

Biochemical Studies of Cytochrome *cbb*₃-type Oxidases from Pseudomonads

Anita Cooper

Submitted in partial fulfillment of the degree of Doctor of Philosophy

31st July 2009

©This copy of the thesis has been supplied on condition that anyone who consults it is understood to recognize that its copyright rests with the author and that no quotations from the thesis, nor any information derived therefrom, may be published without the author's prior written consent.

Abstract

The ability of microorganisms to adapt to low oxygen concentrations confers a considerable growth advantage. Furthermore, the colonization of microaerobic environments by pathogenic bacteria, such as *Pseudomonas aeruginosa* is a significant clinical issue. The *cbb₃* cytochrome *c* oxidases are members of the heme copper oxidase superfamily that regulate microaerobic respiration in diverse Proteobacteria. Cytochrome *cbb₃* oxidases are composed of four non-identical subunits encoded by one or two *ccoNOQP* operons. Surprisingly, the CcoP subunit contains a low potential hexacoordinate heme that binds CO in the reduced state following displacement of the distal endogenous ligand. The biochemical significance of CcoP is poorly understood but the *cbb₃* complex reports the redox status of the cell leading to transcriptional activation of genes involved in energy metabolism via the sensory kinase RegB/RoxS. By expressing the diheme subunit CcoP from the non-pathogenic Pseudomonad, *Pseudomonas stutzeri* in *Escherichia coli*, we have now examined the biochemical properties of the CO binding *c*-type heme. We characterized wild-type and mutant CcoP using mediated redox potentiometry, UV-Visible, magnetic circular dichroism, and electron paramagnetic spectroscopies and have clearly identified two low-spin His/His coordinated *c*-type hemes, with redox potentials of + 185 mV and -15 mV. Examination of the spectral characteristics and oxidase activity of both *cbb₃* oxidase isoforms from the clinically relevant *P. aeruginosa* suggested that the *cbb₃*-1 oxidase has an important metabolic function at high oxygen tensions and the *cbb₃*-2 oxidase has a more significant role under oxygen limiting conditions.

In conclusion, our data suggests a prominent function for the CcoP subunit of cytochrome *cbb₃* oxidases in the adaptive ability of Pseudomonads to colonize diverse environments. Further understanding of this adaptive biochemistry may reveal drugable targets for *P. aeruginosa*.

Acknowledgements

I would like to thank my supervisor, Dr Nick Watmough for his constant encouragement and support throughout the period of study. I would also like to thank, Dr Myles Cheesman for many useful discussions. Dr Sarah Field and Sue Bennett with whom the EPR and MCD was run and interpreted. Everyone I shared a lab with during my research period. Finally, I would like to thank my family, especially Oliver, for being there to listen to the good and the bad and Charlie for being a good sleeper.

Contents

1. Introduction

1.1 Thesis Aims.....	1
1.2 Background and Significance.....	2
1.3 Aerobic Respiration.....	7
1.4 Heme Copper Oxidases.....	15
1.5 Cytochrome <i>cbb</i> ₃ oxidases.....	19
1.6 Microaerobic expression of the cytochrome <i>cbb</i> ₃ oxidases.....	23
1.7 Organization of the cytochrome <i>cbb</i> ₃ oxidase complex.....	25
1.8 Role of cytochrome <i>cbb</i> ₃ oxidases in microaerophilic environments.....	40
1.9 Two Component Regulatory systems.....	43
1.10 Role of <i>cbb</i> ₃ oxidases in two component regulatory systems.....	46
1.11 Heme Sensory Proteins.....	52
1.12 Summary.....	55

2. Materials and Methods

2.1 Bacterial cultivation and strains	
2.1.1 Media and antibiotics.....	56
2.1.2 Bacterial Strains and plasmids.....	57
2.2 General protein biochemistry	
2.2.1 Determination of protein concentration.....	59
2.2.2 Analysis of proteins by SDS-PAGE.....	60
2.2.3 Mass Spectrometry.....	61
2.3 Molecular biology techniques	
2.3.1 Plasmid DNA isolation.....	62
2.3.2 Preparation of competent <i>E. coli</i> cells.....	62
2.3.3 Plasmid Transformations.....	63

2.3.4 Site Directed Mutagenesis.....	63
2.3.5 Restriction Digests.....	65
2.3.6 Agarose gel electrophoresis.....	65
2.3.7 Subcloning.....	66
2.3.8 DNA Sequencing.....	68
2.4 Expression and purification of Full Length CcoP from <i>P. stutzeri</i>	
2.4.1 Expression of full length CcoP in <i>E. coli</i>	68
2.4.2 Purification of full length CcoP.....	69
2.5 Expression and mutagenesis of variant full length CcoP from <i>P. stutzeri</i>	
2.5.1 Site-Directed mutagenesis.....	70
2.5.2 Expression and purification of variant full length CcoP.....	72
2.6 Expression and purification of truncated CcoP from <i>P. stutzeri</i>	
2.6.1 Expression of truncated CcoP.....	72
2.6.2 Purification of truncated CcoP.....	72
2.7 Growth conditions and purification of the two <i>Cbb</i> ₃ isozymes from <i>P. aeruginosa</i>	
2.7.1 Growth conditions of <i>cbb</i> ₃ oxidase.....	74
2.7.2 Preparation of membranes.....	75
2.7.3 Purification of cytochrome <i>cbb</i> ₃ -1 and <i>cbb</i> ₃ -2 oxidase.....	75
2.7.4 Oxidase activity.....	77
2.8 Biophysical Methods	
2.8.1 Electronic absorbance (UV-Visible) Spectroscopy.....	79
2.8.2 Electron paramagnetic resonance (EPR) Spectroscopy.....	80
2.8.3 Magnetic circular dichroism (MCD) Spectroscopy.....	82
2.9 Other Biophysical Methods	
2.9.1 Mediated redox potentiometry.....	84
2.9.2 CO titrations.....	89

3. Biochemical and Spectroscopic Characterization of Full Length CcoP and Truncated CcoP	
3.1 Introduction.....	91
3.2 Results and Discussion.....	94
3.2.1 Optimization of growth and purification	94
3.2.2 UV-Visible Spectroscopy.....	101
3.2.3 Mediated Redox Potentiometry.....	106
3.2.4 EPR Spectroscopy.....	115
3.2.5 MCD Spectroscopy.....	121
3.2.6 CO binding studies.....	133
3.3 Conclusions.....	138
4. Site directed mutagenesis of CcoP	
4.1 Introduction.....	139
4.2 Results and Discussion.....	142
4.2.1 Sequence Alignments and Site Directed Mutagenesis.....	142
4.2.2 Phenotype Characterization of Mutated CcoP.....	143
4.2.3 Biochemical Characterization of Mutated CcoP.....	150
4.2.4 Mediated Redox Potentiometry.....	158
4.2.5 CO Binding Studies.....	163
4.2.6 Comparative EPR Spectroscopy of CcoP variants.....	175
4.3 Conclusions.....	180
5. Cytochrome <i>Cbb</i>₃ oxidases from <i>P. Aeruginosa</i>	
5.1 Introduction.....	182
5.2 Results and Discussion.....	187
5.2.1 Growth in batch culture under different oxygen regimes.....	187
5.2.2 Expression of the two predicted <i>P. aeruginosa cbb</i> ₃ oxidases.....	190
5.2.3 Steady State Assay of Wild-type <i>P. aeruginosa</i> and mutants.....	194
5.3 Conclusions.....	208

6. Biochemical Characterization of *cbb*₃ oxidase isolated from *P. aeruginosa*

6.1 Introduction.....	209
6.2 Results and Discussion.....	209
6.2.1 Purification of cytochrome <i>cbb</i> ₃ oxidase from <i>P. aeruginosa</i>	209
6.2.2 UV-Visible spectroscopy.....	213
6.2.3 TMPD mediated oxygen uptake activity.....	219
6.2.4 Mediated Redox Potentiometry of <i>Cbb</i> ₃ -1 and <i>Cbb</i> ₃ -2.....	222
6.3 Conclusions.....	228
7. General Discussion.....	229
8. References.....	235

Abbreviations

Amp	Ampicillin
ATP	Adenosine Triphosphate
CcO	Cytochrome <i>c</i> oxidase
Cm	Chloramphenicol
CT	Charge transfer
Cyt	Cytochrome
DM	Dodecyl Maltoside
DT	Sodium Dithionite
DTT	Dithiothreitol
EPR	Electron Paramagnetic Resonance
Gm	Gentamicin
HCO	Heme Copper Oxidase
His	Histidine
Kan	Kanamycin
Met	Methionine
MCD	Magnetic Circular Dichroism
PAGE	Polyacrylamide Gel Electrophoresis
Q	Quinol
SDS	Sodium Dodecyl Sulphate
TCA	Tricarboxylic acid cycle
TMPD	N,N,N',N'-tetramethyl p-phenylenediamine
UQ	Ubiquinone
UQH ₂	Ubiquinol

1. Introduction

1.1 Thesis Aims.....	1
1.2 Background and Significance.....	2
1.3 Aerobic Respiration.....	7
1.4 Heme Copper Oxidases.....	15
1.5 Cytochrome <i>cbb</i> ₃ oxidases.....	19
1.6 Microaerobic expression of the cytochrome <i>cbb</i> ₃ oxidases.....	23
1.7 Organization of the cytochrome <i>cbb</i> ₃ oxidase complex.....	25
1.8 Role of cytochrome <i>cbb</i> ₃ oxidases in microaerophilic environments..	40
1.9 Two Component Regulatory systems.....	43
1.10 Role of <i>cbb</i> ₃ oxidases in two component regulatory systems.....	46
1.11 Heme Sensory Proteins.....	52
1.12 Summary.....	55

1.1 Thesis Aims

The aim of the work presented in this thesis was to gain a further understanding of the function of cytochrome *cbb*₃ oxidases in Pseudomonads, in particular the role of the subunit CcoP.

Thesis Aim 1

- Undertake a thorough biochemical and spectroscopic analysis of the *Pseudomonas stutzeri* cytochrome *cbb*₃ subunit, CcoP, to establish a possible role and function of this poorly characterized subunit.

Thesis Aim 2

- Characterize the two *cbb*₃ oxidases, *cbb*₃-1 and *cbb*₃-2, from *Pseudomonas aeruginosa* and compare their biochemical properties.

1.2 Background and significance

Pseudomonas stutzeri was first described in 1895, however, the initial description of a bacterial species belonging to the genus *Pseudomonas* is ambiguous (Van Niel and Allen 1952; Lalucat *et al.* 2006). The genus was first clearly defined in 1966 based on the phenotypic analysis of many different bacterial species, (Palleroni 1975; Palleroni 2003). More recently the phylogenetic affiliation of the genus *Pseudomonas* has been reassessed based on ribosomal RNA homology (Anzai *et al.* 2000; Lalucat *et al.* 2006). A broad phenotype that characterizes members of the genus is Gram-negative, non-spore forming, motile bacilli (Anzai *et al.* 2000; Palleroni 2003; Lalucat *et al.* 2006).

Pseudomonads demonstrate strong nutritional diversity and are able to grow utilizing a variety of carbon sources (Clarke 1975; Spiers *et al.* 2000). The metabolic heterogeneity of this genus affords bacterial cells the ability to adapt to a variety of environmental conditions, therefore enabling the colonization of a wide variety of niches (Dos Santos *et al.* 2004; Williams *et al.* 2007). *Pseudomonads* are facultative aerobes and hence, oxygen is the terminal electron acceptor of choice in the respiratory pathways of this genus (Lalucat *et al.* 2006). Under anaerobic conditions, *Pseudomonads* are able to use nitrogen oxides as alternative terminal electron acceptors (Arai *et al.* 1997; Van Alst *et al.* 2007). Consequently, the genus has an important role in the environment as a denitrifier in the nitrogen cycle (Fig. 1.1 (A and B)).

Denitrification is a process of ecological importance as a key part of the nitrogen cycle (for recent review see Tavares *et al.* 2006). In the biological nitrogen cycle, gaseous nitrogen is the oxidation of ammonia into nitrate and nitrite, in an energy consuming process. The process known as nitrification ensures that a useable form of nitrogen is available for consumption by living organisms. Biological denitrification is the process of reducing nitrate into gaseous nitrogen, therefore completing the nitrogen cycle.

The reaction: $2\text{NO}_3^- + 10\text{e}^- + 12\text{H}^+ \rightarrow \text{N}_2 + 6\text{H}_2\text{O}$

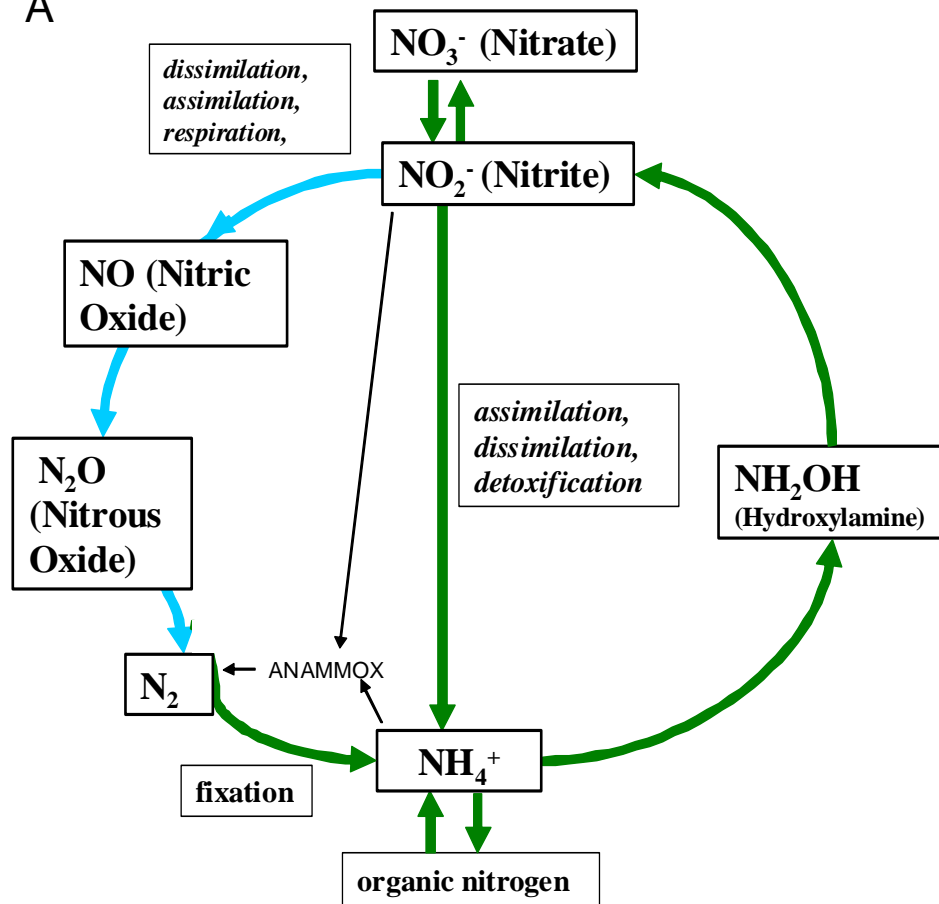
is achieved in four enzymatic steps. The membrane bound enzyme nitrate reductase (NAR) receives electrons from ubiquinol (UQH₂) and nitrate (NO₃⁻) is reduced to nitrite (NO₂⁻). NO₂⁻ is subsequently reduced to nitric oxide (NO) by one of two types of nitrite reductase that are distinguished by their prosthetic group. The cytochrome *cd*₁ and the copper containing nitrite reductase receive electrons from the cytochrome *bc*₁ complex via either cytochrome *c* or a blue copper protein, for example, pseudoazurin. The two types of nitrite reductase are present in strains from the genera *Pseudomonas* and *Alcaligenes*. NO is subsequently reduced by the integral membrane protein, nitric oxide reductase, (NOR) to produce nitrous oxide (N₂O). In the final step of denitrification the enzyme nitrous oxide reductase (N₂OR) reduces N₂O to di-nitrogen (N₂). Each separate enzymatic interconversion is coupled to energy conserving electron transport pathways.

The denitrification process only occurs in oxygen depleted conditions (such as in some soils and seafloor sediments), since oxygen is a more favorable electron acceptor than nitrate. Moreover, in general, anaerobic respiration is less energy efficient than aerobic respiratory pathways (Zumft 1997; Williams *et al.* 2007). The ability of Pseudomonads to exploit the diverse environmental conditions presented is primarily attributed to the complex respiratory system of this genus as shown in Fig. 1.1 (B) (Stover *et al.* 2000; Alvarez-Ortega and Harwood 2007).

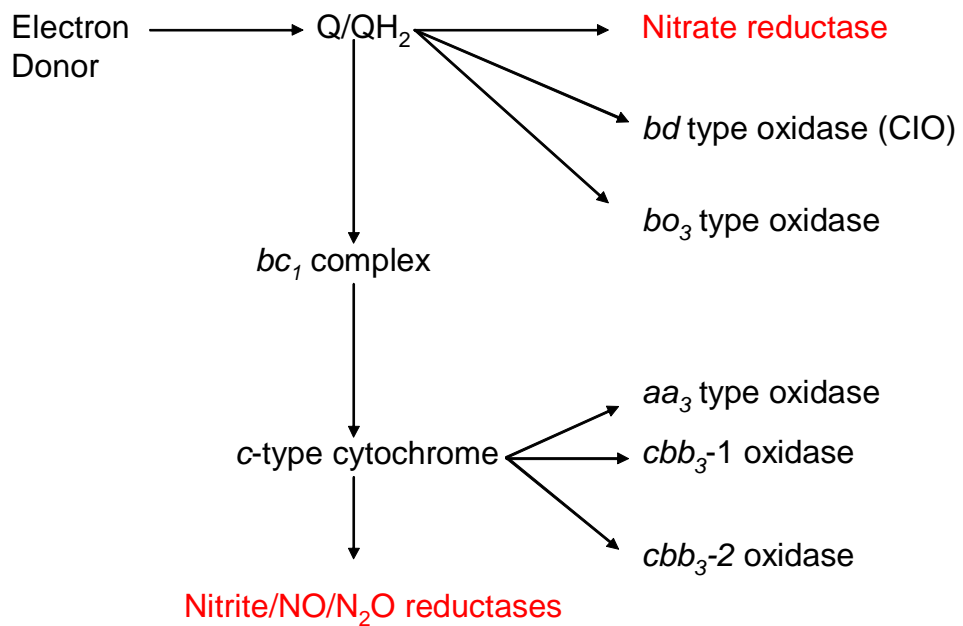
Fig. 1.1 (A) The Biological Nitrogen Cycle. The nitrogen cycle describes an important natural cycle operating in terrestrial ecosystems. Each separate interconversion is catalyzed by a different enzyme. Bacteria play a significant role in the denitrification process and under anaerobic conditions Pseudomonads use nitrates as an alternative final electron acceptor to oxygen, thereby utilizing the denitrification enzyme pathway. ANNAMOX is Anaerobic Ammonium Oxidase. Adapted from (Richardson 2000).

FIG. 1.1 (B) Schematic representation of the *P. aeruginosa* respiratory pathway. This facultative organism can respire anaerobically by denitrification (shown in red) or aerobically using one of two quinol oxidases or one of three cytochrome *c* oxidases. (Adapted from Comolli and Donohue 2004)

A



B



The pseudomonad species, *P. aeruginosa*, is ubiquitous in the environment, but also plays a more significant role as a clinically challenging pathogen responsible for bacteremia, urinary tract infections, respiratory system infections, and soft tissue infections (Govan 1997; Pieracci and Barie 2007; Williams *et al.* 2007; Driscoll *et al.* 2007). Infections caused by *P. aeruginosa* are particularly serious in immunocompromised patients (Pieracci and Barie 2007). For example, patients with cystic fibrosis are characteristically susceptible to chronic infection caused by this organism (Van Alst *et al.* 2007; Williams *et al.* 2007). Individuals with cystic fibrosis are predisposed to thick mucus production in the lungs, which is proposed to provide an ideal habitat for *P. aeruginosa* colonization and a semi-solid substrate for subsequent biofilm formation (Dinwiddie 2000; Matsui *et al.* 2006).

Many Gram-negative bacteria, including Pseudomonads, are naturally resistant to a wide range of antibiotics as the outer membrane lipopolysaccharides (LPS) protect the bacteria from the influx of antimicrobial agents (Meadow 1975; Driscoll *et al.* 2007). Slow influx of antimicrobial agents through the LPS is predicted to act synergistically with an active efflux of the agent from the Pseudomonad cell (Li *et al.* 1994). Moreover, Pseudomonads maintain antibiotic resistance plasmids and are able to transfer these resistance plasmids between generations by means of transduction and conjugation (Towner 1997). Once acquired chronic infections caused by *P. aeruginosa*, prove particularly challenging to treat with the current range of anti-microbial agents (Driscoll *et al.* 2007). In particular, when the organism forms a biofilm, increased resistance to antibiotics is observed meaning that *P. aeruginosa* is responsible for high rates of illness and death in the immunocompromised population (Kirisits and Parsek 2006; Van Alst *et al.* 2007). Consequently, there is a need for new anti-*P. aeruginosa* agents and any new insights into Pseudomonas biology will be valuable (Takeda *et al.* 2007). Advancing our understanding of the biochemistry of Pseudomonads requires the study of a model organism that can be obtained in high yield

and of low pathogenic risk to the user, for example the organism *P. stutzeri*. *P. stutzeri* is a soil dwelling, facultative anaerobe with the capacity to denitrify. This Pseudomonad is non-pathogenic, and can grow easily in minimal, chemically defined media (Lalucat *et al.* 2006). The availability of a complete genomic sequence of *P. stutzeri*, means it remains an ideal organism model to provide insights into physiology of the other pseudomonads, for example, the human pathogen, *P. aeruginosa* (Van Niel and Allen 1952; Lalucat *et al.* 2006; Yan *et al.* 2008).

1.3 Aerobic Respiration

Cellular respiration is the process by which electrons derived from the oxidation of organic compounds are converted into a form of energy that can be used by cells. At the most basic level, respiration integrates a series of oxidation/reduction reactions that conserve energy in the form of a transmembrane electrochemical proton gradient for subsequent use in ATP synthesis. In eukaryotic systems (Fig. 1.2) the enzymatic machinery for respiration is embedded in the inner mitochondrial membrane. In mitochondria, electrons derived from glycolysis and the citric acid cycle enter the respiratory pathway, through the low-redox potential electron carrier nicotinamide adenine dinucleotide (NAD^+) and NADH:ubiquinone oxidoreductase (Complex I). Complex I catalyses the transfer of two electrons from NADH to the lipid-soluble electron carrier ubiquinone (UQ). The reaction is associated with the translocation of protons across the membrane (Nicholls 2002).

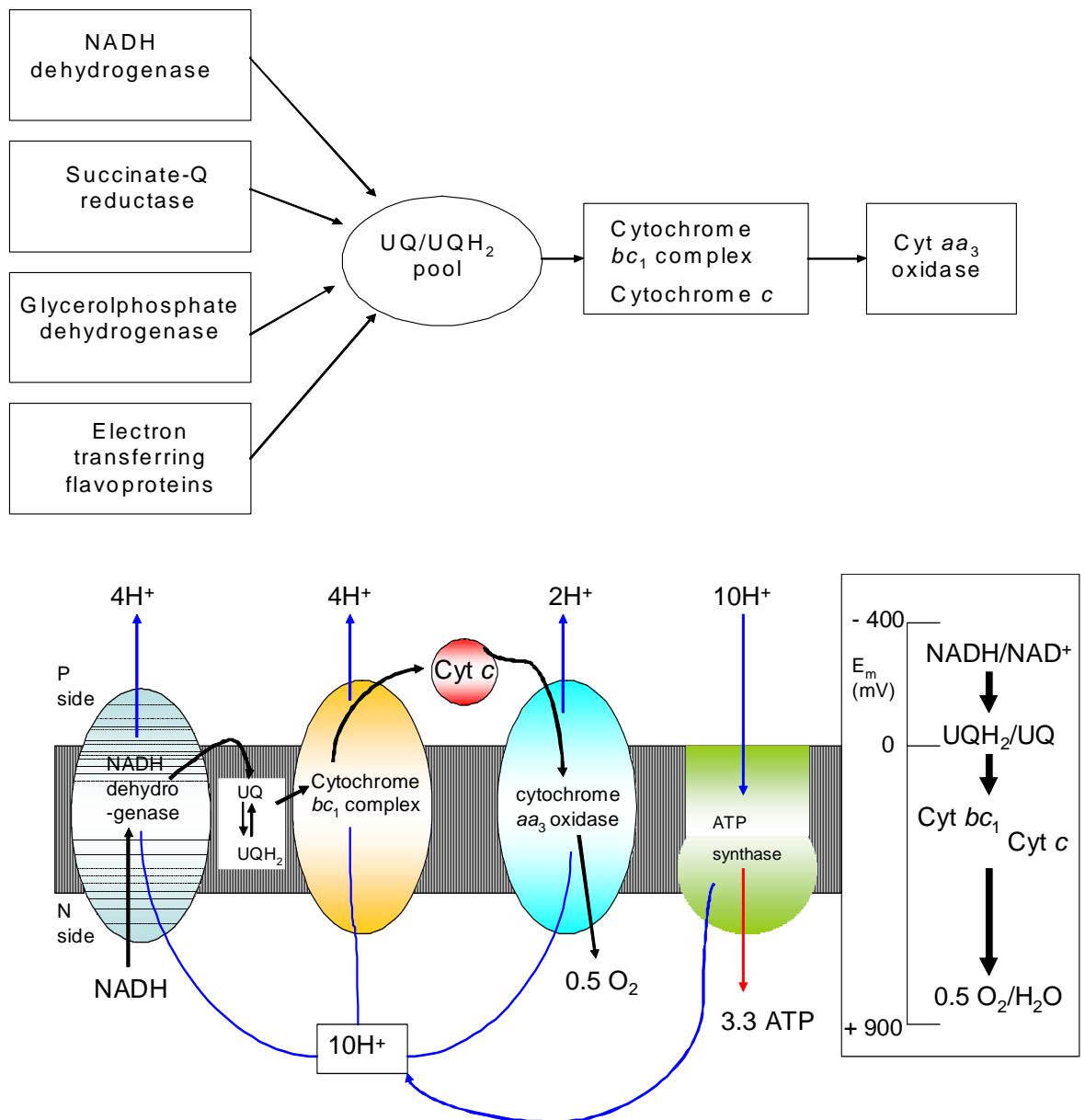


FIG. 1.2 The topology and bioenergetics of a basic aerobic respiratory electron transport system of mammalian mitochondrion. Schematic illustrating the complexes involved in the basic aerobic respiratory electron transport system of a mammalian mitochondrion. Electrons pass along the electron transport chain via a series of integral and peripheral membrane proteins to the terminal electron acceptor, oxygen, which is subsequently reduced to water. The transfer of protons from the mitochondrial matrix (N-side) to the intermembrane space (P-side) accompanies electron flow. The movement of protons across the membrane leads to the generation of a proton motive force that ultimately drives the synthesis of ATP. The scale to the right indicates the redox potential of redox couples in the electron transport system. UQ, ubiquinone; UQH₂, ubiquinol; Cyt, cytochrome. Adapted from (Richardson 2000).

In addition to complex I, at least three other enzymes feed electrons to UQ, as shown in Fig. 1.2. Flavoprotein succinate:ubiquinone oxidoreductase (Complex II), transfers electrons from succinate to fumarate as part of the tricarboxylic acid cycle (TCA). The two electrons are subsequently transferred to the cofactor flavin adenine dinucleotide (FAD) which is reduced to form FADH₂. The transfer of electrons to UQ follows this step, and UQ is reduced to form UQH₂. The second and third enzymes, ETF ubiquinone oxidoreductase and glycerol phosphate dehydrogenase accept electrons from alternative dehydrogenases to succinate, however, similarly to complex II these two enzymes transfer electrons from FADH₂ to UQ. Complex II, ETF ubiquinone oxidoreductase and glycerol phosphate dehydrogenase are not proton pumps as the free energy change of the catalyzed reaction, the transfer of electrons from FADH₂ to UQ, is too small.

The ubiquinol-cytochrome *c* oxidoreductase (cytochrome *bc*₁; Complex III) catalyses the transfer of electrons from ubiquinol (UQH₂) to the water-soluble electron carrier cytochrome *c*. The redox groups in cytochrome *bc*₁ comprise a Fe₂/S₂ centre located on the Rieske protein, two *b* type hemes located on a single polypeptide and the *c* type heme of cytochrome *c*₁. (Fig. 1.3) (Xia *et al.* 1997). The transfer of electrons through the *bc*₁ complex leads to the generation of a proton gradient via the operation of the proton-motive Q-cycle mechanism.

Mitchell first proposed the Q cycle in 1975, which describes a series of redox reactions (Mitchell 1975). The Q cycle relates how the sequential oxidation and reduction of UQ/UQH₂ can result in the net movement of protons across the lipid bilayer (Mitchell 1975) (Fig. 1.3). The overall reaction catalyzed by the *bc*₁ complex involves the release of four protons at one side of the membrane and the uptake of two protons from the opposite side (Crofts *et al.* 2006).

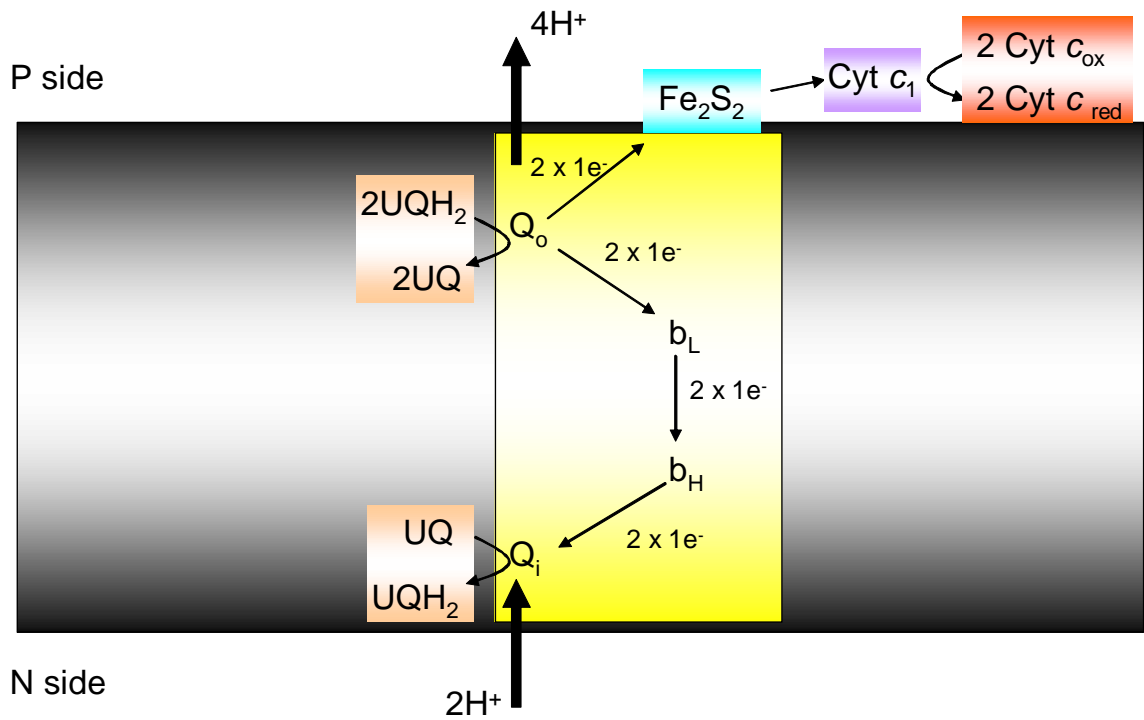


FIG. 1.3 Schematic representation of the Q-cycle in the bc_1 complex in mitochondria. This schematic illustrates the electron transfer events that occur following the oxidation of UQH_2 at the P side of the inner mitochondrial membrane. The oxidation of UQH_2 to UQ occurs in two stages. UQH_2 binds to the Q_o site, close to the P-face of the membrane and an electron is transferred to the adjacent Rieske protein (Crofts *et al.* 2006). The electrons received by the Fe_2S_2 centre, located on the Rieske protein, pass down the chain to cytochrome c_1 , followed by transfer to cytochrome c . The second electron, which was transferred to the b_L heme ($E_m = -100\text{ mV}$) is used to reduce the b_H heme ($E_m = +50\text{ mV}$), which in turn transfers the electron to the ubiquinone bound at the Q_i site, which is reduced to a semiquinone radical ($UQ^{\cdot-}$). In the second half of the Q-cycle a second electron is transferred from b_H reducing the semiquinone species to ubiquinol. Following electron transfer the two protons required for the subsequent reduction of UQ to UQH_2 are taken up from the matrix (N-side). In the bc_1 complex, the movement of electrons by the b -heme chain from Q_o to Q_i sites indirectly achieves proton translocation across the mitochondrial membrane. Adapted from (Crofts *et al.* 2006).

The final step in the electron transport chain of mitochondria and aerobically respiring bacteria is the sequential transfer of four electrons from reduced cytochrome *c* to oxygen forming water in a reaction catalyzed by cytochrome *c* oxidase (CcO) (complex IV). This terminal oxidase, for example, the cytochrome *aa*₃ oxidase in mitochondria, uses the liberated free energy to translocate protons from the N side of the membrane. The proton pumping mechanism in the terminal oxidases will be discussed in more detail in Section 1.7.

The overall transfer of electrons through the respiratory complexes (I-IV) is coupled to the pumping of protons from the mitochondrial matrix (N-side) to the cytosolic side (P-side) of the membrane (Wikstrom 2004). The movement of protons generates a proton electrochemical gradient across the membrane (Wikstrom 1977). The proton motive gradient drives the passage of protons from the intermembrane space into the mitochondrial matrix via the membrane spanning subunits of ATP synthase and the synthesis of ATP from ADP and P_i is catalyzed.

The enzyme, ATP synthase consists of a catalytic domain (F₁) and a membrane domain (F₀) which are linked by a central stalk (γ) as shown in Fig. 1.4 (B) (Zhou *et al.* 1997). In *Escherichia coli*, the F₁ domain consists of five subunits in a $\alpha_3\beta_3\gamma_1\delta_1\varepsilon_1$ stoichiometric ratio (Foster and Fillingame 1982; Schwem and Fillingame 2006). The F₀ domain is composed of three subunits in an $a_1b_2c_{10-12}$ stoichiometric ratio (Foster and Fillingame 1982; Schwem and Fillingame 2006). Protons generated by the electron transport chain move through the F₀ domain from the P to the N side of the membrane (Pedersen and Amzel 1993). The movement of protons generates the rotation of the ring-like formation of *c* subunits arranged around the central stalk of the water-soluble F₁ domain (Duncan *et al.* 1995). As the *c* subunits rotate, the attached stalk also rotates (Duncan *et al.* 1995; Adachi *et al.* 2007). Rotation of the central stalk results in sequential conformational changes in the α

and β subunit of the F_1 domain (Boyer 2002). The proton motive force induced conformational changes occur in the hexamer of alternating α and β subunits (Duncan *et al.* 1995). The conformational changes alter the binding affinity of the subunits to ATP, ADP and P_i (Nicholls 2002). The three catalytic nucleotide binding sites on the β subunits at α/β interfaces exist in three different conformations, each reflecting a different affinity for ATP, ADP and P_i as shown in Fig. 1.4 (Kayalar *et al.* 1977; Duncan *et al.* 1995). The different conformations of each of the three β subunits of the F_1 domain alternate sequentially (Adachi *et al.* 2007). In the “loose” (L) conformation, the β subunit binds ADP and P_i . Next, the β subunit adopts the “tight” (T) conformation in which ADP and P_i react to form ATP. In the last step, the β subunit adopts the “open” (O) conformation to release the newly formed ATP molecule. Energy is not used to form the ATP molecule but to release the tightly bound ATP from the enzyme (Boyer 2002).

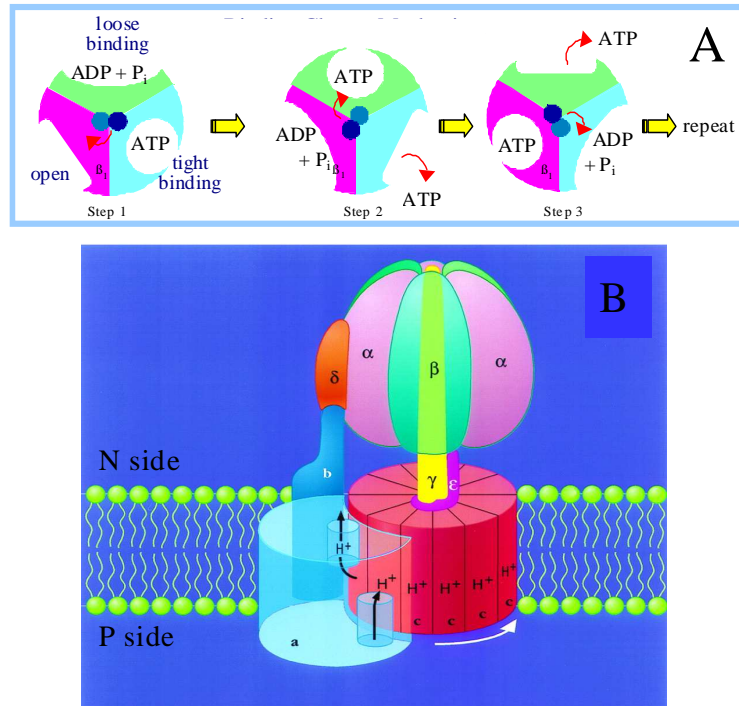


FIG. 1.4 The ATP synthase. (A) Representation of the binding change mechanism looking up at the F_1 domain from the membrane. In the open (O) conformation the β_1 subunit of the F_1 domain is empty. In step (1) the asymmetric γ subunit rotates 120° clockwise driving the conformational change of β_1 (green) to loose. In the loose (L) conformation, the β_1 subunit binds ADP and P_i . In step (2) rotation of the γ subunit changes the conformation of β_1 to tight (T). In the tight conformation, ADP and P_i are combined to form ATP. A further rotation of the γ subunit changes the conformation of β_1 back to open, resulting in the release of a newly formed ATP molecule. These steps occur in each β subunit simultaneously (Adapted from (Zhou *et al.* 1997)).

(B) Schematic of ATP synthase from *E. coli*. The enzyme from *E. coli* has an F_1 portion, which is located within the membrane and has subunits designated as $\alpha_3\beta_3\gamma_1\delta_1\epsilon_1$. The subunits of the F_0 portion are designated $a_1b_2c_{10-12}$ (Zhou *et al.* 1997).

In mammals, a single *aa*₃ type cytochrome *c* oxidase terminates the respiratory chain and catalyses the reduction of oxygen to water. The single *aa*₃ oxidase means that respiratory flexibility to changes in oxygen concentration is restricted in mammals and they compensate by having a highly complex network of organs, which control the uptake, transport and tissue distribution of oxygen (Ludwig and Schatz 1980; Wenger 2002). In contrast, the prokaryotic respiratory system terminates with multiple respiratory enzymes that either catalyze the reduction of alternative terminal electron acceptors or are expressed accordingly, in response to fluctuating levels of oxygen (Kita *et al.* 1986). The variety of respiratory enzymes in prokaryotes allows bacteria to customize their respiratory system in response to changeable environments (Richardson 2000).

The bacterial pathogen *P. aeruginosa* is an example of a bacterial species that express genes which encode distinct respiratory oxidases (Matsushita *et al.* 1980; Stover *et al.* 2000; Williams *et al.* 2007). Publication of the complete genome sequence of *P. aeruginosa* has facilitated the prediction of the respiratory pathways of this opportunistic pathogen, as shown in Fig. 1.1B (Stover *et al.* 2000; Alvarez-Ortega and Harwood 2007). *P. aeruginosa* can respire aerobically using one of two quinol oxidases, (cytochrome *bo*₃ oxidase or *bd*-type oxidase) or one of three cytochrome *c* oxidases, (cytochrome *cbb*₃₋₁, cytochrome *cbb*₃₋₂ or cytochrome *aa*₃). Recent completion of the genomic sequence of *P. stutzeri* revealed that this non pathogenic Pseudomonad also possesses two operons that each potentially encode a *cbb*₃ oxidase (*cbb*₃₋₁ and *cbb*₃₋₂) (Yan *et al.* 2008). The branched respiratory pathway of both Pseudomonad species suggests the potential for significant respiratory flexibility (Baker *et al.* 1998). Each terminal oxidase in *P. aeruginosa* is expressed in response to different oxygen tensions and allows the bacteria to survive in environments with fluctuating oxygen levels (Castresana *et al.* 1994; Baker *et al.* 1998; Williams *et al.* 2007). To survive in anoxic environments, alternative terminal electron acceptors can also be utilized to ensure the continuity of respiration. *P. aeruginosa*

can generate energy anaerobically using N-oxides as terminal electron acceptors using the denitrification pathway, as discussed in section 1.2.

Four of the putative terminal oxidases observed in *P. aeruginosa*, belong to the heme copper oxidases superfamily (HCO) (García-Horsman *et al.* 1994). The fifth terminal oxidase is the cyanide insensitive oxidase (CIO). The CIO is part of the cytochrome *bd* oxidase family, a family of two subunit quinol oxidases, which have no homology to members of the HCO superfamily (Zlosnik *et al.* 2006; Williams *et al.* 2007). The CIO will be discussed in more detail in section 1.10.

1.4 Heme Copper Oxidases

The majority of bacterial oxidases and the single Cytochrome *c* oxidase (CcO), cytochrome *aa*₃, in eukaryotic mitochondria belong to one superfamily, the heme copper oxidases (HCO) (García-Horsman *et al.* 1994). The X-ray crystal structures of the cytochrome *aa*₃ from both *P. denitrificans* and bovine mitochondria have been determined and show that their subunits I and II are remarkably similar (Iwata *et al.* 1995; Tsukihara *et al.* 1995; Ostermeier *et al.* 1997). Membership in the HCO superfamily is based on the presence of a subunit homologous to subunit I (SUI) of the mammalian CcO. SUI comprises at least twelve transmembrane helices and contains the active site, a dinuclear centre formed by the iron of a high-spin heme, to which substrates and other exogenous ligands can bind and an adjacent copper ion (Cu_B) (Stevens and Chan 1981) (García-Horsman *et al.* 1994). A second heme in SUI facilitates the transfer of electrons to the dinuclear centre from either cytochrome *c* or ubiquinol in cytochrome *c* oxidases or quinol oxidases respectively (Brzezinski and Adelroth 2006; Brown *et al.* 1993). The high-spin heme is ligated by a single histidine, the low-spin heme is ligated by two histidines and Cu_B is ligated by three histidines (Shapleigh *et al.* 1992). These six histidines are highly conserved in the HCOs and the *cbb*₃ related NORs.

The prokaryotic heme copper oxidases can be broadly subdivided into one of two classes: quinol oxidases, which terminate bc_1 independent respiratory chains, for example cytochrome bo_3 from *E. coli*, and CcO, such as the aa_3 type oxidases from *Paracoccus denitrificans* (Kita *et al.* 1986; Castresana *et al.* 1994; de Gier *et al.* 1994). Prior to the discovery of the cbb_3 oxidases, a major difference between the two classes of oxidases was considered to be the presence of the redox active metal centre Cu_A in subunit II of CcO which is absent in quinol oxidases (Fig. 1.5).

In CcOs the binding site for the electron donor cytochrome *c* has been localized to subunit II and it is the Cu_A centre in subunit II which receives electrons from cytochrome *c* (Musser *et al.* 1993; Malatesta *et al.* 1998). The dinuclear Cu_A centre is composed of two electronically coupled copper ions mixed valence Cu^I/Cu^{II} which act together in the CcO as a one electron-donor or acceptor. Mixed valence copper complexes as observed in Cu_A are rare (Hwang and Lu 2004).

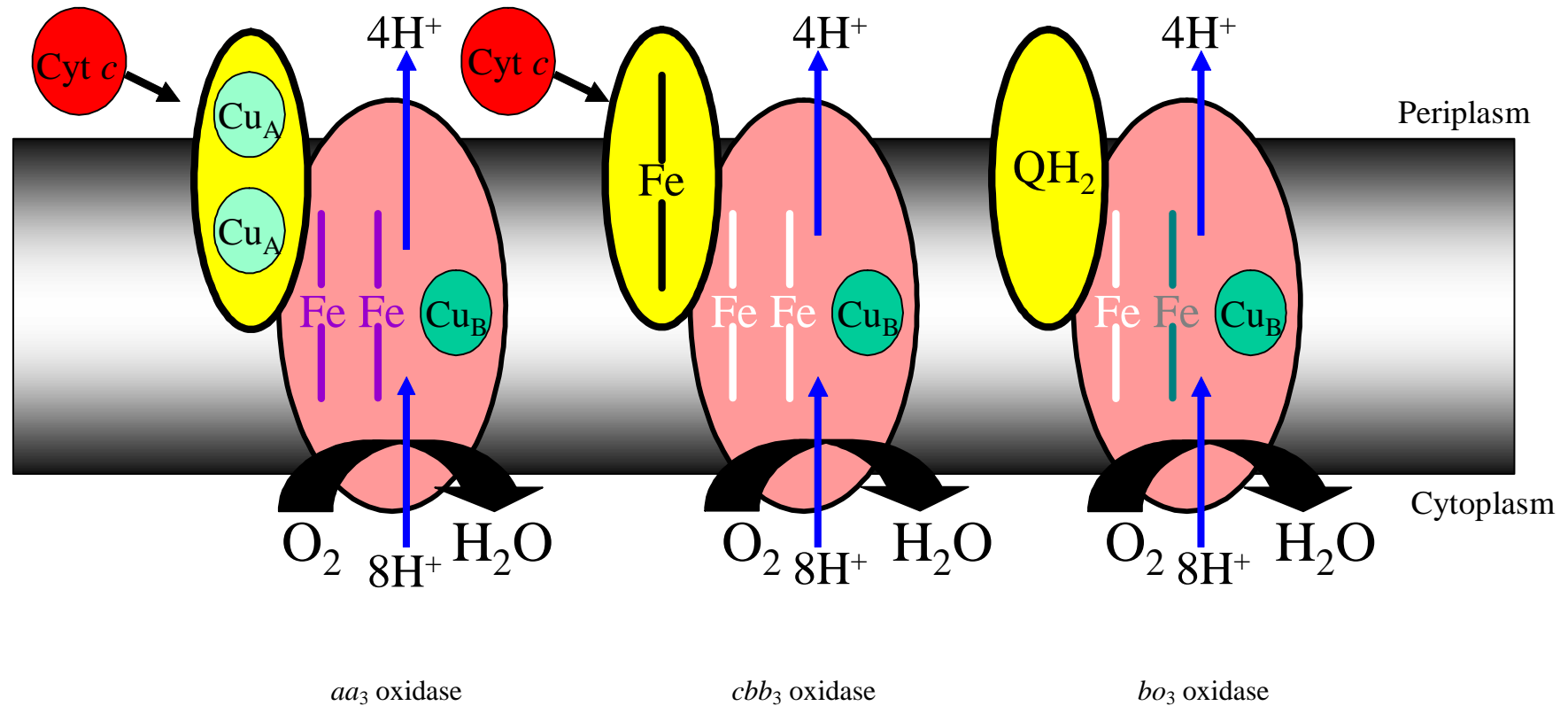


FIG. 1.5 Schematic illustrating the similarities and differences between different subclasses of HCOs. The different heme types in subunit I (pink) are shown, *heme A*, purple, *heme B*, white, and *heme O*, dark cyan. Differences between the electron receiving domains, subunit II, (yellow), and electron donors are shown. The cytochrome *c* dependant enzymes *aa*₃ oxidase and *cbb*₃ oxidase accept electrons from reduced cytochrome *c*. In contrast, Quinol oxidases, for example *bo*₃ oxidases accept electrons directly from the quinone pool. (Adapted from (Richardson 2000)).

Three dimensional structures are known for the CcO from *P. denitrificans* and bovine heart mitochondria (Iwata *et al.* 1995; Tsukihara *et al.* 1995). The primary electron acceptor site Cu_A centre is present in subunit II of CcO but not in the corresponding subunit of the quinol oxidase (Puustinen *et al.* 1991; van der Oost *et al.* 1992). However, hydrophathy analysis of quinol oxidase subunit II suggests it is structurally related to subunit II of the CcO, cytochrome *aa*₃ (Chepuri *et al.* 1990; Musser *et al.* 1993). Sequence alignments of subunit II of the CcO and quinol oxidases indicate that quinol oxidases lack the four putative ligands for Cu_A (two histidines and two cysteines) observed in CcO (Holm *et al.* 1987; Chepuri *et al.* 1990). Moreover, it has been demonstrated that the Cu_A site can be generated within subunit II of the *E. coli bo*₃ type quinol oxidase using site directed mutagenesis to restore the “missing” ligands in the subunit (van der Oost *et al.* 1992). Hence, the main role of subunit II in the quinol oxidases may be analogous to that of subunit II in the cytochrome *c* oxidases, i.e., delivering electrons to the metal centers within subunit I (Welter *et al.* 1994; Puustinen *et al.* 1996). The quinol oxidases do not, however, receive electrons from the water-soluble cytochrome *c* but catalyze the two-electron oxidation of UQH₂ (Musser *et al.* 1993).

The substrate binding site of quinol oxidases is hypothesized to be the membrane spanning region of subunit I, which contains a cluster of polar residues exposed to the interior of the lipid bilayer (Abramson *et al.* 2000). This proposed binding site can therefore accommodate the hydrophobic nature of the substrate, UQH₂ (Gohlke *et al.* 1997). The proposed location of the binding site of UQH₂ within the lipid bilayer suggests that UQH₂ interacts directly with the low-spin heme bound to transmembrane helices of subunit I (Puustinen *et al.* 1996). In contrast, cytochrome *c* binds to the periplasmic surface of the CcO. In subunit II the Cu_A binding region projects into the aqueous phase and is therefore an ideal intermediate for electron transfer due to the cellular location of the electron donor, cytochrome *c* (Gray *et al.* 1994; Farver *et al.* 2007)

A more recently described family of HCO, the cytochrome *cbb*₃ oxidases, has evolved which differ to the models described thus far (Preisig *et al.* 1993). The *cbb*₃ oxidases utilize cytochrome *c* as an electron donor, however subunit II of these oxidases lack a Cu_A site (García-Horsman *et al.* 1994; Gray *et al.* 1994; Kim *et al.* 2007). Using a hydrophobic ubiquinone analogue it has been suggested that UQH₂ does not elicit any oxygen uptake by purified *cbb*₃ oxidase isolated from *Rhodobacter capsulatus* (Gray *et al.* 1994). Evidence therefore suggests that the *cbb*₃ oxidase is not a quinol oxidase, but a CcO. It remains unclear how electrons are received from cytochrome *c* by the *cbb*₃ oxidase. In addition to a subunit homologous to SUI (CcoN) the *cbb*₃ oxidases also have two heme *c* containing subunits (CcoO and CcoP) (Sharma *et al.* 2006). It is speculated that one of these two heme *c* containing subunits receive electrons directly from cytochrome *c*, even in the absence of Cu_A (Gray *et al.* 1994). The subunits CcoO and CcoP will be discussed in more detail in Section 1.7.

1.5 Cytochrome *cbb*₃ oxidases

Cytochrome *cbb*₃ oxidases are the most recently characterized members of the superfamily of HCO (Preisig *et al.* 1993). The *cbb*₃ oxidase was initially identified in the bacterium *Bradyrhizobium japonicum* as the product of an operon (*fixNOQP*) whose expression is required for nitrogen fixation (Preisig *et al.* 1993). It was observed that these genes, designated *fixNOQP*, were expressed under microaerobic conditions in the root nodule where *B. japonicum* lives symbiotically with the legume host plant. Subsequently, the *ccoNOQP* operon was also identified in the non symbiotic nitrogen fixing bacteria *R. capsulatus* (Thöny-Meyer *et al.* 1994).

The *ccoNOQP* operon has been identified in many non-diazotrophic Proteobacteria including human pathogens for example, *P. aeruginosa*, *Helicobacter pylori* and *Campylobacter jejuni* (Thöny-Meyer *et al.* 1994; Preisig *et al.* 1993; Parkhill *et al.* 2000;

Tomb *et al.* 1997). These human pathogens are observed as infectious agents in anoxic environments. For example, *P. aeruginosa* has been isolated from hypoxic mucus regions in the lungs of cystic fibrosis patients and *H. pylori* has been isolated from the microaerophilic environment, the gastric mucosa (Cottet *et al.* 2002; Worlitzsch *et al.* 2002; de Reuse and Bereswill 2007; Williams *et al.* 2007). It is therefore hypothesized, that the *cbb₃* oxidase contributes to the successful colonization of hypoxic tissues and may be an important determinant of pathogenicity (Pitcher and Watmough 2004).

The gene products of the *ccoNOQP* operon encode for the *cbb₃* subunits CcoN, CcoO, CcoP and CcoQ as shown in Fig. 1.6 (A) (Zufferey *et al.* 1996). In most Proteobacteria characterized so far the *ccoNOQP* operon is located immediately upstream of the *ccoGHIS* gene cluster (Koch *et al.* 2000; Kulajta *et al.* 2006). The *ccoGHIS* gene cluster is necessary for the assembly of an active *cbb₃* oxidase complex in the cell.

The *ccoGHIS* operon was first identified, and sequenced from the nitrogen fixing bacterium *Sinorhizobium meliloti* (formally *Rhizobium meliloti*) (Kahn *et al.* 1989). The operon has since been identified in the microaerophilic nitrogen fixing *B. japonicum* and *Azorhizobium caulinodonas* (Preisig *et al.* 1996; Mandon *et al.* 1993). Similarly to the *ccoNOQP* operon expression of the *ccoGHIS* operon is strongly induced in cells grown microaerobically or anaerobically (Preisig *et al.* 1996). Evidence suggests that the four proteins encoded by the *CcoGHIS* operon exist as a multi-subunit membrane protein complex in which they function in concert, since mutations in either one of the genes results in a nitrogen fixation defective strains (Preisig *et al.* 1996; Koch *et al.* 2000).

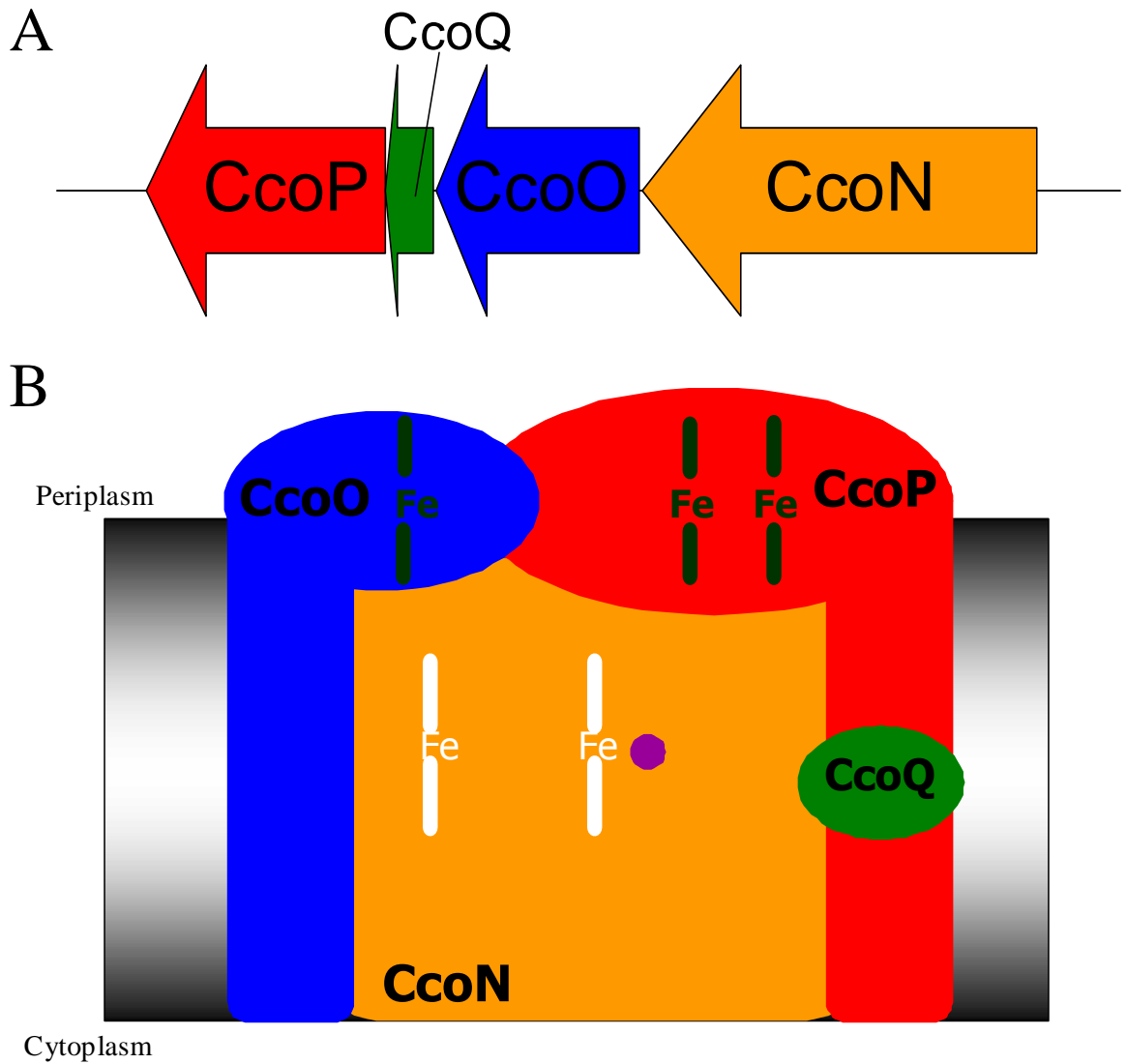


FIG. 1.6 Schematic diagrams illustrating the *ccoNOQP* operon (A) and the proposed organization of the *cbb₃* complex (B). In the schematic of the membrane bound *cbb₃* complex, the individual subunits are annotated accordingly. The *b*-type hemes are coloured white, *c*-type hemes black and Cu_B purple

The CcoG, CcoH, CcoI and CcoS proteins are each proposed to have a specific role in the biogenesis of cytochrome *cbb*₃ oxidase (Preisig *et al.* 1996; Kulajta *et al.* 2006). Sequence similarities between the protein CcoI and *Enterococcus hirae* CopA suggest a function for the CcoI protein (Kahn *et al.* 1989; Preisig *et al.* 1996). CopA is an integral membrane copper-uptake protein that belongs to the family of prokaryotic and eukaryotic P-type ATPases, which are involved in transport of heavy metal ions (Rensing *et al.* 2000). It is proposed that CcoI is involved in Cu delivery to the only Cu containing subunit of *cbb*₃ oxidase, the catalytic subunit, CcoN (Koch *et al.* 2000). Site directed mutagenesis has been used to demonstrate that membranes of a CcoI deletion strain are devoid of the CcoNOQP complex (Kulajta *et al.* 2006). The experimental evidence therefore suggests that Cu incorporation is a pre-requisite for the formation or the stability of the *cbb*₃ oxidase complex.

Sequence similarities between CcoG and the protein RdxA from *Rhodobacter sphaeroides* suggests a function for the protein CcoG (Kahn *et al.* 1989; Preisig *et al.* 1996). RdxA is an integral membrane containing two 4Fe-4S like ferredoxin domains. Based on the sequence similarity to RdxA and other ferredoxins the protein CcoG is proposed to be involved in an unknown oxidation-reduction process (Kahn *et al.* 1989; Neidle and Kaplan 1992; Koch *et al.* 2000). Deletion of CcoG however, appears to have only minor effects on the activity of *cbb*₃ oxidase in *R. capsulatus* membranes compared to the absence of the proteins CcoH and CcoI (Kulajta *et al.* 2006). It is hypothesized that CcoH and CcoI play a role in the assembly of the *cbb*₃ oxidase, therefore a loss of activity of the oxidase is feasible in CcoH and CcoI mutants.

In contrast to CcoI and CcoG, the proteins CcoH and CcoS have no characteristic sequence motifs and share no sequence homology to proteins of known function (Kulajta *et al.* 2006). Analysis of *R. capsulatus* membranes in which *CcoS* had been deleted, indicated

that the *cbb*₃ oxidase complex was fully detectable; however, the assembled *cbb*₃ complex was inactive. It was determined spectroscopically that the inactivity of the complex was due to the absence of a functional heme *b*₃-Cu_B binuclear centre in CcoN (Koch *et al.* 2000). It is therefore suggested that the role of CcoS can be attributed to the insertion of either the *b*-type heme or Cu_B or of both cofactors into CcoN (Kulajta *et al.* 2006).

1.6 Microaerobic expression of the cytochrome *cbb*₃ oxidase

Despite apparent homology of subunit I between members of the HCO superfamily and the cytochrome *cbb*₃ oxidases the latter differs to other members of this family. As previously discussed (Section 1.4), *cbb*₃ oxidases accept electrons from cytochrome *c* but lack the Cu_A electron receiving prosthetic group in subunit II observed in other CcOs (Gray *et al.* 1994; Preisig *et al.* 1996). The *cbb*₃ oxidases also differ from other HCOs with regards to their affinity for oxygen. The *B. japonicum* *cbb*₃ oxidase is induced under microaerophilic conditions and the experimentally determined K_m for dioxygen is 7 nM (Preisig *et al.* 1993; Zufferey *et al.* 1996). The experimental K_m value demonstrates that the *cbb*₃ oxidase has a very high affinity for oxygen, and is therefore consistent with its expression under microaerophilic conditions. The *cbb*₃ oxidase isolated from *C. jejuni* has a slightly higher K_m value for dioxygen than *B. japonicum* of 40 nM (Jackson *et al.* 2006). These experimentally determined K_m values for the *cbb*₃ oxidase are lower than recorded for other HCOs. For example, cytochrome *bo*₃ isolated from *E. coli* has a K_m value of 0.15-0.35 μM (D'Mello *et al.* 1995; Zufferey *et al.* 1996). The substrate affinity of *cbb*₃ oxidases isolated from *B. japonicum* and *C. jejuni* are thus far the only measurements reported. It is assumed that a similar affinity for oxygen would be demonstrated in cytochrome *cbb*₃ oxidases isolated from sources other than those reported.

In principle, the high oxygen affinity of the *cbb*₃ oxidases enables Proteobacteria to colonize microaerobic environments. As previously discussed (Section 1.2) most bacterial

species have multiple respiratory oxidases which allow cells to customize respiratory systems to meet the demands of varying environmental conditions. For example, in the aerobic respiratory chain of *E. coli* there are two distinct respiratory oxidases, cytochrome *bd* and cytochrome *bo₃* (Kita *et al.* 1984). Cytochrome *bd* has a higher affinity for oxygen than cytochrome *bo₃* and is induced to high levels when the oxygen tension in growth medium is low (Fu *et al.* 1991). Similarly, in the *cbb₃* expressing bacteria, under microaerophilic conditions the cytochrome *cbb₃* oxidases predominate (Preisig *et al.* 1993; Marchal *et al.* 1998).

Under microaerophilic conditions, expression of the *ccoNOQP* operon is regulated by the oxygen sensing transcriptional regulator of fumarate and nitrate reductase (FNR) (Vollack *et al.* 1998; Van Spanning *et al.* 1997; Cosseau and Batut 2004). FNR was first identified in *E. coli* and belongs to a large family of regulators that modulate physiological changes in response to various environmental and metabolic changes (Unden and Guest 1985; Crack *et al.* 2007).

FNR is activated under anaerobic conditions by the acquisition of one $[4\text{Fe-4S}]^{2+}$ cluster per protein and which promotes dimerization of FNR (Khoroshilova *et al.* 1995; Moore *et al.* 2006). FNR is active as a dimer and binds to an FNR box sequence (TTGAT-N4-GTCAA) in the promoter region of the target gene. At high oxygen concentrations the $[4\text{Fe-4S}]^{2+}$ cluster undergoes a conversion into a $[2\text{Fe-2S}]^{2+}$ cluster and the conformational change results in loss of the site specific DNA binding (Khoroshilova *et al.* 1997; Crack *et al.* 2006). The role of FNR and FNR analogues in the regulation of the *cbb₃* oxidase under microaerophilic conditions will be discussed in more detail in Section 1.8.

1.7 Organization of the cytochrome *cbb*₃ oxidase complex

Cytochrome *cbb*₃ oxidases have been purified from several species of Proteobacteria including *P. denitrificans* (de Gier *et al.* 1996), *R. sphaeroides* (García-Horsman *et al.* 1994), *B. japonicum* (Preisig *et al.* 1996) and *P. stutzeri* (Urbani *et al.* 2001). Rather poor yields and a tendency for the complex to dissociate have made crystallization difficult and a structure for the *cbb*₃ oxidase is not available (Urbani *et al.* 2001; Geimeinhardt 2006). A schematic of the *cbb*₃ oxidase complex has however been suggested as shown in Fig. 1.6 (García-Horsman *et al.* 1994; Pitcher and Watmough 2004). It is assumed that the structural organization of the subunits of the *cbb*₃ oxidases is similar in all Proteobacteria.

CcoN

The catalytic subunit in all *cbb*₃ oxidases is homologous to SUI of the mammalian CcO and defines these oxidases as a member of the HCO super family (as discussed in section 1.3, Fig. 1.3). The *cbb*₃ operon gene product, CcoN, encodes for the catalytic subunit, SUI. (Preisig *et al.* 1993; García-Horsman *et al.* 1994; Pereira *et al.* 2001).

Hydropathy analysis of the CcoN sequence from *B. japonicum*, predicts a minimum of 12 transmembrane helices, which span the lipid membrane with both the N and C termini facing the cytoplasmic side of the membrane (Preisig *et al.* 1993). The six canonical amino acid residues which ligate the redox centres, the low-spin heme *b* and the high-spin heme *b*₃-Cu_B, are predicted to be located within the transmembrane helices (Zufferey *et al.* 1998; Oh 2006). The high-spin heme is axially coordinated by a single histidine and has one available coordination position providing the oxygen binding site. The Cu_B is ligated by three histidines and the second heme *b* is ligated by two histidines. The ligating histidines are strictly conserved in the CcoN subunit in all *cbb*₃ oxidases identified thus far (Fig 1.7) (Zufferey *et al.* 1998; Oh 2006). The terminal electron acceptor, oxygen, binds at the dinuclear centre of CcoN and the catalytic reaction performed by all terminal oxidases

under aerobic conditions, the reduction of di-oxygen to water, occurs at this site (Section 1.2, 1.3).

For each molecule of di-oxygen reduced by a CcO four protons are taken from the N-side of the cell membrane for the reduction of oxygen to water at the active site and another four protons are translocated across the membrane (Nicholls 2002; Wikstrom 2004). The active site of subunit I in HCOs is embedded deep within the protein to reduce the release of reactive oxygen species during the catalytic reaction (Pereira *et al.* 2001). A pathway for the protons required for the reaction spans the entire thickness of the membrane and is necessary to facilitate proton transfer across the membrane. In addition, because of the location of the oxygen-binding catalytic site in the membrane spanning part of the protein, a pathway is required for the transfer of substrate protons to the catalytic site.

The availability of the 3D structure of the bovine CcO revealed two potential proton uptake pathways within the enzyme, towards the buried heme a_3 -Cu_B active site where O₂ binds to heme a_3 (Tsukihara *et al.* 1995). Additionally there are good crystal structures of the bacterial aa_3 oxidase from *P. denitrificans* and *R. sphaeroides* (Iwata *et al.* 1995; Ostermeier *et al.* 1997; Svensson-Ek *et al.* 2002). Both of these bacterial oxidases are amenable to genetic manipulation leading to the production of informative mutant forms (Shapleigh *et al.* 1992; Svensson-Ek *et al.* 2002). The proton uptake pathways, the so called D and K channel have been further identified using the knowledge gleaned from mutagenesis experiments.

The D channel, leads from a conserved aspartate residue (D124 *P. denitrificans* numbering) on the cytoplasmic surface of subunit I to a proton accepting glutamate residue (E278 *P. denitrificans* numbering) near the active site (Ostermeier *et al.* 1997). The D pathway is utilized for the movement of all the pumped protons and some catalytic protons

(Brzezinski and Adelroth 2006). The second channel, the K channel, is so called after a conserved lysine residue (K354 *P. denitrificans* numbering) in the middle of the proton input channel. The K channel leads directly to the binuclear site in subunit I and translocates catalytic protons (Ådelroth *et al.* 1998). Both the D and K channels contain highly polar ionizable residues that guide the formation of hydrogen bonded water chains within the channels (Wraight 2006). These water chains electrostatically stabilize the transferred proton and assure kinetically competent proton transfer (Wraight 2006; Hemp *et al.* 2007). In the absence of this electrostatic stabilization provided by the protein, protons could be excluded from the water containing pores within the channel.

The D and K channels have been identified in various HCOs, however, amino acid sequence alignments of SUI indicate that the residues of these two channels are not common to all oxidases (Gomes *et al.* 2001; Pereira *et al.* 2001; Wikstrom and Verkhovsky 2007). The CcoN subunit of the *cbb*₃ oxidases, has a low degree of similarity, at the amino acid sequence level, with other members of the HCO family (Preisig *et al.* 1993; Sharma *et al.* 2006). The residues that form the proton channels in other members of the HCO family are not conserved in the CcoN subunit (Sharma *et al.* 2006) (Hemp *et al.* 2007). Proton translocation has however, been demonstrated in cell suspensions in which cytochrome *cbb*₃ oxidase is the only cytochrome *bc*₁ dependant oxidase present in the cytoplasmic membranes (Toledo-Cuevas *et al.* 1998). Moreover, cell suspensions of the cytochrome *cbb*₃ oxidase from *R. sphaeroides* and *P. denitrificans* have been shown to operate as a proton pump (de Gier *et al.* 1996; Toledo-Cuevas *et al.* 1998). Proton translocation from the cytoplasmic side of the inner membrane to the periplasmic space with a stoichiometry of 1 H⁺/e⁻ has been reported for both organisms. This is a slightly higher value than observed in purified cytochrome *cbb*₃ reconstituted into phospholipid vesicles, which varied between 0.2 H⁺/e⁻ and 0.4 H⁺/e⁻ (Arslan *et al.* 2000). The reconstituted *cbb*₃ oxidase does, however, have a substantially lower proton pumping activity than reconstituted *aa*₃

oxidase from *P. denitrificans* (Arslan *et al.* 2000). Experimental results therefore suggest that proton movement does occur during catalytic reactions in cytochrome *cbb*₃ oxidases (de Gier *et al.* 1996; Arslan *et al.* 2000). However, the absence of canonical proton pathway residues in CcoN suggests an alternative route to other CcOs.

Sequence analyses and homology modeling of the *cbb*₃ oxidase subunit, CcoN, from *Vibrio cholerae* and *R. sphaeroides* has been used to identify residues, which have homology to amino acid residues in other HCOs (Sharma *et al.* 2006; Hemp *et al.* 2007). In most HCOs, the D channel leads from an aspartate residue on the cytoplasmic side of subunit I to a proton accepting residue near the active site of SUI (Hemp *et al.* 2007). There are no conserved hydrophilic residues that could form a proton channel analogous to this D channel in the CcoN subunit (Hemp *et al.* 2007; Ozturk *et al.* 2007). The second proton channel in the HCOs, the K channel, leads from a glutamic acid residue near the interface of SUI and SUII on the cytoplasmic side of the membrane to a histidine-tyrosine cofactor. Sequence analysis indicates the conservation of some residues in the CcoN subunit which are spatially analogous to the K channel in other HCOs (Hemp *et al.* 2007; Ozturk *et al.* 2007). Hence, it is suggested that in the *cbb*₃ subunit CcoN, only one channel is used for the input of both catalytic and pumped protons.

In the canonical HCOs there is a fully conserved tyrosine residue (Tyr 244 *Bos taurus* numbering) within the active site of SUI that forms a covalent bond to one of the three histidine ligands of Cu_B (Buse *et al.* 1999; Rauhamaki *et al.* 2006). The cross-linked tyrosine-histidine dimer is at the end of K channel in HCOs and it is hypothesized to be of critical importance in the catalytic mechanism of SUI (Rauhamaki *et al.* 2006; Hemp *et al.* 2007). The tyrosine residue is hypothesized to donate a hydrogen atom (an electron plus a proton) during catalysis to facilitate cleavage of the O-O bond after O₂ binds to the reduced high-spin heme in SUI (Nyquist *et al.* 2003; Hemp *et al.* 2005). In the *cbb*₃ oxidases the

spatially equivalent tyrosine residue to other HCOs is missing but homology modeling has suggested that an alternative tyrosine residue (Tyr 311 *R. sphaeroides* numbering) replaces the missing tyrosine in the active site (Rauhamaki *et al.* 2006). This alternative residue (Y311) is fully conserved amongst the *cbb*₃ oxidases and site directed mutagenesis of Y311 in *R. sphaeroides* resulted in an inactive phenotype suggesting that Y311 fulfills a similar role to the tyrosine residue in the canonical HCOs (Rauhamaki *et al.* 2006). It has been hypothesized that only one channel, the K channel, is used for the input of catalytic and pumped protons in the CcoN subunit, however further evidence is necessary to confirm this proposal (Hemp *et al.* 2007). Confirmation of the presence of the modified tyrosine residue in the *cbb*₃ oxidase at the end of the proposed K channel in CcoN further supports this proposal (Rauhamaki *et al.* 2006).

Similarly to the *cbb*₃ oxidases, the residues that contribute to the D- and K- channels in subunit I of the HCO's are not conserved in the equivalent subunit, NorB of the cNOR nitric oxide reductase family (Thorndycroft *et al.* 2007). Five highly conserved glutamate residues have been identified in the NorB subunit of the cytochrome *c* and quinone dependant NORs (Butland *et al.* 2001; Thorndycroft *et al.* 2007). Using site directed mutagenesis Thorndycroft *et.al.* demonstrated that two of these conserved glutamate residues form the entrance to a proton conducting channel (Thorndycroft *et al.* 2007). The proposed function of this so called "E-channel" is to conduct protons from the periplasm to the active site of the enzyme during turnover (Thorndycroft *et al.* 2007). Based on homology to the proposed proton input channel in the cNOR family, a proton exit pathway for pumped protons has been proposed in the *cbb*₃ oxidases (Hemp *et al.* 2007).

.....MSPGN--ELHNYNTVVRQF

410 420 430 440 450 460 470 480 490 500

1NKYQTQKVMAMLY *Bradyrhizobium japonicum*
1MNYAAGTVLSGLGALFAVLLAGFSH--DELFRTHNVILFATLAIIFTILLNRNAD-YGLTPKKVQSTYNDGPIRYG *Brucella suis*
1MHPGN--ALNYDYTVAKYF *Campylobacter coli*
1MHPGN--YLYDYTVAKYF *Campylobacter jejuni*
1MQENV--PLSYDYTSKLF *Helicobacter pylori*
1METLN-OTQTYNYKVYRQF *Neisseria gonorrhoeae*
1MSTAI-SQTAYNYKVYRQF *Pseudomonas aeruginosa 1554*
1MSTTI-PELAYNYKVYRQF *Pseudomonas aeruginosa 1557*
1MLDTIKLIAIGTIAVLAIAAANYARPDOLAYLVNALIIMLAAGIMFLRVLRQMGNEQPALEPHPETQYMDQVYRAG *Paracoccus denitrificans*
401 WVNGITQGLMWRRAVHEDGTLTYSFVEALVASHPGFVYRFAGGVFLSGMLLNAYNTWRTYRVADERLALSARIAC.FETS **HODSI--ALNYDYTVAKYF** *Pseudomonas fluorescens*
1HSSFHPHLKFSQAVAKPY *Pseudomonas stutzeri*
1MSTTI-SPTAYNYRVYRQF *Pseudomonas syringae*
1MVDYVKLVALGVIALCAAIAANYAR--DLAYMNVNAYSVMLVAGGLFLWQVRRVG-DEYRDKPALQTEYMDGVIYRYG *Rhodobacter sphaeroides*
1NHHHSQPTGADYNYTIVYRQF *Shewanella oneidensis*
1MQHSQEKQLQNYNYTVYRQF *Vibrio cholerae*
1MQHSQVKQLQNYNYTVYRQF *Vibrio parahaemolyticus*

AIATVLVGGVGLVGVLIAAQLVWPDINFD---PYLTFGRIRPLHTNAVIFAAGGSGLFATSYVVVQRTCQTRIFGG---ALAAFTFVGWQAVIVLAA

510 520 530 540 550 560 570 580 590 600

13 FYGALTLFLAQLVGLLAGTIYVLPNTLS---TLLPFNIVRMINTN-ALIVWSLIGFNGATVFLIPEETEYELYSP---LAKIQFVMFFGAAGVAV *Bradyrhizobium japonicum*
74 VIATVFMGVVGFVGVLIAAQLVWPDINL---QPYFNFGRIRPVIHTSAVIFAAGGNALICSSFYVVQRTCARLIFGG---DLAMFVFMGYQLFIYMAA *Brucella suis*
18 MFATILFGIVGMAIGTLIAFQNAYPNLNYLAG--EYATFSRLRPLHTSGVIFGFNLSGIMATWYYIGQRVLKVSMAESKFLHAIQKLFHFLYNYITMIVAV *Campylobacter coli*
18 MFATILFGIVGMAIGTLIAFQNAYPNLNYLAG--EYATFSRLRPLHTSGVIFGFNLSGIMATWYYIGQRVLKVSMAESRFLHAIQKLFHFLYNYITMIVAV *Campylobacter jejuni*
18 LYANVGFGIIGMLIGVIAFAEISFSLNYIAG--EYGIIFGRIRPLHTNAVITGFTLGGVWASWYYIGQRVLKITVHQHPFLKIVGILLHFMWIIILLILGV *Helicobacter pylori*
19 AINTVVMGVVGMVGVVIAAQLVWPDINL---GPFNFGRIRPLHTNAVIFAAGGCGLIGTSYVVVQRTCNTLIFGG---VLPAAFTFVGWQAVIVAAV *Neisseria gonorrhoeae*
19 AVHTVVMGVVGMVGLGVLIAAQLVWPDINFD---LPWTSFGRIRPLHTNAVIFAAGGCA LFATSYVVVQRTCQARLISD---TLAAFTFVGWQAVIVGAV *Pseudomonas aeruginosa 1554*
19 AINTVVMGVVGMVGVVIAAQLVWPDINFD---LPWTSFGRIRPLHTNAVIFAAGGCA LFATSYVAVQRTCQARLISD---TLAAFTFVGWQAVIVLILAA *Pseudomonas aeruginosa 1557*
77 VIATAFMGVVGFVGVVIAFAEISFSLNYIAG--EYGTFSRLRPLHTNNGVVGFMNLSGITATWYYIGQRVLKVSMAESKFLHAIQKLFHFLYNYITMIVAV *Paracoccus denitrificans*
499 MFTTIIIFGIVGMAIGTLIAFQNAYPNLNYLAG--EYGTFSRLRPLHTNNGVVGFMNLSGITATWYYIGQRVLKVSMAESKFLHAIQKLFHFLYNYITMIVAV *Pseudomonas fluorescens*
20 FVFALILFVGQVLFGLINGLQVYVGDVFLF---PLLPFNIVRMINTN-LLIVWLLIFGFMGAAYLIPPEESOCCLHSP---KLAIIIFVFAAAGVLTIV *Pseudomonas stutzeri*
19 AINTVVMGVVGMVGLGVVIAAQLVWPDINL---LEWTFGRIRPLHTNLVIFAAGGCA LFATSYVVVQRTCQTRLISD---GLAAFTFVGWQAVIVGAV *Pseudomonas syringae*
74 VVATAFMGVVGFVGVVIAFAEISFSLNYIAG--EYATFSRLRPLHTSAVIFAAGGNALXATSYVVVQRTCQARLIFGG---NLGMFVFMGYNLFIYVMAA *Rhodobacter sphaeroides*
21 ALTTVLGGIVGMAVGVVIAAQLVWPDINFD---TPWFTYSRLRPLHTNAVIFAAGTSA LFATSYVVVQRTCQTRIFAP---KLAFTFVGWQAVIILSAA *Shewanella oneidensis*
22 TLYTILVGGIVGMAVGVVIAAQLVWPDINFD---TPWLTYSRLRPLHTNAVIFAAGTSA LFATSYVVVQRTCQTRIFGG---PLVPAFTFVGWQAVIIVSAA *Vibrio cholerae*
22 TLYTILVGGIVGMAVGVVIAAQLVWPDINFD---TPWLTYSRLRPLHTNAVIFAAGTSA LFATSYVVVQRTCQTRIFGG---PLVPAFTFVGWQAVIILAAA *Vibrio parahaemolyticus*

XSLPLGYTT-----SKEYAELEWPIDILXIVVAVAVVFFGTIVKRKEKHXYVANWFYGAFLTVAMLIHVNNMAYPVSLF-----KS

610 620 630 640 650 660 670 680 690 700

103 VGYLFHYHE.....GREFLEQPFITKVGIVVYCLMFLFNVTNTALKGRKTTVTNILLGLVGVATFFLFAFYH...PANLA.....Bradyrhizobium japonicum
166 TGYL LGITQ.....SREYAEP EWYVDIMLT IYVAVYL VVFMGTL LRKKEPHIYVANWFYLSFIITITIANLHIINMLAIPVSFLG----VKSS
116 ISL FAGYST.....SKEYAELEWPIOLIVLXVVLVGVVSIFGLIGIRREKTLYISLWYYIATFLGXIAML YLFNNMAYPT YFVAENGKVMHS
116 ISL FMGVTT.....SKEYAELEWPIOLIVLXVVLVGVVSIFGLIGIRREKTLYISLWYYIATFLGXIAML YLFNNMEYPT YFVTGMGKVMHS
116 ISL FAGLTQ.....SKEYAELEWPIOLIVVAVVVLVGVVNHFGSMSVRRRENTIYVSLWYYIATYVGIIVHYL FNNLSYPT YFVADMGSMHS
114 VSL FPMGVTQ.....GKEYAELEWPIOLITLYVAVAVIVFFGTIAKRKV KHIYVANWFYGGF ILAYALHIVNHSIPAGLM-----KS
112 LTL POGFTT.....SKEYAELEWPLAILLA IYVITVAVVFFGTIVKRKV KHIYVGNWFYGA FILVTAMHIVNHMSLPVSMF-----KS
112 ISLPLGYTS.....SKEYAELEWPIOLITVYVAVAVVFFGTIVKRKV KHIYVGNWFYGGF ILYTAMHIVNML ELPVIT-----KS
112 Pseudomonas aeruginosa 1557
273 TGYL LGATQ.....SKEYAELEWYVDIMLT IYVAVYL VVFMGTL LRKKEPHIYVANWFYLSFIIVTITIANLHIIVNMLAIPVSFLG----SKSS
Paracoccus denitrificans
597 VSL FAGLST.....SKEYAELEWPIOLIVVAVVVLVGVVSIFGLIGIRREKTLYISLWYYIATFLGXIAML YLFNNMEYPT RLVS GMGSMHS
Pseudomonas fluorescens
110 LGYLFVPPYAAEAENTRNDLLPTMGR EFLLEQPTITKIGIVVYALGFLYHIGMTHLGRKTYVSTYMMTGLIGLAVFFLFAFYH...PERLS.....Pseudomonas stutzeri
112 VTLP MGVTQ.....TKEYAELEWPIVAILLA IYVAVAVVFFGTIVKRRT RHIVVANWFYGA FIVVTGMHIVNHSIPVSLF-----KS
Pseudomonas syringae
169 QSYL LGATQ.....SKEYAELEWYLDIMLT IYVAVYL VVFMGTL LRKKEPHIYVANWFYLSFIIVTITIANLHIIVNMLAIPVSFLG----SKSS
Rhodobacter sphaeroides
114 ITLP MGYS.....GKEYAELEWPIOLIT IYVAVAVIVFFGTIAKRRT SHIYVANWFYGA FIIIVAVLHIVNSMAYPVSLF-----KS
Shewanella oneidensis
115 ITLP LGYS.....GKEYAELEWPIOLIT IYVAVAVVFFGTIVKRRT SHIYVANWFYGA FIIITVAVLHIVNSMAYPVSMG-----KS
Vibrio cholerae
115 ISLPLGFTS.....GKEYAELEWPIOLIT IYVAVAVVFFGTIVKRRT SHIYVANWFYGA FIIITVAVLHIVNSMAYPVSLG-----KS
Vibrio parahaemolyticus

YSNYAGAYDANYQWVYGHNAVGFLLTAGFLGMNYYFVPKQA--ERPVSYSRLSIVHFVALIFLYIWAGPHHLHYTALPDWAQSLGNVFSLVLIAPSVGGM

710 720 730 740 750 760 770 780 790 800

126 -----YOKHYVYVYVHLWV EGVWELIHASVLA YLNIK LHGIDREVVEKWL YVIIGLAL FSGILGTG--HFFYVIGAP GYVQVIGSLFSTLEVAPFFFTMV Bradyrhizobium japonicum
247 YSAFAGYQDAVYQWYGHNAVAFELTVPFLAMHYYFVPKQA--NRPVYSYRLSIVHFVMSIFLYIWAGPHHLHYTAVPDWAQTLGNVFSIMLWHP SVGGM
Brucella suis
202 VSNYAGTNOALVQWYGHNAVAFVFTVGIIAQIYVFLPKES--GQPIFSYKLSLFAFWGLMFVYLVWAGGHLLIYSTVPDWMQTMG SVF SVVLXLP SVGSA
Campylobacter coli
202 VSNYAGTNOALVQWYGHNAVAFVFTVGIIAQIYVFLPKES--GQPIFSYKLSLFAFWGLMFVYLVWAGGHLLIYSTVPDWMQTMG SVF SVVLXLP SVGSA
Campylobacter jejuni
202 ISKYSGSNOALIQWYGHNAVAFVFTVGIIAQIYVFLPKES--GQPIFSYKLSLFAFWGLMFVYLVWAGGHLLIYSTVPDWMQTLSSVFSVVLXLP SVGTA
Helicobacter pylori
193 YPYYSGAIDANYQWYGHNAVGFLLTAGFLGMNYYFVPKQA--ARPVYSYRLSIVHFVMSIFLYIWAGPHHLHYTALPDWTQSLGNVMSLILFAP SVGGM
Neisseria gonorrhoeae
191 YSAYSGATDANYQWYGHNAVGFLLTAGFLGMNYYFVPKQA--ERPVSYSRLSIVHFVMSIFLYIWAGPHHLHYTALPDWAQSLGNVMSLILLAP SVGGM
Pseudomonas aeruginosa 1557
191 YSLYAGATDANYQWYGHNAVGFLLTAGFLGMNYYFVPKQA--ERPVSYSRLSIVHFVMSIFLYIWAGPHHLHYTALPDWAQSLGNVMSLILLAP SVGGM
Paracoccus denitrificans
254 VQLFSGYQDANTQWYGHNAVGFLLTAGFLGMNYYFVPKQA--ERPVSYSRLSIVHFVMSIFLYIWAGPHHLHYTALPDWAQSLGNVFSIILWHP SVGGM
Pseudomonas fluorescens
603 VSNYAGSNOALVQWYGHNAVAFVFTVGIIAQIYVFLPKES--GQPIFSYKLSLFAFWGLMFVYLVWAGGHLLIYSTVPDWMQTMG SVF SVVLXLP SVGSA
Pseudomonas stutzeri
197 -----ROKFWYVYVYVHLWV EGVWELIHASVLA YLNIK LHGIDREVVEKWL YVIIGLAL FSGILGTG--HFFYVIGAP TVWLWVGSIFSALEPLPFFAMV
Pseudomonas stutzeri
191 YSAFAGATDANTQWYGHNAVGFLLTAGFLGMNYYFVPKQA--ERPVSYSRLSIVHFVMSIFLYIWAGPHHLHYTALPDWAQSLGNVMSLILLAP SVGGM
Pseudomonas syringae
250 VQYFSGYQDANYQWYGHNAVGFLLTAGFLGMNYYFVPKQA--ERPVSYSRLSIVHFVMSIFLYIWAGPHHLHYTALPDWTQSLGNVFSIMLWHP SVGGM
Rhodobacter sphaeroides
193 YSNYS GAVDANYQWYGHNAVGFLLTAGFLGMNYYFVPKQA--GRPVSYSRLSIVHFVMSIFLYIWAGPHHLHYTALPDWTQSLGNVMSLILFAP SVGGM
Shewanella oneidensis
194 YSAYAGAYDANYQWYGHNAVGFLLTAGFLGMNYYFVPKQA--ERPVSYSRLSIVHFVMSIFLYIWAGPHHLHYTALPDWTQSLGNVMSLVL FAP SVGGM
Vibrio cholerae
194 YSAYSGAVDANYQWYGHNAVGFLLTAGFLGMNYYFVPKQA--ERPVSYSRLSIVHFVMSIFLYIWAGPHHLHYTALPDWTQSLGNVMSLVL FAP SVGGM
Vibrio parahaemolyticus

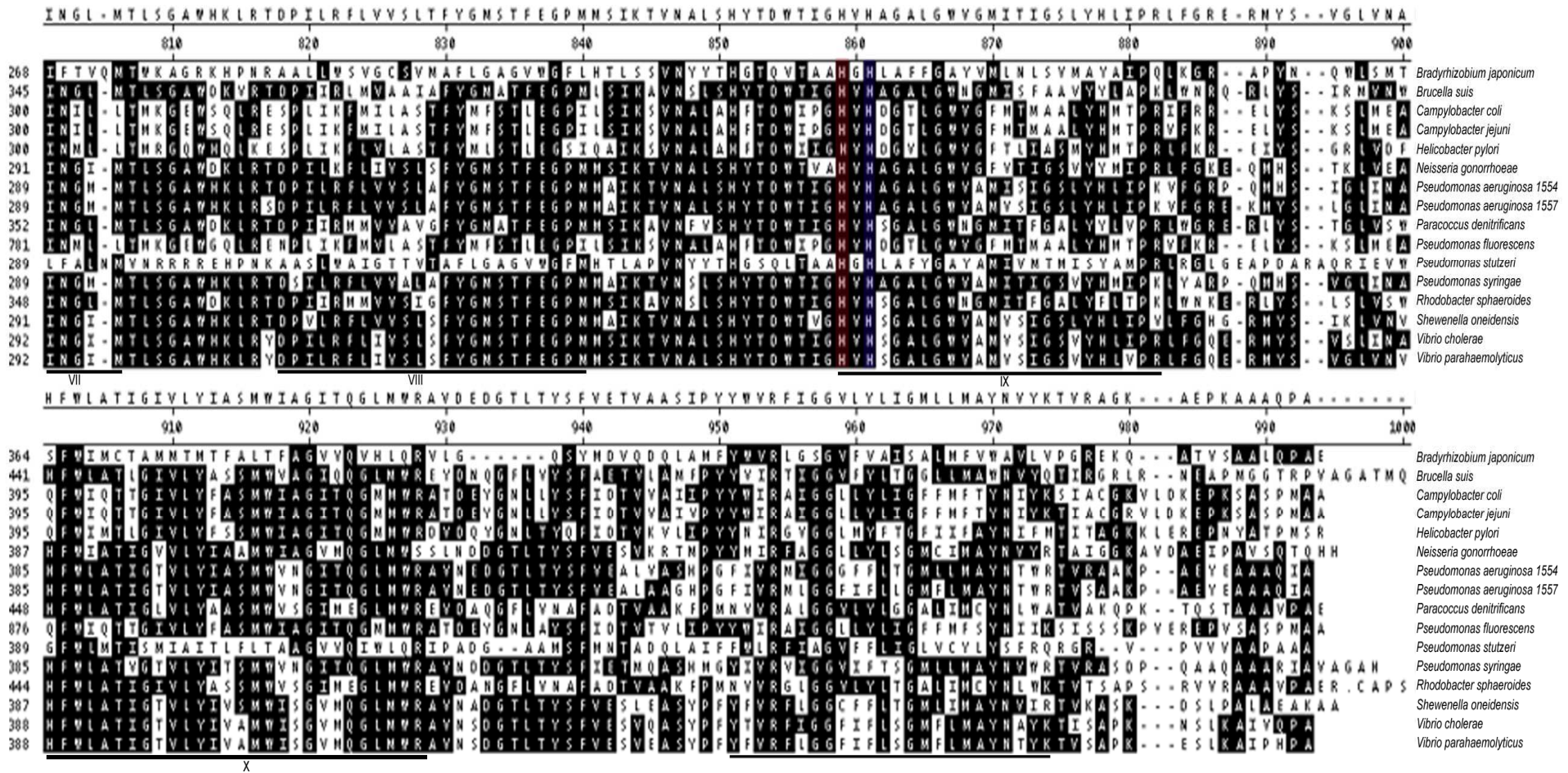


FIG. 1.7 Multiple Sequence alignment of CcoN from ten species. The histidine residues which are predicted to ligate the low-spin and high-spin hemes are coloured blue and red respectively. The histidine residues that ligate the Cu_B site are coloured green. Since the completion of this thesis, the genomic sequence of *P.stutzeri*

has identified two putative *ccb* operons (Yan *et al.* 2008). This alignment refers to CcoN PST 1840.

CcoO

The *ccoO* gene encodes a membrane anchored mono heme cytochrome *c* (Preisig *et al.* 1993). Based on hydropathy analysis, this subunit has a single membrane spanning transmembrane helix near its N-terminus and a hydrophilic domain, which is exposed to the periplasmic side. There is a single CXXCH motif in this hydrophilic domain, which is indicative of a heme *c* binding site (Thöny-Meyer *et al.* 1994). The two cysteines form thioether bonds with the vinyl side chains of the protoheme, and the histidine provides the fifth axial ligand of the heme iron. Previous MCD analysis of *P. stutzeri* cytochrome *cbb*₃ oxidase suggested that the four low-spin hemes in the *cbb*₃ complex are His/His and His/Met coordinated low-spin ferric hemes in a 2:2 ratio (Pitcher 2002). Further MCD analysis of the isolated subunit CcoP suggests that His/His and His/Met ligate the two *c* type hemes in this subunit (Pitcher 2002). The second His/His ligated species observed in the MCD analysis of the complex was assigned to the *b* type heme in CcoN. MCD analysis of the *cbb*₃ oxidase complex therefore infers that the single *c* type heme in CcoO is ligated by a histidine and a methionine in the proximal and distal positions respectively. In the subunit CcoO there is only one fully conserved methionine (M137, *P. stutzeri* numbering) which is therefore predicted to be the sixth ligand to the *c* type heme in this subunit (Fig. 1.8). Confirmation of the hypothesis was attempted during this study using site directed mutagenesis, however the mutagenesis was unsuccessful and due to time constraints was not the focus of this study.

The function of the subunit CcoO is unclear, however it is predicted to be a requirement for assembly and stability of the *cbb*₃ oxidase (Thöny-Meyer *et al.* 1996; Zufferey *et al.* 1996). CcoO has little homology to subunits from other HCO with the exception of NorC a membrane bound cytochrome *c* subunit of the enzyme nitric oxide reductase (NOR), also a member of the HCO superfamily (Preisig *et al.* 1993; Cheesman *et al.* 1998; Sharma *et al.* 2006). Similarly to *cbb*₃ oxidases the enzyme NOR lacks a Cu_A containing electron

receiving domain and NorC had been established as the electron receiving domain of this enzyme (Saraste and Castresana 1994; Thorndycroft *et al.* 2007). Using sequence analogy, it can therefore be hypothesized that the subunit CcoO fulfills the role of electron receiving domain in the *cbb*₃ oxidase. In further support of this theory it has been demonstrated that, the CcoNO subcomplexes isolated from the organisms *P. denitrificans* and *B. japonicum* are both catalytically competent (de Gier *et al.* 1996; Zufferey *et al.* 1996). Topological predictions of the membrane bound subunit CcoO suggests that the *c* type heme is in the periplasmic domain close to the aqueous medium. The heme in CcoO could therefore potentially accept electrons from either cupredoxins or the water soluble cytochrome *c*.

CcoQ

The *CcoQ* gene is predicted to encode a small membrane bound polypeptide (Preisig *et al.* 1993). The CcoQ subunit is the smallest of the *cbb*₃ oxidase, consisting of between 48 and 73 amino acids depending on the organism (Thöny-Meyer *et al.* 1994; Zufferey *et al.* 1996; Pitcher 2002). This subunit has a hydrophobic region near the N terminus and a polar motif at the C terminus and is predicted to be located within the plasma membrane (Thöny-Meyer *et al.* 1994).

Sequence alignments of CcoQ have shown that this subunit does not contain any cofactor binding motifs and shows no similarity to proteins of known function (Toledo-Cuevas *et al.* 1998). The function of this subunit remains unclear, however, in frame deletion of the *CcoQ* gene in *R. sphaeroides* has suggested that CcoQ protects the *cbb*₃ complex from oxidative destabilization in the presence of oxygen (Oh and Kaplan 2002; Oh 2006).

MKF-----HEILEKENVGLLAVFHVLVVSIIGGLVETVPLFFQDATIEPVEGMKPYTAL ELAGRDIIYIREGCYVCHSQMIRPFRAETER YGHYSVAGESVYD Majority

10 20 30 40 50 60 70 80 90 100

1	MSEWTR--	HQVEEKN	SITLIV	GIILV	IAIGGL	VEIT	PLFY	LKST	IEKY	DGVR	PYTP	LELAGR	RVYV	REGCY	U	CHSQ	MIRP	LRDE	EYER	YGHF	SLAA	ESM	FD	<i>Bradyrhizobium japonicum</i>	
1	MSILKN--	HSKLEKN	ATLLI	ASLAV	VTVGG	LVEIT	PLFY	LENT	IEKY	VEGR	HRPYS	PLELAGR	DIYV	REGCY	U	CHSQ	MIRP	FRDE	EYER	YGHY	SLAA	ESM	YD	<i>Brucella suis</i>	
1	-MF----	SWLEKN	PPFFA	VAVFI	VIAYAG	ITIEV	PLFA	ENAR--	PIEG	KRPY	TV	LQLAGR	DIYI	KDSC	NA	CHSQ	LIRP	FKSE	TD	RYGM	YSV	SGE	FAYD	<i>Campylobacter coli</i>	
1	MSIWKH--	HAKFER	HSLL	VVGI	LVSIG	GLVEIT	PLFW	LQGT	IEKY	DGVR	TYTP	LELAGR	DIYV	REGCY	U	CHSQ	MIRP	LRDE	EYER	YGHY	SLAA	ESM	YD	<i>Campylobacter crescentus</i>	
1	-MF----	SWLEKN	PPFFA	VAVFI	VIAYAG	ITIEV	PLFA	ENAR--	PIEG	KRPY	TV	LQLAGR	DIYI	KDSC	NA	CHSQ	LIRP	FKSE	TD	RYGM	YSV	SGE	FAYD	<i>Campylobacter fetus</i>	
1	-MF----	SWLEKN	PPFFA	VAVFI	VIAYAG	ITIEV	PLFA	ENAR--	PIEG	KRPY	TV	LQLAGR	DIYI	KDSC	NA	CHSQ	LIRP	FKSE	TD	RYGM	YSV	SGE	FAYD	<i>Campylobacter jejuni</i>	
1	-MF----	SFLEKN	PPFFT	LAFIF	VATAG	LVEIT	PLFF	KSAR--	PIEG	LRPY	TV	LETAG	VDIY	IQEG	Y	CHSQ	LIRP	FQAE	Y	DRYG	AYSL	SGE	FAYD	<i>Neisseria gonorrhoeae</i>	
1	MK-----	LQQLAE	EKIGV	LIVFT	LVSIG	GLVEIT	PLFA	TKAAT	Q	PAPG	VKPY	NALQ	VAGR	DIYI	REGC	YN	CHSQ	MIRP	FRAE	ETER	YGHY	SVAG	ESVYD	<i>Pseudomonas aeruginosa 1556</i>	
1	MK-----	HEILEKN	VGLL	ALCM	AVAVS	IGGLT	QIVP	LFQD	V	TNT	PVEG	MKPY	TALQ	LEGR	DIYI	REGC	Y	CHSQ	MIRP	FRAE	ETER	YGHY	SVAG	ESVYD	<i>Pseudomonas aeruginosa 1553</i>
1	MKN-----	HEILEKN	VGLL	ALCM	AVAVS	IGGLT	QIVP	LFQD	V	TNT	PVEG	MKPY	TALQ	LEGR	DIYI	REGC	Y	CHSQ	MIRP	FRAE	ETER	YGHY	SVAG	ESVYD	<i>Paracoccus denitrificans</i>
1	MAILEK--	HKYLEKN	ATLLI	VVGI	LVSIG	GLVEIT	PLFY	LQNT	IEKY	DGVR	TYTP	LELAGR	DIYV	REGCY	U	CHSQ	MIRP	MRDE	EYER	YGHY	SLAA	ESM	YD	<i>Pseudomonas fluorescens</i>	
1	MK-----	HEILEKN	VGLL	ALCM	AVAVS	IGGLT	QIVP	LFQD	V	TNT	PVEG	MKPY	TALQ	LEGR	DIYI	REGC	Y	CHSQ	MIRP	FRAE	ETER	YGHY	SVAG	ESVYD	<i>Pseudomonas syringae</i>
1	MKN-----	HEILEKN	VGLL	ALCM	AVAVS	IGGLT	QIVP	LFQD	V	TNT	PVEG	MKPY	TALQ	LEGR	DIYI	REGC	Y	CHSQ	MIRP	FRAE	ETER	YGHY	SVAG	ESVYD	<i>Pseudomonas syringae</i>
1	MK-----	HDVLEKN	IGLLA	IFMVA	ISIGGL	TQIV	PLFF	QD	V	TNQD	PIEG	MKPR	SAL	VEGR	DIYI	ANGC	Y	CHSQ	MIRP	LRAE	ETER	YGHY	SVAG	ESVYD	<i>Rhodobacter sputingae</i>
1	MSIMDK--	HHVLEKN	ATLLI	IFAVI	VITIG	GLVEIT	PLFY	LEN	IEKY	VEGR	HRPYS	PLELAGR	DIYI	REGC	Y	CHSQ	MIRP	MRDE	EYER	YGHY	SLAA	ESM	YD	<i>Rhodobacter capsulatus</i>	
1	MGILAK--	HKILET	NATLL	IFVFI	VITIG	GLVEIT	PLFY	LEN	IEKY	VEGR	HRPYS	PLELAGR	DIYI	REGC	Y	CHSQ	MIRP	MRDE	EYER	YGHY	SLAA	ESM	YD	<i>Rhodobacter sphaeroides</i>	
1	MKFN----	HEILEKN	IGLLA	IFMVA	ISIGGL	TQIV	PLFF	QD	V	TNQD	PIEG	MKPR	SAL	VEGR	DIYI	ANGC	Y	CHSQ	MIRP	LRAE	ETER	YGHY	SVAG	ESVYD	<i>Shewenella oneidensis</i>
1	MSSNSNRR	HEILEKN	VGLL	ALCM	AVAVS	IGGLT	QIVP	LFQD	V	TNT	PVEG	MKPY	TALQ	LEGR	DIYI	REGC	Y	CHSQ	MIRP	FRAE	ETER	YGHY	SVAG	ESVYD	<i>Vibrio cholerae</i>
1	MSNNSNRR	HEILEKN	VGLL	ALCM	AVAVS	IGGLT	QIVP	LFQD	V	TNT	PVEG	MKPY	TALQ	LEGR	DIYI	REGC	Y	CHSQ	MIRP	FRAE	ETER	YGHY	SVAG	ESVYD	<i>Vibrio parahaemolyticus</i>

HPFLVGSKRTGPDLARVGGGRYSDDWHR AHL LNPRSVVPE S IMPAYPWLAENKLOGKTTAAKMKTLR -TVG-----VPTYDDEDIAGAGA DVEAQA-----

110 120 130 140 150 160 170 180 190 200

99	HPFQMGSKRTGPD	LARVGG	AKYS	DDW	HV	T	H	L	T	N	P	R	A	V	P	Q	S	V	M	P	G	V	P	L	S	A	T	E	V	D	P	T	I	A	D	H	M	R	T	L	R	-	T	V	G	-----	V	P	Y	T	D	E	D	I	A	G	A	G	A	D	V	E	A	Q	A	-----	<i>Bradyrhizobium japonicum</i>							
99	HSFQMGSKRTGPD	LARVGG	RYSD	EW	HV	Q	H	L	V	R	P	R	D	V	P	E	S	V	M	P	S	V	A	F	L	K	E	R	P	L	K	A	D	O	I	A	A	H	L	K	A	N	V	-	A	V	G	-----	V	P	Y	T	Q	E	M	I	D	K	A	L	D	D	L	H	A	Q	A	T	P	-	D	A	-----	<i>Brucella suis</i>
92	RPFLMGSKRTGPD	LARVGN	YRT	D	W	H	E	N	H	M	D	P	V	S	V	P	N	S	I	M	P	A	Y	K	H	M	F	K	N	A	O	M	E	T	A	Y	A	E	A	L	T	V	K	K	V	F	N	-----	V	P	Y	D	T	E	N	G	T	K	L	G	T	W	E	E	A	Q	A	E	I	K	A	E	-----	<i>Campylobacter coli</i>
99	HPFQMGSKRTGPD	LARVGG	KYS	D	W	H	R	D	H	L	I	D	P	R	S	V	P	E	S	V	M	P	P	K	F	L	A	T	N	O	L	O	Y	S	D	I	A	D	R	M	E	A	Q	-	T	V	G	-----	V	P	Y	T	A	D	Q	T	N	A	K	D	L	E	A	Q	A	D	P	F	S	T	-----	<i>Campylobacter crescentus</i>		
92	RPFLMGSKRTGPD	LARVGN	YRT	D	W	H	E	N	H	M	D	P	V	S	V	P	N	S	I	M	P	A	Y	K	H	M	F	K	N	A	O	M	E	T	A	Y	A	E	A	L	T	V	K	K	V	F	N	-----	V	P	Y	D	A	E	D	M	P	K	L	G	T	W	E	A	T	Q	A	N	V	K	E	E	-----	<i>Campylobacter fetus</i>
92	RPFLMGSKRTGPD	LARVGN	YRT	D	W	H	E	N	H	M	D	P	V	S	V	P	N	S	I	M	P	A	Y	K	H	M	F	K	N	A	O	M	E	T	A	Y	A	E	A	L	T	V	K	K	V	F	N	-----	V	P	Y	D	A	E	N	G	T	K	L	G	S	W	E	D	A	Q	A	E	V	K	A	E	-----	<i>Campylobacter jejuni</i>
92	RPFLMGSKRTGPD	LARVGN	YRT	D	W	H	E	N	H	M	D	P	V	S	V	P	N	S	I	M	P	A	Y	K	H	M	F	K	N	A	O	M	E	T	A	Y	A	E	A	L	T	V	K	K	V	F	N	-----	V	P	Y	D	T	E	N	G	Y	K	L	G	S	V	E	E	A	K	K	A	Y	L	E	E	-----	<i>Neisseria gonorrhoeae</i>
96	HPFQMGSKRTGPD	LARVGG	RYSD	EW	H	R	I	H	L	N	P	R	D	V	P	E	S	N	M	P	A	F	P	W	L	A	R	N	K	Y	D	V	D	A	T	V	A	N	M	A	L	R	-	K	V	G	-----	T	P	Y	S	D	E	E	I	A	K	A	P	E	A	L	N	K	S	-	-----	<i>Pseudomonas aeruginosa 1556</i>						
95	HPFLMGSKRTGPD	LARVGS	RYSD	D	W	H	R	A	H	L	N	P	R	N	V	P	E	S	K	M	P	A	Y	P	W	L	V	E	N	K	L	O	G	K	D	I	E	K	K	L	E	V	M	R	-	T	L	G	-----	V	P	Y	T	D	E	D	I	K	G	A	K	D	S	L	K	G	K	-	-----	<i>Pseudomonas aeruginosa 1553</i>				
96	HPFLMGSKRTGPD	LARVGG	RYSD	EW	H	R	A	H	L	N	P	R	N	V	P	E	S	N	M	P	A	F	P	W	L	V	E	N	K	L	O	G	K	D	T	A	T	K	M	E	V	L	R	-	K	L	G	-----	V	P	Y	T	D	E	D	I	A	G	A	R	E	A	V	K	-----	<i>Paracoccus denitrificans</i>								
99	HPFQMGSKRTGPD	LARVGG	RYSD	EW	H	D	H	L	V	D	P	A	V	P	E	S	I	M	P	K	Y	G	L	N	R	Q	V	D	A	S	N	M	Q	R	L	K	T	D	A	-	L	G	G	-----	V	P	Y	D	D	A	M	I	A	A	G	E	D	F	R	V	Q	A	A	P	-	D	A	-----	<i>Pseudomonas fluorescens</i>					
95	HPFLMGSKRTGPD	LARVGG	RYSD	EW	H	R	A	H	L	N	P	R	N	V	P	E	S	N	M	P	A	F	P	W	L	V	E	N	K	L	O	G	K	D	T	A	T	K	M	E	V	L	R	-	K	L	G	-----	V	P	Y	T	D	E	D	I	A	G	A	T	A	T	L	K	G	K	-	-----	<i>Pseudomonas stutzeri</i>					
96	HPFLMGSKRTGPD	LARVGG	RYSD	EW	H	R	A	H	L	N	P	R	N	V	P	E	S	N	M	P	A	F	P	W	L	V	E	N	K	L	O	G	K	D	T	A	K	M	S	A	L	R	-	M	L	G	-----	V	P	Y	T	E	E	D	I	A	G	A	R	D	A	V	R	G	K	-	-----	<i>Pseudomonas syringae</i>						
95	HPFLMGSKRTGPD	LARVGG	RYSD	EW	H	R	V	H	L	N	P	R	D	V	P	E	S	T	S	I	M	P	A	Y	P	L	A	E	R	K	I	D	S	T	Q	T	A	K	K	L	Q	V	L	R	-	T	L	G	-----	T	P	Y	T	D	A	D	I	A	G	E	A	A	V	Q	G	K	-	-----	<i>Pseudomonas syringae</i>					
99	RPFLMGSKRTGPD	LARVGG	RYSD	EW	H	V	E	H	L	I	N	P	Q	S	V	P	E	S	V	M	P	K	Y	G	L	A	K	V	P	L	O	S	S	H	T	E	T	K	L	M	R	-	T	L	G	-----	V	P	Y	T	D	E	I	A	G	A	T	A	T	L	K	G	K	-	-----	<i>Rhodobacter capsulatus</i>								
99	HPFQMGSKRTGPD	LARVGG	RYSD	EW	H	D	H	L	V	D	P	A	V	P	E	S	I	M	P	K	Y	G	L	N	R	Q	V	D	A	S	N	M	Q	R	L	K	T	D	A	-	L	G	G	-----	V	P	Y	D	D	A	M	I	A	A	G	E	D	F	R	V	Q	A	A	P	-	D	A	-----	<i>Rhodobacter sphaeroides</i>					
97	HPFLMGSKRTGPD	LARVGG	RYSD	EW	H	R	V	H	L	I	N	P	R	D	V	P	E	S	N	M	P	A	F	P	W	L	V	E	N	K	L	O	G	K	D	T	A	K	M	S	A	L	R	-	M	L	G	-----	V	P	Y	T	E	E	D	I	A	G	A	R	D	A	V	R	G	K	-	-----	<i>Rhodobacter sphaeroides</i>					
101	HPFLMGSKRTGPD	LARVGG	RYSD	EW	H	R	V	H	L	N	P	R	D	V	P	E	S	N	M	P	A	F	P	W	L	V	E	N	K	L	O	G	K	D	T	A	K	M	S	A	L	R	-	M	L	G	-----	V	P	Y	T	D	E	D	I	A	G	A	T	A	T	L	K	G	K	-	-----	<i>Shewenella oneidensis</i>						
101	HPFLMGSKRTGPD	LARVGG	RYSD	EW	H	R	V	H	L	N	P	R	D	V	P	E	S	N	M	P	A	F	P	W	L	V	E	N	K	L	O	G	K	D	T	A	K	M	S	A	L	R	-	M	L	G	-----	V	P	Y	T	D	E	D	I	A	G	A	T	A	T	L	K	G	K	-	-----	<i>Vibrio cholerae</i>						
101	HPFLMGSKRTGPD	LARVGG	RYSD	EW	H	R	V	H	L	N	P	R	D	V	P	E	S	N	M	P	A	F	P	W	L	V	E	N	K	L	O	G	K	D	T	A	K	M	S	A	L	R	-	M	L	G	-----	V	P	Y	E	D	E	T	I	A	N	A	K	E	V	E	G	K	-	-----	<i>Vibrio parahaemolyticus</i>							



FIG. 1.8 Multiple sequence alignments of CcoO. Conserved residues are shaded black. Predicted transmembrane segments are underlined.

The predicted heme c binding sites are coloured red. The predicted distal heme residue, Met137, (P. stutzeri numbering) is highlighted in blue.

Since the completion of this thesis, the genomic sequence of *P.stutzeri* has identified two putative *cbb*₃ operons (Yan *et al.* 2008). This alignment refers to CcoO PST 1839.

The subunit CcoQ has also been proposed to transduce an inhibitory signal, related to electron flow through the *cbb*₃ oxidases, to the PrrBA two component system (Oh and Kaplan 1999). The CcoQ subunit does not however contain any redox active cofactors that could sense electron flow (Toledo-Cuevas *et al.* 1998; Oh and Kaplan 1999). This subunit would therefore have to respond to a change in the environment that was sensed elsewhere in the *cbb*₃ complex. The evidence that the heme content in the subunit CcoP is affected by deletion of *CcoQ* suggests a connection between the two subunits CcoQ and CcoP (Oh and Kaplan 2002). In biological heme based sensors, a regulatory heme-binding domain or subunit controls a neighboring transmitter region of the same protein (Gilles-Gonzalez and Gonzalez 2005). It could be speculated that the subunits CcoP and CcoQ act cooperatively as a heme based sensor. Two component systems, heme based sensors and the potential role of the subunits CcoQ and CcoP in this system will be discussed in more detail in section 1.10 and 11.

CcoP

The *CcoP* gene encodes a membrane bound diheme cytochrome *c*. This subunit has a putative hydrophobic transmembrane helix near its N terminus and similarly to CcoO, a hydrophilic domain which, based on hydropathy analysis, is exposed to the periplasmic side. There are two cytochrome *c* binding CXXCH motifs in the hydrophilic domain of this subunit which are indicative of two heme *c* binding sites (Thöny-Meyer *et al.* 1994). The two cysteines form thioether bonds with the vinyl side chains of the protoheme, and the histidines provides the fifth axial ligand of the heme iron. It is not known which residues provides the sixth ligand to the heme irons in CcoP but they are predicated to be a histidine and a methionine (Pitcher 2002). MCD analysis of the isolated CcoP subunit suggests that one of the *c* type hemes is His/His ligated and one is His/Met ligated. As in the subunit CcoO it is unconfirmed which specific residues provide the sixth ligands to the heme irons but these are predicated to be the fully conserved histidine His42 and the fully conserved

methionine, Met272 based on the proximity of surrounding proline residues (Fig. 1.9) (Pitcher 2002; Yan *et al.* 2008).

The function of CcoP is not clear, however it is possible that the presence of this subunit is not required for catalytic activity of the *cbb*₃ oxidase. In the *B. japonicum* *cbb*₃ oxidase, the *fixP::aphII* insertion mutant had a slightly higher oxidase activity than the Δ *fixN* and the Δ *fixO* deletion mutant. (Zufferey *et al.* 1996). Furthermore, deletion of CcoP from the *cbb*₃ complex does not appear to affect the stability of the subunits CcoN and CcoO in microaerobically grown cells (Zufferey *et al.* 1996).

It was previously observed that the oxygen analogue, carbon monoxide (CO) bound to one of the *b*-type hemes in CcoN in *R. capsulatus* and *B. japonicum* (Gray *et al.* 1994; Preisig *et al.* 1996). CO binding was presumed to bind at the high-spin heme in CcoN as this is the site of oxygen binding during the catalytic reduction of oxygen to water. It was however, also speculated that in *B. japonicum* CO bound to one of the *c*-type heme in CcoP or CcoO (Preisig *et al.* 1996). Carbon monoxide binding provides the most convenient method for distinguishing heme proteins in which the iron has an absent or replaceable sixth ligand, which bind CO, from those in which all ligands are stable, which do not bind CO (Wood 1984). Using the *cbb*₃ oxidase isolated from *P. stutzeri*, Pitcher *et al.* confirmed the hypothesis that CO binds to one of the *c*-type hemes in the *cbb*₃ oxidase (Pitcher *et al.* 2003). In contrast, the *cbb*₃ oxidase purified from *P. denitrificans*, which loses the CcoP subunit during purification, does not bind CO to a *c*-type heme (de Gier *et al.* 1996; Pitcher *et al.* 2002).

To further investigate the observation that CO binds to one of the *c*-type hemes in the *cbb*₃ oxidase CcoP was isolated from the *P. stutzeri* *cbb*₃ oxidase complex (Pitcher *et al.* 2002; Pitcher *et al.* 2003). It was recognized that the stoichiometry of CO binding to the hemes in

the separately expressed CcoP subunit was 1:1, but only following full reduction with sodium dithionite (Pitcher *et al.* 2003). UV-visible and MCD spectroscopy of the isolated CcoP subunit indicate that both *c*-type hemes are low-spin, therefore suggesting that one of the ligands to the *c*-type heme which binds CO is displaced to bind the exogenous ligand (Pitcher *et al.* 2002). Upon addition of CO, the complex that is formed with the *c*-type heme contains an Fe(II)-CO bond that is photo-labile (Pitcher *et al.* 2003). Transient illumination of the His-Fe (II)-CO species in the CcoP subunit leads to photolysis of the Fe(II)-CO species resulting in a pentacoordinate species, which can undergo competing reactions (Pitcher *et al.* 2003). Either the pentacoordinate species can react with the endogenous ligand to yield a six-coordinate ferrous heme or it can recombine with CO. The CO recombination kinetics displayed by some plant hexa-hemoglobins (Hbs) involved in physiological stress responses such as hypoxia are similar to those of displayed by CcoP (Hargrove 2000; Hebelstrup *et al.* 2007).

Many proteins with hexacoordinate heme irons function in reversible binding of ligands rather than transfer of electrons (Gilles-Gonzalez and Gonzalez 2005). For example, the *E. coli* protein *EcDos*, and the protein CcoA isolated from *Rhodospirillum rubrum* (Delgado-Nixon *et al.* 2000; Ibrahim *et al.* 2006). These proteins are classed as heme based sensors, a group of proteins, which are the important regulators of adaptive responses to fluctuating oxygen, carbon monoxide and nitric oxide levels (Gilles-Gonzalez and Gonzalez 2005). In heme based sensors, the distal ligand is displaced to bind an exogenous ligand and a conformational switch of the protein upon binding of its signal ligand is a common observation in this group of proteins (Delgado-Nixon *et al.* 2000; Hargrove 2000; Youn *et al.* 2003; Gilles-Gonzalez and Gonzalez 2005; Ibrahim *et al.* 2006). Displacement of a protein residue and consequential binding of an exogenous ligand is a very direct and straightforward way for ligand binding to induce a conformational change in the protein (Delgado-Nixon *et al.* 2000). It is speculated that the

displacement of the distal ligand to one of the hemes in CcoP, evidenced by the binding of CO, is connected with the binding of available oxygen. It could therefore be argued that CcoP behaves like a heme based sensor and that the binding of oxygen to the heme in CcoP induces a conformational change in this subunit that allows the signal to be transduced and for the organism to respond.

Two component systems and heme based sensors will be discussed in more detail in sections 1.10-12.

1.8 Role of cytochrome *cbb*₃ oxidases in microaerophilic environments

Bacterial species with multiple terminal oxidases have the ability to sense and adapt to changes in the redox environment. The need for this adaptation is to select the energetically most efficient respiratory pathway for the prevailing conditions. As discussed in Section 1.5, the global regulator, FNR (fumarate nitrate reductase) controls transcription of genes whose functions facilitate adaptation to variations in cellular oxygen status (Spiro and Guest 1991; Crack *et al.* 2007). A consensus sequence (TTGAT-N4-GTCAA) that recognizes members of the FNR family is located -88 and -102 base pairs upstream of the *ccoN* start codon in *P. stutzeri* (Pitcher *et al.* 2002). A binding site for an FNR homologue, Anaerobic Nitrate Reductase (ANR) (TTGAT-N4-ATCAA), is present in *P. aeruginosa* (Vollack *et al.* 1998; Comolli and Donohue 2004). The binding site is located 100 nucleotides upstream of the transcription initiation point of the *ccoN* in the *ccoNOQP* operon (Stover *et al.* 2000). The presence of the FNR analogue in *P. aeruginosa* is consistent with the observation that ANR is required by *P. aeruginosa* for the expression of the *cbb*₃ oxidase under micro-aerobic conditions (Ray and Williams 1997; Comolli and Donohue 2004).

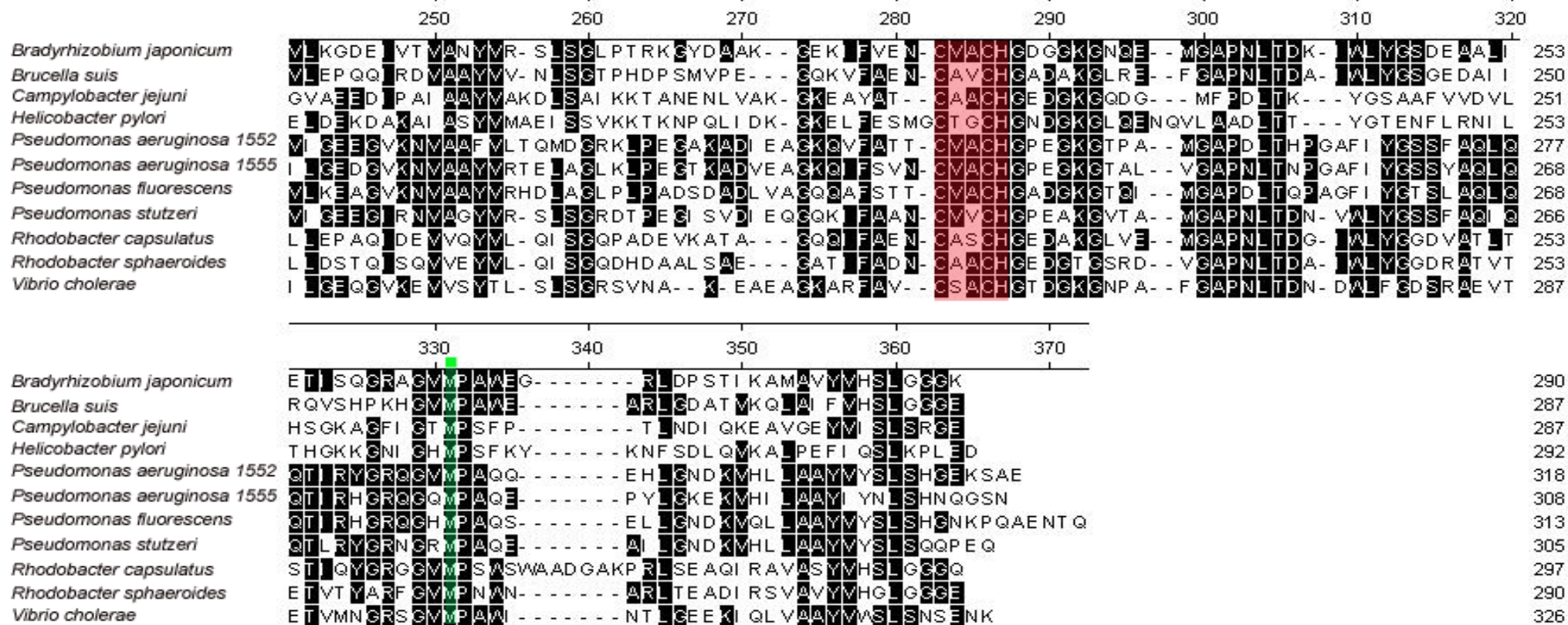


FIG. 1.9 Multiple sequence alignments of CcoP. Conserved residues are shaded in black. Predicted transmembrane segments are underlined. The predicted heme c binding sites are coloured red. The predicted distal heme residues His 42 (*P. stutzeri* numbering) is highlighted in blue, the fully conserved methionine Met 272 (*P. stutzeri* numbering) is highlighted in green. Since the completion of this thesis, the genomic sequence of *P. stutzeri* has identified two putative *cbb*₃ operons (Yan *et al.* 2008). This alignment refers to CcoP PST 1837.

It has been suggested that FNR is not the only regulatory protein sensing intracellular oxygen tension and alternative proteins are involved in the respiration-linked regulation of cytochrome *cbb₃* expression (Van Spanning *et al.* 1997; Cosseau and Batut 2004). A regulatory effect involving the *cbb₃* subunit, CcoQ, has been described and it is has been suggested that the *cbb₃* oxidases plays a role as a sensor of the cell's redox status (Eraso and Kaplan 2000; Oh *et al.* 2000). The proposal is that electron flow through the *cbb₃* oxidase generates a signal under aerobic conditions, which is sensed and transduced by the two-component system, PrrBA (Eraso and Kaplan 2000; Oh *et al.* 2000). The PrrBA two component system has been shown to play a pivotal role in the induction regulation of photosynthesis (PS) gene expression in nonsulfur photosynthetic bacteria in response to changes in oxygen tension (O'Gara *et al.* 1998; Kim *et al.* 2007),

1.9 Two component regulatory systems

Bacteria are constantly regulating their structure, physiology and behavior in order to respond and adapt to their environment (Richardson 2000). This requires bacteria to have evolved molecular systems that can both sense environmental cues and elicit an appropriate response for the cell. The term signal transduction refers to any process by which a cell converts one kind of signal or stimulus into another, most often involving ordered sequences of biochemical reactions to elicit a cell response, for example gene activation. Signal transduction is the process observed in the “two component” regulatory systems (Parkinson 1995; Marina *et al.* 2005).

Two-component systems regulate protein transcriptional activators of pre-existing proteins in response to environmental stimuli, for example, changes in oxygen tension or changes in pH, resulting in an altered cellular state (Parkinson 1995). These systems consist of two proteins, a sensor protein and a response regulator protein (Parkinson and Kofoid 1992; Marina *et al.* 2005; Kim *et al.* 2007). In a typical two component regulatory system, as

shown in Fig. 1.10, the sensor protein is a protein kinase. The chemical activity of a protein kinase involves removing a phosphate group from ATP and covalently attaching it to an amino acid residue. In prokaryotes, the kinase protein is commonly a histidine kinase, in which a specific histidine residue undergoes ATP-dependant phosphorylation (Dutta *et al.* 1999; Marina *et al.* 2005). This sensor protein is usually located within the cell membrane and is responsible for detecting changes in the cellular environment directly and communicating that information to a second protein, the response regulator (Parkinson 1995; Marina *et al.* 2005).

The mechanism of communication between the sensor protein and the response regulator protein occurs through phosphorylation-dephosphorylation reactions. The N-terminal domain of the histidine kinase protein functions as the input region, sensing a specific environmental stimulus directly or interacting with an upstream receptor (Parkinson 1995; Mascher *et al.* 2006). Recognition of the signal by the histidine kinase, which possesses autokinase activity, promotes phosphorylation of a histidine residue in a conserved domain (Marina *et al.* 2005). The phosphate group is then transferred from the histidine residue to an aspartate residue in the cytoplasmic response regulator protein (Parkinson 1995). The aspartyl phosphate residue is active in signaling and the appropriate cellular reaction is triggered in response to the extracellular physicochemical conditions. Types of cellular responses include activation of genes, for example, photosynthesis genes (Oh and Kaplan 2000; Kim *et al.* 2007). The relative equilibrium between the kinase and phosphatase activities of the histidine kinase is altered to elicit an appropriate response under specific conditions (Marina *et al.* 2005). This response mediated by the signal is recognized by the histidine kinase, through either direct binding to the kinase or protein-protein interactions between the kinase and other sensory proteins (Russo and Silhavy 1993).

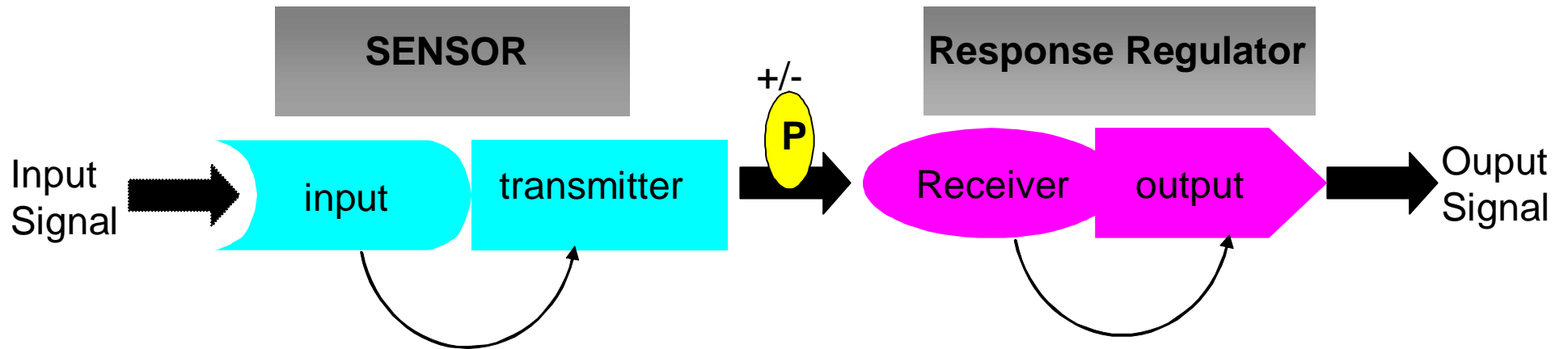


FIG. 1.10 Schematic diagram illustrating the two component regulatory system. The sensory protein kinase (shown in cyan) is activated by environmental stimuli and the protein undergoes autophosphorylation. Subsequent phosphorylation of the response regulator protein (shown in magenta) occurs. Upon activation of the response regulator protein, repression or transcription of target genes occurs. (Adapted from (Parkinson 1995).

1.10 Role of *cbb*₃ oxidases in two component regulatory systems

The primary role of the *cbb*₃ oxidases is likely to be energy generation as part of the electron transport chain (Comolli and Donohue 2004). The *cbb*₃ oxidases have also been implicated as regulators of gene expression by controlling the equilibrium of phosphate kinase activity in the PrrBA two component system (Oh *et al.* 2000). PrrBA and RegBA were originally identified in the anaerobic induction of the photosystem in *R. sphaeroides* and *R. capsulatus* respectively (Mascher *et al.* 2006). The PrrBA/RegBA two component system, as shown in Fig. 1.11, consists of the membrane associated sensory histidine kinase protein, PrrB/RegB, and response regulator, PrrA/RegA. The PrrBA/RegBA system is one of the major regulatory systems involved in the control of photosynthetic (PS) gene expression in phototrophic bacteria (O'Gara *et al.* 1998; Kim *et al.* 2007). Unlike other two component systems PrrBA/RegBA does not have a separate sensory domain and responds to environmental changes in oxygen tension and determines the presence or absence of the genes required for regulation of photosynthesis in bacterial cells (Oh *et al.* 2004).

The PrrBA two component system in the Gram negative non sulphur purple bacteria *R. sphaeroides* controls the expression of the PS genes either directly or indirectly in response to changes in oxygen tension (Eraso and Kaplan 1994; Kim *et al.* 2007). Under conditions of high oxygen an “inhibitory” signal shifts the relative equilibrium of PrrB activity shifts from the kinase mode to the phosphatase-dominant mode (Oh *et al.* 2001; Kim *et al.* 2007). This results in the silencing of PS gene expression (Oh *et al.* 2001; Kim *et al.* 2007). In the absence of oxygen, the inhibitory signal is weak and the kinase activity of PrrB is increased relative to its phosphatase activity. PrrA is phosphorylated and the cellular response, the expression of PS genes, is activated (Fig. 1.10) (Oh *et al.* 2001).

Previous studies by Oh and Kaplan established that mutation of the *cbb*₃ operon in *R. sphaeroides* resulted in the induction of the photosynthetic apparatus under aerobic

growth conditions accompanied by increased PS gene expression (Oh and Kaplan 1999; Kim *et al.* 2007). The regulation of PS genes is a response to anaerobic conditions and therefore high levels of PS gene expression under aerobic conditions suggests a disruption in the PrrBA regulatory system (O'Gara *et al.* 1998; Oh and Kaplan 1999). The observation generated a model proposing that at high oxygen levels increased electron flow through the *cbb₃* oxidase generates a strong inhibitory signal that alters the PrrB kinase/phosphatase activity towards the phosphatase dominant mode and expression of PS genes is minimal (Fig. 1.10) (Oh and Kaplan 1999; Kim *et al.* 2007). At low oxygen levels reduced electron flow through the *cbb₃* oxidase decreases the inhibitory signal, causes the equilibrium to shift and PrrB returns to the kinase dominant mode. At low oxygen levels, PrrA is phosphorylated and PS gene expression is induced (Oh and Kaplan 1999; Kim *et al.* 2007). This model suggests that the *cbb₃* oxidases can function to report the redox status of the bacterial cell to the PrrBA system.

On the basis of genetic and biochemical studies the cytochrome *cbb₃* oxidases have been proposed to play a role as an oxygen sensor controlling the equilibrium between the PrrB kinase/phosphatase activities in response to changes in oxygen availability (O'Gara *et al.* 1998; Ouchane and Kaplan 1999; Oh *et al.* 2001; Kim *et al.* 2007). Based on the hypothesis that the histidine kinase PrrB does not sense environmental stimuli directly, it has been proposed that the volume of electron flow through the *cbb₃* complex is monitored by the *cbb₃* oxidase subunit, CcoQ (Oh and Kaplan 1999; Oh and Kaplan 2000). However, as discussed previously, the CcoQ subunit does not contain any redox active cofactors that could sense electron flow (Toledo-Cuevas *et al.* 1998; Oh and Kaplan 1999). This subunit would therefore have to respond to a change in the environment that was sensed elsewhere in the *cbb₃* complex. Evidence suggests that the heme content in the subunit CcoP is affected by the absence of CcoQ from the *cbb₃* complex (Oh and Kaplan 2002). Based on this experimental evidence a connection between the two subunits CcoQ and CcoP could

be suggested (Oh and Kaplan 2002). In biological heme based sensors, a regulatory heme-binding domain or subunit controls a neighboring transmitter region of the same protein (Gilles-Gonzalez and Gonzalez 2005). It could therefore be speculated that the subunits CcoP and CcoQ act concomitantly as a heme based sensor.

Genetic studies have lead to the postulation that the gene encoding for the membrane-bound PrrC protein, is located immediately upstream of *prrA* (Eraso and Kaplan 2000; Kim *et al.* 2007). The protein PrrC has no definable role in the signal transduction pathway (Badrick *et al.* 2007). It is hypothesized however, that PrrC is located between the *cbb₃* oxidase, adjacent to CcoQ, and PrrB (Oh *et al.* 2004). It is proposed that the inhibitory signal is transduced to the PrrBA through the membrane-localised PrrC protein via CcoQ (Eraso and Kaplan 2000; Oh *et al.* 2000).

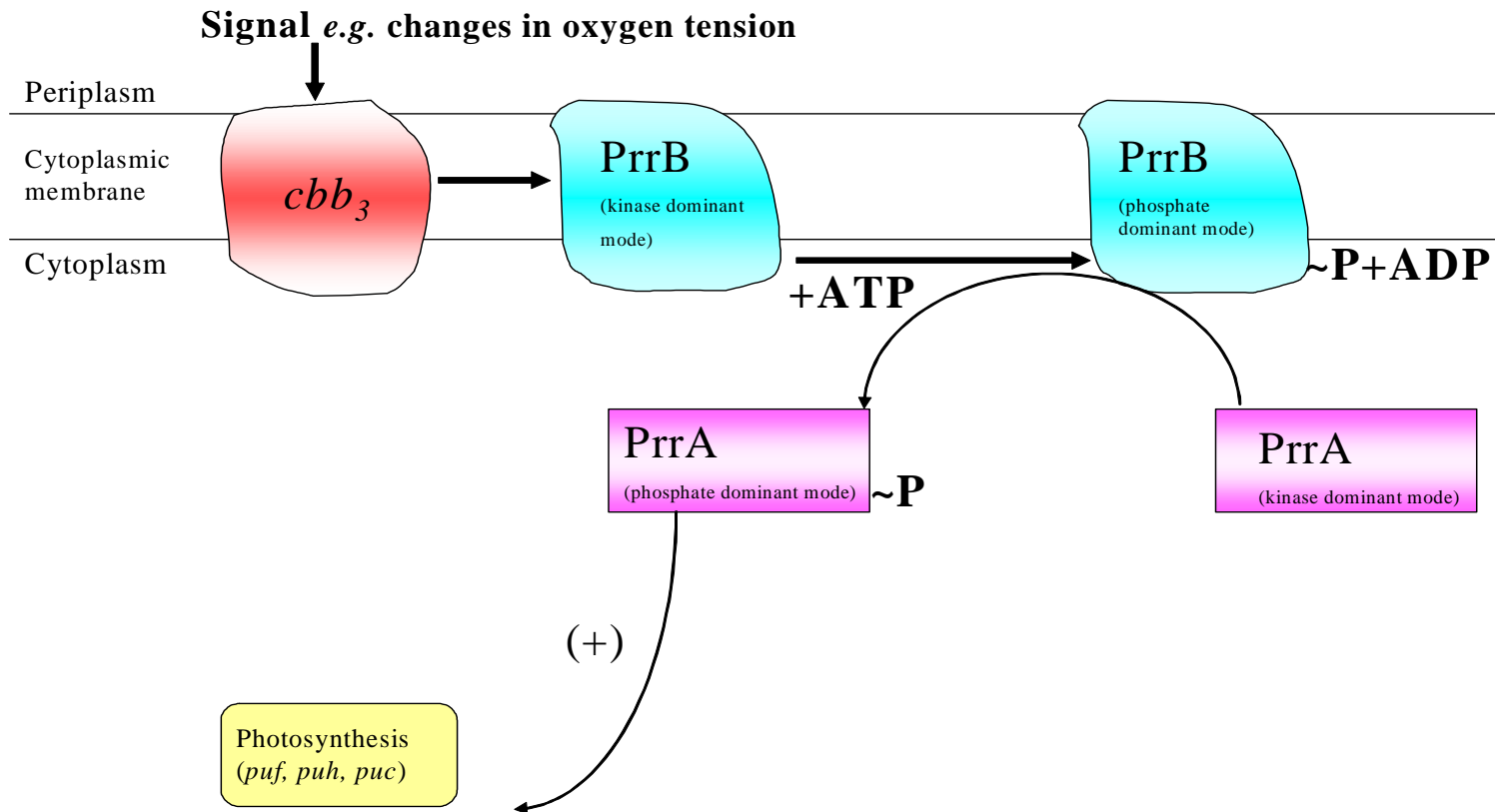


FIG. 1.11 Schematic demonstrating the PrrBA regulatory system in *R. sphaeroides*. In the presence of oxygen, electron flow through the *cbb₃* oxidase generates an inhibitory signal. The equilibrium shift of PrrB from the kinase dominant mode to the phosphate dominant mode leads to dephosphorylation of PrrA. In the absence of oxygen, electron flow through the *cbb₃* oxidase is minimized. PrrB is returned to the kinase dominant mode. This leads to phosphorylation of the PrrA resulting in the induction of PS gene.

A regulatory system similar to the PrrBA regulatory system is observed in the organism *P. aeruginosa*. The RoxRS regulatory system, a homologue of the PrrBA system, controls expression of the cyanide insensitive oxidase (CIO), which terminates one of the branches of the *P. aeruginosa* respiratory pathway (Fig. 1.2) (Comolli and Donohue 2002; Williams *et al.* 2007). The CIO has been shown to be resistant to the potent respiratory inhibitor cyanide, allowing respiration to proceed in the presence of > 1 mM potassium cyanide whilst respiratory oxidases sensitive to cyanide are routinely inhibited by concentrations of the order of 100µM or lower (Cunningham and Williams 1995). It is therefore postulated that the CIO enables the organism *P. aeruginosa* to survive in an environment with increased levels of cyanide (Cunningham and Williams 1995). Cyanide is produced by some bacteria, *P. aeruginosa* for example, and levels of this potent poison can build up when host cells are significantly infected by a cyanogenic pathogen (Blumer and Haas 2000). The ability of *P. aeruginosa* to respire under cyanogenic conditions therefore allows the organism to compete successfully with other infecting bacteria in mixed populations (Carterson *et al.* 2004).

The CIO in *P. aeruginosa* is encoded for by the *CioAB* operon, and has homology to the cytochrome *bd* quinol oxidase (García-Horsman *et al.* 1994; Cunningham and Williams 1995; Cunningham *et al.* 1997; Zlosnik *et al.* 2006). The spectral features of *P. aeruginosa* suggest, however, that instead of a high-spin heme *d*, the second heme is likely to be a high-spin heme *b* (Cunningham *et al.* 1997). The CIO shows no homology to members of the HCO superfamily (Zlosnik *et al.* 2006; Williams *et al.* 2007). The cytochrome *bd* quinol oxidases are oxygen regulated in many bacterial species, *E. coli* for example. *E. coli* cytochrome *bd* oxidases have a very high affinity for oxygen consistent with a role at low oxygen tensions and are regulated by the transcriptional regulator FNR (Zlosnik *et al.* 2006). However, this is not universally the case; for example, the cytochrome *bd* oxidase of *Azotobacter vinelandii* has a low affinity for oxygen compared to the *E. coli* *bd* oxidase

and is induced by high levels of oxygen (Junemann and Wrigglesworth 1995; Junemann 1997). In comparison, variant oxygen concentrations in batch cultures of *P. aeruginosa* have been shown to have no effect on CIO expression and no correlation was observed between CIO induction and the dissolved oxygen levels in the growth medium (Cooper *et al.* 2003). It has however, been demonstrated that mutation of the oxygen sensitive transcriptional regulator ANR, an FNR analogue, led to a marked increase in CIO activity in an oxygen sensitive manner with the highest induction occurring under low oxygen conditions (Cunningham *et al.* 1997; Cooper *et al.* 2003). The genes regulating CIO expression, *cioAB*, contain two consensus ANR binding sites within the promoter region. The results presented by Cunningham *et al.* therefore suggests that CIO expression can respond to a signal generated by low oxygen levels, but the response is controlled by ANR repression (Cunningham *et al.* 1997).

The *E. coli* terminal oxidases are regulated in response to oxygen by the ArcAB two component system, in which the *ArcAB* regulatory proteins sense the redox state of the quinone pool (Junemann 1997; Zlosnik *et al.* 2006). In *R. sphaeroides* the two component system, PrrBA, is proposed to regulate PS genes in response to electron flow through the *cbb₃* oxidase (Oh 1999) (Section 1.10). The RoxRS regulatory system, a homologue of the PrrBA system, controls expression of the cyanide insensitive oxidase (CIO) (Comolli and Donohue 2002; Williams *et al.* 2007). It is therefore postulated that the RoxRS system controls gene expression of CIO in a similar manner to which the PrrBA system controls PS gene expression (Comolli and Donohue 2002). In a comparable signaling system to the PrrBA system, increased levels of cyanide would decrease electron flow through the *cbb₃* oxidase by inhibiting the ability of the oxidase to reduce oxygen. Subsequently, the RoxRS regulatory system would be activated and expression of the CIO stimulated through up regulation of the *CioAB* operon.

It is speculated therefore that *cbb*₃ oxidase also plays a role in sensing the environment and influences gene expression accordingly. It has been recognized that many heme-protein enzymes are signal transducers where the heme center is directly concerned with regulation rather than catalysis (Gilles-Gonzalez *et al.* 1991; Garbers and Lowe 1994; Shelver *et al.* 1997; Gilles-Gonzalez and Gonzalez 2005). As discussed previously a CcoNO subcomplex of the *cbb*₃ oxidase isolated from the organism *P. denitrificans* and *B. japonicum* were both catalytically competent (de Gier *et al.* 1996; Zufferey *et al.* 1996). It could be postulated that the CcoNO complex functions to catalyze the reduction of oxygen to water, whereas the *cbb*₃ subunits CcoP and CcoQ collectively act as a heme sensor and monitor electron flow through the *cbb*₃ complex.

1.11 Heme Sensory Proteins

The role of the *cbb*₃ oxidases in the two component system PrrBA has been speculated, however it remains unclear if all or only some of the subunits of the *cbb*₃ oxidase are involved in monitoring electron flow (Oh and Kaplan 2002; Oh 2006; Kim *et al.* 2007). Recent evidence has suggested that redox signaling through the CcoN subunit, is part of the pathway by which the *cbb*₃ oxidase affects the relative kinase/phosphate activity of membrane bound PrrB (Kim *et al.* 2007). However, the underlying mechanism by which the *cbb*₃ oxidase communicates with the PrrB histidine kinase to control activity is not understood. It has been suggested that the subunit CcoQ transponds a signal via the adjacent PrrC protein to PrrBA which ultimately controls gene expression (Oh and Kaplan 1999).

The *cbb*₃ oxidase subunit CcoQ contains no redox factors and the absence of CcoQ from the *cbb*₃ oxidase complex appears to affect only the CcoP subunit (Toledo-Cuevas *et al.* 1998; Oh and Kaplan 2002). It could be speculated that the CcoQ and CcoP subunits are collectively involved in the PrrBA signal transduction pathway. It has been recognized that

many heme-protein enzymes are signal transducers where the heme center is directly concerned with regulation rather than catalysis (Gilles-Gonzalez *et al.* 1991; Garbers and Lowe 1994; Shelver *et al.* 1997; Gilles-Gonzalez and Gonzalez 2005). It is therefore hypothesized that the *cbb*₃ subunits CcoP and CcoQ act together to form a heme sensory protein.

Groups of proteins termed “heme based sensors” are the key regulators of adaptive responses to fluctuating oxygen levels within the bacterial environment (Gilles-Gonzalez *et al.* 1994; Gilles-Gonzalez and Gonzalez 2005). These sensors carry out important roles in biological signaling in prokaryotic and eukaryotic organisms responding to the presence of physiologically important gases using heme cofactors. Examples of heme based sensors include the FixL protein of Rhizobia, the soluble guanylyl cyclase of vertebrates, and the CooA protein of *Rhodospirillum rubrum* that sense dioxygen, nitric oxide and carbon monoxide respectively (Gilles-Gonzalez *et al.* 1991; Garbers and Lowe 1994; Shelver *et al.* 1997). In these proteins the heme cofactor not only binds the regulator molecule but also controls associated enzymatic function via heme and protein conformational changes (Gilles-Gonzalez *et al.* 1994). For example, in the heme based oxygen sensor FixL, conformational changes induced by oxygen binding to the heme sensor domain regulates the activity of a neighboring histidine kinase (Tuckerman *et al.* 2002). The conformational change restricts expression of specific genes explicitly to hypoxic conditions.

In a biological heme sensor, a regulatory heme binding domain or subunit controls a neighboring transmitter region of the same protein (Gilles-Gonzalez *et al.* 1991). In the *cbb*₃ oxidase it can be speculated that the regulatory heme binding domain is fulfilled by the subunit CcoP and the transmitter region fulfilled by the small hydrophobic *cbb*₃ subunit CcoQ. As discussed previously, it was recognized that electron flow through the *cbb*₃ oxidase generates a signal under certain environmental conditions, which is mediated by

the PrrBA two component system (Oh and Kaplan 1999). In purple photosynthetic bacteria the response to this inhibitory signal is repression of photosynthetic gene expression (O'Gara *et al.* 1998). When the gene for subunit CcoQ was deleted from the *cbb₃* operon, repression of the photosynthetic genes was not observed (Oh and Kaplan 2002). However, in the presence of oxygen, the absence of CcoQ leads to the loss of heme from the *cbb₃* complex (Oh and Kaplan 2002). This loss of heme destabilized the *cbb₃* complex into a degradable form. As discussed the CcoQ subunit does not contain any redox active cofactors that could sense electron flow directly (Toledo-Cuevas *et al.* 1998). It is therefore not unreasonable to postulate that the CcoP subunit fulfills the sensory heme binding domain and transmits the appropriate signal via CcoQ. This would elucidate a role for these two subunits, which appear to be redundant in the *cbb₃* oxidase. The redundancy of the subunits CcoP and CcoQ in the *cbb₃* oxidase are highlighted by the observation that a CcoNO complex is catalytically competent (de Gier *et al.* 1996; Zufferey *et al.* 1996).

1.12 Summary

Since their discovery over a decade ago, a number of questions remain regarding the *cbb₃* oxidases. This distinctive class of HCO's is expressed primarily under micro-aerobic conditions permitting bacterial colonization of oxygen-limited environments. The cytochrome *cbb₃* oxidase catalyses the four electron reduction of oxygen to water and subsequently uses the liberated free energy to translocate protons across the periplasmic membrane. Energy generation is understood to be the primary role of this class of oxidases; however, a redox-sensing role has also been suggested. Through molecular dissection and spectroscopic analysis, it is anticipated that the mechanism and roles in anaerobic metabolism of this class of HCO's will become fully understood

2. Materials and Methods

2.1 Bacterial cultivation and strains

2.1.1 Media and antibiotics.....	56
2.1.2 Bacterial strains and plasmids.....	57

2.2 General protein biochemistry

2.2.1 Determination of protein concentration.....	59
2.2.2 Analysis of proteins by SDS-PAGE.....	60
2.2.3 Mass spectrometry.....	61

2.3 Molecular biology techniques

2.3.1 Plasmid DNA isolation.....	62
2.3.2 Preparation of competent <i>E. coli</i> cells.....	62
2.3.3 Plasmid Transformations.....	63
2.3.4 Site-Directed Mutagenesis.....	63
2.3.5 Restriction Digests.....	65
2.3.6 Agarose gel electrophoresis.....	65
2.3.7 Subcloning.....	66
2.3.8 DNA sequencing.....	68

2.4 Expression and purification of Full Length CcoP

from *P. stutzeri*

2.4.1 Expression of full length CcoP in <i>E. coli</i>	68
2.4.2 Purification of full length CcoP.....	68

2.5 Expression and mutagenesis of variant full length CcoP

from *P. stutzeri*

2.5.1 Site-Directed mutagenesis.....	69
2.5.2 Expression and purification of mutated full length CcoP.....	72

2.6 Expression and purification of truncated CcoP

from *P. stutzeri*

2.6.1 Expression of truncated CcoP.....	72
2.6.2 Purification of truncated CcoP.....	72

2.7 Growth conditions and purification of the two *Cbb*₃

isozymes from *P. aeruginosa*

2.7.1 Growth conditions of <i>cbb</i> ₃ oxidase.....	74
2.7.2 Preparation of membranes.....	75
2.7.3 Purification of cytochrome <i>cbb</i> ₃ -1 and <i>cbb</i> ₃ -2 oxidase.....	75
2.7.4 Oxidase Activity.....	77

2.8 Biophysical Methods

2.8.1 Electronic absorbance (UV-Visible) Spectroscopy.....	79
2.8.2 Electron paramagnetic resonance (EPR) Spectroscopy.....	80
2.8.3 Magnetic circular dichroism (MCD) Spectroscopy	82

2.9 Other Biophysical Methods

2.9.1 Mediated redox potentiometry.....	84
2.9.2 CO titrations.....	89

2. Methods and Materials

2.1 Bacterial cultivation and strains

2.1.1 Media and antibiotics

Bacteria were routinely cultured on sterile LB broth (10 g tryptone, 5 g yeast extract, 10 g NaCl per litre, pH 7.0) was the media of choice. Solid LB medium was prepared with the addition of agar (1.5% (w/v)) to the liquid medium prior to autoclaving.

For the expression of full length CcoP and all CcoP variants in *E. coli*, growth was carried out in sterile Tryptone Yeast Phosphate Broth (TYP) (2.3 g KH_2PO_4 , 12.5 g K_2HPO_4 12 g Tryptone, 24 g Yeast Extract, 5 g NaCl, made up to 1 litre with distilled water (pH 7). 4 ml 100% sterile glycerol was added after the media was autoclaved.

For the growth of *Pseudomonas aeruginosa* strains L-asparagine minimal medium was the medium of choice (2 g L-Asparagine, 7 g Tri sodium citrate, 2 g KH_2PO_4 , 2 g $\text{MgSO}_4 \cdot 7\text{H}_2\text{O}$, 10 g NaCl, 0.1 g $\text{CaCl}_2 \cdot 2\text{H}_2\text{O}$, 0.025 g $\text{FeCl}_3 \cdot 6\text{H}_2\text{O}$, 0.00017 g $\text{CuCl}_2 \cdot 2\text{H}_2\text{O}$, made up to 1 litre with distilled water, adjusted to pH 8.0 with NaOH).

All media used was supplemented with the appropriate antibiotics (Table 2.1) according to the antibiotic resistance marker carried by the vector. The addition of antibiotics is essential to prevent the growth of bacterial strains, which do not harbor the strain of interest. The antibiotics were made up in distilled water and passed through a sterile filter prior to use, with the exception of chloramphenicol, which was made up in ethanol.

Antibiotic	Stock Concentration (mg/ml)	Working Concentration (µg/ml)
Ampicillin	100	100
Chloramphenicol*	34	34
Kanamycin	30	30
Gentamicin	20	20

Table 2.1 Concentration of antibiotics used in this study

* The antibiotics were made up in distilled water and passed through a sterile filter prior to use, with the exception of chloramphenicol, which was made up in ethanol

2.1.2 Bacterial Strains and plasmids

The strains used in this work and their relevant characteristics are shown in Table 2.2.

Strain or plasmid	Description or genotype	Source or Reference
<i>E.coli</i> JM109 (DE3)	<i>supE44, recA1, endA1, gyrA96, hsdR17, relA,1 thi, Δ (lac-proAB) λ (DE3)</i>	Lab Stock
<i>E.coli</i> DH5α	<i>supE44 Δ (lacU169)(ø80 lacZ Δ M15) recA1 endA1 gyrA96 thi-1 hsdR17 relA1</i>	Lab Stock
pEC 86	pACYC184 expression vector containing <i>ccmABCDEFGH</i> gene cluster	(Arslan <i>et al.</i> 1998)
pCcoPall	pET21a containing entire <i>ccoP</i> gene from <i>P.stutzeri</i> as an <i>NdeI-SacI</i> fragment	(Pitcher 2002)

Table 2.2 List of Bacterial Strains and Plasmids used in this study

Strain or plasmid	Description or genotype	Source or Reference
pCcoPsol	pET22b containing soluble region of <i>ccoP</i> from <i>P. stutzeri</i> (missing 80 N-terminal residues) as a <i>MscI-SacI</i> fragment	(Pitcher 2002)
pET 24a	Expression vector under control of T7 promoter with kanamycin resistance	Novagen
pCcoPallH42A	pET 24a containing mutated <i>ccoP</i> gene from <i>P.stutzeri</i> as an <i>NdeI-SacI</i> fragment	This work
pCcoPallH42C	pET24a containing mutated <i>ccoP</i> gene from <i>P.stutzeri</i> as an <i>XbaI-XhoI</i> fragment	This work
pCcoPallH42M	pET24a containing mutated <i>ccoP</i> gene from <i>P.stutzeri</i> as an <i>XbaI-XhoI</i> fragment	This work
PAK	Wild type <i>P. aeruginosa</i>	(Comolli and Donohue 2004)
Cco1.1	PAK <i>cbb₃-1 Δ BstB1 - EcoRI :: Gm^r</i>	(Comolli and Donohue 2004)
Cco2.2	PAK <i>cbb₃-2 Δ AccI - Bg II:: Gm^r</i>	(Comolli and Donohue 2004)
CcoΔ1	PAK <i>cbb₃-1/ cbb₃-2 Δ XhoI – EcoRI</i>	(Comolli and Donohue 2004)
CoxΔ1	PAK <i>aa₃ :: Gm^r</i>	(Comolli and Donohue 2004)

Table 2.2 (cont'd) List of bacterial strains and plasmids used in this study

2.2 General protein biochemistry

2.2.1 Determination of protein concentration

The total protein concentration of solutions were determined by the bicinchoninic acid (BCA) protein assay (Pierce, Rockford, USA) according to manufacturer's instructions (Smith *et al.* 1985). Briefly, under alkaline conditions chelation of Cu^{2+} ions and the peptide bonds of protein form a coloured complex. The formation of the coloured complex is followed by the reduction of the complexed Cu^{2+} ions to Cu^{1+} ions. Following an incubation period at 37 °C for 30 minutes, BCA forms a complex with the Cu^{1+} - protein complex resulting in a coloured solution with an absorbance maximum at 562 nm. The intensity of the colour produced is proportional to the number of peptide bonds participating in the reaction, and hence the concentration of protein present. A standard curve was prepared according to protocol using 10 – 100 μl aliquots of Bovine Serum Albumin (1 mg/ml). The absorbance at 562 nm of the standard protein and test protein was recorded and plotted in excel. The gradient of each curve was calculated and the protein concentration of the test sample was determined using the equation:

$$\text{Protein concentration (mg/ml)} = (\text{gradient of curve of unknown sample} / \text{gradient of curve of standard}) \times 1 \text{ mg/ml} \times \text{dilution factor}$$

In work with membrane proteins the BCA method is tolerant to the presence of detergent in the samples, dodecyl maltoside (DM) and Sodium dodecyl sulphate (SDS), for example.

2.2.2 Analysis of proteins by SDS-PAGE

The technique, SDS PAGE, separates proteins according to electrophoretic mobility and was used to qualitatively analyze *E. coli* whole cells, membrane fractions, and purified protein from column chromatography. Gels used contained 15% (w/v) resolving gel (2.5 ml polyacrylamide (30% acrylamide: 0.8% w/v bis-acrylamide), 1.25 ml 1.5 M Tris pH 8.8, 1.2 ml dH₂O, 50 µl 10% APS, 8 µl TEMED, 50 µl 10% SDS) and 5 % stacking gel (330 µl polyacrylamide (30% acrylamide: 0.8% w/v bis-acrylamide), 250 µl 0.5M Tris pH 6.8, 1.4 ml dH₂O, 20 µl 10% APS, 8 µl TEMED, 20 µl 10% SDS) and were prepared as per Sambrook (Sambrook 1989). Samples were loaded into the resolving gel via a 5% (w/v) polyacrylamide stacking gel, to ensure the proteins moved freely and concentrated under the effects of the electric field applied.

Samples were prepared for electrophoresis by the addition of sample buffer (6 M Urea, 5% SDS, 0.1% Glycerol, 0.05% Bromophenol blue) in a 1:1 ratio and heated at 50 °C for 10 minutes before loading onto the gel. Samples were only heated to 50°C as proteins containing significant stretches of hydrophobic amino acids (such as the transmembrane helices of membrane proteins) tend to aggregate when boiled (Scopes 1994). To ensure optimized protein separation during SDS PAGE, typical sample loads were 5 - 40 µg per well.

For analysis of total protein, proteins were visualized by staining the gel with Coomassie blue (40% (v/v) Methanol, 10% (v/v) Glacial acetic acid, 0.1% (w/v) Coomassie blue R250) for 30 minutes at room temperature. The gel was subsequently submerged in destain solution (25% Methanol, 10% Glacial acetic acid) overnight. The destain solution was used to remove unbound background dye from the gel, leaving stained protein visible

as blue bands on a clear background. The molecular weight of the separated proteins was estimated by reference to dual colour markers (Bio-Rad, UK) (10 - 250 kDa). The gels were recorded and archived using an imaging system (Bio-Rad, UK).

Following separation by gel electrophoresis, the *c*-type cytochromes were specifically identified by their intrinsic heme peroxidase activity by incubating the gel in 70 mls 250 mM sodium acetate pH 5 for 15 minutes, to which 30 ml 6.3 mM 3,3',5,5'-tetramethylbenzidine dissolved in methanol was added. The reaction was incubated in the dark for a further 30 minutes. The gel was developed with the addition of 300 μ l 30% H₂O₂ and was incubated in the dark until light blue bands developed indicating the presence of heme containing proteins (approx. 10 mins). The reaction was stopped by washing the gel in distilled water. This staining procedure was performed under dark conditions at room temperature (Goodhew 1986).

2.2.3 Mass spectrometry

The molecular mass of CcoP was determined by mass spectrometry using the MALDI (Matrix Assisted Laser Desorption/Ionisation) technique (Ultraflex TOF/TOF Bruker Daltonics, Germany). Samples were diluted with 0.1 % TFA to a final concentration of 20 pmol/ μ l. The diluted samples were mixed with appropriate amounts of two proteins for calibration, trypsinogen (23982 Da) and enolase from yeast (46671.9 Da). This sample was mixed with MALDI matrix solution (saturated solution of sinapinic acid in 30% acetonitrile, 0.1% TFA) in a 1:1 ratio and spotted on a steel target plate. MALDI TOF spectra were acquired using several hundred-laser shots of 45 – 55 % of the laser point until reasonable peaks were obtained. Mass spectroscopy was performed at the John Innes Centre, Norwich by Dr G Saalbach.

2.3 Molecular biology techniques

2.3.1 Plasmid DNA isolations

Extraction of plasmid DNA for cloning and sequencing was carried out using a plasmid midi or mini prep kit (Qiagen, UK) according to the manufacturer's instructions. Centrifugation speeds and reaction times were dependant upon the use of either the plasmid midi or mini prep kit. The *E. coli* strain DH5 α was used to propagate the plasmid of interest. *E. coli* cells from an overnight bacterial culture were harvested and lysed under alkaline conditions. The lysis time suggested by the manufacturers is optimized to allow maximum release of plasmid DNA without release of chromosomal DNA. The lysate was centrifuged to remove cell debris and precipitated protein. The supernatant was neutralized and adjusted to high-salt conditions. The high salt concentration causes any remaining denatured proteins and chromosomal DNA to precipitate, while the smaller, plasmid DNA remains in solution. Following centrifugation to sediment the precipitated proteins, the supernatant was applied to a silica membrane column, specific for the selective adsorption of plasmid DNA. After thorough washing of the column with high salt buffer the plasmid DNA was eluted under low salt conditions and was precipitated with isopropanol to yield ultra-pure DNA.

2.3.2 Preparation of competent *E. coli* cells

Cells were grown overnight at 37°C with shaking (200 rpm) in 50 ml LB medium and were harvested by centrifugation at 10,000 g, 4 °C for 20 minutes. The cell pellet was subsequently, re-suspended in ice-cold 50 mM calcium chloride and incubated on ice for 30 minutes. Treatment of the bacterial cells with Ca²⁺ at 4°C makes the cell wall permeable to DNA, and therefore induces the bacteria to take up plasmid DNA during plasmid transformation. Following the incubation period, the cells were harvested by centrifugation at 10,000 g, 4°C for 20 minutes. The cell pellet was re-suspended in ice-cold 50 mM

calcium chloride/25% glycerol. Addition of glycerol to the re-suspension solution acts as a protectant against cell damage during thawing of the cells following storage (Acha *et al.* 2005). The competent cells were pipetted into 200 μ l aliquots, rapidly frozen in liquid nitrogen and stored at - 80 °C.

2.3.3 Plasmid transformations

A 200 μ l aliquot of competent cells was thawed on ice for approximately five minutes. The thawed cells were then inoculated with 1 - 5 μ g of DNA pertaining to the plasmid of interest, and incubated on ice for a minimum of 30 minutes to allow the DNA to bind to the receptor sites on the cell surface. Following the incubation period, the cells were heat shocked at 42 °C for 60 seconds to increase the permeability of the cell membranes, allowing the plasmid DNA to enter. The transformed cells were incubated on ice for 2 minutes, followed by the addition of 1 ml LB and further incubation at 37 °C for 1 hour allowed the cells time to recover. Following sedimentation at 3,000 g for 2 minutes the cells were carefully resuspended in 400 μ l un-supplemented LB. A 200 μ l aliquot of the transformed cells was spread on a LB agar plate containing the appropriate antibiotics. The plates were incubated overnight at 37 °C. As a negative control untransformed cells were treated the same as transformed cells, through the heat shock and recovery steps. The cells were plated onto LB agar and LB agar supplemented with the appropriate antibiotics. As a positive control competent cells were transformed with pET21a, pET22b or pET24a as appropriate. The cells were plated onto LB agar and LB agar supplemented with the appropriate antibiotics

2.3.4 Site-directed mutagenesis

Substitution of a single amino acid in a protein is achieved by site-directed mutagenesis (SDM) of the gene which encodes the protein. Mutation of plasmid borne genes was

created by PCR amplification, using a modification of the “QuikChange” method (Stratagene, UK). The technique of SDM was employed using mutagenic oligonucleotide primers (Sigma, UK.) designed to bind to opposite complementary strands of the plasmid. The primers were designed to incorporate unique or additional restriction sites for easy identification of the mutated clones.

All reactions were carried out in 0.5 ml thin walled eppendorf tubes, which ensures ideal contact with the heat block of the thermocycler (Primus, MWG-Biotech, Germany).

The sample reactions were prepared as below

5 μ l 10x reaction buffer

5 - 50 ng dsDNA template

X μ l (100 μ M) oligonucleotide primer #1

X μ l (100 μ M) oligonucleotide primer #2

1 μ l dNTP mix

1 μ l *Pfu-Turbo* DNA polymerase (2.5 U/ μ l)

made up with the appropriate volume of sterile water to a total volume of 50 μ l.

Pfu-Turbo DNA polymerase was used for all amplifications due to the additional exonuclease activity of the enzyme that acts as a proof reading mechanism, thereby increasing the fidelity of the PCR reaction.

PCR reactions were initiated by 2 mins at 94 °C, followed by 30 cycles of denaturation (30 secs, 94 °C), annealing (30 secs, 55 °C) and extension (2 min/1 kb 72 °C). After the final cycle, a further incubation at 72 °C for 10 minutes was included to ensure completion of polymerization.

Following PCR, the total product was treated with the restriction enzyme Dpn1 for 60 minutes, at 37 °C (Roche, UK) to digest the dam methylated (parental non-mutated) DNA. Following the incubation period, the restriction enzyme was inactivated at 65 °C for 15 minutes before the total final product was transformed into 200 µl DH5α competent cells using the protocol outlined in section 2.3.3.

2.3.5 Restriction digests

Restriction enzymes were used for routine analysis of plasmid DNA. Purified plasmid DNA, typically 1-2 µg, was digested in a total volume of 10 µl: 1 µl 10x digest buffer, 1 µl restriction enzyme, X µl DNA made up with the appropriate volume of sterile distilled water to a total volume of 10 µl.

The digest buffer was specific to the restriction enzyme in accordance with optimal reaction conditions as suggested by the manufacturers (Roche, UK/Promega, UK). When multiple restriction enzymes were used, a buffer compatible with both enzymes were identified. The restriction digest reactions were incubated at 37 °C for 90 minutes. Following incubation DNA loading dye was added and the samples were analyzed by size fractionation using agarose gel electrophoresis as outlined in section 2.3.6. As a negative control, the restriction enzyme was omitted and the total volume made up with distilled water.

2.3.6 Agarose gel electrophoresis

DNA fragments from PCR or restriction digests were analyzed by ethidium bromide treated agarose gel. The appropriate amount of agarose (0.8-2 % (w/v) depending upon predicted size of DNA fragment) was dissolved in TAE Buffer (40 mM Tris-HCl (pH 8.0), 1.142% (v/v) acetic acid, 1 mM EDTA) and supplemented with ethidium bromide (0.5µg/ml final concentration) (Sigma, UK). Samples were prepared for electrophoresis by

the addition of 6x DNA loading buffer (10 mM Tris-HCl pH 7.5, 50 mM EDTA, 10% Ficoll 400, 0.4% Orange G) in a 6:1 ratio. The gel was immersed in running buffer (TAE buffer) and current was applied for approximately 1 hour, at 80 Volts, in accordance with protocol (Sambrook 1989). Standards (1 Kb ladder, Invitrogen) were run adjacent to the DNA fragments. Following separation, the DNA fragments were visualized under UV light.

2.3.7 Subcloning

During SDM, amplification of the entire plasmid can result in the introduction of secondary mutations. The mutagenized insert was, therefore, re-cloned into the kanamycin resistant vector, pET 24a.

1. Restriction Digests

The plasmid containing the mutagenised insert and the vector were digested separately essentially utilizing the methods outlined in section 2.3.5. 10 µg of DNA (plasmid and vector) was digested at 37 °C overnight with 4 µl of one of the chosen restriction enzymes in a total volume of 100 µl. Following the incubation period, an additional 1 µl of the appropriate restriction enzyme buffer and 3 µl of a second restriction enzyme were added to the digested product. The restriction digest was re-incubated at 37 °C for a further five hours. Following the incubation period, the reaction mixture was analyzed by agarose gel electrophoresis.

2. Purification of DNA

DNA fragments were purified from agarose gel using the Quiaquick gel extraction kit (Qiagen, UK) according to manufacturer's instructions. The gel was visualized using a UV light source and the DNA fragments excised using a sharp scalpel. The agarose slice containing the DNA was dissolved in high salt buffer, pH 7.5 at 50 °C for 10 minutes and applied to a silica membrane column, which specifically binds DNA. Following thorough

washing using an ethanol based buffer the DNA was eluted from the column with distilled water.

3. Quantification of DNA

The DNA yield following gel extraction was quantified spectroscopically, considering 1 absorbance unit at 260 nm equals 50 mg DNA/ml (Sambrook 1989). To confirm the purity of the DNA, the absorbance at A_{280} was also recorded. The sample was considered to be of sufficient purity if $A_{260}:A_{280}$ was greater than 1.5.

4. Dephosphorylation of vector DNA

The cut ends of the vector DNA digested for subsequent sub-cloning were dephosphorylated to minimize vector re-circularization in the subsequent ligation step. Shrimp Alkaline phosphatase (Roche) was used to remove any terminal phosphate groups from the linearized vector. The dephosphorylation reactions were carried out in a total volume of 30 μ l: 10 μ l DNA (30 – 600 ng), 3 μ l 10x Reaction Buffer, 1 μ l shrimp alkaline phosphatase, made up to 30 μ l with sterile distilled water. The reaction was incubated at 37 °C for 30 minutes, and the reaction was stopped by incubating at 65 °C for 15 minutes.

5. Ligations

Following dephosphorylation, the DNA fragments (insert and vector) were annealed using T4 DNA ligase (Roche, UK). A series of ligation reactions were performed in tandem, considering 1:1, 1:3 and 1:5 vector:insert ratios. The ligations were carried out in a total volume of 20 μ l: 4 μ l ligase buffer, X μ l insert, 1 μ l vector, 2 μ l ligase (Invitrogen, UK), made up to 20 μ l with distilled water, and incubated overnight at 4 °C. Following the incubation period, the total ligation reaction was transformed into *E. coli* DH5 α competent cells, following the protocol outlined in section 2.3.3. For each set of ligation reactions, a control containing no insert was also included to check the non-recombinant background. Transformation of this control reaction should not yield antibiotic resistant colonies.

2.3.8 DNA sequencing

DNA sequencing was performed on all PCR amplified products to ensure they contained the mutation of interest and no undesirable mutations occurred during genetic manipulation of the DNA. Sequencing was performed by MWG Biotech (Germany) using standard T7 forward and reverse primers.

2.4 Expression and purification of full length CcoP from *P. stutzeri*

2.4.1 Expression of full length CcoP in *E. coli*

A single colony of JM109 (DE3) cells co-transformed with pEC 86 and pCcoPall was selected from antibiotic supplemented LB agar plates. The colony was used to inoculate 50 mls LB medium, which was incubated overnight at 37 °C while being shaken (200 rpm). 4 mls of the bacterial suspension was used to inoculate 400 mls TYP medium in a 2 L baffled flask and grown at 30 °C for 30 hours while being shaken (200 rpm). As required, appropriate antibiotics were added to all media.

2.4.2 Purification of full length CcoP

The cells were harvested by centrifugation at 10,000 g, 4 °C, for 20 minutes and resuspended in cold 20 mM Tris-HCl, 5 mM EDTA pH 8. The bacterial cells were disrupted by two passes through a French pressure cell operated at 1200 p.s.i. To digest the DNA during cell lysis, and hence to reduce the viscosity of the sample, DNase (Sigma, UK) was added to the cell suspension prior to French press. Following cell breakage the protease inhibitors: AEBSF (1 mM), leupeptin (1 µM), pepstatin (1 µM), MgCl (2 mM) and EDTA (5 mM) were added. The solution was centrifuged at 5,000 g, 4 °C, for 10 minutes to remove any unbroken cells and the supernatant was centrifuged for a further 2 hours at 186,000 g, 4 °C. Following centrifugation the pellet containing the cell membranes was resuspended in 20 mM Tris-HCl, 50 µM EDTA, 500 mM NaCl, pH 8. An

equal volume of 10 M Urea was added to wash the membranes. The resulting suspension was centrifuged at 142,000 g, 4 °C for 1 hour. Following centrifugation the membranes were resuspended in 20 mM Tris-HCl, 50 µM EDTA, 100 mM NaCl, pH 8.

Solubilisation of the membrane proteins was achieved by stirring the resuspended membranes in 20 mM Tris-HCl, 50 µM EDTA, 100 mM NaCl, pH 8, with the appropriate amount of DM (2.5g of DM per g of protein) overnight at 4°C. The total protein concentration of the resuspended membranes was determined using the bicinchoninic acid protein assay as described in Section 2.2.1. Following solubilisation, the protein solution was centrifuged at 142,000g, 4 °C for 45 minutes. The resulting supernatant was diluted three fold in 20 mM Tris-HCl, 50 µM EDTA, 25mM NaCl, pH 8 and loaded onto a DEAE Fast Flow 75 ml anion exchange column pre-equilibrated with 20 mM Tris-HCl, 50 µM EDTA, 25 mM NaCl, 0.05 % w/v Triton, pH 8. The bound protein was washed for 10 column volumes with 20 mM Tris-HCl, 50 µM EDTA, 50 mM NaCl, 0.05 % w/v Triton, pH 8 and elution of the sample was achieved by a stepwise salt gradient (20 mM Tris-HCl, 50 µM EDTA, 100 - 150 mM NaCl, 0.05 % w/v Triton, pH 8). Following each 25mM increment of NaCl the column was washed for 3 column volumes. CcoP eluted with 125 mM NaCl.

Chromatographic fractions enriched in *c*-type heme were combined and concentrated using an Amicon ultrafiltration cell (Amicon, MA, USA) with a 30,000 kDa cut off membrane (YM30). The concentrated protein was diluted 5 fold in 20 mM Tris-HCl, 50 µM EDTA, 25 mM NaCl, 0.02% w/v DM, pH 8 and loaded onto a 5 ml Q Sepharose HP column (GE Healthcare, UK) pre-equilibrated with 20 mM Tris-HCl, 50 µM EDTA, 25 mM NaCl and 0.02% w/v DM, pH 8. The bound protein was washed with the same buffer for a minimum of 10 column volumes. The purpose of this chromatographic step was not only further protein purification but also to exchange the detergent Triton X-100 for DM.

The detergent, Triton X-100 has an absorbance of A_{280} , and the replacement detergent, DM does not. It was therefore possible to monitor the column eluent for successful detergent exchange. Once the Triton X-100 used for separation chromatography was exchanged for DM, the bound protein was eluted with 20 mM Tris-HCl, 50 μ M EDTA, 300 mM NaCl, 0.02% w/v DM, pH 8 using a linear NaCl gradient (25 – 300 mM NaCl) over 10 column volumes. The chromatographic fractions containing *c*-type heme were combined and concentrated using an Amicon ultrafiltration cell with 30,000 kDa cut off membrane (YM30). The concentrated protein was snap frozen in liquid nitrogen and stored at -80°C .

2.5 Expression, purification and mutagenesis of variant full length CcoP from *P. stutzeri*

2.5.1 Site-directed mutagenesis

Site-directed mutagenesis was performed to change a single amino acid in *ccoP* to an alanine (pCcoPallH42A), cysteine (pCcoPallH42C) and methionine (pCcoPallH42M). Site-Directed mutagenesis was carried out using the methods outlined in section 2.3.4.

Complementary forward and reverse mutagenic oligonucleotide primers were designed to include a unique restriction site as shown in table 2.3. The unique restriction site allows for quick and easy screening of the mutants.

	Primer	Restriction Site incorporated
CcoPH42A (H42A)	GAAACCGTCGGG GCTAGC TATGACGGC CTTTGGCAGCCC CGATCG AATACTGCCG	Nhe1
CcoPH42C (H42C)	GAAACCGTCGGG TGCTCA TATGACGGC CTTTGGCAGCCC ACGAGT AATACTGCCG	Nde1
CcoPH42M (H42M)	GAAACCGTCGGG ATGTCA TATGACGGC CTTTGGCAGCCC TACAGT AATACTGCCG	Nde1

Table 2.3 Primers designed for Site-Directed Mutagenesis of CcoP. The oligonucleotides were designed to encode a new restriction site within the gene, which was used to screen colonies for confirmation of successful mutagenesis. The restriction sites incorporated for each mutation are indicated. The mutated amino acids are indicated in red.

The reagents for the preparation of each mutated plasmid are indicated in Table 2.4.

	pCcoPallH42A	pCcoPallH42C	pCcoPallH42M
10x reaction buffer	5 µl	5 µl	5 µl
DsDNA template (CcoPall)	5 ng	5.4 ng	5.7 ng
oligonucleotide primer #1 (100µM stock)	0.5 µl	0.5 µl	0.5 µl
oligonucleotide primer #2 (100µM stock)	0.5 µl	0.5 µl	0.5 µl
dNTP mix	1 µl	1 µl	1 µl
Pfu polymerase (2.5U stock)	1 µl	1 µl	1 µl

Table 2.4 Reagents used for Site-directed mutagenesis of full length CcoP. Each reaction was made up to a total volume of 50 µl using sterile distilled water

The PCR conditions were as outlined previously in section 2.3.4. and were the same for each mutant generated.

2.5.2 Expression and purification of variant full length CcoP

Expression and purification of variant full length CcoP was prepared using the same conditions set out for recombinant full length CcoP (Section 2.4.1 and 2.4.2).

Throughout this study recombinant full length CcoP will be referred to as CcoP and the variants CcoPH42A, CcoPH42C and CcoPH42M will be referred to as H42A, H42C and H42M, respectively. The truncated soluble form of CcoP, described in section 2.6, will be referred to as truncated CcoP (tr-CcoP).

2.6 Expression and purification of truncated CcoP from *P. stutzeri*

2.6.1 Expression of truncated CcoP

A colony of JM109 (DE3) cells co-transformed with pEC 86 and pCcoPsol was selected off antibiotic supplemented LB agar plates. The colony was used to inoculate 50 mls LB medium, which was incubated overnight at 37 °C while being shaken (200 rpm). 4 mls of the bacterial suspension was used to inoculate 400 mls TYP medium in a 2 L baffled flask that was grown at 30 °C for 30 hours while being shaken (200 rpm). As required, appropriate antibiotics were added to all media.

2.6.2 Purification of truncated CcoP

The cells were harvested by centrifugation at 10,000 g, 4 °C for 20 minutes and the cell pellet was resuspended in cold sphaeroplast buffer (100 mM Tris-HCl, 500 mM sucrose, 1 mM EDTA, pH 8). The resuspended cells were incubated on ice for 10 minutes and the

following additions were made 1 mM AEBSF, 1 μ M leupeptin, 1 μ M pepstatin, 2 mM $MgCl_2$. The solution was centrifuged at 10,000 g, 4 °C for 10 minutes to sediment unbroken cells. The resulting supernatant was incubated at 4 °C and stirred while solid ammonium sulphate was slowly added to 30 % saturation. This solution was centrifuged at 20,000 g for 30 minutes at 4 °C, and the precipitate of unwanted proteins discarded. The orange supernatant was reincubated at 4 °C and was taken to 70 % saturation by the further addition of ammonium sulphate. The solution was centrifuged at 20,000 g for 30 minutes, 4 °C, and the pale yellow supernatant discarded. The red precipitate containing tr-CcoP was resuspended in a minimum volume of 20 mM Tris HCl, 50 μ M EDTA, 25 mM NaCl, pH 8 and dialyzed at 4 °C overni ght against the same buffer.

The dialyzed protein was loaded onto a DEAE Fast Flow 75 ml anion exchange column equilibrated with 20 mM Tris-HCl, 50 μ M EDTA, 25 mM NaCl, pH 8. The bound protein was washed for 2 column volumes with 20 mM Tris-HCl, 50 μ M EDTA, 50 mM NaCl, pH 8 and elution of the sample was achieved by a stepwise salt gradient, in the elution buffer, 20 mM Tris-HCl, 50 μ M EDTA, 100 - 200 mM NaCl, pH 8. Following each increment of 50 mM NaCl, the column was washed for 3 column volumes. Tr-CcoP eluted from the column with 150mM NaCl. Chromatography fractions enriched in *c*-type heme were combined and concentrated to 2 ml using an Amicon ultrafiltration cell with a 10,000 kDa cut off membrane (YM10). The concentrated protein was rapidly frozen in liquid nitrogen and stored at – 80 °C.

2.7 Growth conditions and purification of the two *Cbb*₃ isozymes from *P. aeruginosa*

2.7.1 Growth conditions of *Cbb*₃ oxidase

Large scale expression of the cytochrome *cbb*₃ oxidases was initiated by inoculation of 5 mls LB with 15µl of appropriate glycerol stock. Following incubation for 6 hours at 37 °C, with shaking at 200 rpm, 1 ml of this culture was used to inoculate 50 ml flasks of LB, which were incubated overnight at 37 °C, with shaking at 200 rpm. From this overnight culture 25 mls was used to inoculate asparagine medium. For the growth of aerobic cultures the total volume of asparagine medium was 500 mls in a baffled flask. The cells were continuously shaken (200 rpm) during growth. For the growth of semi aerobic cells the total volume of asparagine medium was 1 L in 2 L unbaffled flasks. The cells were grown with slow agitation (135 rpm). Under both conditions the cells were grown to mid-log phase (approx. 24 hours). Following the appropriate incubation period the cells were harvested by centrifugation at 10,000 g, 4 °C for 20 minutes and the whole cells were rapidly frozen in liquid nitrogen and stored at - 80 °C.

The strain CoxΔ1 was not propagated directly from the glycerol stock. 20 µl of the glycerol stock was used to inoculate a gentamicin supplemented agar plate which was incubated overnight at 37 °C. A single colony was used to inoculate 5 mls LB which was incubated at 37 °C for 16 hours, shaking at 200 rpm. 50 µl of this bacterial culture was used to inoculate 50 ml flasks of LB which were incubated overnight at 37 °C, with shaking at 200 rpm. From this overnight culture 25 mls was used to inoculate asparagine medium. All cultures were supplemented with the appropriate antibiotics.

2.7.2 Preparation of membranes

The cells were harvested by centrifugation at 10,000 g, 4 °C for 20 minutes and the cell pellet was resuspended in 20 mM Tris-HCl, 50 µM EDTA, pH 8.5 followed by the addition of 5 µg DNase. Two passes through a French pressure cell operated at 1200 p.s.i disrupted bacterial cells in the suspension. After breaking the cells the following additions were made: 1 mM AEBSF, 1 µM leupeptin, 1 µM pepstatin, 2 mM MgCl and 5 mM EDTA. The solution was centrifuged at 5,000 g, 4 °C for 10 minutes to remove any unbroken cells. The resulting supernatant was spun for 2 hours at 186,000 g, 4 °C. Following centrifugation the pellet, containing the cytoplasmic membranes, was resuspended in 40 ml 20 mM Tris-HCl, 2.5 mM EDTA, pH 8.5. To remove any peripheral proteins 100 ml Tris-HCl, 2.5 mM EDTA, 500 mM NaCl , 0.08% (w/v) sodium deoxycholate (DOC), pH 8.5 was added drop wise while the protein suspension was being stirred on ice. Following addition of the buffer containing DOC the suspension was stirred continuously on ice for 15 mins and re-sedimented by ultracentrifugation at 142,000 g, 4 °C for 1 hour. The resulting membranes were resuspended in 20 mM Tris-HCl, 50 µM EDTA, 25 mM NaCl, pH 8.5. The total protein concentration was determined by the BCA protein assay (section 2.2.1).

2.7.3 Purification of cytochrome *cbb₃-1* and *cbb₃-2*

Solubilisation of the membrane proteins was achieved by stirring a suspension of the *cbb₃* oxidase containing membranes in 20 mM Tris-HCl, 50 µM EDTA, 100mM NaCl, pH 8.5 with the appropriate amount of DM (2.5 g of DM per g of protein) overnight at 4 °C. The supernatant, obtained after centrifugation at 142,000g for 45 minutes at 4 °C, was diluted three fold in 20 mM Tris-HCl, 50 µM EDTA, 25 mM NaCl, pH 8.5 and loaded onto a Q

Sepharose Fast Flow 100ml anion exchange column equilibrated with 20 mM Tris-HCl, 50 μ M EDTA, 25 mM NaCl, 0.02% w/v DM, pH 8.5. The elution buffer was 20 mM Tris-HCl, 50 μ M EDTA, 500 mM NaCl, 0.02% w/v DM, pH 8.5 and elution of the *cbb*₃ oxidase was achieved with the application of a stepwise gradient. The column was washed with 50 mM NaCl, the NaCl concentration was increased to 200 mM and stepwise increments of 50 mM NaCl were applied to a final concentration of 300 mM. At each step, the column was washed for 2 column volumes. Following the final stepwise increment, the NaCl concentration was increased to 500 mM and washed for 2 column volumes.

Fractions enriched in *c*-type heme were combined and concentrated using an Amicon ultrafiltration cell using a membrane with a 30,000 kDa cut off (YM30). The concentrated protein was diluted 5 fold in 20 mM Tris-HCl, 250 mM NaCl, 0.02% w/v DM, pH 8.5 and loaded onto a 5 ml Hi trap metal chelating column pre-equilibrated with 20 mM Tris-HCl, 250 mM NaCl and 0.02% w/v DM, pH 8.5 following which the column was washed with the same buffer for 5 column volumes. The elution buffer was 20 mM Tris-HCl, 250 mM NaCl, 10 mM imidazole, 0.02% w/v DM, pH 8.5 and elution of the *cbb*₃ oxidase was achieved with the application of a stepwise gradient. The column was washed with 2 mM imidazole and then the imidazole concentration was increased stepwise by 2 mM to a final concentration of 10 mM. At each step the column was washed for 4 column volumes. The fractions containing *c*-type heme were combined and concentrated using an Amicon ultrafiltration cell with a membrane with a 30,000 kDa cut off (YM30). The combined fractions were dialyzed by exchange of buffer to 20 mM Tris-HCl, 50 μ M EDTA, 25 mM NaCl, 0.02% w/v DM, pH 8.5 using an Amicon ultrafiltration cell. Following buffer exchange the protein was applied to a 5 ml fast flow DEAE column (GE Healthcare, UK) which had been equilibrated with 20 mM Tris-HCl, 50 μ M EDTA, 25 mM NaCl, 0.02% w/v DM, pH 8.5. The elution buffer was 20 mM Tris-HCl, 50 μ M EDTA, 500 mM NaCl, 0.02% w/v DM, pH 8.5 and elution of the *cbb*₃ oxidase was achieved with the

application of a stepwise gradient. The column was washed with 50 mM NaCl, the NaCl concentration was increased to 200 mM and stepwise increments of 50 mM NaCl were applied to a final concentration of 300 mM. At each step the column was washed for 4 column volumes. Following the final stepwise increment, the NaCl concentration was increased to 500 mM and washed for 2 column volumes.

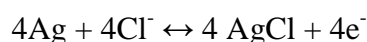
Following chromatography purified *cbb*₃ oxidase was concentrated in an Amicon pressure cell using a membrane with a 30,000 kDa cut off (YM30). The purified protein was analyzed spectroscopically and by SDS-PAGE before being rapidly frozen in liquid nitrogen and stored at – 80 °C.

2.7.4 Oxidase activity

The consumption of oxygen by *P. aeruginosa* membranes grown in aerobic and semi-aerobic conditions was measured using a Clark type oxygen electrode (Oxytherm, Hansatech Instruments, UK) The oxygen electrode is an electrochemical cell containing a platinum cathode and a silver anode. At the platinum cathode oxygen is reduced to water:



The cathode is polarized at - 0.7 V with respect to the Ag:AgCl reference anode. Saturated KCl, which surrounds the anode, allows current to flow between the cathode and anode and silver chloride is formed on the silver anode:



The silver/silver chloride anode provides electrons for the cathode reaction.

The reductive removal of the oxygen at the cathode surface allows more oxygen in the test solution to diffuse across the permeable membrane of the cathode and for the process of

reduction to continue. The reduction of oxygen allows a current to flow between the cathode and anode, which creates a potential difference. In PC operated electrode control units the potential difference between the cathode and anode is monitored, recorded and converted into graphs using oxygraph software (Hansatech Instruments, UK). The trace is thus a measure of the oxygen activity of the reaction mixture.

The platinum electrode (cathode) was covered with a thin layer of KCl and a PTFE membrane (12.5 μM thickness) was used as a gas permeable barrier to protect the cathode from the reactants in the chamber. The Ag electrode (anode) was bathed in saturated KCl. The reaction chamber was stirred constantly during the assays and the temperature of the chamber was kept constant at 25 °C.

P. aeruginosa membranes were prepared as described in Section 2.6.2 from PAK, Cco1.1, Cco2.2, Cco Δ 1 and Cox Δ 1. The Clark-type electrode used for the measurements of oxidase activity was set up on the day of measurement, and calibrated by performing a 2-point calibration routine using air-saturated buffer and zero oxygen buffer.

Membrane samples (approx. 500 μg) or purified protein (3 - 10 μM) were diluted into 20 mM Tris-HCl, 50 μM EDTA, 100 mM NaCl, pH 8.5 in the 2 ml electrode chamber. Protein concentrations were estimated using the BCA assay method (section 2.2.1). The reaction mixture was stirred rapidly and once a steady state of oxygen consumption was achieved the appropriate electron donor was added. The concentrations of the different electron donors are outlined in table 2.5. Following injection of the electron donor, a decrease in the signal was observed as the membranes consumed the available oxygen. The rate of oxygen consumption by the membranes was calculated from the time taken for 30 % of oxygen to be consumed.

Electron Donor	Concentration
NADH	0.5 mM
Cytochrome <i>c</i> *	90 μ M
Azurin*	90 μ M
TMPD*	0-1500 μ M

Table 2.5 Concentration of electron donors used in the measurement of oxidase activity in *P. aeruginosa* membranes. * 5mM ascorbate was also added to the reaction to reduce the electron donor.

As a control the auto-oxidation of the electron donors was tested but no significant oxidation occurred. Three independent measurements were made for each membrane sample and the error bars in the presented data indicate the standard deviation (section 5.2.3).

2.8 Biophysical Methods

2.8.1 Electronic Absorbance (UV-Visible) Spectroscopy

Absorption spectra were measured at room temperature with a Hitachi U-3100 spectrophotometer or a Cary UV-50 using a quartz cuvette of 1 cm path length. Sample spectra were saved as ASCII files and re-plotted using the scientific graph software Origin.

For UV-visible spectroscopy, oxidation of the sample was achieved with the addition of potassium ferricyanide, which was subsequently removed by passing the sample down a PD-10 desalting column (Bio-Rad). Reduction of the sample was achieved by either the addition of small aliquots of sodium dithionite (Final concentration approx. 50 μ M) or ascorbate (Final concentration approx. 1mM).

2.8.2 Electron Paramagnetic Resonance (EPR) Spectroscopy

EPR is a spectroscopic technique that probes the environment of a paramagnetic centre by defining the size and shape of the magnetic moment produced by the unpaired electron (for review see More *et al.* 1999). An unpaired electron can be viewed as spinning upon its own axis, giving rise to a magnetic moment (m_s). When placed in an external magnetic field (B) the spin of the unpaired electron can align itself parallel ($m_s = + 1/2$) or antiparallel ($m_s = - 1/2$) to the field. These two electron alignments have specific energies. The parallel alignment corresponds to the lower energy state, and the separation between the lower and the upper energy, or antiparallel state, is described by the equation:

$$\Delta E = g_e \beta B$$

In the equation, g_e is the delocalized electron g value $g = 2.0023$, β is a physical constant of magnetic moment, and B is the external magnetic field. In other words, the splitting of the energy levels is proportional to the magnetic field applied, as shown in Fig. 2.1. The energy required to cause the resonance between the two parallel and antiparallel states can be induced by the application of radiation. The resonance condition can be written as:

$$h\nu = g\beta B$$

where h is Planck's constant and ν is the frequency of radiation, and g is the g factor. In an EPR experiment, g can be determined by measuring the magnetic field and the frequency at which resonance occurs. When a heme protein is placed in a magnetic field the unpaired electron in the protein resonates between the two spin states (parallel and antiparallel). The energy absorbed as it does so is converted into the EPR spectrum. For localized electrons the g value deviates from the free electron value and is determined by the environment of the unpaired electron. The g values of localized electrons can therefore give further information regarding the structure of the molecule.

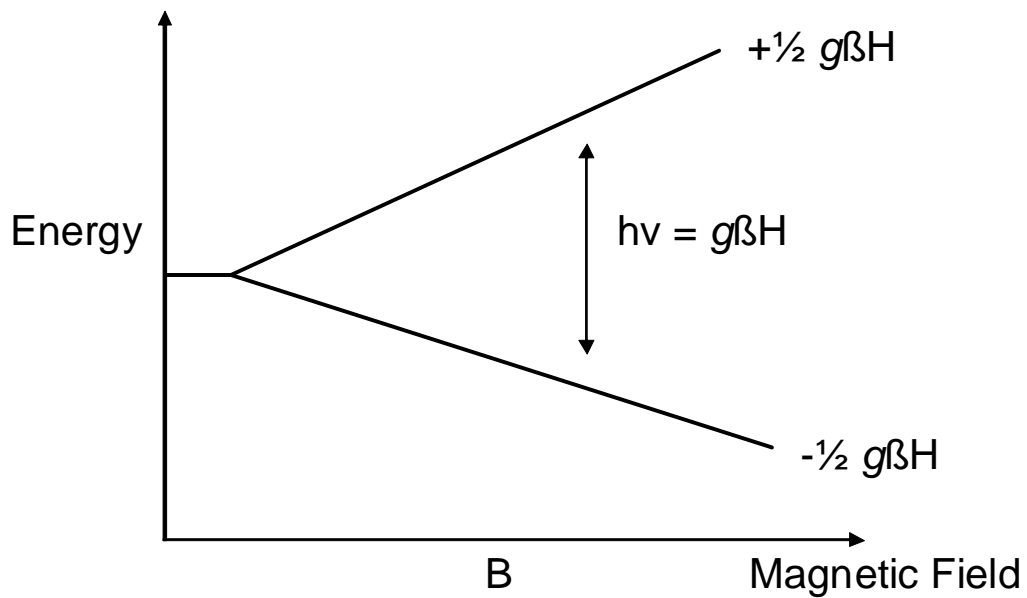


Fig. 2.1 The main condition of electron paramagnetic resonance origin. Under the influence of the external magnetic field the energy levels of the unpaired electron are split between the parallel ($m_s = + \frac{1}{2}$) and anti-parallel state ($m_s = - \frac{1}{2}$) Adapted from (Saifutdinov 2000).

EPR measurements were made by changing the magnetic field and using a constant frequency radiation. EPR spectra were recorded on a Bruker ESP-300 instrument. The spectra were recorded at 15 K, 9.68 GHz frequency radiation and 2 mW microwave power.

Samples were prepared to a concentration of approx 200 μ M in a total volume of 200 μ l. All samples were prepared in 20 mM Tris-HCl, 50 μ M EDTA, 0.02 % DM pH 8 and were oxidized using potassium ferricyanide. Quantitation of the low spin ferric heme giving rise to the EPR signals was achieved by the integration method using 1mM Cu (II) EDTA as a spin concentration standard (Aasa and Vänngård 1975).

2.8.3 Magnetic Circular Dichroism (MCD) Spectroscopy

Magnetic circular dichroism is the differential absorption of left and right circular polarized light induced in a molecule by the application of a magnetic field (for review see Kirk and Peariso 2003). MCD measurements are made by taking a circular dichroism measurement of the protein of interest with the magnetization oriented in the positive sense, and then repeating the measurement with the magnetization oriented in the negative sense. The two signals are subtracted to give the MCD spectrum.

MCD spectroscopy can be used to probe the electronic structure of metalloenzymes. Orbital overlaps between the π orbitals of the porphyrin ring and the d-orbitals of the heme iron results in distinct MCD spectral features. Specifically, bands in the UV-visible region (300-600 nm) of heme MCD spectra are diagnostic for the spin state and concentration of ferric hemes. In the near infrared (NIR) region (600-2500 nm) of the spectrum, features that arise from porphyrin to metal charge transfer (CT) transitions are observed. The positions of the high-spin and low-spin CT transitions are sensitive to the nature of the axial ligands of the heme centre (Fig. 2.2).

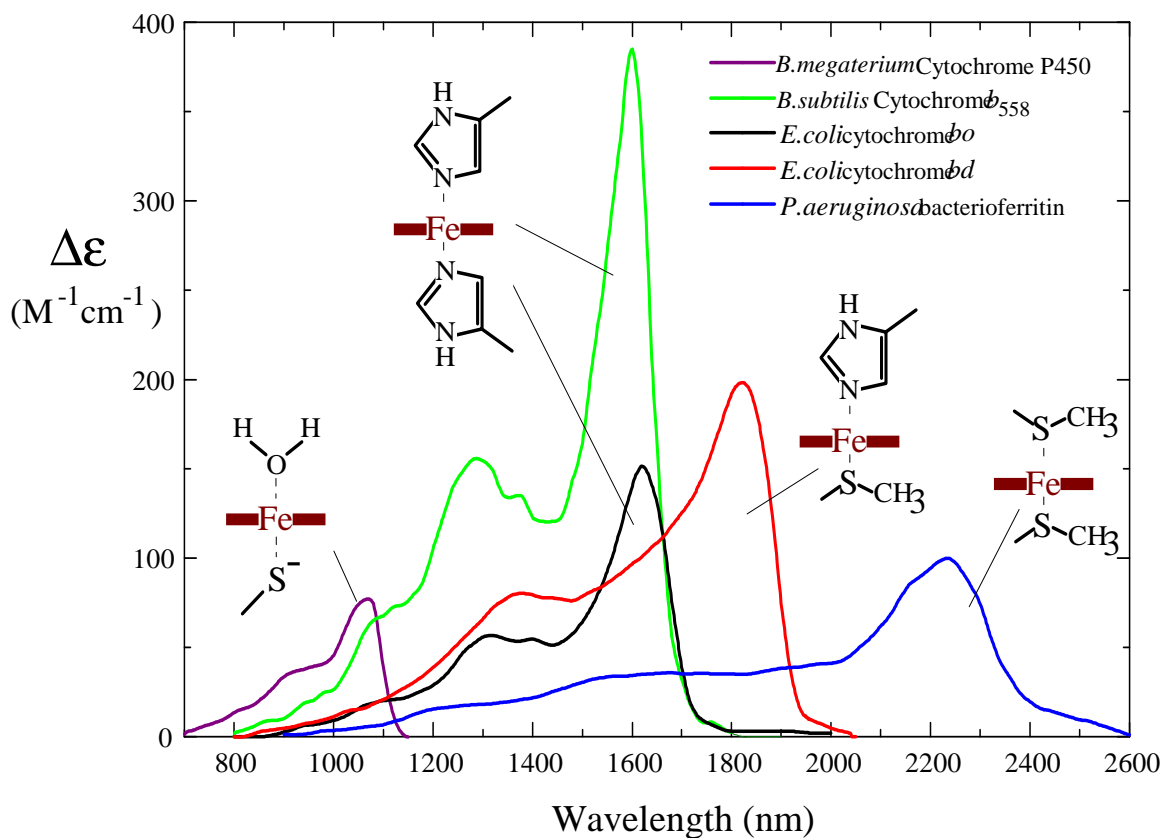


FIG. 2.2 The energy of the low-spin ferric heme transitions in the Near infrared region (NIR) is sufficiently sensitive to coordination of the heme to identify axial ligands. The NIR-MCD of several proteins is shown and the ligation state of the heme is indicated: Purple line, Cytochrome P₄₅₀ from *Bacillus megaterium*; Green line: Cytochrome b_{558} from *Bacillus subtilis*; black line: Cytochrome bo_3 oxidase from *E. coli*; red line; Cytochrome bd oxidase from *E. coli*, blue line: bacterioferritin from *P. aeruginosa*. All the samples were recorded at 4.2 K (Cheesman 2006).

MCD measurements were recorded on either a JASCO J-500D for the wavelength range 280-1000 nm or a JASCO J-730 circular dichrograph for the range 800-2000 nm using a split coil superconducting solenoid capable of generating magnetic fields up to 6 T. MCD spectra were obtained at room temperature (RT-MCD) and at low temperature (LT-MCD). All samples for magneto-optical spectroscopy were prepared in deuterated 20 mM Tris-HCl, 50 μ M EDTA, 0.02% DM, pH 8. All samples were oxidized using potassium ferricyanide. For low temperature MCD measurements, the glassing agent glycerol was added to samples to a level of 50 % (v/v).

2.9 Other Biophysical Methods

2.9.1 Mediated Redox Potentiometry

The midpoint reduction potential (E°) is the solution potential at which the concentration of oxidized heme protein equals the concentration of reduced protein. Mediated spectrophotometric redox potentiometry was undertaken essentially as described by Dutton (Dutton 1978).

Titration were performed in a specially designed 1 cm path length quartz cuvette (Fig. 2.3). The cuvette had a large septum through which the platinum Ag/AgCl combination electrode (Metrohm) with an attached digital display (Mettler Toledo) was immersed into the protein for monitoring the solution potential. The electrode was calibrated prior to the each titration using a saturated solution of quinhydrone (hydroquinone/benzaquinone 1:1 complex; $E^\circ = + 295$ mV) in 20 mM Tris-HCl pH 8 for 30 minutes. The resting potential of the electrode should be 295 mV relative to the standard hydrogen electrode (SHE). The difference between 295mV and the potential recorded for the hydroquinone complex was added to each reading. For example, if the quinhydrone-immersed electrode showed a

solution potential of + 74 mV, every measurement required the addition of 221 mV to the reading so the potential readings were standardized against SHE.

To maintain anaerobicity of the protein during the titration, the sample was flushed with Argon via the glass side arms of the cuvette. The redox mediators were introduced to the sample through a third side arm of the cuvette. All the glass side arms were sealed with rubber septa for the duration of the experiment. Redox mediators are electron buffering agents and were present throughout the titration to stabilize the potential of the solution. Electron transfer to and from the active sites of redox enzymes is sometimes difficult to achieve because they are buried in an insulating protein shell. In addition to stabilizing the potential of the solution, redox mediators also shuttle electrons between the protein and electron donor. The reduction potential of each redox mediator and the concentrations used are listed in Table 2.6. All the mediators were purchased from Sigma. Following the addition of redox mediators and the oxidizing agent to the protein, the cuvette system was deoxygenated for at least one hour with argon. This allowed the system to equilibrate before the addition of reducing agents. A small magnetic stirring bar was placed at the bottom of the cuvette to mix the reagents after additions.

When the system had reached equilibrium, a UV-visible spectrum of the initial sample was recorded using a U3100 Hitachi Spectrophotometer. During the experimental period, a circulating water bath attached to the spectrophotometer was set at 25°C to maintain the temperature of the instrument. Stock solutions of 10 – 100 mM DTT or 100 mM DT in degassed buffer were used as the reducing agent. Aliquots of the appropriate reducing agent (0.1 - 2 μ l) were added to the sample as appropriate. Following addition of the reducing agent, the sample was stirred and the system allowed to re-equilibrate for ten minutes. Following equilibration the UV-visible spectrum and solution potential were recorded. The titration was continued until the sample solution was maximally reduced

with DTT (- 330 mV) then the reducing agent was changed to DT (- 420 mV) to ensure complete reduction of the hemes in the protein.

Mediator	Approx. EmV (pH7)	Working concentration
Potassium ferricyanide	+430	25 μ M
Quinhydrone *	+295	saturated
2,3,5,6,-Tetramethyl phenylenediamine diaminodurol or DAD)	+260	10 μ M
2,6 dimethylbenzoquinone	+180	10 μ M
1,2, naphthoquinone	+140	10 μ M
N-methyl phenazonium methosulfate (PMS)	+80	10 μ M
N-ethyl phenazonium ethosulfate (PES)	+55	10 μ M
Duroquinone	+5	10 μ M
N-Methyl-1-hydroxyphenazonium methosulfate (pyocyanine)	-34	10 μ M
Menadione	-70	10 μ M
2-Hydroxyl-1,4-naphthoquinone	-152	10 μ M
Anthraquinone-2,6-disulfonate	-185	10 μ M
Anthraquinone-2-sulfonate	-225	10 μ M
Benzyl viologen	-252	10 μ M
N,N-dimethyl-4,4-bipyridinium dichloride (methyl viologen)	-430	10 μ M

Table 2.6 Midpoint Potential of the mediators used for redox titrations

* Not added to the sample. Used to calibrate the electrode prior to the start of each titration

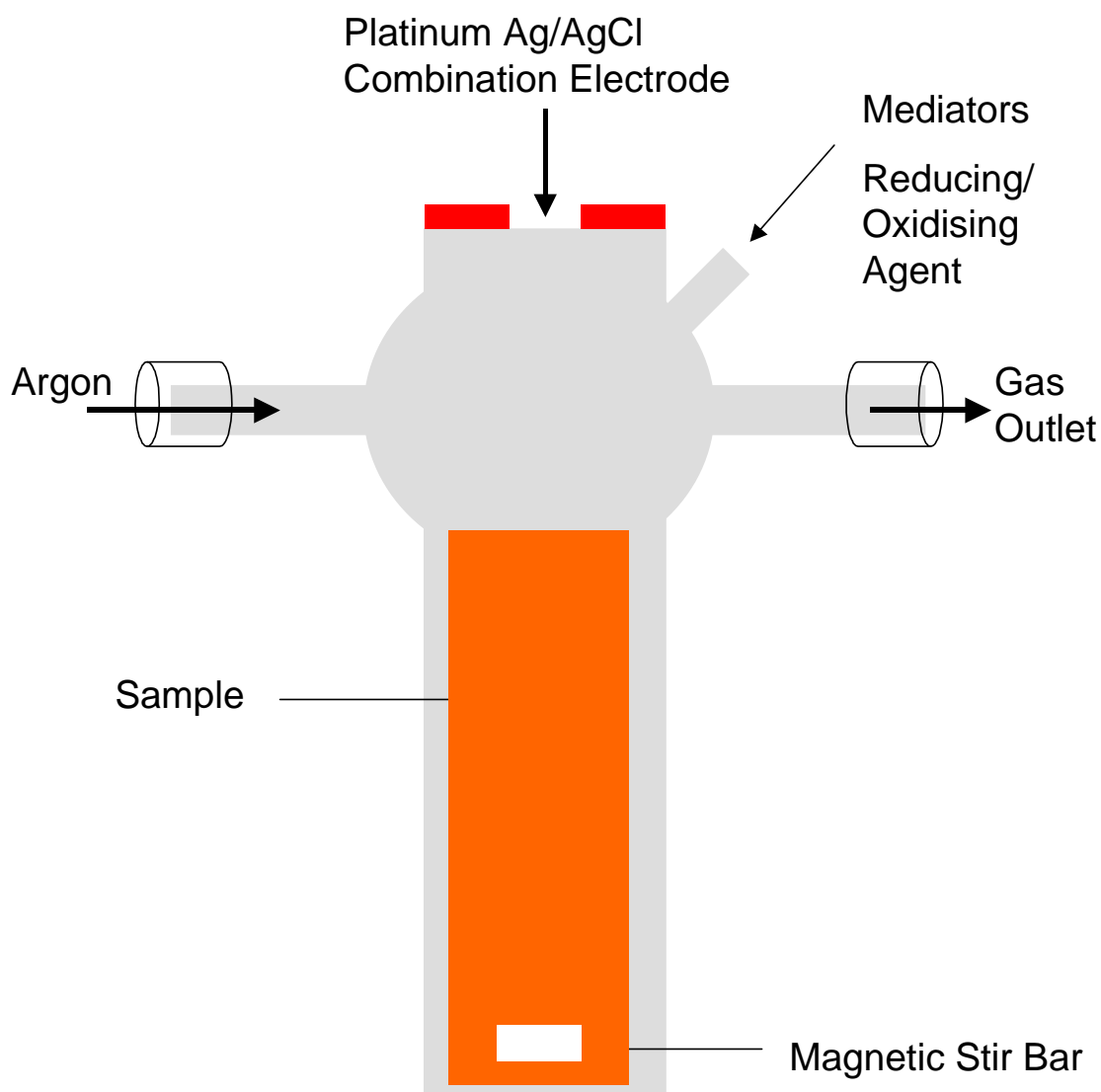
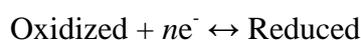


FIG. 2.3 Schematic Diagram of 1 cm quartz cuvette used for redox titrations

Redox titration data was exported as ASCII files and imported into Excel. The difference between the absorbance at the α -max wavelength for the reduced cytochrome and the absorbance at an isosbestic point were calculated using Excel and the absorbance difference was plotted against the potential of the system using Origin (OriginLab). A customized program in Table-curve 2D (Jandel Scientific) was used to fit the data points to a number of Nernstian components.

The experimental redox potential (E) for the redox couple:



is given by the Nernst equation:

$$E = E^\circ + 2.3 (RT/nF) \log_{10} [\text{oxidized}]/[\text{reduced}]$$

where E° is the standard reduction potential, R is the universal gas constant, T is the absolute temperature, n is the number of electrons and, F is the Faraday constant.

The Nernst equation can be written in Table Curve as:

$$F1=(x/[1+EXP (0.038* [X-\#A])])$$

$$Y=F1+\#B$$

This is the equation for a single electron reaction where $n = 1$. The parameter x represented the total amplitude of the absorbance change. The equation can be used to derive a Nernstian curve fit to the data points. The coefficient of determination (r^2), also known as the goodness of fit, for each Nernstian curve fit is noted in the appropriate figure legends. It is computed as the fraction of the total variation of the Y values of data points that is attributable to the assumed model curve. As a fit becomes more ideal the r^2 value approaches 1. A value of 0 represents a complete lack of fit.

2.9.2 CO Titrations

Under anaerobic conditions, purified CcoP (2 - 4 μM) was placed into a 3 ml cuvette, reduced with excess sodium dithionite and left to equilibrate for 30 minutes. The cuvette was sealed and the UV-visible spectrum of the sample was recorded. To prepare the saturated CO solution (1 mM), CO gas was bubbled through oxygen free buffer (20 mM Tris-HCl, 50 μM EDTA, 0.02% DM, pH 8) for approximately 15 minutes (Hargrove 2000).

Using a gas tight syringe, the initial 0.5 μl aliquot of CO equilibrated buffer (1 mM) was added, and the system was allowed to equilibrate for 10 minutes. Following equilibration, the UV-visible spectrum was recorded (Fig. 2.4). The binding of CO to a heme iron induces visible spectroscopic changes in the absorption spectrum of the heme. Upon CO binding to fully reduced CcoP the Soret band shifts from 417 nm to 416 nm, an increase in intensity of the Soret band can be observed and a decrease in the intensity of the β and α bands at 525 nm and 550 nm respectively. These features were used to monitor CO binding to the ferrous *c*-type heme. The addition of CO saturated buffer and subsequent steps were repeated until no further spectral changes were observed. Data was exported as ASCII files and exported to Excel. The fractional saturation (Y), the ratio of the observed A_{415} to A_{415} recorded after complete formation of the CO adduct, was plotted against CO concentration (μM) using the scientific graph software Origin. The K_d values were obtained by fitting the experimental data to a hyperbolic function using non-linear least squares using Table Curve 2D.

$$Y = 1 * ((\#B * X) / (1 + (\#B * X)))$$

where #B is the K_d and assuming that CO only binds to a single heme.

Anaerobic conditions were maintained throughout by using a gas tight syringe for all additions of CO. The titrations were performed at room temperature.

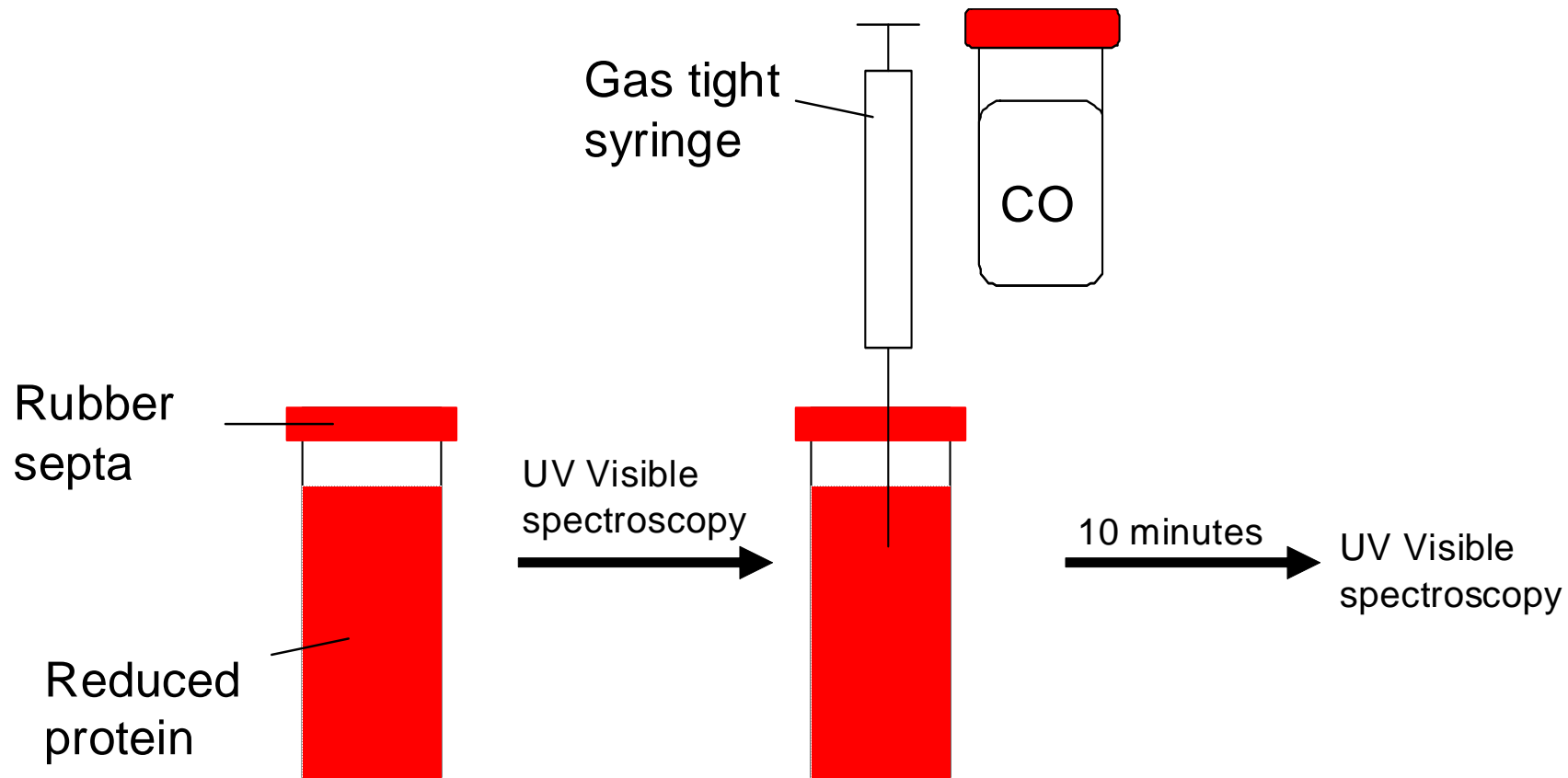


FIG 2.4 Schematic representation of CO titration protocol

3. Biochemical and Spectroscopic Characterization of Full Length CcoP and Truncated CcoP

3.1 Introduction.....	91
3.2 Results and Discussion.....	94
3.2.1 Optimization of Growth and Purification.....	94
3.2.2 UV-Visible Spectroscopy.....	101
3.2.3 Mediated Redox Potentiometry.....	106
3.2.4 EPR Spectroscopy.....	115
3.2.5 MCD Spectroscopy.....	121
3.2.6 CO Binding Studies.....	133
3.3 Conclusions.....	138

3.1 Introduction

Cytochrome *cbb*₃ oxidases are bacterial heme copper oxidases that are predicted to contain four membrane-bound subunits, CcoN, CcoO, CcoQ and CcoP (Chapter 1, Section 1.5). However, in none of the cytochrome *cbb*₃ oxidase preparations reported to date has there been any evidence of CcoQ being part of the enzyme complex after purification (Preisig *et al.* 1996; Pitcher, 2002; Hemp *et al.* 2007). The subunit CcoN harbours the binuclear centre (active site) heme *b*₃-Cu_B and a low spin heme *b* (Zufferey *et al.* 1998). A subunit analogous to CcoN is common to all members of the heme copper oxidase superfamily (García-Horsman *et al.* 1994). The subunit CcoO is homologous to the Nitric Oxide Reductase subunit NorC (Preisig *et al.* 1993; Saraste and Castresana 1994; Sharma *et al.* 2006). In the divergent heme-copper oxidase NOR, the NorC subunit serves as the electron receiver for periplasmic donors (Saraste and Castresana 1994; Thorndycroft *et al.* 2007). Consequently, it is proposed that electrons are transferred to the catalytic subunit CcoN by the monoheme subunit CcoO (Pitcher *et al.* 2002; Verissimo *et al.* 2007). The function of the diheme *cbb*₃ subunit, CcoP, remains unclear. However, the observed catalytic competency of the CcoNO sub complex suggests that CcoP does not necessarily play a role in electron transfer, therefore supporting the suggestion that the electron transfer role is fulfilled by the subunit CcoO (de Gier *et al.* 1996; Zufferey *et al.* 1996).

Evidence suggests that the one of the heme centers in the CcoP subunit is able to bind CO, an analogue of oxygen (Pitcher *et al.* 2003). Previously it was believed that only penta-coordinate ferrous hemes could bind exogenous ligands. However, a class of heme based sensors have been described in which the heme iron is coordinated at both axial ligands by amino acid residues (Gilles-Gonzalez and Gonzalez 2005). In heme based sensors, one of the amino acids must be displaced to bind exogenous ligands, this is commonly observed in hemes that play a regulatory role in the protein (Shelver *et al.* 1997; Delgado-Nixon *et al.* 2000). The *c*-type hemes in the diheme, *cbb*₃ subunit CcoP are reported to be

hexacoordinate and it has previously been suggested that in CcoP, CO binding is preceded by displacement of an endogenous ligand (Pitcher *et al.* 2002; Pitcher *et al.* 2003). Plant and vertebrate globins have also been reported that bind CO in the ferrous state and are hexa-coordinate and appear to have some role in the physiological responses to hypoxia (Arredondo-Peter *et al.* 1998; Sowa *et al.* 1998; Sun *et al.* 2001). It is not clear if the binding of CO, an analogue of O₂ and NO, observed in CcoP indicate any physiological significance.

A spectroscopic characterization of recombinant CcoP from *P. stutzeri* has previously been completed (Pitcher 2002; Pitcher *et al.* 2002). NIR-MCD analysis of CcoP suggested that one of the *c*-type hemes of this subunit has His/Met ligation and the second heme is His/His coordinated (Pitcher 2002). It has not been possible, however, to confirm these ligations structurally, since it has proved difficult to crystallize the membrane protein, *cbb*₃ oxidase, and the individual subunit, CcoP, for structural determination (Geimeinhardt 2006). Obtaining well diffracting crystals of membrane proteins, including the *cbb*₃ oxidases, can be affected by the presence of detergent (Columbus *et al.* 2006; Prive 2007). The use of detergent in purified membrane proteins is, however essential to maintain the protein in a functional folded state in the absence of a lipid membrane (Prive 2007). The crystallization of soluble proteins is not as challenging due to a lack of detergent in the protein buffers (McPherson *et al.* 1986; Prive 2007). An alternative approach was to construct an expression vector that expressed only the heme *c* containing domain of CcoP (Pitcher 2002). Using methods similar to those reported by Bamford *et al.* this heme containing soluble domain was cloned into the expression vector pET 22b (Novagen, UK) to create the construct, truncated CcoP (Bamford *et al.* 2002; Pitcher 2002). The vector pET 22b carries an N-terminal *pelB* signal sequence to direct export of the polypeptide to the periplasmic region and ensures posttranslational modification of the protein by covalent attachment of the two hemes.

Using hydrophobic analysis, a predication of the transmembrane topology of a given protein can be made. The software program, TMHMM, (Center for Biological Sequence Analysis, Denmark), gives the probable location and orientation of transmembrane helices in the sequence by using an algorithm of all paths through the model with the same location and direction of the helices (Krogh *et al.* 2001). The TMHMM program was used in this study to analyse the primary structure of CcoP from the DNA sequence, and hence confirm the location of the soluble domain of CcoP used by Pitcher *et.al.* for construction of the plasmid tr-CcoP. The CcoP subunit in *cbb₃* oxidases is predicated to have two transmembrane helices spanning amino acids 1-79. Amino acids 4 - 26 are predicated to form the first transmembrane helix, with amino acids 27 - 56 spanning the two helices on the cytoplasmic side of the membrane. Amino acids 57 – 79 are predicted to form the second transmembrane helix from the cytoplasmic side to the periplasm. The soluble domain of CcoP, amino acids 80 - 301, is located in the periplasm and includes the two-heme binding domains of CcoP.

The water-soluble form of CcoP (truncated CcoP) can be purified without the use of detergent so the protein could be used for crystallization trials. This soluble form of CcoP has not previously been characterized. Therefore, prior to crystallisation trials it was important to determine whether the biophysical properties of tr-CcoP were identical to full length CcoP.

Previously a combination of UV-visible spectroscopy, mediated redox potentiometry, EPR and MCD spectroscopy were used to identify the axial ligands to the two *c*-type hemes in CcoP (Pitcher 2002). CcoP was predicted to have one His/His ligated heme and one His/Met ligated heme. A similar approach was used to determine whether the axial ligands to the hemes in tr-CcoP were identical to those in the full length protein.

Recent completion of the genomic sequence of *P. stutzeri* revealed that this γ -Proteobacterium contains a pair of *ccoNOQP* operons that each potentially encode a *cbb*₃ oxidase (*cbb*₃-1 and *cbb*₃-2) (Yan *et al.* 2008). A consensus sequence (TTGAT-N4-GTCAA), that recognizes members of the FNR family of transcriptional regulators is located 100 base pairs upstream of the *ccoN* start codon on one of the *P. stutzeri cbb*₃ operons (Yan *et al.* 2008). This is consistent with the observation that FnrA is required by *P. stutzeri* for the expression of cytochrome *cbb*₃ under microaerophilic conditions (Vollack *et al.* 1999). The other *P. stutzeri cbb*₃ operon does not have an FNR or FNR homologue binding site. These observations suggest that the two *P. stutzeri ccoNOQP* operons are independently regulated from distinct promoters. The *P. stutzeri* CcoP subunit used throughout this study is isolated from the FNR independent *cbb*₃ operon.

3.2 Results and Discussion

3.2.1 Optimization of growth and purification

Purification of full length CcoP

In my hands, the method reported by Pitcher *et al.* to grow and purify CcoP did not yield sufficiently pure protein (Pitcher *et al.* 2002). Cytochrome *bd* oxidase is a quinol oxidase from *E. coli* which is optimally expressed under microaerophilic conditions (Yang *et al.* 2007). Under the micro-aerobic conditions, required for the expression of CcoP, cytochrome *bd* is therefore also expressed and was readily identifiable by its characteristic spectrum with absorption peaks at 431, 560 and 630 nm. However, cytochrome *bd* oxidase proved difficult to separate from CcoP because it eluted from the first anion exchange column immediately prior to CcoP. The initial chromatographic step employed was the anion matrix DEAE sepharose. Additional chromatographic steps using a Hi-trap chelating column and a Mono Q column failed to produce improved resolution and a significant number of contaminating proteins including cytochrome *bd* were observed on Coomassie stained SDS PAGE and spectroscopically. Cytochrome *bd* oxidase was recognized as a

major contaminating protein as it was identified spectroscopically following the final purification step.

In an attempt to improve the purity of the final product, various modifications of the purification protocol were devised. The buffer used in the initial purification method outlined by Pitcher *et al.* was 20 mM sodium phosphate, pH 7.5 (Pitcher *et al.* 2002). However, ideally simple counter ions (e.g. Cl⁻, acetate) are used as buffering agents in anion exchange chromatography (Scopes 1994). Hence, to refine the purification procedure the buffer was therefore changed to Tris-HCl pH 8. Compared to phosphate buffers, Tris (pKa = 8.06) has a good buffering capacity above pH 7.5, (Good *et al.* 1966).

The purity of CcoP did not however improve significantly when the protein was chromatographed using Tris-HCl buffer. As no change in purity of CcoP was observed, following the change of buffer the effect of different detergents on the purification of CcoP was investigated. The non-ionic detergent Dodecyl maltoside (DM) is commonly used in the purification of membrane proteins and was therefore the first detergent of choice in the purification of CcoP. DM is effective at solubilizing membrane proteins while maintaining the functional properties of the protein (Lund *et al.* 1989; Prive 2007). In some cases, however, the detergent used to mimic the lipid bilayer in transmembrane proteins may not be able to fully mask the hydrophobic regions of a protein (Prive 2007). These hydrophobic regions can cause proteins to aggregate in order to isolate the hydrophobic surfaces from the hydrophilic environment. It was therefore hypothesized that the protein of interest, CcoP and the contaminating proteins were aggregating together. Reduced concentrations of DM in the chromatography buffers did not improve the chromatographic resolution. The use of an alternative detergent was therefore trialed for use in chromatography buffers. The detergent that yielded optimal chromatographic resolution was Triton X-100. The use of Triton X-100 in the chromatography elution buffers

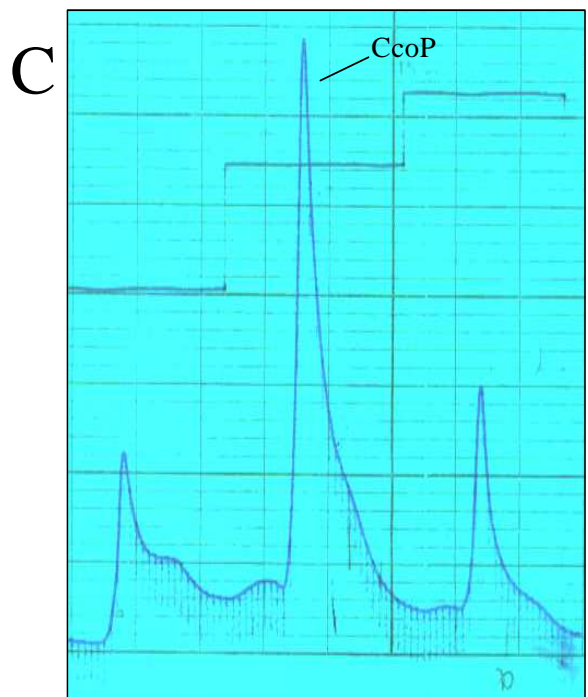
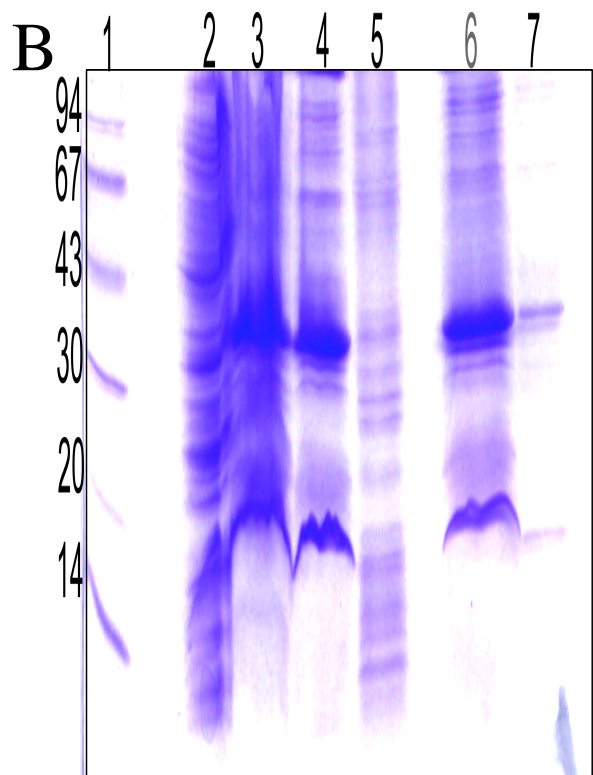
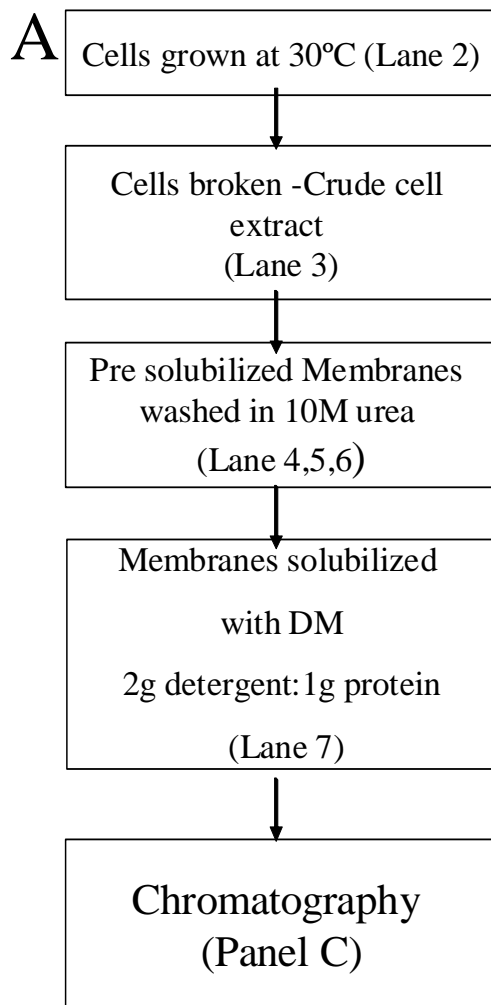
successfully separated CcoP from cytochrome *bd*. The choice of Triton X-100 did however have disadvantages. This detergent is heterogeneous and contaminants such as peroxide can arise from the manufacturing process (Bhairi 2001; Prive 2007). Moreover, Triton X-100 has an absorbance at 280 nm, therefore the detergent had to be removed from the purified CcoP prior to any spectroscopic experiments. Following purification of CcoP Triton X-100 was, exchanged for DM using chromatographic methods before accurate spectroscopic analysis of the purified protein was made. Furthermore, stability of membrane proteins is strongly dependant upon the nature of detergent used for storage (Gall and Scheer 1998). For this reason, the use of DM was maintained for solubilisation and storage of CcoP.

Throughout the purification of CcoP samples were taken at each purification step as shown in Fig. 3.1. The CcoP obtained using this revised protocol, although not 100 % pure as judged by SDS-PAGE, was spectroscopically pure; the only hemes present in the purified protein were those found in CcoP (Fig.3.2). The apparent molecular mass of the subunit was 34 kDa as judged by SDS-PAGE and was in good correspondence with a mass of 34,970 Da obtained by MALDI-TOF (Chapter 4, Section 4.2.2).

Figure 3.1 Flow diagram illustrating purification stages of CcoP from *P.stutzeri* heterologously expressed in *E. coli* (A). Corresponding gel lanes (B) are indicated in brackets.

(B) SDS PAGE of *P.stutzeri* heterologously expressed in *E. coli*. Proteins were visualized by Coomassie blue staining a 15 % resolving gel. Each sample loaded consisted of 10 µl protein sample and 10 µl 2x SDS loading buffer containing 6M Urea, to denature the protein, 5% SDS, to give the proteins a uniform net charge, 0.1% glycerol to increase the density of the sample/buffer and 0.05% Bromophenol blue as a tracking dye. Protein samples were denatured in SDS loading buffer at 50 °C for 10 minutes before being run on SDS-PAGE. Lane 1 Molecular low weight markers (Amersham Bioscience #17-0446-01), Lane 2 Whole cells, Lane 3 membranes, Lane 4 Pre solubilized membranes-pre urea wash, Lane 5 Proteins removed by Urea wash, Lane 6 Pre solubilized membranes post urea wash, Lane 7 Solubilized membranes, Pre DEAE Sepharose Column.

(C) Column Chromoatography profile of solubilized membranes of *P.stutzeri* heterologously expressed in *E. coli*



Purification of tr-CcoP

In developing a strategy for expressing a soluble form of CcoP, the DNA encoding N-terminal membrane anchor region of CcoP was removed using molecular biology techniques (Pitcher 2002). This has provided a water-soluble form of CcoP that could be easily purified in the high yields required for crystallization studies. The methods used for expression of tr-CcoP were as described previously for CcoP (section 2.5.1).

High expression levels of tr-CcoP were observed in cells grown in TYP media. Following the appropriate growth period, the harvested cells were gently broken using osmotic shock and the bacterial cell walls disrupted resulting in the liberation of soluble proteins. The techniques employed for purification of tr-CcoP differed to those used for CcoP as described in section 2.5.2. To ensure the inclusion of all the periplasmic proteins in the preparation, and considering the view of colleagues that periplasmic extraction methods can be inefficient, the cultures of tr-CcoP were not separated into periplasmic and cytosolic fractions. Methods developed for the purification of the water soluble heme containing oxidase cytochrome *c* peroxidase have resulted in high purification levels and high yields of protein, therefore, the methods employed for the purification of tr-CcoP were based on this method (Echalier *et al.* 2008).

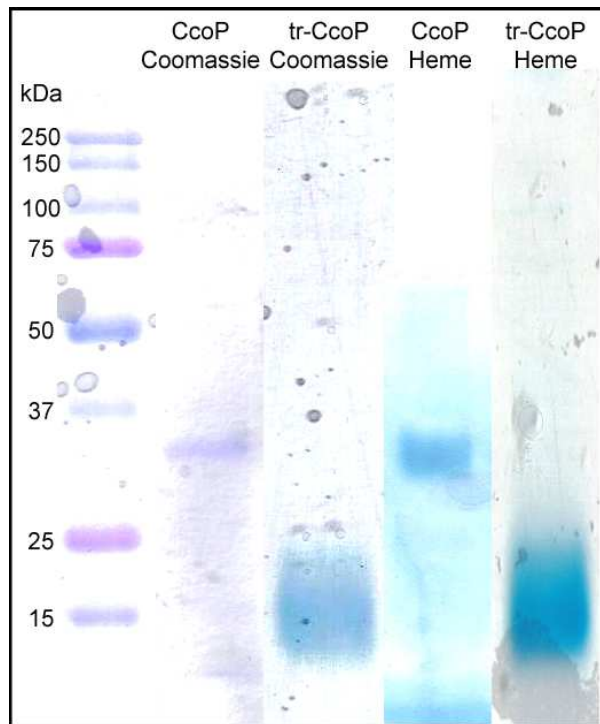


FIG. 3.2 SDS PAGE of concentrated CcoP and tr-CcoP following purification.

The proteins were purified using the methods outlined in Section 2.4.1/3.2.1. The proteins were visualized by Coomassie blue staining and heme staining a 15% resolving gel. The sample load consisted of protein sample and 2x SDS loading buffer containing 6M Urea, to denature the protein, 5% SDS, to confer an overall negative charge to the proteins in the sample, 0.1% glycerol to increase the density of the sample/buffer, and 0.05% Bromophenol blue as a tracking dye. The protein sample was denatured in SDS loading buffer at 50 °C for 10 minutes before being run on SDS-PAGE. Sample lanes are as marked (CcoP 34 kDa, tr-CcoP 24 kDa).

Following osmotic shock of the bacterial cells, the soluble proteins were subject to an ammonium sulphate precipitation at 30% and 70% saturation. The method of ammonium sulphate precipitation is a useful first step in the purification of soluble proteins. The addition of the ammonium sulphate salt ions increases the ionic strength of the solution. As the salt concentration increases, water molecules in contact with hydrophobic patches on the surface of the protein are removed to help solvate the salt molecules. As the water molecules are removed the hydrophobic patches on the protein surface become exposed. These exposed hydrophobic patches interact with each other causing aggregation of protein molecules and consequently precipitation of the protein. Consequently, it is possible to selectively separate proteins from a mixture based on relative hydrophobicity by gradually increasing the concentrations of ammonium sulphate. The protein is not irreversibly denatured by ammonium sulphate precipitation and the precipitated protein can be redissolved in low ionic strength buffer. Following ammonium sulphate fractionation it was necessary to dialyse the partially purified tr-CcoP to remove excess salt. After overnight dialysis in chromatography buffer, the remaining proteins were separated by chromatography using a DEAE anion exchange column. Only one chromatographic step was required to obtain tr-CcoP with a high degree of purity (>95%) as indicated by SDS PAGE (Fig. 3.2). The apparent molecular mass of the subunit was estimated to be 24 kDa by SDS-PAGE.

3.2.2 UV-Visible Spectroscopy

CcoP

CcoP was purified in the partially reduced state. Fully oxidized CcoP was obtained by the addition of potassium ferricyanide, which was subsequently removed by passing the protein through a PD-10 desalting column (Bio-Rad, USA), in the same buffer and detergent. The electronic absorption spectrum of fully oxidized CcoP shows a Soret maximum of 408 nm and a broad band in the α/β region (500-600 nm) (Fig. 3.3). There

was no feature beyond 551 nm that would indicate the presence of penta-coordinate ferric heme, suggesting that both of the *c*-type hemes in CcoP are in the six-coordinate state. Upon complete reduction of CcoP with excess sodium dithionite the Soret band shifted to 417 nm and an increase in intensity was observed. The α and β bands in the visible region intensified upon reduction at 551 nm and 521 nm, respectively. These features are characteristic of ferrous *c*-type hemes and the intensity of the band at 551 nm was consistent with the reduction of two *c*-type hemes (Moore and Pettigrew 1990). There was no evidence of bands near 560 nm or 630 nm that would correspond to contamination with heme *b*.

Tr-CcoP

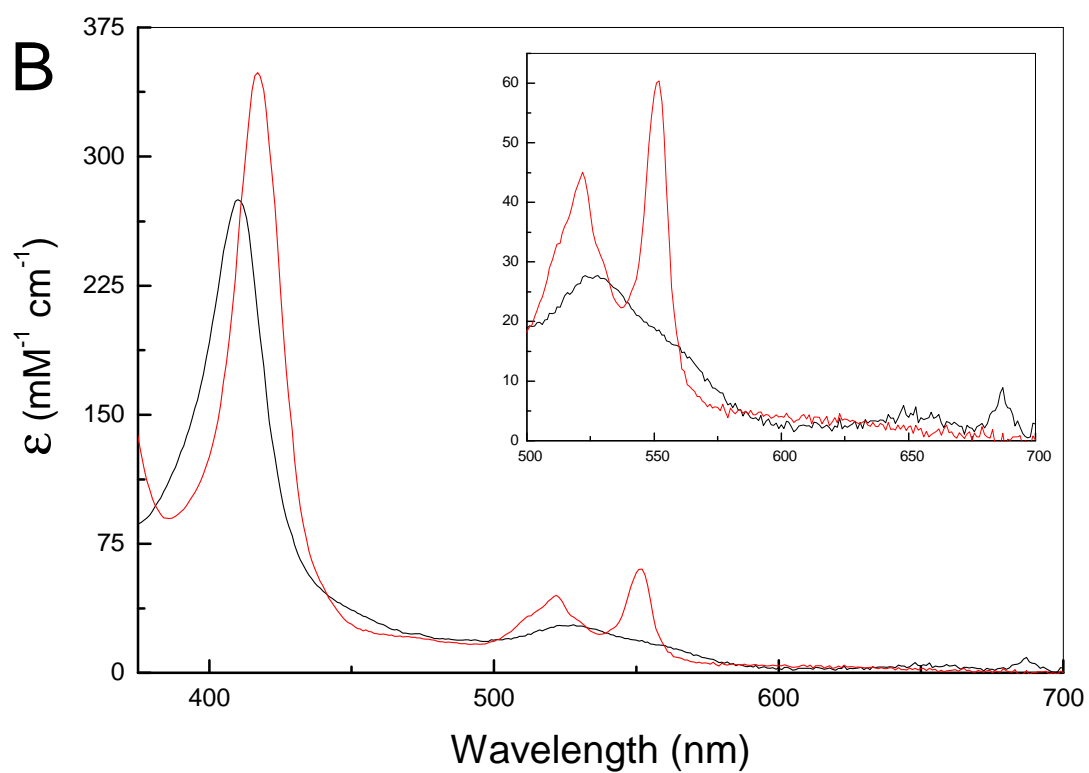
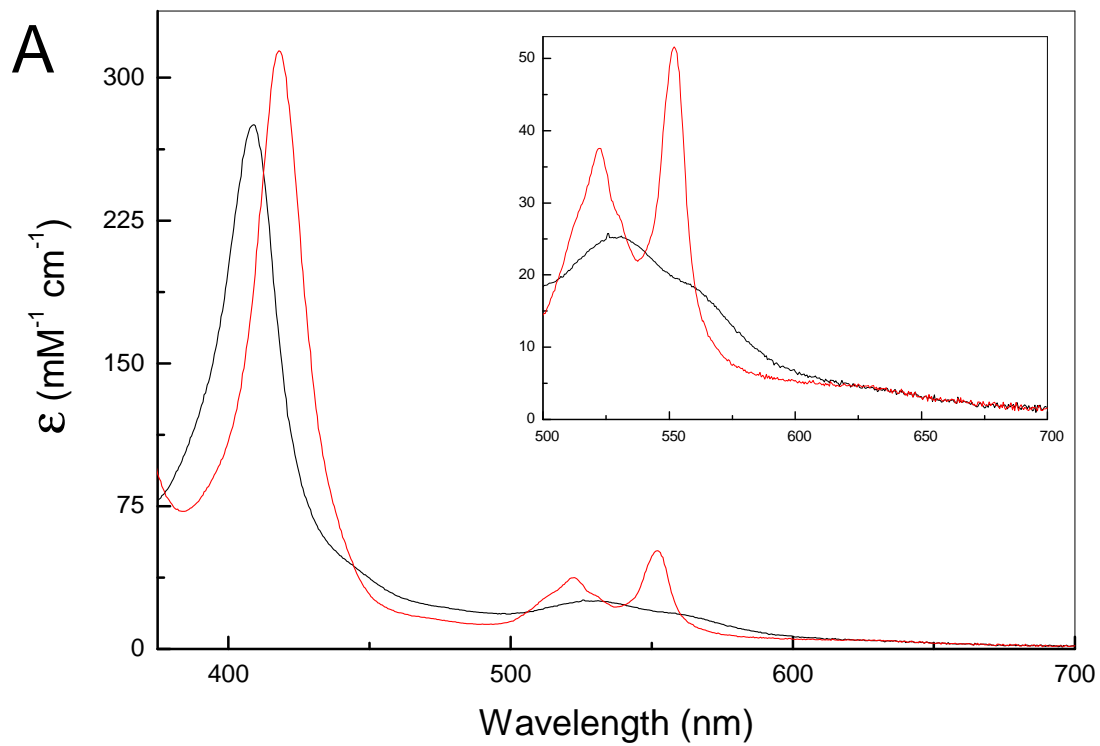
The electronic absorbance spectra of fully oxidized and reduced tr-CcoP resemble that of CcoP, but some additional features were observed (Fig. 3.3B). The spectrum of fully oxidized tr-CcoP shows a broad and slightly shifted Soret with a maximum of 410 nm, compared to CcoP. A broad band in the α/β region (500-600 nm) can be observed in the spectra of tr-CcoP. In addition, a CT band at approximately 650 nm observed in the electronic absorbance spectrum of tr-CcoP, which was not observed in the spectrum of CcoP. This type of CT band is consistent with histidine/H₂O axial (Moore and Pettigrew 1990). The characteristic CT band in the electronic absorbance spectrum of tr-CcoP could therefore suggest a displacement of the sixth axial ligand or replacement of the sixth axial ligand with H₂O.

FIG. 3.3 UV-Visible absorption spectra of recombinant full length *P. stutzeri* CcoP (A) and recombinant truncated *P. stutzeri* CcoP (B).

(A) The black trace shows CcoP fully oxidized with potassium ferricyanide. The red trace depicts the spectrum of the fully reduced enzyme after the addition of excess sodium dithionite. The insert shows a close up of the α and β regions of reduced CcoP with peaks at 551 nm and 521 nm respectively. Upon reduction, a shift of the Soret band from 408 nm to 417 nm was observed. The protein concentration was 2.6 μ M in 20 mM Tris-HCl, 50 μ M EDTA and 0.02% DM, pH 8. The spectrum was recorded at room temperature.

(B) The black trace shows tr-CcoP fully oxidized with potassium ferricyanide. The red trace depicts the spectrum of the fully reduced enzyme after the addition of excess sodium dithionite. The insert shows a close up of the α and β regions of reduced tr-CcoP with peaks at 551 nm and 521 nm respectively. Upon reduction, a shift of the Soret band from 410 nm to 417 nm was observed. The protein concentration was 2.7 μ M in 20 mM Tris-HCl, and 50 μ M EDTA, pH 8. The spectrum was recorded at room temperature.

The protein concentrations are based on the CcoP extinction coefficient previously reported by Pitcher *et. al.* (Pitcher *et al.* 2002).



In the oxidized spectra of tr-CcoP a second CT band was visible, in the 695 nm region. A CT band at this wavelength is characteristic of a low intensity ligand to metal charge transfer transition that is present when a low spin ferric heme possesses at least one of the sulphur ligands, methionine or cysteine (Moore and Pettigrew 1990). Pitcher *et al.* previously reported that the hemes in CcoP are His/His and His/Met ligated, therefore, the presence of a CT band in the spectrum of tr-CcoP was not surprising (Pitcher *et al.* 2002). However, the 695 nm charge transfer (CT) band is not apparent in the electronic absorbance spectrum of CcoP. The absence of this CT band in the CcoP spectrum is not, however, conclusive proof that one of the hemes in CcoP is not His/Met ligated (Moore and Pettigrew 1990).

The apparent 695 nm band in the electronic absorbance spectrum of tr-CcoP does not resemble that previously reported for other proteins, for example, cytochrome *c*₅₅₁ oxidase isolated from *Pseudomonas perfectomarinus* (Liu *et al.* 1983). In the spectrum of tr-CcoP the CT band is asymmetrical and the peak is intense. The expected extinction coefficient for a CT band at 695 nm is 0.5-1 mM⁻¹ cm⁻¹ (Moore and Pettigrew 1990). As observed in Fig. 3.3B the extinction coefficient for the CT band in tr-CcoP is 5 mM⁻¹ cm⁻¹. However, despite the intense peak of the CT band it is favourable to assign the CT band to a His/Met ligated heme, possibly that previously observed by Pitcher *et al.* or a second His/Met ligated heme resulting from the deletion of His 42 from CcoP (Pitcher *et al.* 2002).

Upon complete reduction of tr-CcoP with excess sodium dithionite, the Soret band shifted to 417 nm and increased in intensity. The α and β bands in the visible region intensified upon reduction at 551 nm and 521 nm respectively. These features are characteristic of ferrous *c*-type hemes and, similarly to CcoP, the intensity of the band at 551 nm was consistent with the reduction of two *c* type hemes. There was no evidence of bands at 560 nm or 630 nm that would correspond to contamination with heme *b*.

3.2.3 Mediated Redox Potentiometry

The midpoint redox potential (E_m) is the potential at which the concentration of oxidized protein equals the concentration of reduced protein. The midpoint redox potential of a protein indicates the tendency of a redox couple to donate or accept electrons. In heme proteins, the immediate environment of the heme influences the midpoint redox potential of the protein. A difference in the electron donor-acceptor power of the heme axial ligands also affects the midpoint redox potential. In His/Met ligated *c*-type hemes the methionine sulfur is a good electron acceptor and therefore, favors a relatively electron-rich reduced state resulting in a more positive redox potential (Moore and Pettigrew 1990). Typically, hemes with His/Met ligation have redox potentials greater than + 150 mV. In contrast, *c*-type cytochromes that have histidine as the second axial ligand generally have a reduced ability to stabilize ferrous iron. Hemes with this axial ligation therefore have a lower midpoint redox potential, less than + 50 mV (Moore and Pettigrew 1990).

The midpoint potentials of the two *c*-type hemes in CcoP and tr-CcoP were determined by mediated redox potentiometry using the methods described previously in materials and methods (Section 2.8.1). Samples of the protein (6-8 μ M) were reduced incrementally using the electron donating agent DTT ($E_m = - 330$ mV). The reduced and oxidized states of heme proteins are spectroscopically different. These spectral differences were therefore used to monitor the changes in population of the oxidized (Fe^{3+}) and reduced (Fe^{2+}) states of CcoP and tr-CcoP as shown in Fig. 3.4. These spectroscopic differences allow easy quantification of the relative proportions of each species during the mediated redox titration. As the reduction of CcoP and tr-CcoP proceeds, an isosbestic point can be clearly observed in tr-CcoP at 560 nm (Fig. 3.4B). However, an isosbestic point was not observed in the spectra of CcoP (Fig. 3.4A). Observation of an isosbestic point may be taken as evidence that a single set of reactants gives a single set of products in constant proportions. The isosbestic point is the wavelength at which oxidized and reduced species have the

same extinction coefficient. The absence of an isosbestic point in the spectra of CcoP therefore suggests that the proportions of oxidized and reduced heme varies in the two *c*-type hemes in CcoP so each heme has a different extinction coefficient.

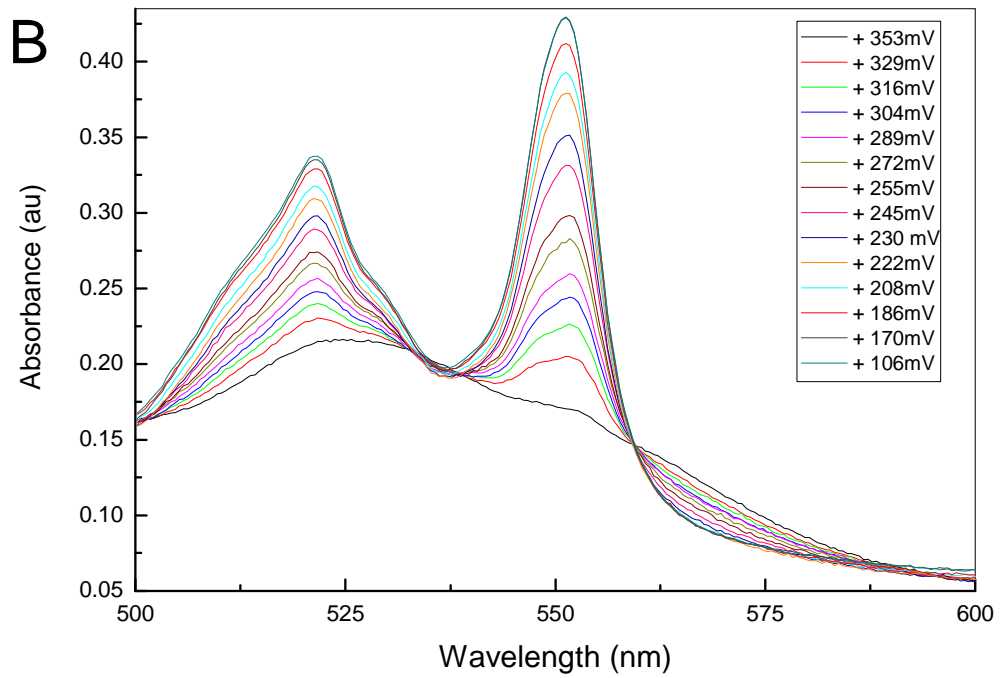
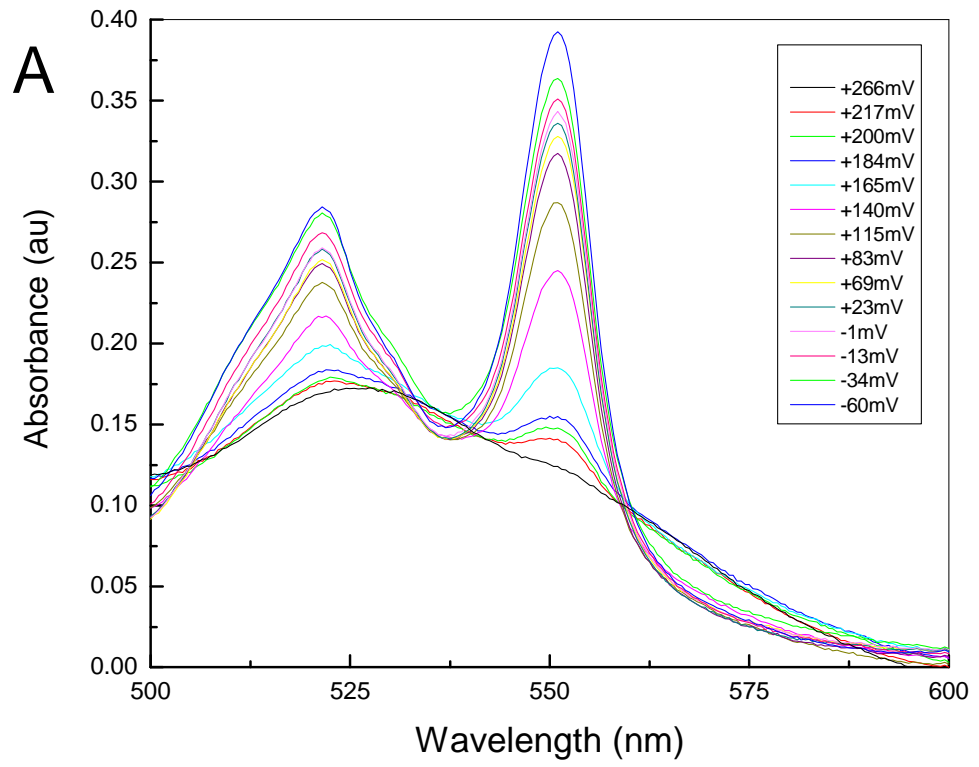
The isosbestic point provides a convenient reference point between the oxidized and reduced state as it remains constant throughout the experiment. The spectral changes occurring during the redox titration (*i.e.* the absorbance at the α band maximum, 550 nm, *minus* the absorbance at an isosbestic point) were plotted relative to the redox potential observed during reduction of the protein as shown in Fig. 3.5. The absorbance at 560 nm was used as a reference point for the calculation of the observed absorbance change during the reduction of CcoP. The Soret region was not used to monitor the redox changes as several of the mediators added to the protein during the titration also absorb in this region (Dutton 1978). The mediators used in these titrations were described in more detail in section 2.8.1.

Full length CcoP

Mediated reduction potentiometric titrations of CcoP indicated the presence of two low-spin *c*-type hemes with midpoint redox potentials of $+ 188 \pm 12$ mV and $- 15 \pm 4$ mV *vs.* SHE at pH8 (Fig. 3.6). These midpoint redox potentials are consistent with the two *c*-type hemes in tr-CcoP having His/Met and His/His ligation respectively. The experimental midpoint redox potentials disagree with those previously reported by Pitcher *et.al.* (Pitcher 2002). Pitcher *et.al.* concluded that the His/Met and His/His ligated *c*-type hemes observed in the MCD spectrum of CcoP had redox potentials of $+ 142$ mV and $+ 111$ mV respectively. As discussed hemes with His/Met and His/His ligation favour midpoint potentials in the range of $> + 150$ mV and $< + 50$ mV respectively (Moore *et al.* 1986). Therefore, the experimental mediated redox potentials reported for CcoP in this study concur with redox potentials expected for hemes with these axial ligands.

FIG. 3.4 Representative spectra of optical changes observed in the 500 - 600 nm regions during a reducing titration of full length CcoP (A) and truncated CcoP (B).

The concentration of the CcoP and tr-CcoP was 7.5 μ M in 20 mM Tris-HCl, 50 μ M EDTA, 0.02% DM, pH 8 and 7 μ M in 20 mM Tris-HCl, 50 μ M EDTA, pH 8 respectively. The mediators used were: 10 μ M each of diaminodurol, 2,6 dimethylbenzoquinone, N-methyl phenazonium methosulfate (PMS), N-ethyl phenazonium ethosulfate (PES), Duroquinone, Pyocyanine, Menadione, 2-Hydroxyl-1,4-napthoquinone, Anthraquinone-2,6-disulfonate, Anthraquinone-2-sulfonate, Benzyl Viologen, Methyl Viologen. The sample was reduced by the successive additions (0.1 - 2 μ l) of 1, 10 or 100 mM DTT as appropriate. Spectra were recorded 10 minutes after each addition of the reducing agent. Reduction of the enzyme was monitored using the α -max band at 550nm, which increases in intensity upon reduction. The protein was stirred under an argon atmosphere during the experiment to maintain anaerobicity. The reference wavelength was 700 nm. The spectra were recorded at 25°C.



To obtain satisfactory fits of the redox potentiometric titration data it was necessary to use two independent $n = 1$ Nernstian components as shown in Fig. 3.5 (A) as the redox potentials of both hemes are well spaced. The best fit of the data using two independent $n = 1$ Nernstian components was obtained when it was assumed that the two hemes did not contribute equally to the absorption amplitude of the 551 nm band, of the fully reduced sample. The high potential heme contributed 68% and the low potential heme contributed 32% to the absorbance change in the α -band maximum. The unequal contribution of the hemes to the absorption amplitude possibly indicates that a change in the spin state of CcoP is observed upon reduction. Upon reduction of a high spin heme, the contribution of the spectral change to the height of the 550 nm α band is not as great as the observed spectral increase upon reduction of a low-spin heme. The unequal contribution of the low and high potential heme to the spectral change observed for CcoP may correspond with the low potential heme becoming high-spin, five coordinated upon reduction. In this scenario, displacement of the distal ligand to the low potential heme, following full reduction of the high potential heme would result in an open axial position able to bind oxygen.

Following full reduction of the two *c* type hemes in CcoP, the protein was oxidized by titrating 10 mM potassium ferricyanide into the reduced protein. The titration was performed using the same methods employed for the reductive titration (Chapter 2, Section 2.8.1). The results were plotted as described for the reductive titration. The oxidative titration was performed to ensure that the titration was reversible within reasonable parameters and to determine if any ligand switching was occurring upon reduction of the protein.

Mediated oxidation potentiometric titrations indicated that the two low-spin *c*-type hemes in CcoP have midpoint redox potentials of $+ 178 \pm 10$ mV and $+ 14 \pm 2$ mV. The midpoint redox potential of the previously observed high potential heme was therefore shifted

negatively (+ 188 mV to + 178 mV) and the midpoint potential of the low potential heme was shifted positively (- 15 mV to + 14 mV) compared with the reductive titration. Similarly to the reductive titration to obtain satisfactory fits of the data it was necessary to use two independent $n = 1$ Nernstian components as shown in Fig. 3.5 (B). In the reductive direction, the hemes did not contribute equally to the fit, however, in the oxidative direction each component contributed equally to the fit.

The redox titrations of CcoP were fully reversible as exemplified by the profiles presented in Fig. 3.5 (C and D). Fig. 3.5 (C) shows the overlay of the reductive and oxidative redox titration curves of CcoP. If a simple mediated redox reaction takes place, during the mediated redox titration the midpoint potentials of the oxidized and reduced titrations should be identical (Moore and Pettigrew 1990). Fig. 3.5 D shows the reductive and oxidative points fit with a single titration curve. To obtain satisfactory fits of the redox potentiometric titration data it was necessary to use two independent $n = 1$ Nernstian components with midpoint redox potentials of + 187 mV and + 10 mV vs. SHE at pH8. The reversible redox titration of CcoP increases confidence that the titration was performed at equilibrium.

FIG. 3.5 Reductive and oxidative titrations of CcoP.

The titrations of CcoP were performed using the conditions outlined in Fig. 3.4. Values obtained for $A_{550}-A_{560}$ (i.e. the absorbance of the A_{MAX} wavelength for reduced *c*-heme minus the absorbance at an isosbestic point) were plotted as a function of potential.

(A) The solid line represents the theoretical Nernst curve for two electron reduction (■) of CcoP and corresponds to a best fit between the normalised data with two $n = 1$ Nernstian components centred at $+188 \pm 12$ mV and -15 ± 4 mV assuming one heme contributes 68% and the second heme contributes 32% to the absorbance change in the α -band maximum in the spectrum. r^2 value = 0.994

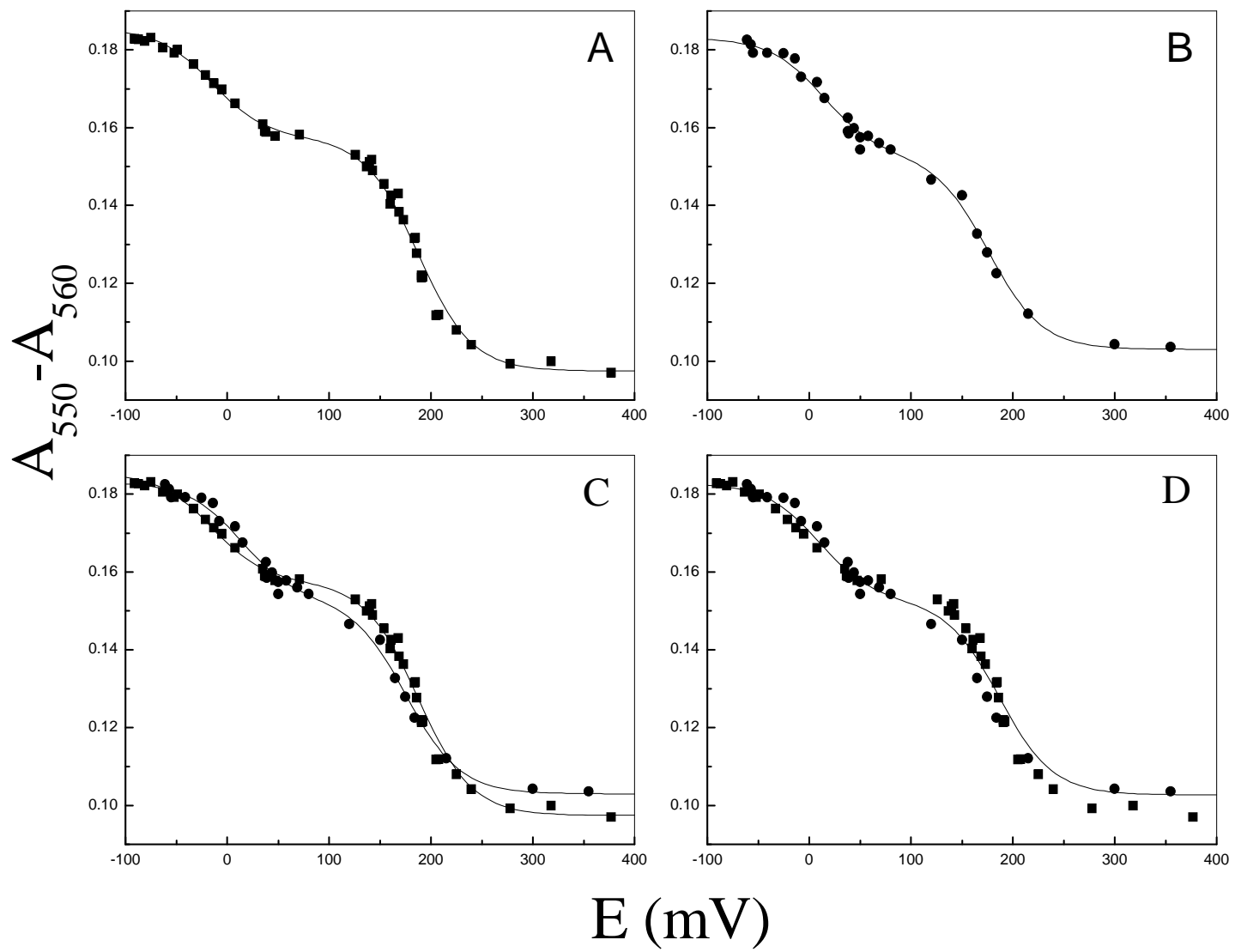
The sample was reduced by the successive additions (0.1-2 μ l) of 10mM DTT

(B) The solid line represents the theoretical Nernst curve for two electron oxidation (●) of CcoP and corresponds to a best fit between the normalised data with two $n = 1$ Nernstian curves centred at +178 mV and +14 mV assuming each heme contributes 50% to the absorbance change in the α -band maximum in the spectrum. r^2 value = 0.995

The sample was oxidized by the successive additions (0.1-2 μ l) of 10mM potassium ferricyanide.

(C) The solid lines represent the theoretical Nernst curves for two electron reduction (■) and oxidation (●) of CcoP.

(D) The solid line represents the theoretical Nernst curve for data gathered during the reduction (■) and oxidation (●) titrations of CcoP The curve corresponds to a best fit between the normalised data with two $n = 1$ Nernstian curves centred at +187 mV and +10 mV assuming the high potential heme contributes 62% and the low potential heme contributes 38% to the absorbance change in the α -band maximum in the spectrum. r^2 value = 0.984



The midpoint redox potentials reported in this study for the two hemes in CcoP (+ 188 mV and -15 mV) suggest that only the heme with a redox potential of + 188 mV could potentially act as an electron receiving domain in CcoP. However, the previously reported redox potential of CcoO, (+ 265 mV to + 320 mV) suggests that CcoO could potentially act as an electron-receiving domain in the *cbb₃* complex (Gray *et al.* 1994; Pitcher 2002). Based upon the similarity between the CcoO subunit and the electron receiving subunit, NorC, the suggestion that CcoO is the electron receiving subunit in the *cbb₃* oxidase is viable (Preisig *et al.* 1993; Saraste and Castresana 1994; Pitcher *et al.* 2002; Verissimo *et al.* 2007).

Tr-CcoP

The mediated redox potentials of the two hemes in tr-CcoP differ to those observed in CcoP. Mediated reduction potentiometric titrations of tr-CcoP indicated the presence of two low-spin *c*-type hemes with midpoint redox potentials of + 300 mV and + 220 mV. The high potential of the two hemes in tr-CcoP are consistent with both hemes having His/Met ligation. Recall that the redox potentials reported for CcoP (+ 185 mV and – 15 mV) are consistent with a His/Met ligated high potential heme and a His/His ligated low potential heme. It is proposed that variations in the mediated redox potentials of the hemes in CcoP and tr-CcoP are due to differences in the protein environment of the hemes in the soluble protein, tr-CcoP compared to CcoP. The results, however, also suggests disruption of the ligands to the low potential heme, observed in CcoP. Sequence alignments of the amino acid sequence of CcoP indicate that there is only one fully conserved histidine (His-42) which could act as a distal ligand in CcoP. This histidine could conceivably fulfill the role of distal ligand to the low potential heme in CcoP. His 42 is located in the hydrophobic tail in CcoP. In tr-CcoP, His-42 has therefore been deleted and it is reasonable to suggest that the distal histidine to the low potential heme in CcoP has been disrupted and the distal histidine has been replaced by

methionine. This proposal would therefore correspond with the fact that the heme with a potential of -15 mV observed in CcoP is not observed in tr-CcoP.

To obtain satisfactory fits of the tr-CcoP mediated redox potentiometry data it was necessary to use two $n = 1$ Nernstian components as shown in Fig. 3.6 (A). It was assumed that the two hemes contributed equally to the absorption change of the fully reduced sample at 550 nm. The tr-CcoP redox titration data was also analyzed using a single $n = 1$ Nernstian component as shown in Fig. 3.6 (B). The resulting poor fit indicates that the reduction of tr-CcoP is two distinct $n = 1$ steps and not two closely occurring $n = 1$ titrations despite the suggestion that the two hemes in tr-CcoP are both His/Met ligated.

The redox titration of tr-CcoP did not display the same reversible properties as CcoP. The tr-CcoP protein was relatively unstable in the oxidized state, which meant gathering data by oxidizing the protein was not possible. The reason for the instability of the oxidized state is not clear and may be due to structural differences between CcoP and tr-CcoP.

3.2.4 EPR Spectroscopy

The spectroscopic techniques EPR and MCD are used in combination to identify axial ligands in low-spin ferric hemes. EPR is a technique for studying chemical species that have one or more unpaired electron, such as ferric ion. In this study, EPR was used to investigate the identity of the suggested His/Met and His/His ligated *c*-type hemes in CcoP.

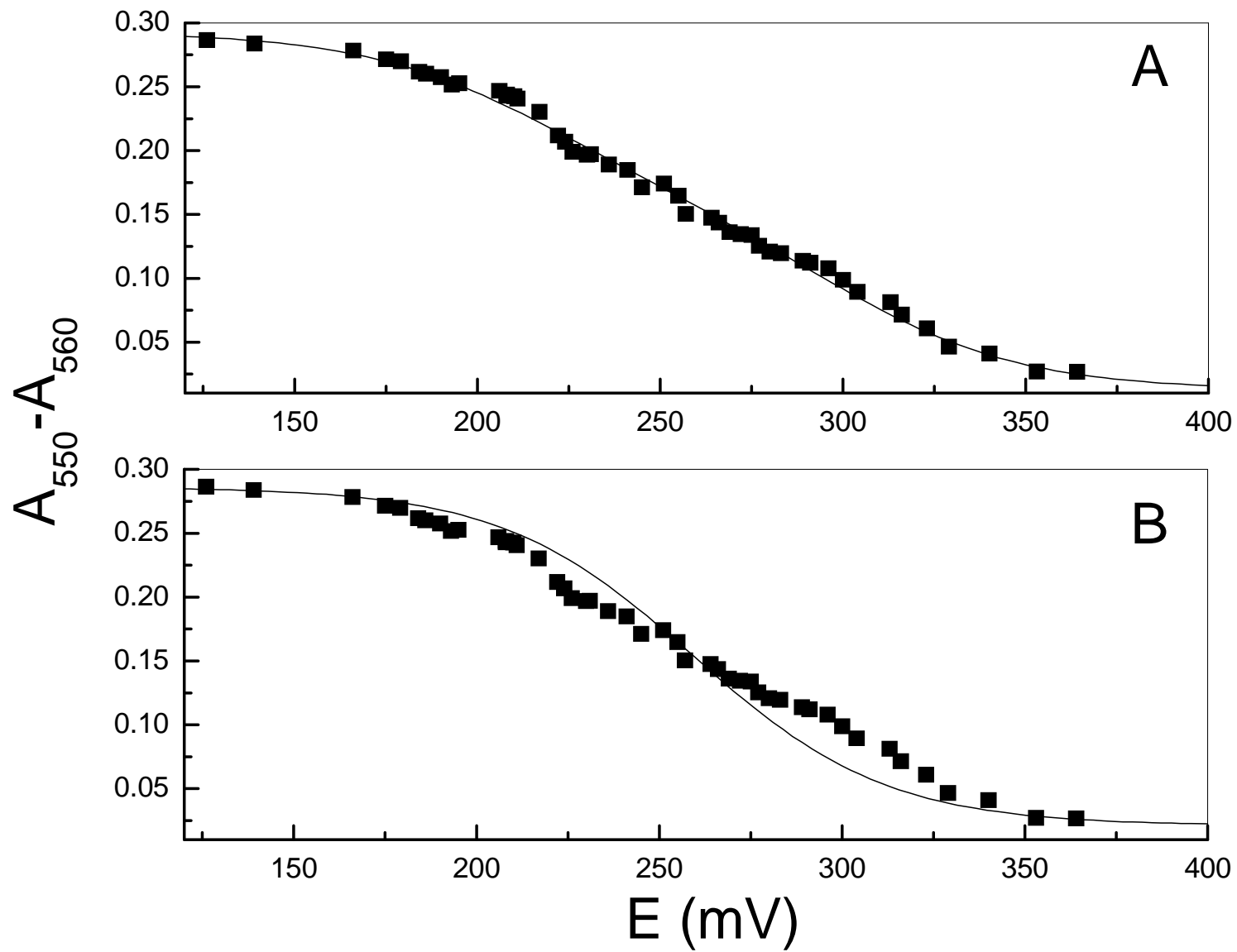
FIG. 3.6 Reductive Titrations of Truncated CcoP.

The titrations of tr-CcoP were performed using the conditions outlined in Fig. 3.4. Values obtained for $A_{550}-A_{560}$ (i.e. the absorbance of the A_{MAX} wavelength for reduced c-heme minus the absorbance at an isosbestic point) were plotted as a function of potential.

(A) The solid line represents a fit of the data to two theoretical $n = 1$ Nernst equations. The curve corresponds to a best fit between the normalised data with two $n = 1$ Nernstian curves centred at $+300 \pm 7$ mV and $+220 \pm 10$ mV assuming both hemes contribute equally to the absorbance change in the α -band maximum in the spectrum. r^2 value = 0.996.

The sample was reduced by the successive additions (0.1-2 μ l) of 10mM DTT

(B) The solid line represents a fit of the data to one theoretical $n = 1$ Nernst equations. The curve corresponds to a best fit between the normalised data with one $n = 1$ Nernstian curves centred at $+ 259 \pm 5$ mV assuming both hemes contribute equally to the absorbance change in the α -band maximum in the spectrum. r^2 value = 0.958



Full length CcoP

The X-band EPR spectrum of fully oxidized CcoP from *P. stutzeri* (Fig. 3.7 A) recorded at 15 K shows three features at $g = 2.97, 2.27, 1.53$ typical of a low-spin ferric heme with rhombic symmetry. The parallel orientation of axial ligands around a heme group gives rise to a rhombic signal and this type of spectrum is typically observed for hemes with two histidine ligands (Moore and Pettigrew 1990). A rhombic signal can, however, also arise from hemes with His/Met ligation (Cheesman *et al.* 1998). The rhombic spectrum observed in the EPR spectrum of CcoP, can be assigned therefore to a His/His or the His/Met ligated *c*-type heme, the identity of which was suggested previously based on MCD data and further supported by mediated redox titrations in this study (Pitcher 2002) (Section 3.2.3).

The concentration of the species giving rise to the low-spin ferric rhombic trio (2.97, 2.27 and 1.53) was estimated by integration of the g_z feature ($g = 2.97$) using 1 mM Cu (II) EDTA as a spin standard. The results indicated that the species giving rise to the g_z feature accounts for *ca.* 65% of the total low-spin heme in the EPR absorption spectra. Heme quantification by this method is only considered accurate to within 10%; it can therefore be assumed that the rhombic trio, 2.97, 2.27 and 1.53, accounts for one low-spin heme with His/His or His/Met ligation. Previously Pitcher *et. al.* assigned the rhombic trio $g = 2.97, 2.27$ and 1.53 observed in the EPR spectroscopy of CcoP to a His/His ligated heme (Pitcher 2002). In addition to the rhombic trio, Pitcher *et.al.* observed a shoulder at $g = 3.19$, which was assigned to a heme with His/Met ligation (Pitcher 2002). The $g = 3.19$ feature was not observed in EPR spectra performed during this study. The absence of this feature is possibly a reflection on differences in the preparation of the CcoP samples in this study and samples prepared by Pitcher *et. al.* (Pitcher *et al.* 2002).

The second low spin heme in CcoP is unaccounted for in the EPR spectrum. As the additional low-spin ferric heme is not evident in the EPR spectrum, it is suggested that the

heme may be spin-coupled to another paramagnetic centre (Cheesman 2006). It has been assumed that the rhombic trio (2.97, 2.27 and 1.53) correspond to 100% of one of the heme species in CcoP and the proposed spin coupled heme accounts for the second heme centre. It is however, possible that the rhombic trio accounts for 50 % of the His/His species and 50 % of the His/Met species. The other 50 % of each heme species are conceivably spin-coupled to each other thereby inducing an EPR silent paramagnetic centre.

Features near $g = 6$, $g = 4.3$ and $g = 2$ observed in the spectra of CcoP (Fig. 3.6A) represent minor amounts of high-spin ferric heme, small amounts of free Fe(III), and small amounts of Cu (II) respectively. These small quantities represent no more than a few percent in terms of enzyme concentrations.

Truncated CcoP

Similarly to full length CcoP, the X band EPR spectrum of fully oxidized tr-CcoP (Fig. 3.7 B) at 15 K shows three features at $g = 2.99$, 2.27, 1.53, typical of a low-spin ferric heme with rhombic symmetry with either His/His or His/Met ligation. The concentration of the species giving rise to this low-spin ferric rhombic trio was estimated by integration of the g_z feature ($g = 2.99$) using 1 mM Cu (II) EDTA as a standard. Integration of the g_z feature demonstrates that the species giving rise to the $g = 2.99$ feature accounts for *ca.* 50% of the total low-spin heme in the EPR absorption spectra of tr-CcoP. The rhombic trio in the EPR spectrum of tr-CcoP is consistent with the rhombic trio observed in the EPR spectrum of CcoP.

Further study of the $g = 2.99$ feature in the EPR spectrum of tr-CcoP reveals a broad underlying signal visible at $g = 3.54$ to the left of the $g = 2.99$ feature as indicated by the red arrow shown in Fig. 3.7(B). This high g -value of the signal together with the asymmetrical shape suggests that it is one component of a rhombic trio, in which the g_y

and g_x features are broad and not easily detected (Cheesman *et al.* 1998). This leads overall to a broad “large g_{\max} ” type EPR spectrum. Samples of metalloproteins studied by EPR are frozen solutions in which the molecules are randomly oriented. The orientation of the heme molecules can affect the EPR signals which arise, and large g_{\max} signals can be observed when the ligand planes have a perpendicular orientation rather than a parallel orientation (More *et al.* 1999). A broad g_{\max} is typically observed for hemes with two perpendicular orientated histidine ligands, but can also arise in hemes with histidine-methionine ligation, for example the $g_z = 3.54$ signal observed in the EPR spectrum of NorC from *P. stutzeri* (Cheesman *et al.* 1998). This signal at $g_z = 3.53$ in the EPR spectrum of tr-CcoP was therefore assigned as the g_z feature of the spectrum of a low-spin heme with His/Met ligands. Quantification of the species contributing to the large g_{\max} signal by EPR spin integration is less straightforward than quantification of the species contributing to a rhombic trio (Cheesman *et al.* 1998). The species contributing to the large g_{\max} signal was therefore not determined.

Mediated redox titrations of both CcoP and tr-CcoP identified high potential hemes in these proteins with redox potentials of + 188 mV and + 220 mV respectively (Section 3.2.3). It could be postulated that the rhombic trio, 2.99, 2.27, 1.53, observed in the EPR spectrum of both CcoP and tr-CcoP correspond to the hemes in these proteins with corresponding midpoint redox potentials. Previously reported MCD spectra suggested that the high potential heme in CcoP is His/Met ligated (Pitcher 2002). It is therefore proposed that the high potential *c*-type hemes in both CcoP and tr-CcoP have His/Met ligation.

The $g = 3.53$ signal observed in the EPR spectrum of CcoP is consistent with a heme with His/Met ligation. Based on the EPR spectrum of tr-CcoP it is therefore postulated that the unassigned high potential heme observed in tr-CcoP (+ 300 mV) is His/Met ligated (Section 3.2.3). These results therefore suggest that the two hemes in tr-CcoP are both

His/Met ligated. It is proposed that the high potential heme in CcoP is His/Met ligated and the low potential heme is His/His ligated. The results observed for tr-CcoP therefore lead to the suggestion that the distal histidine to the low potential heme in CcoP is replaced by a methionine in tr-CcoP. Mediated redox potentiometry indicates that the lowest potential heme in tr-CcoP is + 220 mV, compared to - 15 mV in CcoP. The redox potentiometry results therefore further support the suggestion that the lower potential heme in tr-CcoP does not have the same axial ligands as the low potential heme in CcoP.

As observed in the EPR spectrum of CcoP, the tr-CcoP EPR spectrum indicates signals at $g = 4.3$ and $g = 2$ representing small amounts of free Fe(III) and Cu (II) respectively. A $g = 6$ signal was not however apparent.

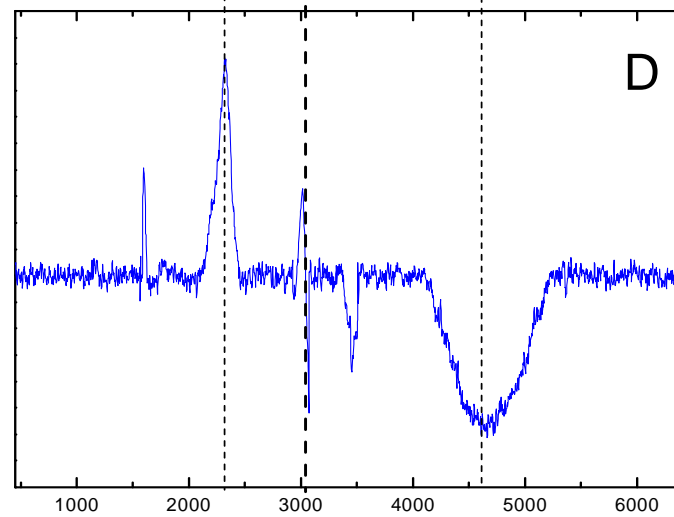
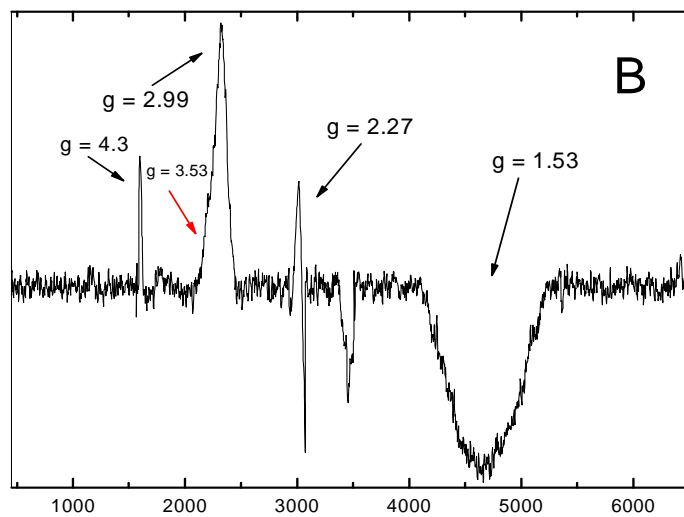
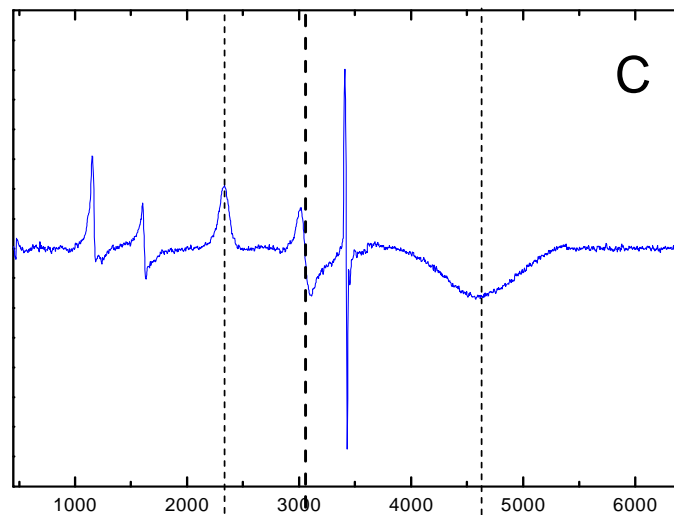
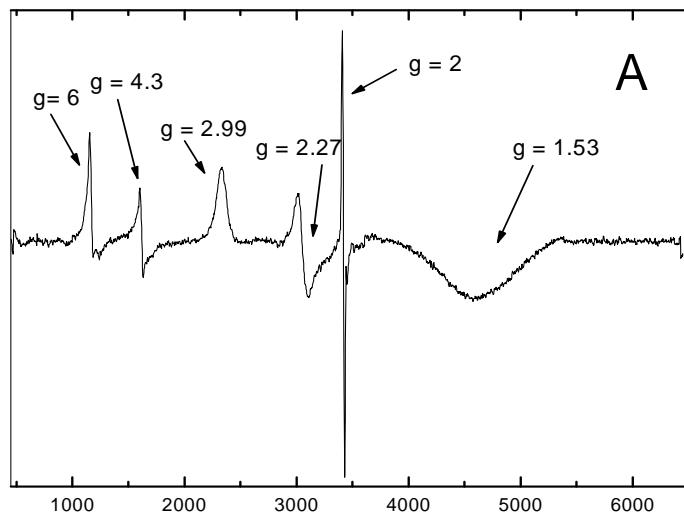
Mediated redox potentiometry and EPR spectra suggest that the two *c*-type hemes in CcoP are His/His and His/Met ligated and the two hemes in tr-CcoP are both His/Met ligated. MCD spectroscopy of the proteins was performed to confirm these results.

3.2.5 MCD Spectroscopy

Magnetic Circular Dichroism is an optical probe of paramagnetism that detail the electronic and magnetic properties of the ground states of metal centers and is therefore a good technique for characterizing the secondary structure in metalloproteins. The differential absorption of left and right-circularly polarized light induced by the presence of a longitudinal magnetic field produces spectra that are rich in information about the chromophores under study. These spectra define heme oxidation, spin, and ligation state of the protein when in solution.

FIG. 3.7 X-band EPR spectra of full length CcoP (A) and truncated CcoP (B) from *P. stutzeri*.

- A) The protein concentration was 179 μM in 20 mM Tris-HCl, 50 μM EDTA, 0.02% DM, pH 8 and was fully oxidized with potassium ferricyanide. The spectrum was recorded at 15 K, using 2 mW of microwave power, and 1 mT modulation amplitude. The g -values of features indicated are discussed in the text.
- B) The protein concentration was 185 μM in 20 mM Tris-HCl, 50 μM EDTA, pH 8 and was fully oxidized with potassium ferricyanide. The spectrum was recorded at 15 K, using 2 mW of microwave power and 1 mT modulation amplitude.
- Comparison of EPR spectrum of CcoP (C) and tr-CcoP (D) as shown in panel A and B. Dashed lines indicate positions of corresponding features



Magnetic Field (G)

Optical absorption bands in the UV-Visible MCD spectrum to the high-energy side, 600 nm, arise from π - π^* transitions of the porphyrin and are sufficiently sensitive to the properties of the iron. Bands that arise from these transitions can be diagnostic of the spin and oxidation state of the heme. The NIR-MCD spectrum diagnoses the axial ligands of low-spin ferric hemes. At longer wavelengths, charge transfer (CT) bands involving porphyrin (π) to ferric transitions are detected in the MCD spectrum. The energy of the low-spin ferric heme CT transition is shifted by changes in heme coordination. The CT band for low-spin hemes, which occurs in the NIR region (800-2000 nm), is rarely detectable by absorption spectroscopy but it readily located by MCD and the spectral peak is diagnostic of the heme ligands.

Full Length CcoP

The derivative shaped Soret absorption band, that is characteristic of low-spin ferric hemes, dominates the RT-UV-Visible MCD spectrum of oxidized CcoP shown in Fig. 3.8A. At these energies, the low-spin ferric heme dominates the contribution from any high-spin heme, which could potentially be observed in the Soret band (Babcock *et al.* 1976; Cheesman *et al.* 1998). In the α region, the intensity of the derivative shaped band with extremes at 551 nm and trough at 569 nm is typical for two low-spin hemes. A band at 695 nm would be observed if a heme possessing a sulfur ligand was present, however, there is no band visible beyond 600 nm. In the room temperature NIR-MCD spectrum of oxidized CcoP, shown in Fig. 3.8B, an intense band was observed with maxima at 1585 nm. This band represents a porphyrin (π) to ferric charge transfer transition for a heme with His/His ligation. A small peak was apparent at 1825 nm, which is consistent with a His/Met ligated heme, however, the relative intensities of the two features were not at a 1:1 ratio as expected for two hemes with His/His and His/Met ligation as predicted for CcoP. The intensity of the peak at 1585 nm indicates that two hemes are present (Cheesman *et al.* 1998; Cheesman 2008). The MCD data therefore suggest that the two hemes in CcoP are

both His/His ligated. To ensure that the ligation state of the hemes was not temperature dependant, MCD spectra were obtained at room temperature and under low temperature conditions.

As previously discussed, it is typically observed that hemes with His/His ligation have a redox potential of less than + 50 mV. As demonstrated in this work one of the hemes in CcoP has a positive redox potential (+ 188 mV), which is uncommon for a heme with His/His axial ligation. A high potential His/His ligated heme is not, however, a feature unique to the *cbb*₃ subunit. In the multi-heme nitrite reductase, ccNIR, one of the four His/His ligated heme in the subunit NrfA is reported to also have a high redox potential of + 150 mV (Almeida *et al.* 2003). The occurrence of high potential His/His ligated hemes is an atypical observation however, encapsulation of the heme group in a hydrophobic area can cause a positive shift in the midpoint redox potential of a heme (Shifman *et al.* 2000). The structure of CcoP or the proximity of CcoP to the other *cbb*₃ subunits is unknown and this is a tangible explanation for the somewhat high potential of one of the His/His ligated heme.

Tr- CcoP

Similarly, to CcoP, the Soret absorption band dominates the UV-Visible room temperature MCD spectrum of tr-CcoP as shown in Fig. 3.9A. This Soret band is characteristic of two low-spin ferric hemes. In the α region, the intensity of the derivative shaped band with extremes at 551 nm and a trough at 569 nm is also typical for two low-spin hemes. The minor trough observed at 630 nm is due to a high-spin His/water coordinated heme, which represents no more than ~3% of the heme species (Cheesman *et al.* 2001). The observed trough is consistent with the CT band observed at 638 nm in the electronic absorbance spectrum of tr-CcoP (Section 3.2). A derivative shaped band is clearly seen at 695nm. This band suggests the presence of a heme possessing a sulfur ligand, methionine or

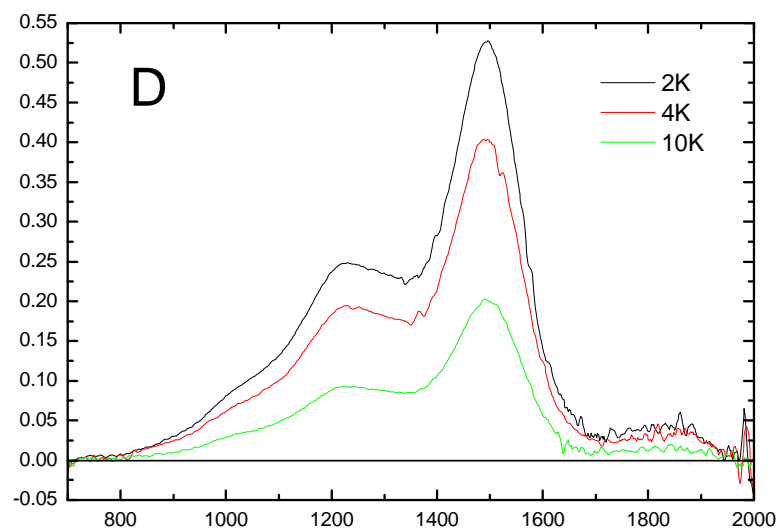
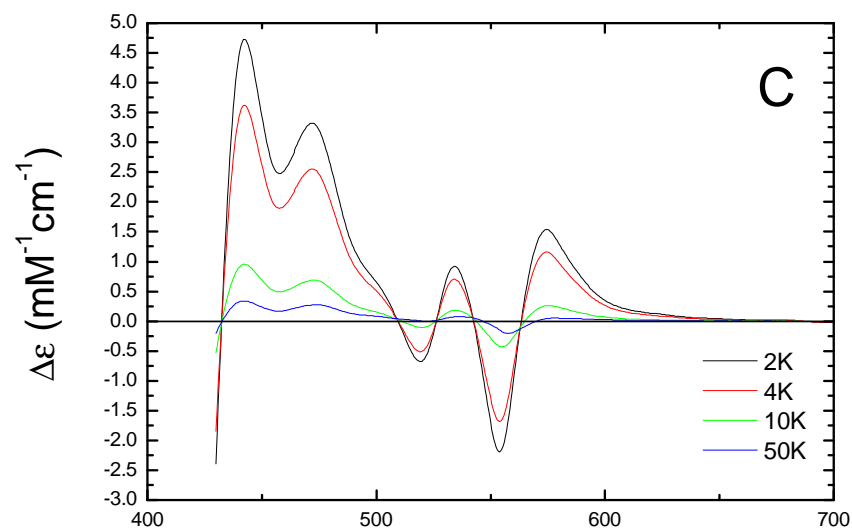
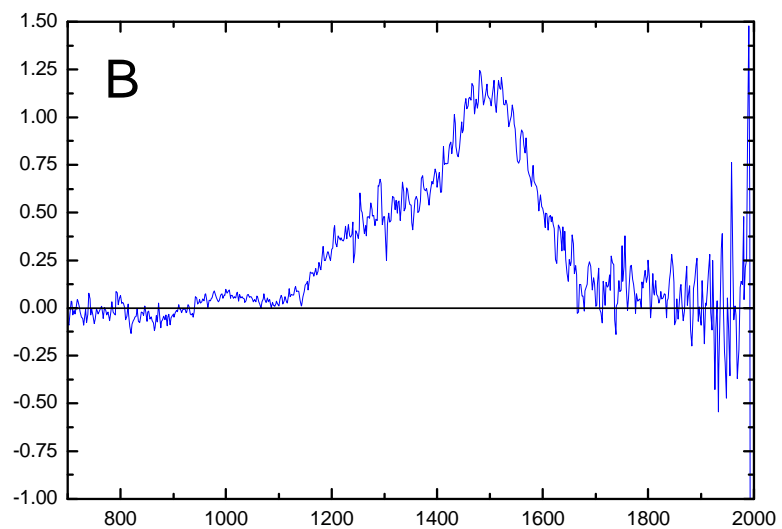
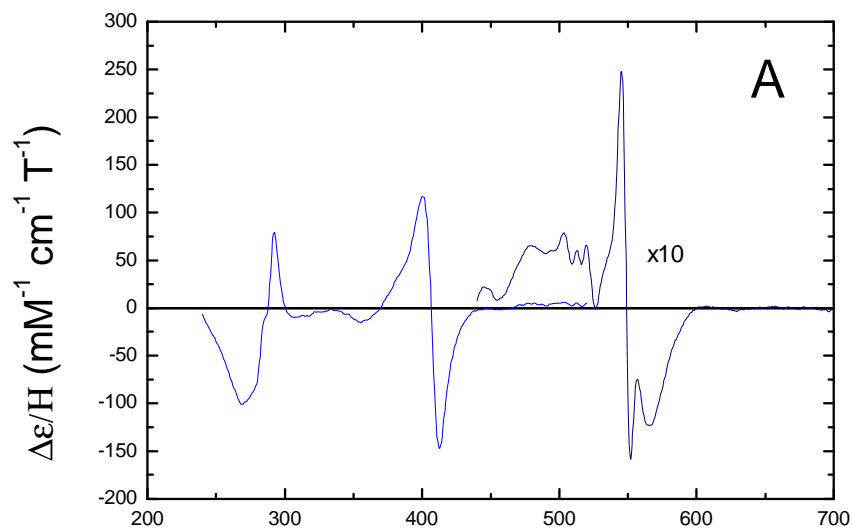
cysteine for example and is consistent with the 695 nm band observed in the electronic absorbance spectrum of tr-CcoP (Section 3.2). Previously the 695 nm band in the electronic absorbance spectrum of tr-CcoP was concluded to be a spectroscopic artifact. Considering the extinction coefficient and the asymmetrical shape of the band, it is still reasonable to conclude that the band can be attributed to an artifact. However, the presence of an underlying CT band is therefore not possible to deconvolute.

In the room temperature NIR MCD spectrum of oxidized tr-CcoP, two intense bands were observed with maxima at 1585 nm and 1825 nm. These bands represent a porphyrin (π) to ferric charge transfer transition for a heme with His/His ligation and a heme with His/Met ligation respectively. The intensity of the peaks indicates that the two hemes are present in equimolar quantities. The intensity of the His/His ligated heme at 4.2 K of $190 \text{ M}^{-1}\text{cm}^{-1}$ is considered acceptable for a heme with a standard rhombic type EPR spectrum. However, in contrast $250 \text{ M}^{-1}\text{cm}^{-1}$ is above average for a rhombic His/Met (Cheesman 2008). The MCD spectra of CcoP indicated that the two *c*-type hemes in this protein both have His/His ligation. It was anticipated that one of the *c*-type hemes in tr-CcoP would be His/His ligated, however it was unclear if both hemes would be His/His ligated. Sequence alignments of the amino acid sequence indicate that there is only one fully conserved histidine in CcoP (His-42). His 42 is located in the hydrophobic tail of CcoP, therefore, in the construction of tr-CcoP His-42 has been deleted. It is reasonable to suggest that His 42 is one of the distal ligands to the His/His ligated heme in CcoP but due to its absence in tr-CcoP, the distal ligand is replaced by a methionine.

FIG. 3.8 UV-Visible and Near Infrared (NIR) MCD of oxidized *P. stutzeri* CcoP performed at room temperature and low temperature.

- Room-temperature UV-Visible (A) and NIR MCD spectra (B). The sample concentration used was 138 μM . The spectrum was recorded using a magnetic field of 5T.
- Low-temperature UV-Visible (C) and NIR MCD spectra (D). The sample concentration used was 138 μM . The spectrum was recorded using a magnetic field of 5T. Temperatures used were 2 K, 4 K and 10K.

The enzyme was fully oxidized with potassium ferricyanide. Buffers were as described in materials and methods.

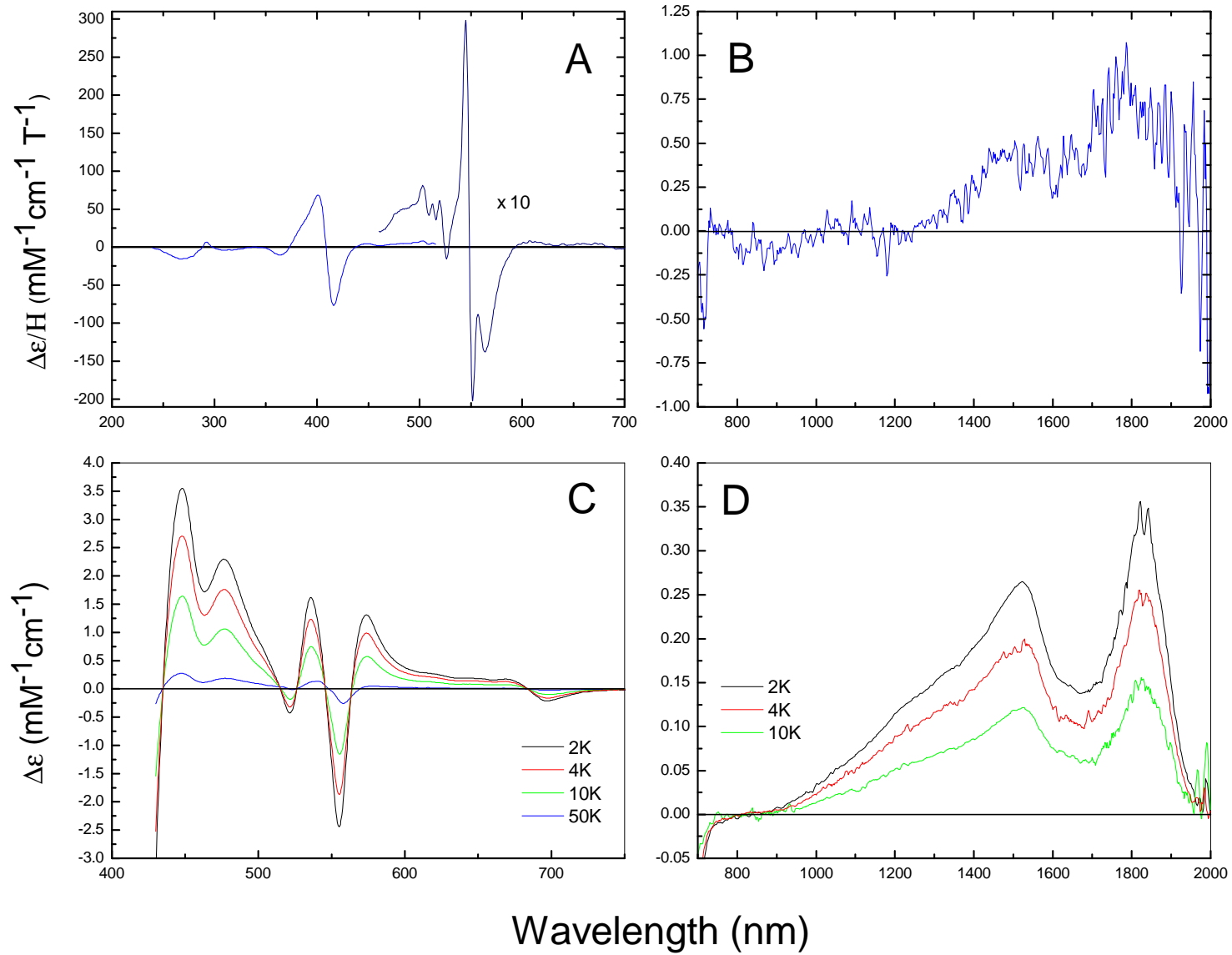


Wavelength (nm)

FIG. 3.9 UV-Visible and NIR MCD of oxidized *P. stutzeri* Truncated CcoP performed at room temperature and low temperature.

- Room-temperature UV-Visible (A) and NIR-MCD spectra (B). The sample concentration used was 115 μM . The spectrum was recorded using a magnetic field of 5T.
- Low-temperature UV-Visible (C) and NIR-MCD spectra (D). The sample concentration used was 115 μM . The spectrum was recorded using a magnetic field of 5T. Temperatures used were 2 K, 4 K and 10K.

The enzyme was fully oxidized with potassium ferricyanide. Buffers were as described in materials and methods.



Based on earlier results it was speculated that the heme with a midpoint redox potential of + 188 mV observed in CcoP and the heme with a midpoint redox potential of + 220 mV in tr-CcoP correspond with each other. Due to the high redox potential, it was speculated that these corresponding hemes in CcoP and tr-CcoP have His/Met ligation. However, considering a His/Met ligated heme was not observed in the MCD spectra of CcoP, it is concluded that these two hemes are His/His ligated. The 1585 nm band observed in the NIR-MCD spectra of both CcoP and tr-CcoP is therefore assigned to the species responsible for the rhombic trio ($g = 2.97, 2.25, 1.53$) observed in the EPR spectrum of both proteins (Fig. 3.7).

The low potential heme (- 15 mV) observed in CcoP is not seen in tr-CcoP; however a heme with a mediated redox potential of + 300 mV is apparent. Based on the MCD spectra of CcoP and tr-CcoP it is proposed that these hemes are His/His and His/Met ligated respectively. The results therefore suggest that the distal histidine to the low potential heme in CcoP has been replaced by a methionine in the soluble form of CcoP, tr-CcoP. As discussed previously it can be concluded that the histidine, which is replaced in tr-CcoP, is His 42. The 1825 nm MCD band observed in the tr-CcoP spectra can therefore be assigned to a His/Met species giving rise to the $g = 3.54$ EPR signal in the EPR spectra of tr-CcoP.

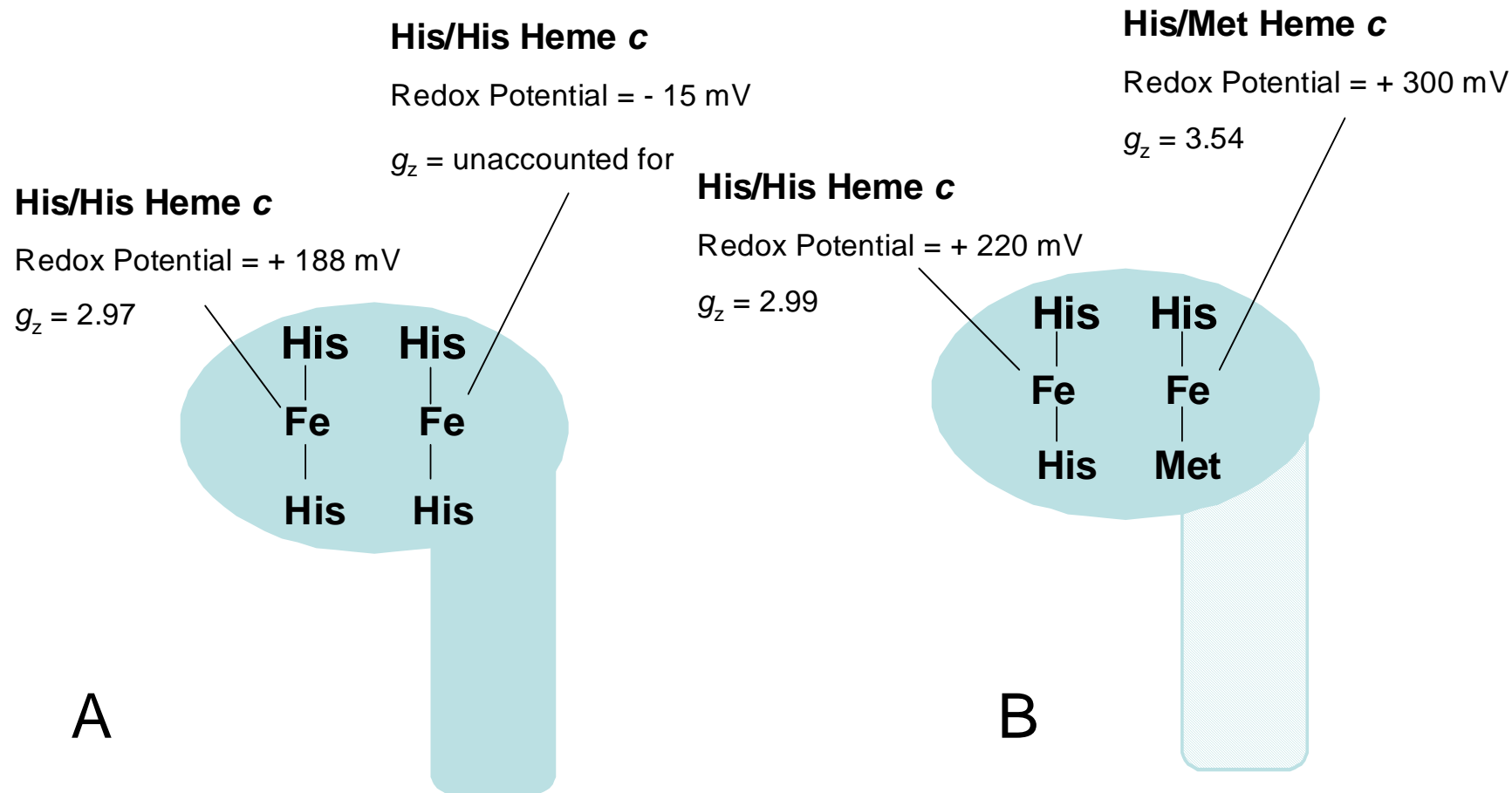


FIG. 3.10 Assignment of individual redox potentials and EPR signals to specific hemes in CcoP (A) and tr-CcoP (B). The assignments were based a combination of the redox potentiometry, EPR and MCD spectra of CcoP and tr-CcoP reported in this chapter.

3.2.6 CO binding studies

Carbon monoxide binding provides a convenient method for distinguishing heme proteins in which the distal ligand is absent, or can be displaced to bind an exogenous ligand from those in which all ligands are stable. The properties of protein/CO binding therefore provide a convenient method for distinguishing between heme proteins with different ligation states and/or differing axial ligands. MCD spectra of CcoP and tr-CcoP indicate that the distal ligands to the two *c*-type hemes in these proteins differ. In CcoP, both hemes are His/His ligated, however, in tr-CcoP, one heme is His/His and the other heme is His/Met ligated (Section 3.2.5).

It has been shown previously that hexa-coordinate CcoP binds the exogenous ligand CO, presumably following displacement of the endogenous distal ligand (Pitcher *et al.* 2003). The question therefore arises; do the different distal ligands in CcoP and tr-CcoP alter the CO binding properties of these proteins? The binding of CO to a heme iron induces distinguishable spectroscopic changes at the Soret region in the characteristic absorption spectrum of the heme. Upon CO binding to a fully reduced *c*-type heme the Soret band shifts from 417 nm to 415 nm and an increase in intensity of the Soret band can be observed. These features were used to monitor CO binding to the ferrous *c*-type hemes in CcoP and tr-CcoP (Fig. 3.11).

CcoP

The effect of CO binding to fully reduced CcoP is readily seen in the electronic absorbance spectrum (Fig. 3.11A). Upon CO binding, the Soret band shifts from 417 nm to the slightly shorter wavelength, 415 nm. The band also increases in intensity in comparison to the fully reduced state. The increase of the absorption intensity in the Soret band is coupled with a decrease in the α and β bands. Fig. 3.11B shows the difference spectrum of CcoP (dithionite reduced with CO bound *minus* dithionite reduced). The difference spectrum

shows a sharp band with a maximum at 415 nm and a minimum at 428 nm. A trough centered at 551 nm can also be observed. This pattern is typical of CO binding to a ferrous *c* type heme (Wood 1984). As discussed previously, it was generally believed that only penta-coordinated ferrous hemes could bind CO. As shown previously UV-Visible spectroscopy indicates that the two *c*-type hemes in CcoP are both six-coordinate, suggesting that CO does not bind to the heme via a vacant distal site (Section 3.2.2). The CO binding results of CcoP therefore suggest that the ligand to one of the *c*-type hemes in CcoP is displaced by the exogenous ligand, CO, prior to binding. The results presented here are concurrent with those previously reported by Pitcher *et al.* (Pitcher *et al.* 2003).

From the electronic absorbance spectrum of CcoP it is not possible to recognize whether CO is binding to one or both hemes. Previously Pitcher *et al.* reported that ascorbate-reduced CcoP does not bind CO and showed that spectral changes associated with CO binding were only fully developed when both hemes were completely reduced with dithionite, suggesting that CO only binds to the low potential heme (Pitcher 2002; Pitcher *et al.* 2003). Only hemes with redox potentials above + 60 mV are reduced with ascorbate, therefore the data suggests that CO binds to the low potential heme only (- 15 mV) in fully reduced CcoP, which is predicted to be His/His ligated. It is therefore speculated that the distal histidine to the low potential heme is displaced by the exogenous ligand, CO, prior to binding.

Truncated CcoP

In contrast to CcoP, CO binding to one of the *c*-type hemes in tr-CcoP is not observed in the electronic absorbance spectrum of tr-CcoP (Fig. 3.11C). A shift or an increase in the intensity of the Soret band was not observed upon addition of CO to reduced tr-CcoP. As shown by the difference spectra, a sharp band with a maximum at 415 nm and a minimum at 428 nm and a trough centered at 551 nm were not observed. The observed spectral

pattern of tr-CcoP following the addition of CO has not been reported in any *c*-type heme that binds CO and therefore suggests that CO does not bind to the ferrous *c*-type hemes in tr-CcoP (Wood 1984). It has been proposed that in CcoP the distal histidine ligand to the low potential heme is displaced to bind CO (Pitcher *et al.* 2003). The observation that CO does not bind to tr-CcoP suggests that the distal axial ligand that displaces to bind CO in CcoP is absent in tr-CcoP.

It is proposed that the amino acid residue, His 42, is the distal ligand to the low potential heme in CcoP. Redox potentiometry, EPR and MCD spectroscopy indicates that the low potential His/His ligated heme is not apparent in tr-CcoP. A His/Met ligated heme is observed in the MCD spectra of tr-CcoP (Section 3.2.5). It is therefore concluded that in tr-CcoP, His 42 has been replaced by a distal methionine. Tr-CcoP does not bind CO suggesting that the distal methionine that substitutes for the distal histidine observed in CcoP, does not displace to bind CO. CcoP does bind CO, therefore suggesting that it is the distal histidine, His 42, which displaces to bind CO.

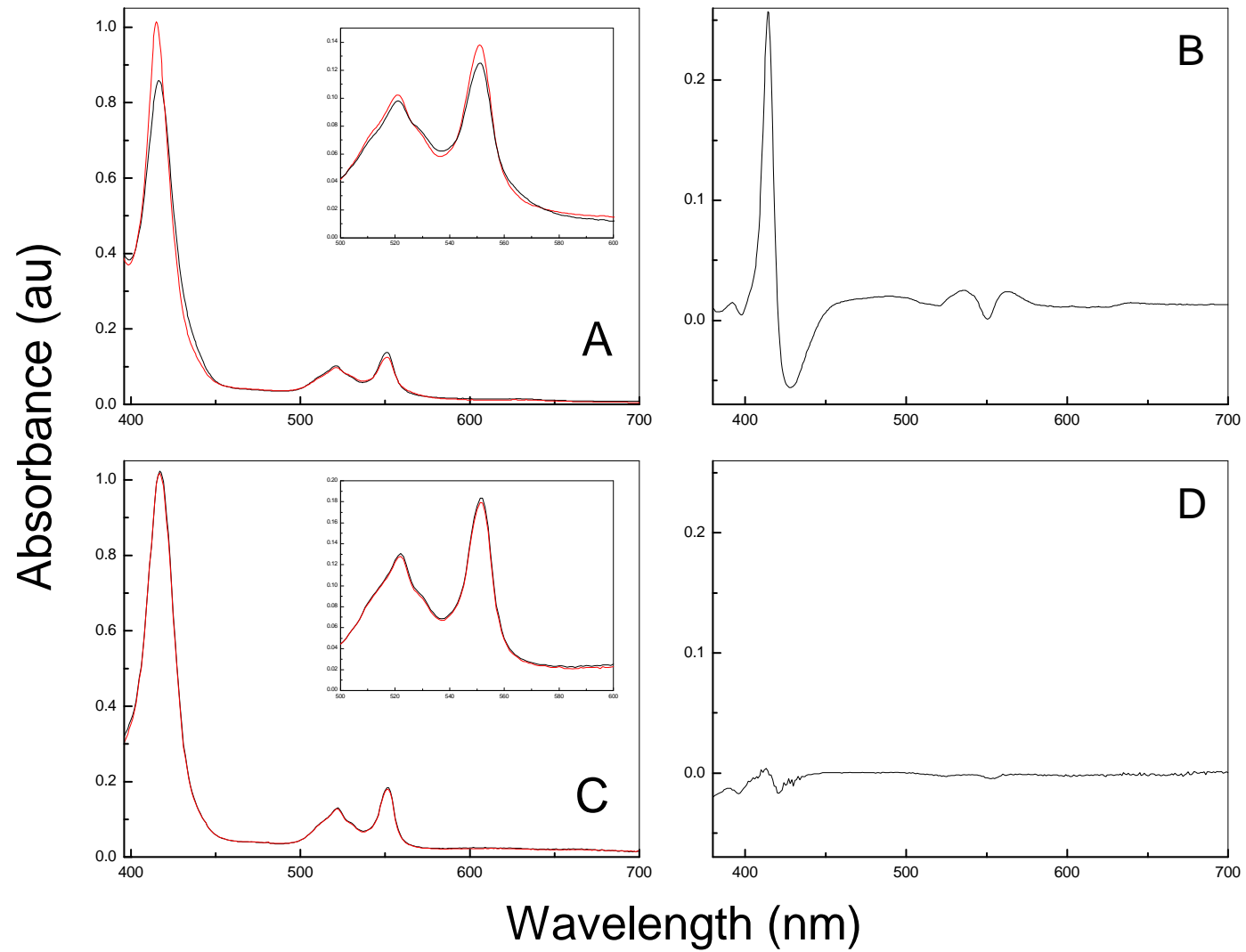
FIG. 3.11 UV-Visible absorption spectrum of fully reduced CcoP (A) and tr-CcoP (C) prior to (black trace) and after the additions of CO (red trace)

(A) The protein concentration was 2.5 μM in 20 mM Tris-HCl, 50 μM EDTA, 0.02% DM, pH 8. After the addition of excess sodium dithionite, the reduced spectrum was recorded (black trace). Following the addition of 1 mM CO (red trace) the spectrum clearly shows a shift of the Soret band from 417 nm to 415 nm and an increase in intensity. The insert shows a close up of the α and β regions of reduced CcoP (black trace) and reduced CcoP plus CO (red trace) with peaks at 550 nm and 521 nm respectively. Upon binding of CO a decrease in the α and β bands is observed. The spectrum was recorded at room temperature.

(B) CO difference spectrum (reduced plus CO *minus* reduced) of CcoP

(C) The protein concentration was 3 μM in 20 mM Tris-HCl, 50 μM EDTA, pH 8. After the addition of excess sodium dithionite, the reduced spectrum was recorded (black trace). Following the addition of 1 mM CO (red trace) the spectrum clearly shows no shift of the Soret band from 417 nm to 415 nm and no change in intensity. The insert shows a close up of the α and β regions of reduced tr-CcoP (black trace) and reduced tr-CcoP plus CO (red trace) with peaks at 550 nm and 521 nm respectively. Upon binding of CO no change in the α and β bands is observed. The spectrum was recorded at room temperature.

(D) CO difference spectrum (reduced plus CO *minus* reduced) of tr-CcoP



3.3 Conclusions

This study presents the results of the first comparative investigation of the *cbb*₃ subunit, CcoP, and the soluble heme-containing domain of CcoP. Using the combined approach of UV-Visible spectroscopy, EPR, MCD and redox potentiometry, evidence indicates that the two low spin hemes in CcoP are His/His ligated.

Parallel spectroscopic studies of CcoP and tr-CcoP, indicate that the distal ligand to one of the hemes in the water-soluble form of CcoP differs to that observed in CcoP. The low potential His/His ligated heme observed in CcoP is not detected in tr-CcoP but a high potential His/Met ligated was distinguished using spectroscopic techniques. In the absence of the low potential His/His ligated heme, tr-CcoP no longer binds CO, suggesting that it is the distal ligand to the low potential heme in CcoP which is displaced by the exogenous ligand, CO prior to binding. It is appealing to suggest that the sole fully conserved histidine in the CcoP subunit, His 42, is the displaceable distal ligand to the low potential heme. Mutating the His 42 residue using Site-directed mutagenesis and investigating the biochemical characteristics of the mutants can be used to explore the identity of the distal ligand further.

4. Site Directed Mutagenesis of CcoP

4.1 Introduction.....	139
4.2 Results and Discussion.....	142
4.2.1 Sequence Alignments and Site Directed Mutagenesis.....	142
4.2.2. Phenotype Characterization of Mutated CcoP.....	143
4.2.3 Biochemical Characterization of Mutated CcoP.....	150
4.2.4 Mediated Redox Potentiometry.....	158
4.2.5 CO Binding Studies.....	163
4.2.6 Comparative EPR Spectroscopy of CcoP variants.....	175
4.3 Conclusions.....	180

4.1 Introduction

Spectroscopic studies have revealed that both *c* type hemes in the *ccb*₃ subunit, CcoP are His/His ligated in the ferric form (Chapter 3). Despite having the same ligation state, one of these *c* type hemes has a high midpoint redox potential and one has a low midpoint redox potential (Chapter 3, Section 3.2.3). CO binding studies reveal that the low midpoint redox potential heme in CcoP binds CO when in the ferrous state (Chapter 3, Section 3.2.4). The low midpoint redox potential heme in CcoP remains six-coordinated in the ferrous state therefore, CO binding to this heme must be preceded by displacement of the distal ligand. The displacement mechanism is possibly mimicked *in vivo* in the presence of an exogenous ligand, for example, oxygen or nitric oxide. The identity of this displaceable distal histidine to the low midpoint redox potential heme is not confirmed. However, the residue His 42 is the only fully conserved histidine observed in the alignment of sequences of the CcoP subunit from a variety of species from all sub-divisions of the Proteobacteria group. It is assumed that a distal ligand, which is proposed to have such a direct function in the protein, would be conserved throughout the species. It is therefore appealing to suggest that His 42 is the distal ligand to the low midpoint redox potential heme. Moreover, CO binding is not observed in water-soluble form of CcoP (tr-CcoP) in which His 42 is deleted (Chapter 3, Section 3.2.4).

Using protein topology prediction methods, the conserved histidine residue, His 42, in the CcoP subunit, is indicated to be located in the cytoplasm (Krogh *et al.* 2001). The two *c*-type heme binding motifs of CcoP are predicted to be located in the periplasm. The residue, His 42, and the two hemes would therefore be placed on opposite sides of the membrane. This structural suggestion would preclude His 42 from serving as an axial ligand to either of the *c*-type hemes in CcoP. These topological predictions are based on the N-terminus of CcoP being located in the periplasm and the presumption that CcoP has two transmembrane helices, as shown by the schematic in Fig. 4.1A. Alternatively a

membrane protein can be monotopic and anchored via an amphipathic helix inserted in a parallel way to the membrane interface, so called in-plane membrane anchors (IPM) (Fig. 4.1B and C) (Penin *et al.* 2004; Sapay *et al.* 2006). IPM anchored proteins are not uncommon, however, this suggested topology has not been reported in a heme protein (Sapay *et al.* 2006). A model predicting IPM anchors in CcoP would infer that the N-terminus of this subunit is directed to the cytoplasm and would result in an upside down L-shaped topology of the subunit, as depicted by the schematic in Fig. 4.1B. This structural suggestion would place the conserved histidine residue, His 42, and the *c*-type heme binding motifs in the periplasm. In this scenario the fully conserved histidine residue, His 42 could feasibly ligate the low potential *c*-type heme in CcoP.

Having established that His 42 could feasibly be the distal ligand to the low midpoint redox potential heme in CcoP, we combined mutagenesis and spectroscopic approaches to confirm the identity of this displaceable distal ligand.

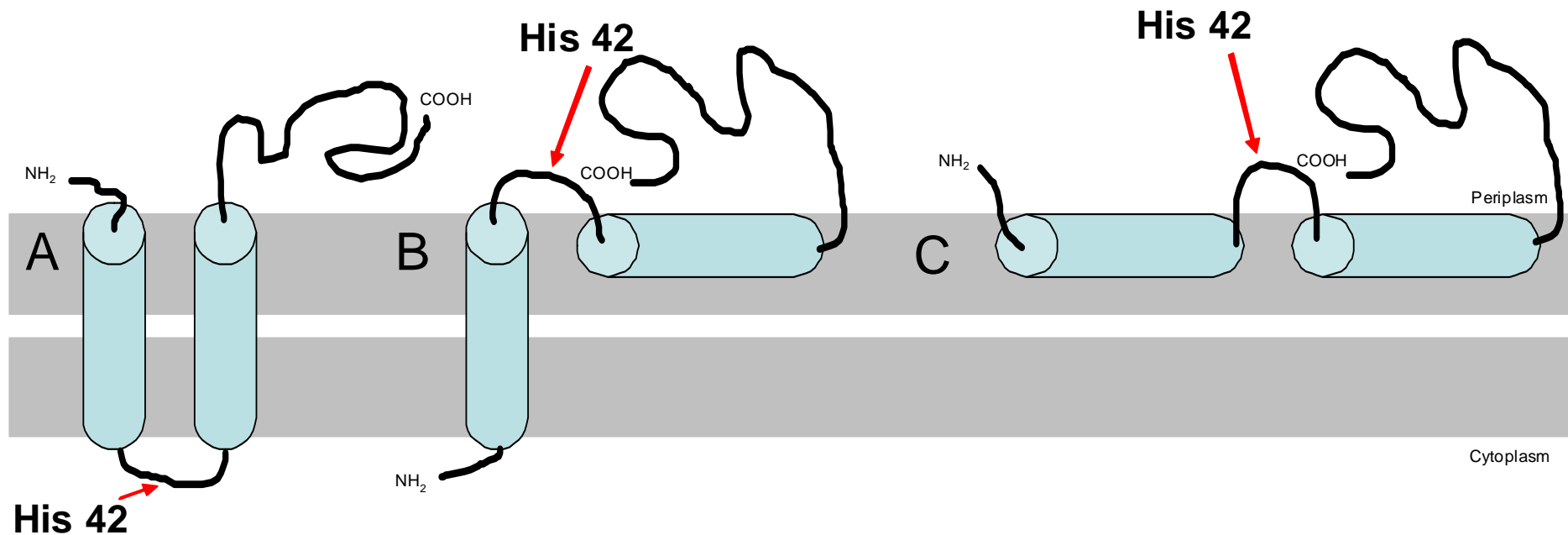


FIG. 4.1 Possible topology of the *cbb*₃ subunit CcoP. CcoP contains one fully conserved histidine residue, His 42, which is predicted to be located in the cytoplasm. The periplasmic domain of CcoP contains two heme *c* binding motifs. (A) Both hydrophobic transmembrane helices traverse the membrane. Consequently, the histidine residue, His 42 cannot ligate either heme iron. (B) Only one hydrophobic stretch traverses the membrane and the second hydrophobic stretch runs parallel to the membrane plane. This places His 42 in the periplasm and can therefore potentially ligate one of the *c*-type hemes. (C) Neither of the hydrophobic regions traverse the membrane but run parallel to the membrane plane. This places His 42 in the periplasm.

4.2 Results and Discussion

4.2.1 Sequence Alignments and Site Directed Mutagenesis

The multiple sequence alignment of CcoP from 10 bacterial species (Fig. 4.2) demonstrates the presence of a single fully conserved histidine (His 42). It is appealing to suggest that this sole conserved histidine is the displaceable axial ligand to the low midpoint redox potential *c* type heme in CcoP. To test this hypothesis the amino acid His42 was substituted with alanine (H42A), cysteine (H42C) or methionine (H42M) by site-directed mutagenesis (SDM).

Substitution of a single amino acid in a protein is achieved by SDM of the gene that encodes the protein. When choosing residue substitutes in SDM it is important that disturbances of the protein fold and structural characteristics are kept to a minimum (Bordo and Argos 1991). Histidine is a polar amino acid, which is unique with regard to its properties. Histidine has a pKa of 6.0, near to that of physiological pH, meaning that the side chain readily accepts and donates protons. This property means that this residue does not substitute particularly well with other amino acids (Bordo and Argos 1991; Betts 2003). The amino acid substitutes for His 42 were therefore chosen based on functional rather than structural replacements.

The amino acids substituted for His 42 in CcoP were alanine, cysteine and methionine. Alanine is a small non-polar amino acid and is therefore less disruptive to protein structure than many other amino acid substitutions. Alanine was an ideal neutral substitute to gather general information regarding the effect of point mutagenesis on the CcoP subunit. It was predicted that the mutant strain, H42A would create a five coordinate heme as the alanine residue would not ligate to the heme iron. In contrast, by changing the histidine to a cysteine it was postulated that a permanently six-coordinated heme would result. Cysteine is a non-polar amino acid and similarly to methionine, the amino acid cysteine ligates to the heme

iron via the sulfur iron in the amino acid. Cysteine is also very electronegative and lowers the reduction potential of the heme iron typically to *ca* -200mV. Methionine is a non-polar neutral amino acid with a sulfur group, which is commonly observed as a heme ligand (Moore and Pettigrew 1990). Using MCD spectroscopy it has been identified that a methionine residue replaces the missing His 42 residue in the water-soluble form of CcoP, tr-CcoP (Chapter 3, Section 3.2.5). The substitution of a methionine residue for His 42 (H42M) was therefore chosen to investigate any interchangeable ligand properties between histidine and methionine.

4.2.2. Phenotype Characterization of Mutated CcoP

The individual mutant proteins were grown and purified using the methods utilized for CcoP, as described previously (Chapter 2, Section 2.4.2). The protein concentrations for each CcoP mutant are based on the calculation of the CcoP extinction coefficient, previously reported by Pitcher *et al.* (Pitcher *et al.* 2002). Previous calculation of the extinction coefficient of CcoP at 408 nm (the Soret maximum of the oxidized protein) yielded a value of $2.7 \times 10^5 \text{ M}^{-1} \text{ cm}^{-1}$.

Following purification of the proteins the yield of the CcoP variants, was compared with that of wild type CcoP. The protein yield of the variants differed slightly compared to CcoP, as shown in Table 4.1. The protein yield of the alanine mutant, H42A, was consistent with CcoP, suggesting that this ligand replacement was tolerated and therefore behaved as CcoP (Wallace and Clark-Lewis 1992). In comparison, the yield of the methionine mutant, H42M, increased slightly, but reproducibly.

Pseudomonas stutzeri -----MTSFWSWYVTLTSLGLTIAALVWLLLATRKGQRPDSTEETVGHSYDGI 47
Pseudomonas aeruginosa 1552 -----MTTFWSLYITALTLGLTLLALTWLIIFATRKGQRSSTTDETVGHSYDGI 47
Pseudomonas aeruginosa 1555 -----MTTFWSLYITALTVGTLIALLLWLVFATRKGAEAKGTTEKTMGHSYDGI 47
Vibrio cholerae -----MTTFWSLWIIIVITVGTLLGCAILLVWCLKDKMGVEEGVDMGHEYDGI 47
Brucella suis -----MTDK-QIDEVSGVSTTGHEWDGI 31
Bradyrhizobium japonicum -----MTDHSEFDSVSGKTTTGHEWDGI 42
Rhodobacter sphaeroides -----MSVKPTKQKPGEPPTTGHSDGI 28
Rhodobacter capsulatus -----MSKKPTTKK--EVQTTGHQWDGI 30
Helicobacter pylori -----MDFLN--DHINVFLIAALVILVLTIIYESSLIKEMRDSKSSQGELMENGHLIDGI 53
Campylobacter jejuni -----MQWLNLEDNVNLLSLIGAILIILITLVIVGRMFKQMKEKKGESELS--HSWDGI 55

*** **

Pseudomonas stutzeri EEYDNPLPRWWFMLFVGTIVIFALGYLVLYPGLGNWKGILPG-----YEG-----GWTQVKEWQREMDKANEQY 127
Pseudomonas aeruginosa EEYDNPLPKWWFMLFVGTLVFVAVGYLALYPGLGTWKGLMPG-----YQSADEFADKEKGWTGVHQWEKEMAKADEKY 127
Pseudomonas aeruginosa EEYDNPLPKWWFMLYIGTIVFSVGYLVLYPGLGNWKGVLPG-----YEG-----GWTQDKQWEREMNIAQEKY 127
Vibrio cholerae RELNNPLPKWWTYLFIGTFIFAAYIYLTLYPGLGSFKGILGWQSSDQTVRSLEESRASIAAAQONKQLVQYSKELDDAEAYY 127
Brucella suis KELDNPMRWWLWTFYATIFWAIAYVIAYPAWPLISG-STAG-----LTGWSSRGQFWQENAKIAASR 102
Bradyrhizobium japonicum KELNTPLPRWWVICFYLTIVWAIGYWIYPAWPLISS-NTTG-----LFGYSSRADVAVELANLEKIR 102
Rhodobacter sphaeroides EEFDNPMRWWLWTFYVTIVWAIGYSILYPAWPLING-ATNG-----LIGHSTRADVQRDIEAFEAEN 102
Rhodobacter capsulatus EELNTPLPRWWLWTFYATIIWGVAYSAMPWPIFSDKATPG-----LLGSSTRADVEKDIAKFAEMN 101
Helicobacter pylori GEFANNVPVGVWIASFMCTIVWAFWYFFFYGYPLN-----SFSQIGQYNEEVKAHNQKF 131
Campylobacter jejuni GEYKNAVPTGWAVVFFLTIVWAIWYFLWGYPLN-----SFSSIGQYNEEVATHNTKF 131

Pseudomonas stutzeri GPLYAKYAAMP-----VEEVAKD----PQALKMGGRLFASNCVCHGSDAKGAYGFPNLTDWLDWGGEPETIKTTILH 180
Pseudomonas aeruginosa GPIFAKFAAMP-----IEEVAKD----PQAVKMGGRLFASNCI CHGSDAKGAYGFPNLTDADWRWGGEPEPETIKTTIMA 177
Pseudomonas aeruginosa GPIFAKYAAMP-----IEEVAKD----EHAMKMGSRMFATYCSI CHGSDAKGALGFPNLADNEWRWGGDPQSIETTILG 177
Vibrio cholerae GEAFKRLAYQDGTTLNREIPDIAAD---SDALKVQRLFLQNC SQCHGSDARGQKGFNPNTDDAWLYGGEPQAIVTTIRH 202
Brucella suis QGIIDQIKAKD-----VHEILADEELRQYAIAGGAAAFRVN CVQCHGSGAQGAPGYPNLNDDDWLWGGSIDDIVTTIRH 155
Bradyrhizobium japonicum GDKMAALGAAS-----LADVEKDPALLALARAKGKTIVFGDNCAP CHGSGGAGAKGFNPNLDDDWLWGGTLDQIMQTIQF 156
Rhodobacter sphaeroides ATIRQQLVNTD-----AIAADPNLLQYATNAGAAVFRTN CVQCHGSGAAGNVGYPNLLDDDWLWGGDIESIHTTVTH 156
Rhodobacter capsulatus KAVEEKLVDATD-----LTAIAADPELVTYTRNAGAAVFRTWCAQCHGAGAGGNTGFPSLLDGDWLHGGAIETIYTNVKH 155
Helicobacter pylori EAKWKNLGQKE-----LVDMGQGI FLVHCSQCHGITAEG LHGS---AQNLVRWGKE-EGIMDTIKH 159
Campylobacter jejuni EEKFKNLSPED-----KIAMGQNI FLVQCSACHGITGDGINGK---AQNLNIWGSE-EGIIINVIKH 159

* * * * * * * * * *

```

Pseudomonas stutzeri      GRQAVMP-----GWKDVIGEEGIRNVAGYVR-SLSGRDTPEGISVDIEQGQKIFAANCVVCHGPEAKGVTA 248
Pseudomonas aeruginosa    GRHAAMP-----AWGEVIGEEGVKNVAAFVLTQMDGRKLPEGAKADIEAGKQVFATTCVACHGPEGKGTTPA 249
Pseudomonas aeruginosa    GRHAIMA-----AWGDILGEDGVKNVAAYVRTELAGLKLPEGTKADVEAGKQIFSVNCVACHGPEGKGTAL 270
Vibrio cholerae           GRIGQMP-----AWKDILGEQGVKEVVSYYTL-SLSGRSVNA---KEAEAGKARFAV-CSACHGTDGKGNPA 270
Brucella suis             GVRSPDDPETRLS-EMTAFAD--VLEPQQIRDVAAYVV-NLSGTPHDP---SMVPEGQKVFAENCAVCHGADAKGLRE 232
Bradyrhizobium japonicum GARS-GHAKTHEG-QMLAFGKDGVLKGDEIVTVANYVRSL-SGLPTRKG--YDAAKGEKIFVENCVACHGDGGKGNQE 255
Rhodobacter sphaeroides  GIRNTTD-DEARYSEMPRFGADGLLDSTQISQVVEYVL-QISGQDHDA---ALSAEGATIFADNCAACHGEDGTGSRD 235
Rhodobacter capsulatus   GIRDPLDPDPTLLVANMPAHLTDELLEPAQIDEVVQYVL-QISGQPADE---VKATAGQQIFAENCASCHGEDAKGLVE 235
Helicobacter pylori       GSKGMDYLAGEMP-----AMELDEKDAKAIASYVMAEISSVKKTKNPQLIDKGKEQIFAENCASCHGNDGKGLQE 235
Campylobacter jejuni      GSKGMNFPGGEMLG-----AADLGVAEEDIPAIAAYVAKDLSAIKKTANENLVAKGKEAYAT--CAACHGEDGKGQDG 238
*                                                                    *   ***   *

Pseudomonas stutzeri      MGAPNLTDN-VWLYGSSFAQIQOTLRYGRNGRMPAQE-----AILGNDKVHLLAAYVYSLSQQPEQ-- 305
Pseudomonas aeruginosa    MGAPDLTHPGAFIYGSSFAQLQOTIRYGRQGVMPAQE-----EHLGNDKVHLLAAYVYSLSHGKSAE 308
Pseudomonas aeruginosa    VGAPNLTNPGAFIYGSSYAQLQOTIRHGRQGMMPAQE-----PYLGKEKVHILAAYIYNLSHNQGSN- 308
Vibrio cholerae           FGAPNLTDN-DWLFGDSRAEVTETVMNGRSGVMPAWI-----NTLGEEKIQLVAAYVWVSLSNSENK----- 326
Brucella suis             FGAPNLTDN-IWLYGSGEDAIRQVSHPKHGVMPAWE-----ARLGDATVKQLAIFVHSLGGGE----- 287
Bradyrhizobium japonicum MGAPNLTDK-IWLYGSDEAALIETISQGRAGVMPAWE-----GRLDPSTIKAMAVYVHSLGGGK----- 290
Rhodobacter sphaeroides  VGAPNLTDN-IWLYGGDRATVTETVTYARFGVMPNWN-----ARLTEADIRSVAVYVHSLGGGE----- 290
Rhodobacter capsulatus   MGAPNLTDG-IWLYGGDVATLTSTIQYGRGGVMPSSWSWAADGAKPRLSEAQIRAVASYVHSLGGGQ----- 297
Helicobacter pylori       N-QVLAADLTTYGTENFLRNILTHGKKGNIGHMPSFKY-----KNFSDLQVKALPEFIQSLKPLED----- 292
Campylobacter jejuni      ----MFPDLTKYGSAAFVVDVLHSGKAGFIGTMPSFP-----TLNDIQKEAVGEYVISLSRGE----- 287
* **                                                                    *

```

FIG. 4.2 Multiple sequence alignments of CcoP. Conserved residues are marked with an asterisk. The predicted heme binding sites of CcoP are coloured red. The fully conserved histidine residue (His 42) is highlighted in blue. The semi conserved histidine residues are highlighted in pale blue. The sole fully conserved methionine residues are highlighted in green and the semi conserved methionine residues are highlighted in pale green. The predicted transmembrane helices of *P. stutzeri* CcoP are underlined. Since the completion of this thesis, the genomic sequence of *P. stutzeri* has

identified two putative *ccb* operons (Yan *et al.* 2008). This alignment refers to CcoP PST 1837.

CcoP Strain	Protein Yield (mg)/ Wet Cells (g)
CcoP	8.63 ± 0.42 mg/25 g
H42A	8.7 ± 0.8 mg/25 g
H42C	5.33 ± 0.71 mg/25 g
H42M	11.4 ± 0.7 mg /25 g

Table 4.1 Protein Yield typical of a 2.4 L grow up of CcoP, H42A, H42C and H42M.

Interestingly, the yield of the cysteine mutant, H42C, decreased compared to CcoP. The difference in protein yield suggests that the H42C mutation resulted in reduced translation of the amino acid sequence by the cell, possibly because the cysteine replacement is not tolerated at the His 42 position (Wallace and Clark-Lewis 1992). Poor expression of the mutant would result in a reduction in heme content of the protein variant relative to CcoP. A homogeneous product was however, obtained that satisfied analytical criteria with physicochemical properties that emulated those reported for CcoP. Therefore, despite speculation, the reason for the discrepancy in apparent protein yields was unclear.

CcoP and the three mutant strains were evaluated using SDS-PAGE, which was stained specifically to detect the presence of *c*-type cytochromes by analyzing the proteins for intrinsic peroxidase activity using 3,3',5,5'-tetramethyl benzidine and H₂O₂ as shown in Fig. 4.3 (Chapter 2, Section 2.2.2). The analysis of proteins using gel electrophoresis is a qualitative method and CcoP was clearly visible as a band at ~35 kDa in all the mutant strains. Despite not being a quantitative method, gel analysis of the purified mutants does indicate a slight difference in the intensity of the band specific to the *c*-type hemes in CcoP when a comparable protein concentration was used. The ability of the mutated enzyme to bind heme should not be affected by the SDM as the proximal histidine has not been

altered. However, these results suggest that the level of CcoP expression is influenced by the presence of the mutation. It is therefore possible that the site specific mutations cause destabilization of the structure of CcoP.

Following SDM the mutated CcoP plasmids were sequenced using standard T7 forward and reverse primers for confirmation of successful mutagenesis (Chapter 2, Section 2.3.8). A technical limitation with this method is that it does not allow for the mapping of post-translational modifications. Protein Mass Mapping using mass spectrometry compares the mass of peptides released by enzymatic digestion of a protein followed by mass analysis of the resulting peptide mixture. Comparison of the mass of the peptides that are released by such treatment makes it possible to identify similar peptides in which amino acid differences occur. The mass spectrometry comparisons of CcoP and the mutants H42A and H42M are shown in Fig. 4.4.

MALDI-TOF experiments performed on covalently heme bound CcoP gave a single peak with a mass of 35047 Da. This mass corresponds with the single peak with a mass of $35,000 \pm 81$ Da for CcoP previously observed by Pitcher *et. al.* and is in good agreement with the molecular mass predicted from the confirmed gene sequence (34,984 Da) (Pitcher 2002).

The corresponding signal in the spectrum of the mutant H42A was 34979 Da. Allowing for experimental error, this signal is consistent with the difference in mass of 66 Da between histidine and alanine. In comparison, the signal in the spectrum of H42M does not differ to the CcoP signal and was observed at 35045 Da. The DNA sequencing confirmed the His to Met mutation and the MALDI-TOF result is consistent with an amino acid change in which the residues only differ in size by 6 Da.

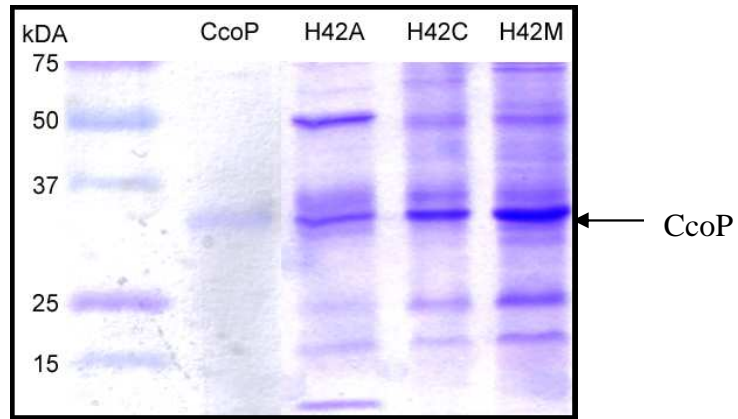
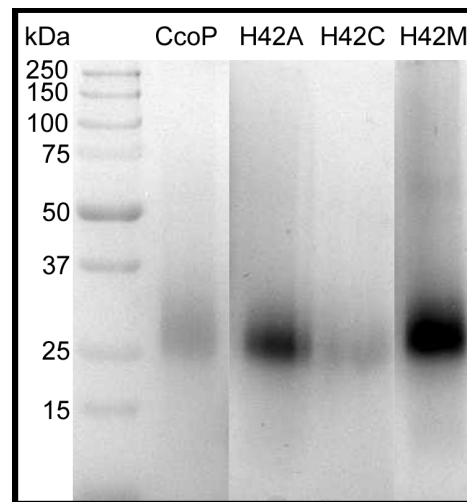
A**B**

FIG. 4.3 SDS PAGE of WT and mutated CcoP.

The proteins were purified using the methods outlined previously. The purified proteins were visualized by (A) Coomassie blue stain for total protein and (B) Heme stained specifically for *c* type hemes. The sample loaded consisted of 10 μ l protein sample and 10 μ l 2x SDS loading buffer containing 6M Urea, to denature the protein, 5% SDS, to confer an overall negative charge to the proteins in the sample, 0.1% glycerol to increase the density of the sample/buffer, and 0.05% Bromophenol blue as a tracking dye. The protein sample was denatured in SDS loading buffer at 50 °C for 10 minutes before being run on SDS-PAGE. Sample lanes are as marked.

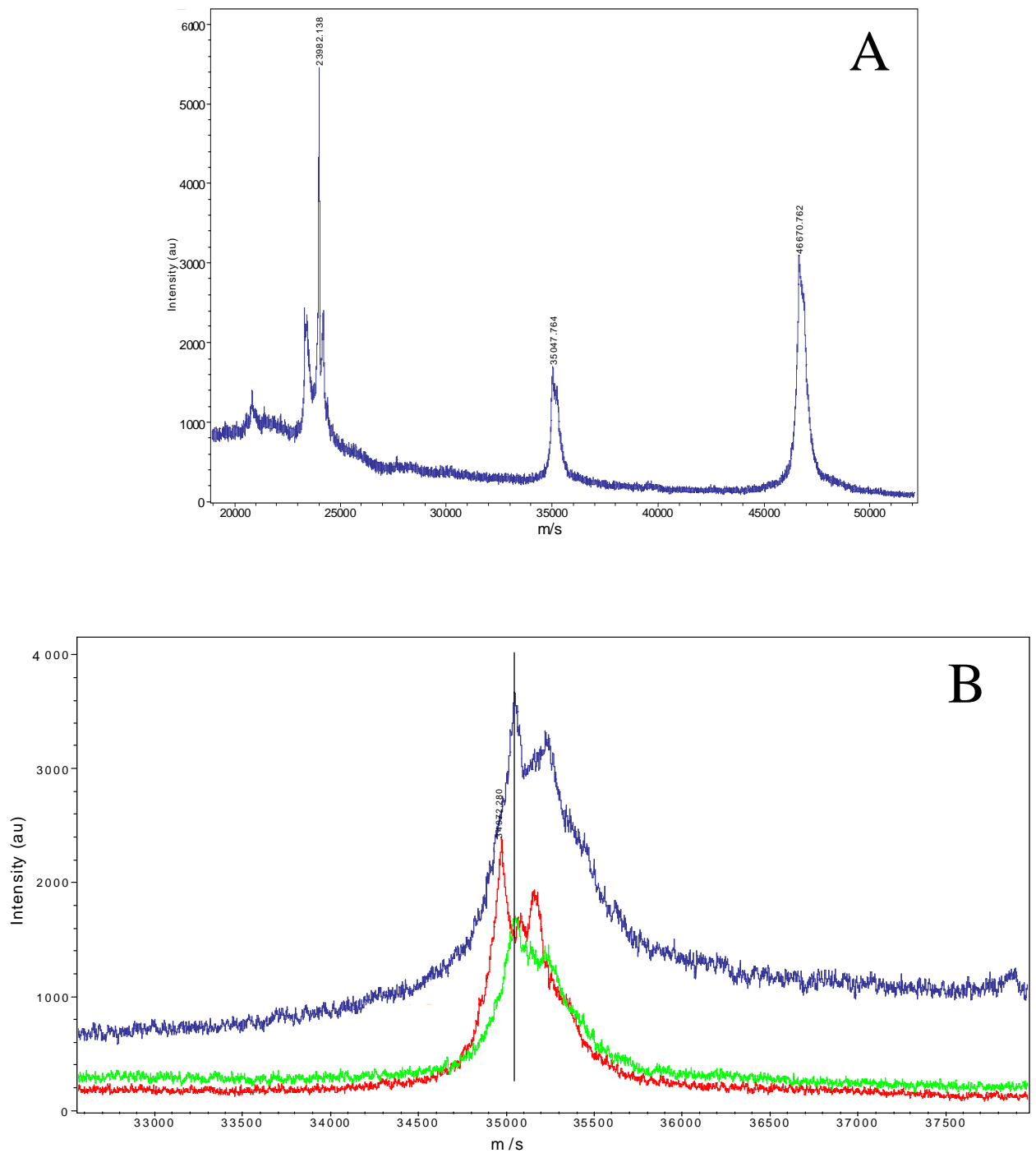


FIG. 4.4 Comparison of the MALDI-TOF mass spectra resulting from the trypsin digest of CcoP and mutants H42A and H42M. A) CcoP showing a peak at 35047 Da. Peaks corresponding to the calibrants, Trypsinogen (23982 Da) and Endolase from yeast (46671.9 Da) are shown. B) Close up of peaks obtained for CcoP, 35047 Da (Green), H42A, 34972 Da (Red) and H42M, 35045 Da (Blue).

Protein	Calculated average mass (Da)	Mass difference with respect to CcoP (Da)
CcoP	35047 ± 2.12	-
H42A	34979 ± 1	- 68
H42C	-	-
H42M	35045 ± 1.82	- 2

Table 4.2 Calculated average mass of CcoP and CcoP mutants and mass differences with respect to CcoP

A strong signal was not obtained for the mutant strain, H42C at 35,000 Da using mass spectrometry. The result suggests, as previously predicted, that this mutation caused instability in the structure of CcoP. All samples were analyzed in duplicate and good reproducibility was observed.

4.2.3 Biochemical Characterization of Mutated CcoP

The UV-Visible spectra of all the CcoP mutants were measured in the ferric and ferrous forms and compared to the UV-Visible spectra of CcoP. A Soret maximum of 408 nm and a broad band in the α/β region (500-600 nm) can be observed in the electronic absorption spectrum of fully oxidized mutated CcoP strains (Fig. 4.5). Upon complete reduction of all the mutants, with excess sodium dithionite, the Soret band shifted to 417 nm and an increase in intensity was observed (Fig. 4.6). The α and β bands in the visible region intensified upon reduction at 551 nm and 521 nm respectively. These features are characteristic of ferrous low spin *c*-type hemes. The intensity of the symmetrical 551 nm band of CcoP was consistent with the reduction of two *c* type hemes. This band, however, has a lower intensity in all of the mutants compared with that exhibited by CcoP, relative to the concentration of the protein. The discrepancy in the height of the band is consistent

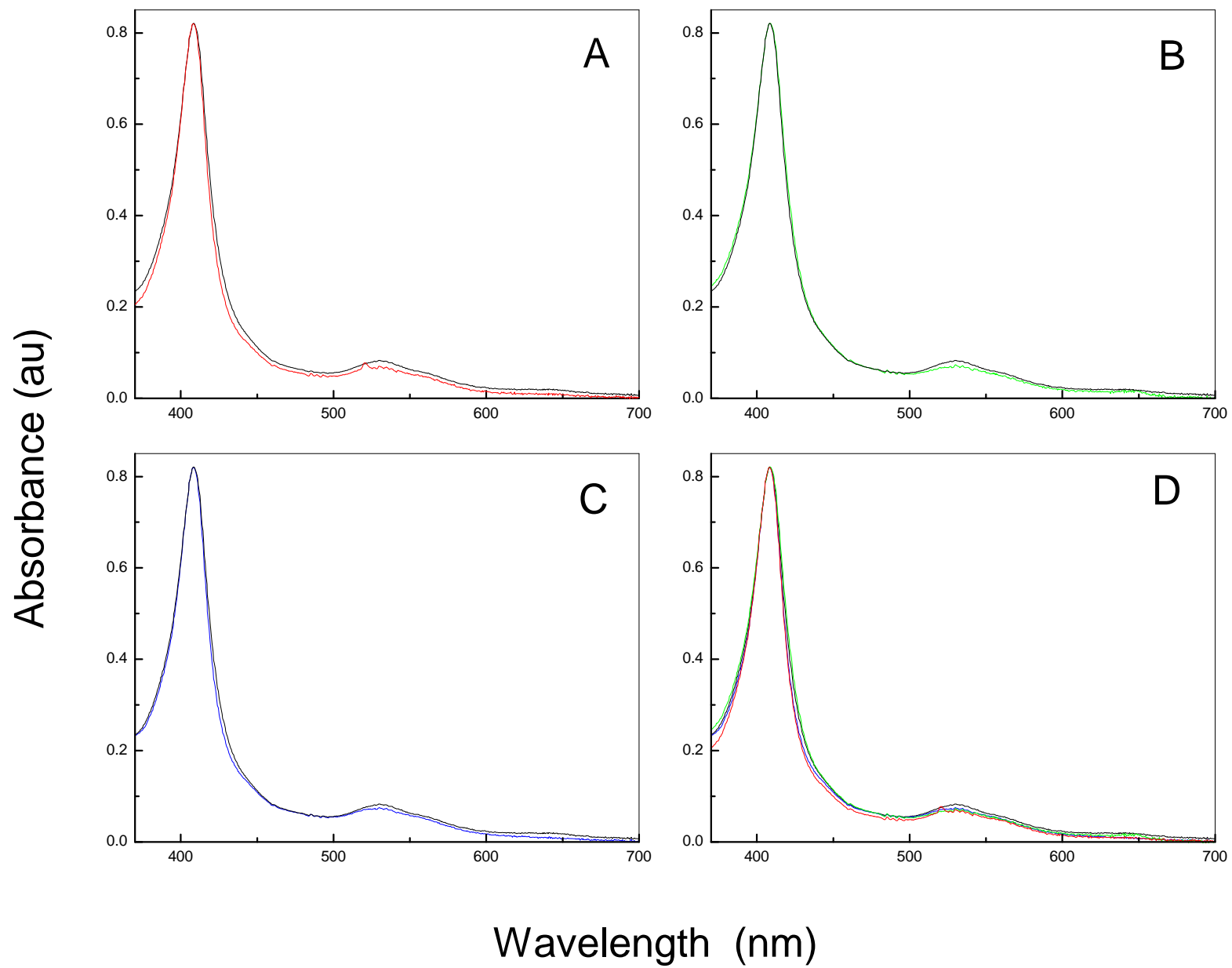
with the mutation of a distal ligand because spectral changes are commonly observed in proteins in which one of both of the axial ligands has been replaced (Wallace and Clark-Lewis 1992). Any differences in the heights and symmetry of the Soret, α or β bands observed can be a reflection of the heme geometry upon the axial heme coordination and heme environment (Kamen *et al.* 1973; Moore and Pettigrew 1990).

The spectra of oxidized and reduced H42C and H42M resemble the spectra of CcoP. This result was anticipated as both cysteine and methionine residues can potentially serve as axial heme ligands (Moore and Pettigrew 1990; Wallace and Clark-Lewis 1992). The spectra therefore suggests that the low midpoint redox potential heme, to which it is assumed the distal ligand has been altered by SDM, remains six-coordinate. Surprisingly, the electronic absorbance spectrum of H42C and H42M showed no evidence of a 695 nm charge transfer band. A 695 nm charge transfer band is characteristic of a low intensity ligand to metal charge transfer transition that is observed when a low spin ferric heme possesses at least one of the sulphur containing residues, methionine or cysteine, as ligands (Moore and Pettigrew 1990). This band is not always visible using absorption spectroscopy and the absence of this band is not diagnostic of the lack of a sulfur ligand to the heme. In the H42C and H42M mutants it is reasonable to predict that the substitution of cysteine and methionine respectively would lead to His/Cys and His/Met coordination of the heme iron if the histidine residue at position 42 provides the distal ligand. This however is not guaranteed. SDM of the distal ligand to one of the *c*-type hemes in the soluble protein, fumarate reductase from *Shewanella frigidimarina* resulted in ligation of the iron by a water molecule not the methionine substitute (Rothery *et al.* 2003).

FIG. 4.5 UV-Visible absorption spectra of recombinant CcoP from *P. stutzeri* and mutated recombinant CcoP from *P. stutzeri* in the oxidized form. The amplitude of the Soret of oxidized mutated CcoP was normalized to the Soret of oxidized recombinant CcoP so the spectra could be easily compared. To demonstrate the influence of the amino acid substitutions on the absorption spectrum of CcoP, the spectrum of CcoP and mutated CcoP are superimposed as indicated:

- A) Oxidized spectra of purified H42A (red trace) and purified CcoP (black trace).
- B) Oxidized spectra of purified H42C (green trace) and purified CcoP (black trace).
- C) Oxidized spectra of purified H42M (blue trace) and purified CcoP (black trace).
- D) Overlay of purified CcoP (black trace), H42A (red trace), H42C (green trace) and H42M (blue trace).

All samples were in 20 mM Tris-HCl, 50 μ M EDTA, 0.02% DM, pH 8. All the samples were oxidized with potassium ferricyanide which was subsequently removed by passing the sample through a PD10 desalting column. The spectra were recorded at room temperature.



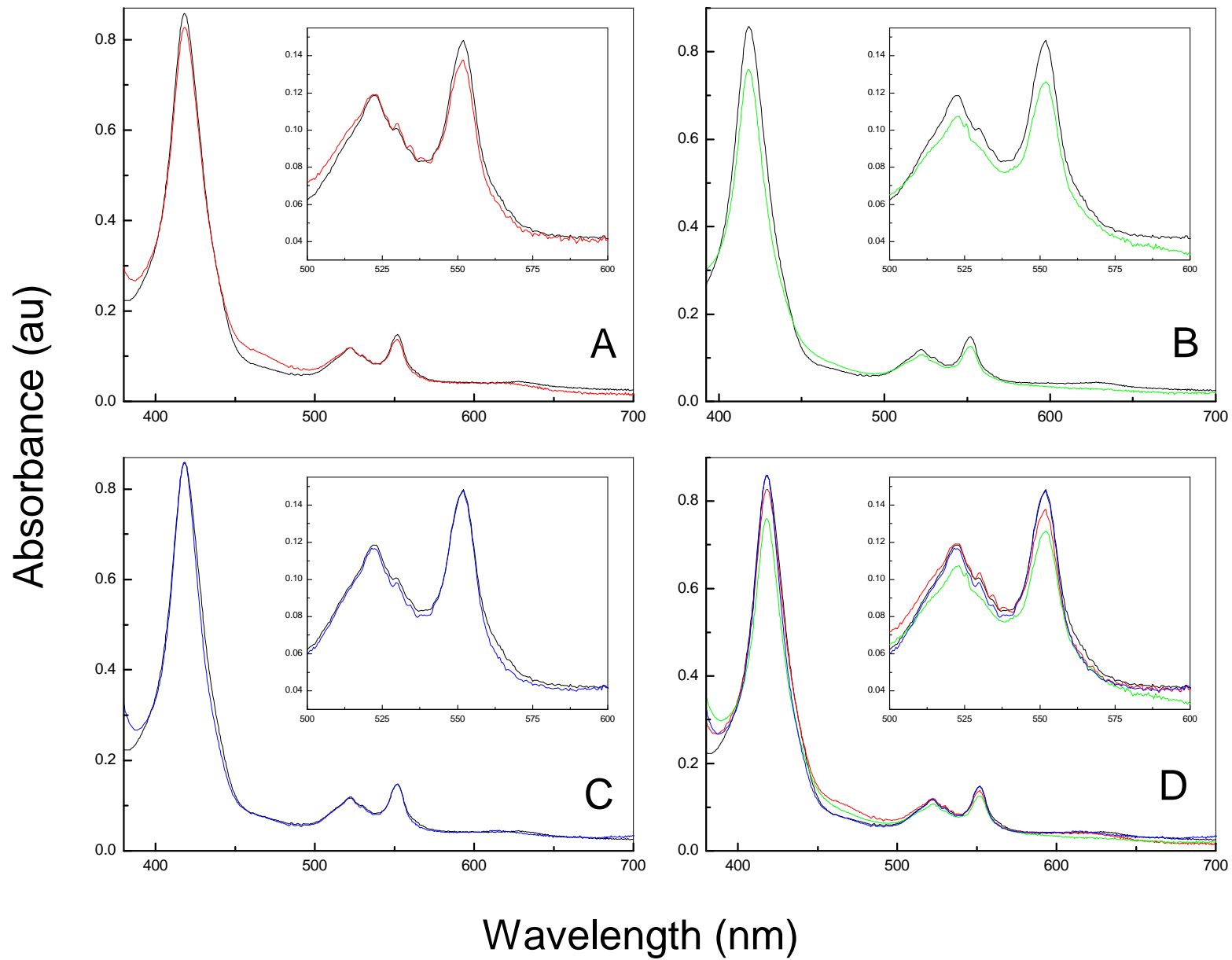
There was no feature beyond 551 nm in the spectra of fully reduced mutated CcoP strains that would indicate the presence of high-spin ferric heme, suggesting that both *c*-type hemes in all the mutants remained in the low-spin state, despite the amino acid substitutions. The aliphatic amino acid residue alanine is not a good donor or π acceptor and saturated carbon atoms do not coordinate metal ions (Wallace and Clark-Lewis 1992). The electron absorbance spectrum of H42A was therefore surprising as it was expected that substitution of His 42 with an alanine residue would result in the low midpoint redox potential heme becoming five coordinate. Any coordination change would alter the appearance of the spectra of H42A compared to CcoP as the low midpoint redox potential heme would be high spin. Features beyond 551 nm are not, however always apparent because of the low extinction coefficient of the high spin signal at 640 nm so high protein concentrations are necessary to visualise any high-spin features spectroscopically (Moore and Pettigrew 1990). Moreover, the spectral features of a low spin *c*-type heme, the distinct α and β bands, can mask the broad band of a high spin *c*-type heme in the same sample (Wood 1984). It should therefore be considered that the spectra of H42A, reflects that His 42 is not the distal ligand, therefore the alanine-histidine substitution has no effect. However, the distal site vacated by the histidine may have been fulfilled by an alternative amino acid or exogenous ligand. In the recently described six-coordinate vertebrate globin, neuroglobin, it has been suggested that alternative residues compete with the distal histidine for the sixth coordination site (Uno *et al.* 2004). It could be speculated that in the absence of His 42 the role of a distal ligand to the low potential heme in CcoP is fulfilled by an alternative amino acid, which would normally compete with His 42, for example one of the conserved methionine residues. Recall, in water-soluble tr-CcoP, His 42 was deleted during the removal of the hydrophobic tail of CcoP (Chapter 3) and one of the two conserved methionine residues in tr-CcoP replaced His 42 as the distal ligand. Methionine did not, however fulfil the role of His 42 in tr-CcoP as the truncated protein does not bind the exogenous ligand CO, but in contrast, CcoP does bind CO (Chapter 3, Section 3.2.4.).

It was therefore concluded that His 42, the only fully conserved histidine in CcoP, is the displaceable distal ligand in the *ccb*₃ subunit CcoP. However, considering the UV-visible spectroscopy of H42A, H42C and H42M the results suggest that His 42 is not the distal ligand to the low midpoint redox potential heme in CcoP. Recall that, the spectra of the mutant H42A suggests the presence of two low spin hemes, compared to the anticipated one low spin and one high spin and a 695 nm charge transfer band was not observed in the oxidized spectra of H42C or H42M. These spectroscopy results were not however conclusive enough to suggest that further investigation of these mutants was unnecessary. A similar pattern of experiments used to investigate CcoP, as described in chapter 3, were therefore repeated using the mutants, H42A, H42C and H42M.

FIG. 4.6 UV-Visible absorption spectra of recombinant CcoP from *P. stutzeri* and mutated recombinant CcoP from *P. stutzeri* in the reduced form. The amplitude of the Soret of reduced mutated CcoP was normalized to the Soret of oxidized recombinant CcoP (Fig. 4.5) so the spectra could be easily compared. To demonstrate the influence of the amino acid substitutions on the absorption spectra of CcoP, the spectrum of CcoP and mutated CcoP are superimposed in panels as indicated.

- A) Reduced spectra of purified H42A (red trace) and purified CcoP (black trace).
- B) Reduced spectra of purified H42C (green trace) and purified CcoP (black trace).
- C) Reduced spectra of purified H42M (blue trace) and purified CcoP (black trace).
- D) Overlay of purified reduced CcoP (black trace), H42A (red trace), H42C (green trace) and H42M (blue trace).

All samples were in 20 mM Tris-HCl, 50 μ M EDTA, 0.02% DM, pH 8. All samples were reduced with Sodium Dithionite. The insert shows a close up of the α and β regions with peaks at 550 nm and 521 nm respectively. A slight shift of the Soret band from 408 nm to 417 nm can be observed upon reduction. The spectra were recorded at room temperature.



4.2.4 Mediated Redox Potentiometry

Mediated redox potentiometry of CcoP demonstrated that one of the two *c*-type hemes in this di-heme subunit has a high midpoint redox potential (+ 188 mV) and one has a low midpoint redox potential (- 15 mV). The ligands coordinating the hemes have a significant influence on the midpoint redox potential of the heme, and redox potentiometry can be employed to probe and compare any ligand changes in a protein (Moore *et al.* 1986). The consequences of mutating the proposed distal ligand to the low potential heme in CcoP, was therefore further characterized using redox potentiometry. Mediated redox potentiometric titrations were carried out using the methods previously described in materials and methods (Chapter 2, Section 2.8.1).

The midpoint redox potentials of each strain are given in Table 4.3 and the Nernstian fits of the titration data are shown in Fig. 4.7. The potentiometric titration data indicates only small variations between the midpoint redox potential of the high midpoint redox potential heme in CcoP and the three mutants, H42A, H42C and H42M. Mediated redox titrations of H42A and H42M estimated one *c*-type heme to have a high midpoint redox potential and the other *c*-type heme to have a low midpoint redox potential heme. In contrast, both *c*-type hemes in H42C have high midpoint redox potentials.

The titration curve fit for the high midpoint redox potential heme in H42A (Fig. 4.7A) resembles CcoP. Moreover, the high potential heme of H42A (+185 mV) has a similar midpoint redox potential to CcoP suggesting no disruption to the high midpoint redox potential heme had occurred as a result of the mutation. The titration curve for H42C is steeper than CcoP and reveals a midpoint redox potential for the high potential heme of +176 mV, 9 mV less than the high potential heme in CcoP. The mediated redox potentiometry data can be fitted with a single component $n = 1$ equation (Fig.4.7B). This experimental data therefore suggests that the two *c*-type hemes in H42C have similar

potentials and both *c* type hemes in this mutant become reduced together. It is possible that only one heme is present, in H42C, possibly the high midpoint redox potential heme and the low midpoint redox potential heme was affected by the mutagenesis. However, the absorbance change observed in the α -band during the redox titration suggests the presence of two low spin *c*-type hemes. The Nernstian fit for the H42M mutant is slightly right shifted from that of CcoP, reflected in the higher midpoint redox potential of + 190 mV, for the high potential component.

The midpoint redox potential of the high midpoint redox potential heme in CcoP differed by no more than 5 % in the mutated strains compared to CcoP. The effects on individual heme reduction potentials are complex therefore it is difficult to make any definitive conclusions. However, these results suggest that the high midpoint redox potential heme in the CcoP mutants is stable and the heme ligands remained unaltered.

Strain	Redox Potential of high midpoint redox potential heme (mV)	Redox Potential of low midpoint redox potential heme (mV)
CcoP	+ 188 \pm 12	- 15 \pm 4
H42A	+ 185 \pm 10	+ 25 \pm 8
H42C	+ 176 \pm 49	+ 174 \pm 40
H42M	+ 190 \pm 5	+ 40 \pm 10

Table 4.3 Redox potentials of high and low midpoint redox potential hemes in CcoP, H42A, H42C and H42M determined from reductive potentiometric titrations. Conditions were as outlined previously (Chapter 2, Section 2.8.1).

In CcoP, the low potential heme has His/His heme ligation and it is proposed that His 42 is the distal ligand to this low potential heme. In comparison to the midpoint redox potential

of the high potential heme, the mediated redox potential of the low potential heme differs significantly in mutated CcoP to CcoP. The potential of the low potential heme differs by more than 50% for all three mutants. The Nernstian curve fit for the low midpoint redox potential heme in H42A indicates a redox potential of $+ 25 \pm 8$ mV. The redox titration curve is shifted by approximately $+ 39$ mV compared to that of CcoP, which has a low midpoint redox potential of -15 mV. As previously discussed the titration curve for the H42C mutant is sharper than that observed for CcoP and the other mutants. The Nernst curve resulting from the titration of H42C suggests that both hemes are titrating together and this is reflected in the potentials of the hemes in H42C, which differs to the low midpoint redox potential heme in CcoP by $+ 188$ mV. A decrease in the reduction potential of the low potential heme would be expected in the variant H42C if His42 is the distal ligand to the low potential heme.

The midpoint redox potential of the low midpoint redox potential heme in the mutant H42M is shifted positively and differs to CcoP by $+ 54$ mV. The midpoint potential differences observed in the low potential heme of the mutants compared to CcoP correlate with the mutated amino acid residue, His 42, being the distal ligand to this heme. It would be expected that the low midpoint redox potential heme of the variant H42M would shift to a more significantly positive potential, consistent with the role of this ligand as a good electron acceptor (Moore and Pettigrew 1990). The low midpoint redox potential heme is however, likely to be influenced by the high midpoint redox potential His/His ligated heme, the heme pocket and the other surrounding amino acid residues.

FIG. 4.7 Reductive titrations of Mutated CcoP. The titrations of H42A, H42C and H42M were performed using the conditions outlined previously. Values obtained for $A_{550}-A_{560}$ (*i.e.* the absorbance of the A_{MAX} wavelength for reduced *c*-heme minus the absorbance at an isosbestic point) were plotted as a function of potential.

(A) The black trace represents the theoretical Nernst curve for the two electron reduction of H42A. The curve was fit with two $n = 1$ Nernstian curves centred at +185 mV and + 25 mV assuming one heme contributes 69% and the second heme contributes 31% to the absorbance change in the α -band maximum in the spectrum. r^2 value = 0.9935

The red trace represents the theoretical fit of H42A with one $n = 1$ Nernstian equation with midpoint potentials centred at + 168 mV for both hemes. r^2 value = 0.9411

(B) The black trace represents the theoretical Nernst curve for the two electron reduction of H42C. The curve was fit with two $n = 1$ Nernstian curves centred at + 176 mV and + 174 mV assuming each heme contributes 50% to the absorbance change in the α -band maximum in the spectrum. r^2 value = 0.9946

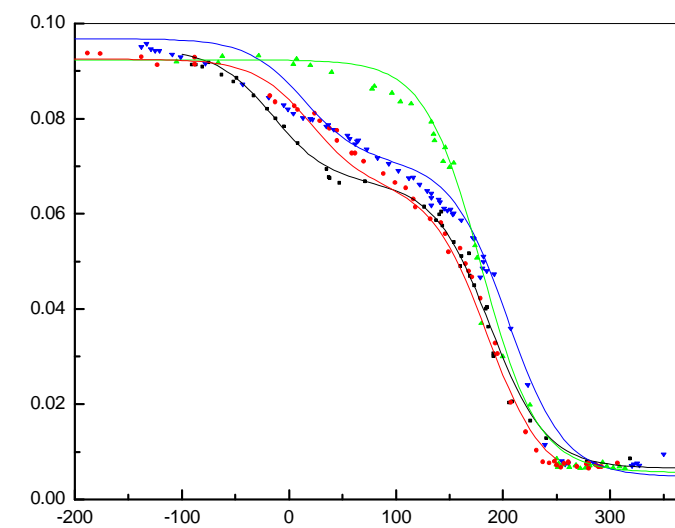
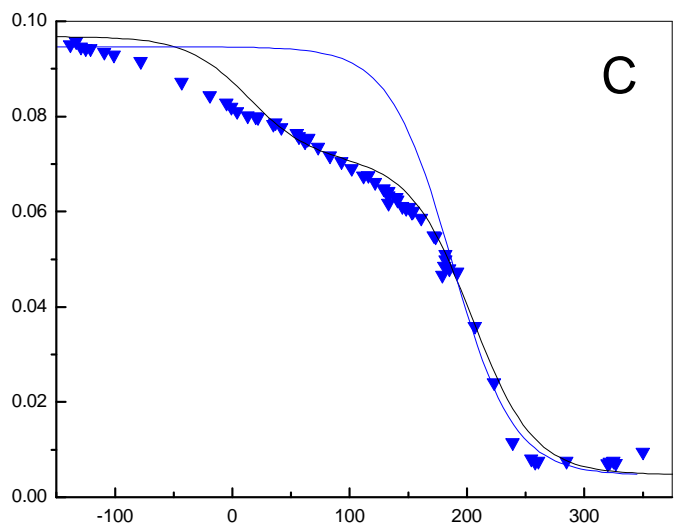
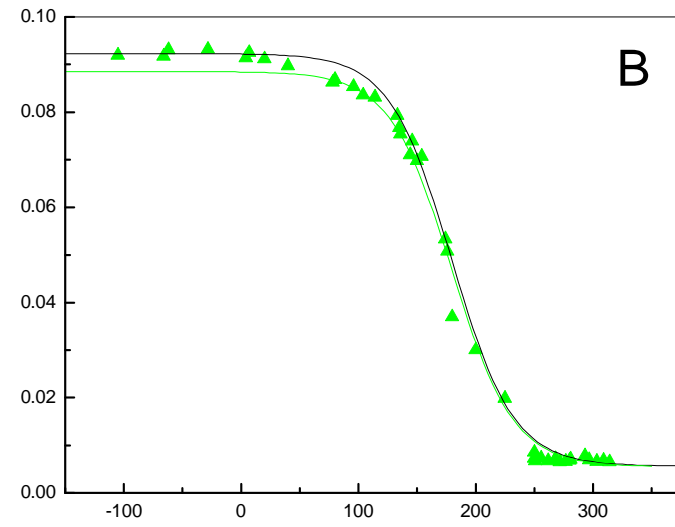
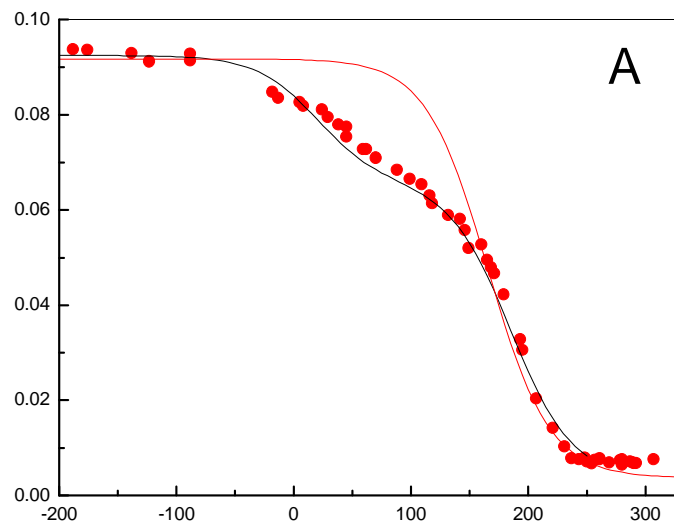
The green trace represents the theoretical fit of H42C with one $n = 1$ Nernstian equation with midpoint potentials centred at + 180 mV for both hemes. r^2 value = 0.9932

(C) The black trace represents the theoretical Nernst curve for the two electron reduction of H42M. The curve was fit with two $n = 1$ Nernstian curves centred at + 190 mV and + 40 mV assuming one heme contributes 72% and the second heme contributes 28% to the absorbance change in the α -band maximum in the spectrum. r^2 value = 0.9895

The blue trace represents the theoretical fit of H42M with one $n = 1$ Nernstian equation with midpoint potentials centred at + 195 mV for both hemes. r^2 value = 0.8507

(D) Overlay of redox potentiometry fits of CcoP (Black trace), H42A (red trace), H42C (green trace), H42M (blue trace)

A550-A560



E (mV)

To analyze the redox titrations it was necessary to simulate the data theoretically, assuming Nernstian behavior. As with CcoP the data was fit with two $n = 1$ Nernst equations. There was, however, discontinuity in the Nernst fit of the titration data for H42A and H42M in the + 125 mV to – 100 mV range. The data was therefore, also fitted using one $n = 1$ Nernstian fit as shown in Fig. 4.7 (A and C respectively). If a protein with two redox centres have similar potentials the experimental data can be fitted with a single component $n = 1$ equation despite the transfer of two electrons (Dutton 1978). However, if these redox centres are well spaced, the data must be fitted with two $n = 1$ Nernst equations. The fit of the data using only one $n = 1$ Nernstian equation was also unsatisfactory and it was therefore assumed that disruption to the low midpoint redox potential heme in the mutant strains, H42A and H42M accounted for any discontinuity in the Nernstian fits using two $n = 1$ Nernstian equations. The midpoint redox potential of the low potential *c*-type heme in mutated CcoP differed to CcoP and differences in the polarity of the substituted amino acid residues is not enough to account for the variations in redox potential of the low redox potential heme (Mauk 1997). The results of the mediated redox potentiometry therefore suggest that His 42 is the distal ligand to the low midpoint potential heme.

4.2.5 CO Binding Studies

As previously discussed, the *cbb*₃ subunit, CcoP binds the exogenous ligand, CO (Chapter 3, Section 3.2.4). It is proposed that the distal ligand to the low midpoint redox potential heme in CcoP displaces to bind CO. CO binding in CcoP variants in which the proposed distal ligand had been mutated was therefore investigated.

The effect of CO binding to fully reduced CcoP is readily seen in the UV-visible spectroscopy (Chapter 3, Section 3.2.4.). Upon binding CO the Soret band shifts from 417 nm to the shorter wavelength, 415 nm. The band also increases in intensity in comparison to the fully reduced state. The increase of the absorption intensity in the Soret

band is coupled with a decrease in the intensity of the α and β bands. Fig. 4.8 shows the reduced spectrum of the CcoP mutants (black trace) and the CO bound spectrum (coloured trace). The UV-visible spectra of CO bound mutated CcoP shows that all of the mutants bind the exogenous ligand CO as indicated by an increase in the Soret band, a shift from 417 nm to 415 nm and a decrease in the intensity of the α and β bands can be observed.

It was hypothesized that the alanine mutant, H42A, would bind CO as mutation of His42 to an alanine would create a five-coordinated heme, since the distal ligand site would be vacant. However, from the oxidized and reduced UV- visible spectroscopy of this mutant, it was concluded that the low midpoint redox potential heme in H42A remained six coordinate. Binding of CO to one of the hemes in H42A therefore suggests that CO displaces the distal ligand to the heme, as is observed in CcoP (Chapter 3, Section 3.2.4).

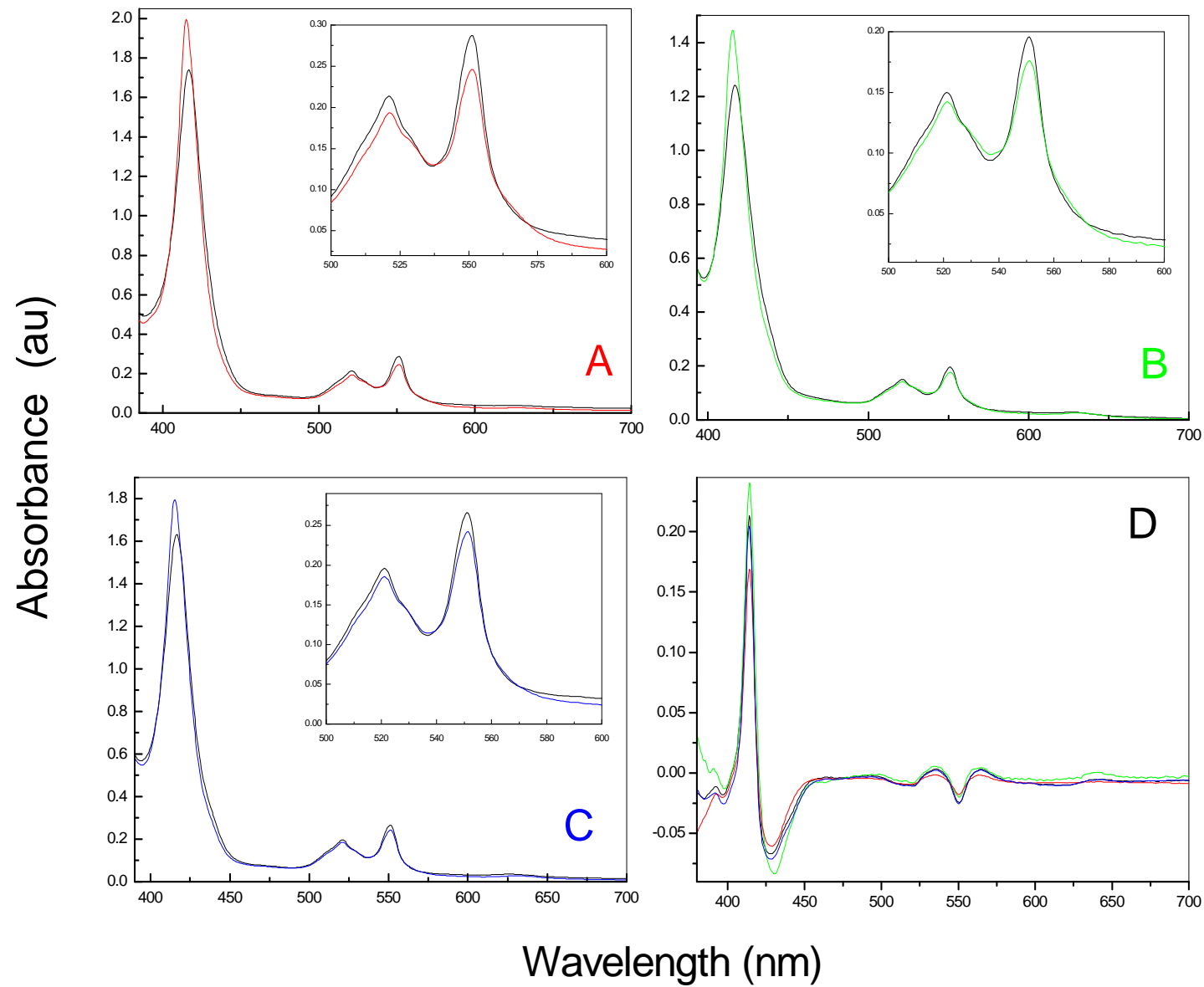
The choice of cysteine and methionine as substitutes for His 42 was based on the assumption that the cysteine and methionine residue replacements would create a strong bond to the heme iron, which would not be displaced by an exogenous ligand. It was therefore surprising that the CcoP variants, H42C and H42M bound CO. It is possible, however, that the residue replacing the histidine forms a weak bond with the heme, which is readily displaced by an exogenous ligand as observed in the heme sensor protein *EcDos* (Gonzalez *et al.* 2002). It should also be considered, however, that His 42 residue is not the distal ligand to the low midpoint redox potential heme in CcoP. Therefore, CO binding would still be observed in all the CcoP variants as SDM would not have altered the ligands to the low potential heme.

FIG. 4.8 UV-Visible absorption spectra of fully reduced H42A (A), H42C (B) and H42M (C) prior to and after the additions of CO

Panels A-C: The proteins are in 20 mM Tris-HCl pH 8, 50 μ M EDTA, 0.02% DM. After the addition of excess sodium dithionite, the reduced spectrum was recorded (black trace). Following the addition of 1 mM CO (coloured trace) the spectra clearly show a shift of the Soret band from 417 nm to 415 nm and an increase in intensity. The insert in each panel shows a close up of the α and β regions of reduced mutated CcoP (black trace) and reduced mutated CcoP plus CO (coloured trace) with peaks at 550 nm and 521 nm respectively. Upon binding of CO a decrease in the α and β bands is observed. The spectra were recorded at room temperature.

(D) CO difference spectrum (reduced plus CO minus reduced) of CcoP

(Black trace), H42A (Red trace), H42C (Green trace) and H42M (Blue trace).



The CcoP variants H42A, H42C and H42M, all bind the exogenous ligand CO. The CO bound difference spectra of the CcoP mutants in Fig. 4.8D, demonstrates however that the mutants bind CO to different extents. The differences can be observed by the variations in the height of the Soret band and the troughs at 550 nm (Wood 1984). The difference spectra therefore suggest that the distal coordination sites of the heme that binds CO differ in CcoP and the CcoP variants. The CO binding properties of the low midpoint redox potential heme in CcoP and the variants were therefore investigated further.

Stoichiometry of CO binding to CcoP

The dissociation constant (K_d) gives an experimentally determined value for the affinity of a ligand for the receptor *i.e.* how tightly a ligand binds to a specific protein. A decreased affinity of the receptor (the low midpoint redox potential heme) for an exogenous ligand is largely associated with steric interactions at the heme coordination site (Antonini 1971). To investigate the affinity of the low midpoint redox potential heme in CcoP for CO the change in the intensity of the Soret band relative to the concentration of CO added was monitored. Using this technique the dissociation constant (K_d) could be determined.

To estimate the K_d for the binding of CO to CcoP, the change in absorbance of the Soret band at 415 nm monitored following consecutive additions of aliquots of CO equilibrated buffer (1 mM) to the fully reduced enzyme was monitored. Additions of CO saturated buffer were made until no further change in absorption was observed when it was assumed that saturation of the receptor, the low midpoint redox potential heme, had been achieved. Fig. 4.8A shows the absorbance maximum of the Soret band at 415 nm and absorbance minimum at 428 nm observed when CO binds to the low midpoint redox potential *c*-type heme in CcoP. The observed absorbance change, (the observed maximum at A_{415} minus the observed minimum at A_{428}) was recorded after complete formation of the CO adduct. The absorbance change was normalized to the fraction of bound CO (fractional saturation)

and plotted as a function of CO concentration (Fig. 4.9B). The experimental data yielded a dissociation constant (K_d) of 1.1×10^{-6} M for CcoP.

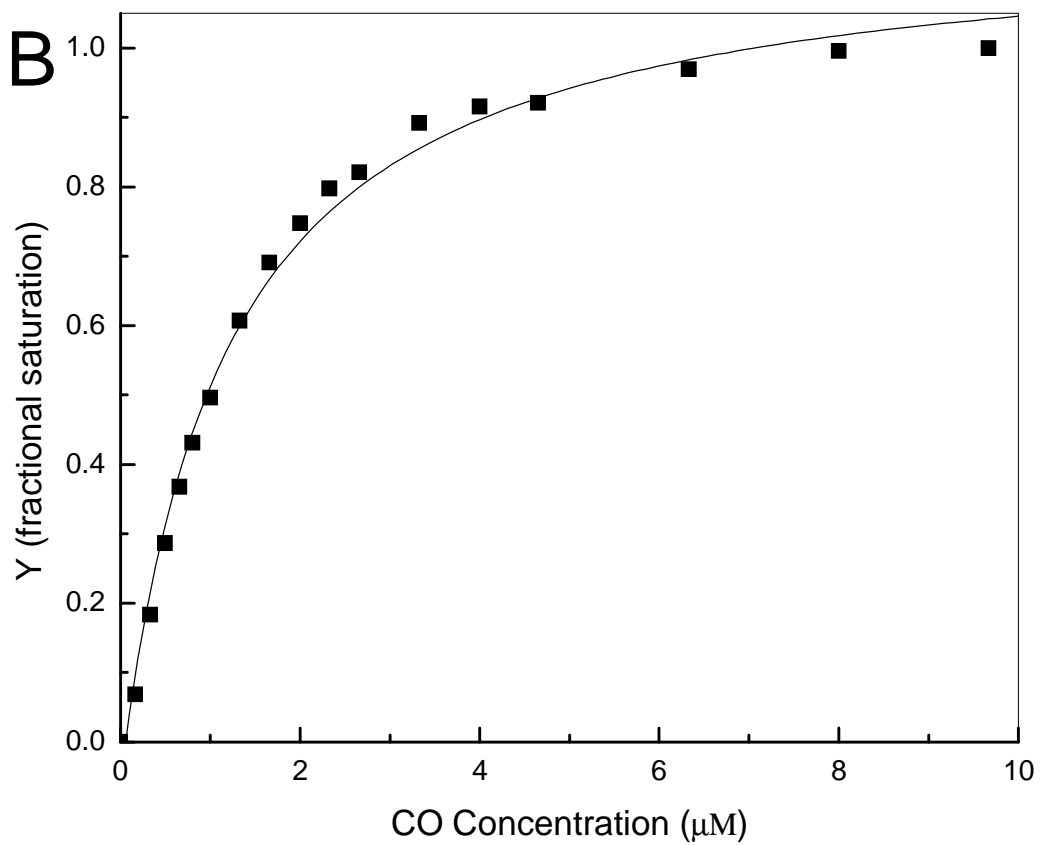
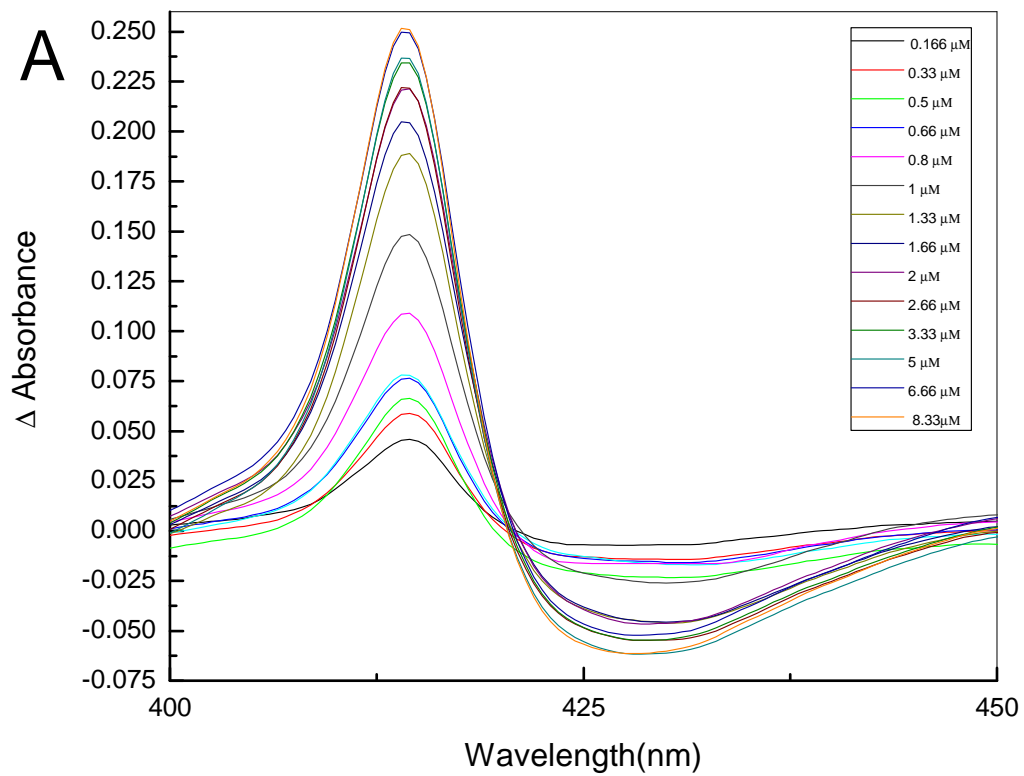
The spectral changes observed in CcoP, which were associated with CO binding, were only fully developed when both *c*-type hemes were fully reduced with dithionite. This is consistent with CO binding only to the low midpoint potential heme, as was also observed previously by Pitcher *et al.* (Pitcher *et al.* 2003).

Fitting the experimental yielded a K_d of 1.1×10^{-6} M for CO binding to CcoP Fig. 4.9B). This result is comparable to the result obtained previously by Pitcher *et al.*, ($K_d = 2.2 \times 10^{-6}$ M) (Pitcher *et al.* 2003). The interaction of CcoP with CO reflects the high affinity of CcoP for CO, an analogue of both O₂ and NO.

It was speculated that SDM of the proposed distal ligand in CcoP would affect the affinity between an exogenous ligand and the protein. The CO dissociation rate of the CcoP variants was investigated to highlight any differences in the affinity of CcoP and CcoP variants for the exogenous ligand CO.

FIG. 4.9 Optical Changes observed during the CO titration of ferrous CcoP.

- (A) The enzyme concentration was 2 μM in 20 mM Tris HCl, 50 μM EDTA, 0.02% DM, pH 8. The enzyme was reduced in a quartz cuvette by the addition of excessive sodium dithionite under anaerobic conditions. The cuvette was sealed with a rubber septum. Absorption at 415 nm was recorded after CO was added incrementally to the sample cuvette from a concentrated stock solution (1 mM) of CO equilibrated buffer (20 mM Tris HCl, 50 μM EDTA, pH 8). The concentration of CO added at each increment is recorded in the figure legend. Following complete formation of the CO adduct (10 minutes) a new spectrum was recorded. The observed absorbance change, (the observed maximum at A_{415} minus the observed minimum at A_{428}) was recorded. All spectra were recorded at room temperature. Each measurement was repeated in triplicate
- (B) CO saturation curve of CcoP monitored at 415 nm. The fractional saturation (Y) is the ratio of the observed A_{415} to the observed maximum A_{415} recorded after complete formation of the CO adduct. The fractional saturation was plotted as a function of the total CO concentration.



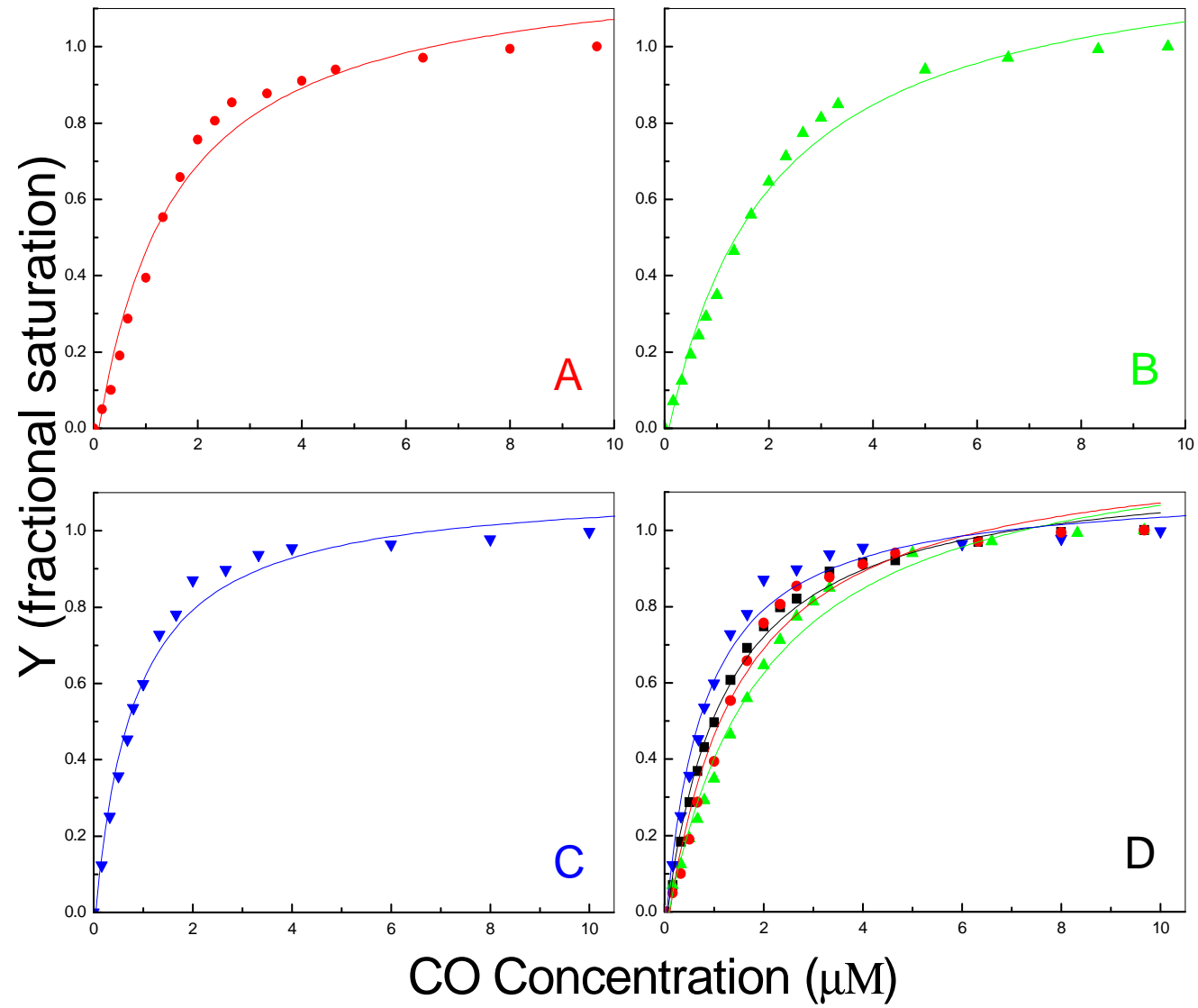
The CO dissociation constants of CcoP and the mutated strains are as shown in Table 4.4. The CcoP variant, H42A, yielded a K_d of 1.2×10^{-6} M that does not differ from the K_d yielded for CcoP (Table 4.4). This result therefore suggests that the binding of CO to H42A did not differ to the binding of CO to CcoP. The binding of CO to H42C yielded a K_d of 1.35×10^{-6} M, which was weaker compared to CcoP. Surprisingly, the binding of CO to the methionine-substituted CcoP variant, H42M, yielded a K_d of 0.67×10^{-6} M. The result therefore suggests that the binding of CO to the low midpoint redox potential heme H42M was stronger than to the heme of CcoP. The overlay of all the saturation curve of all the mutants and CcoP demonstrates the small but observed differences in CO binding (Fig. 4.10).

Strain	Dissociation Constant (M)
CcoP	$1.1 \times 10^{-6} \pm 0.03 \times 10^{-6}$
H42A	$1.2 \times 10^{-6} \pm 0.05 \times 10^{-6}$
H42C	$1.35 \times 10^{-6} \pm 0.11 \times 10^{-6}$
H42M	$0.67 \times 10^{-6} \pm 0.23 \times 10^{-6}$

Table 4.4 Dissociation constants (K_d) of the binding of CO to CcoP, H42A, H42C and H42M

FIG. 4.10 CO saturation curves of CcoP and mutated CcoP

The enzymes were reduced in a quartz cuvette by the addition of excessive sodium dithionite under anaerobic conditions. The cuvette was sealed with a rubber septum. Absorption at 415 nm was recorded after CO was added incrementally to the sample cuvette from a concentrated stock solution (1 mM) of CO equilibrated buffer (20 mM Tris HCl pH 8, 50 μ M EDTA). 10 minutes after each addition a new spectrum was recorded. The fractional saturation (Y) is the ratio of the observed A_{415} to the observed maximum A_{415} recorded after complete formation of the CO adduct. The fractional saturation of each protein was plotted as a function of the total CO concentration. The strains analyzed were CcoP (black trace), AC1 (red trace), AC2 (green trace) and AC3 (blue trace). All spectra were recorded at room temperature. Each measurement was repeated in triplicate



It has been hypothesized that CO binds to CcoP following displacement of the distal ligand (Pitcher *et al.* 2003). The experimentally determined K_d for the binding of CO to the mutants H42A, H42C and H42M do not differ significantly to the K_d for the binding of CO to CcoP. These results therefore suggest that similarly to CcoP, CO binding to the CcoP variants is preceded by displacement of the distal ligand to the low midpoint redox potential heme. It is suggested that in CcoP, the displaced distal ligand stabilizes the bound CO. As previously discussed, it was expected that the H42A mutant would yield a 5C heme, which would not bind CO since there would be no displaced distal ligand present to stabilise the bound CO. It was also hypothesized that as a cysteine ligated to a heme can not be displaced easily by an exogenous ligand this CcoP mutant strain would not bind CO (Antonini 1971). In the mutant strain H42M it is not clear however if the distal ligand, possibly methionine, stabilized the exogenous ligand once it had been displaced by the CO. This would be similar to the CO binding mechanism observed in the sensory protein, *EcDos*. The distal methionine ligand to the *b*-type heme in *EcDos* is displaced by the exogenous ligand, CO and the displaced methionine stabilizes the CO once it is bound to the heme (Gonzalez *et al.* 2002). It is hypothesized that a similar binding mechanism occurs in H42M and the displaced methionine ligand stabilizes the exogenous ligand, CO, therefore maintaining the tight binding.

Amino acid side chains closely surround the active site of heme proteins in a manner that provides steric hindrance to entering ligands and CO affinities in hemes are affected by structural change (Antonini 1971; Traylor 1981). Since no change in the affinity for CO has been observed in the mutant strains compared to CcoP, it is, reasonable to suggest that mutation of the proposed distal ligand to the low redox potential heme in CcoP did not affect the structure of the heme.

4.2.6 Comparative EPR Spectroscopy of CcoP variants

The results presented thus far do not support or dispel the suggestion that His42 is the distal ligand to the low midpoint redox potential heme in the *cbb*₃ subunit CcoP. Mediated redox potentiometry of CcoP variants indicates that the low midpoint redox potential heme of H42A, H42C and H42M, differs to the equivalent heme in CcoP (Section 4.2.4). The redox potentiometry result therefore suggests that one of the ligands to the low midpoint redox potential heme in the CcoP variants differs to the ligand in CcoP. In contrast, however, the CO binding observed in the CcoP variants is comparable to CO binding observed in CcoP (Section 4.2.5). Contradicting the redox potentiometry results, the observed CO binding suggests that the distal ligand to the low midpoint redox potential heme in the CcoP variants does not differ to the distal ligand in CcoP.

Electron paramagnetic resonance is a spectroscopic technique in which the ligation state of the heme gives rise to specific signals. The signal for the high potential His/His ligated heme in CcoP can be observed in the EPR spectra as a rhombic trio. The signal for the low potential heme with proposed His/His ligation is unaccounted for in the EPR spectra (Chapter 3, Section 3.2.5). EPR spectroscopy was used to probe the ligation states of the two hemes in the CcoP variants.

The X-band EPR spectra of the fully oxidized CcoP variants, H42A, H42C and H42M shows two low spin rhombic species (Fig. 4.11). The rhombic trio, with *g* values of 2.99, 2.25 and 1.53 can be observed in the EPR spectra of all the mutants. The equivalent rhombic trio was previously assigned to the high midpoint redox potential His/His ligated heme observed in CcoP and tr-CcoP (Chapter 3 Section 3.2.5). Mediated redox potentiometry of the CcoP variants suggested that the high midpoint redox potential heme in all the mutants had not been affected by SDM (Section 4.2.4). The EPR spectra of H42A, H42C and H42M confirm that SDM of His 42 does not affect the high midpoint

redox potential heme. The concentration of the species giving rise to the low-spin ferric rhombic trio $g = 2.99, 2.25$ and 1.53 in the EPR spectrum of H42A was estimated by integration of the g_z feature ($g = 2.99$) using 1 mM Cu (II) EDTA as a spin standard. The results indicated that the species giving rise to this g_z feature accounts for *ca.* 50% of the total low-spin heme in the EPR absorption spectrum. It can therefore be concluded that the rhombic trio, $2.99, 2.25$ and 1.53 accounts for one low-spin heme in H42A. It is assumed that the $g = 2.99$ feature also accounts for one low spin heme in the EPR spectrum of H42C and H42M.

The second low spin rhombic trio observed in the EPR spectrum of the CcoP variants has g values of $2.43, 2.25$ and 1.93 . This trio of signals is consistent with a heme with His/Hydroxide ligation (Moore and Pettigrew 1990). From the intensity of the signals, the contribution of the his/hydroxide low spin species differs in each of the mutants. The signals are likely to arise from a heme or hemes in which one of the ligands has become detached or damaged possibly as a result of reduced translation of the sequence by the cell in the initial grow up stage of the strain (Wallace and Clark-Lewis 1992). Despite being present in the spectra of all the mutants, this rhombic trio ($2.43, 2.25$ and 1.93) probably accounts for only a small proportion of the preparation, which has been damaged (Cheesman 2006). Interestingly, however, the presence of a His/OH⁻ ligated heme would explain the observation that all the CcoP mutants bind CO, as the hydroxide ligand of a six-coordinated heme would be easily displaced by an exogenous ligand.

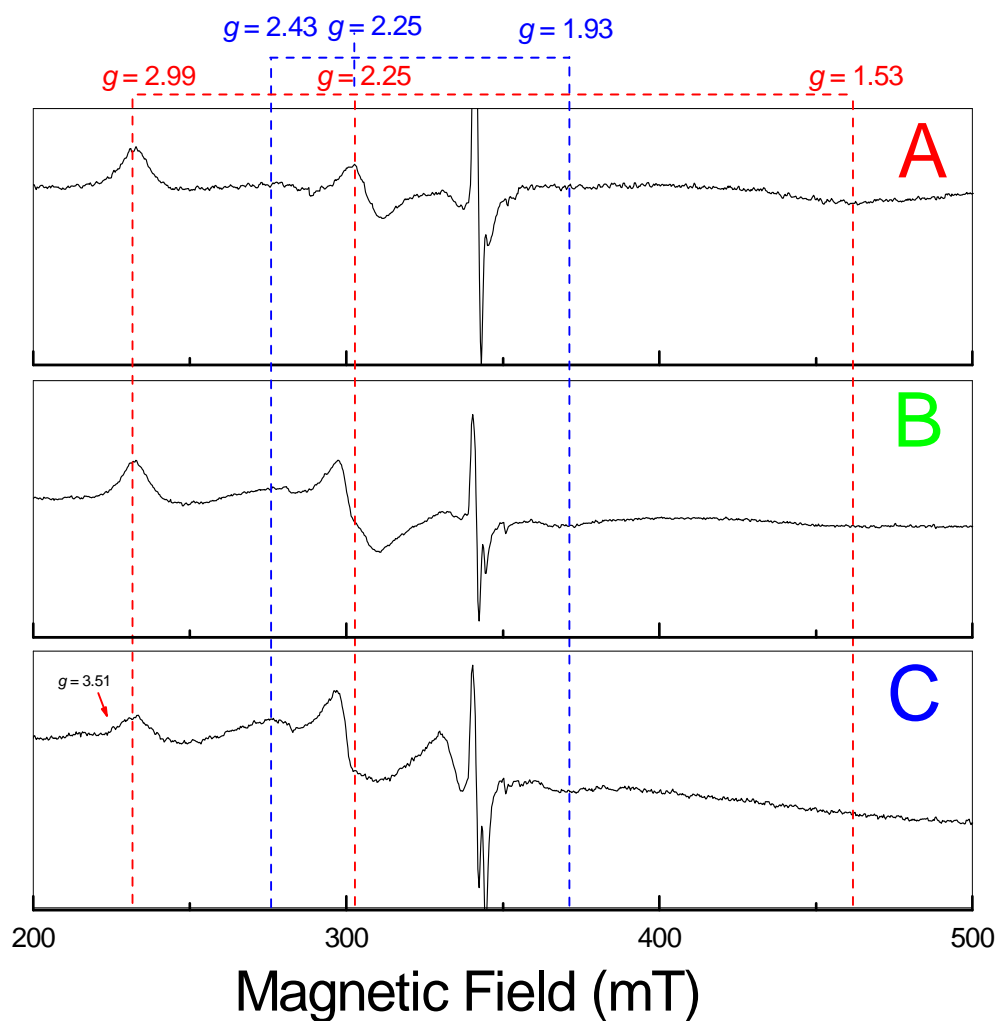


FIG. 4.11 X-band EPR of H42A (A), H42C (B) and H42M (C). The enzymes were in 20 mM Tris-HCl pH 8, 50 μ M EDTA, 0.02%DM and were fully oxidized with Potassium Ferricyanide. The spectra were recorded at 15 K, using 2 mW of microwave power, and 1 mT modulation amplitude. The g -values of features indicated are discussed in the text and in relation to the EPR spectra of CcoP and tr-CcoP (Section 3.2.5).

Features near $g = 6$, $g = 4.3$ and $g = 2$ observed in the spectra of all the mutants represent minor amounts of high-spin ferric heme, small amounts of free Fe(III), and small amounts of Cu(II) respectively. These features represent small quantities of each species in terms of enzyme concentrations.

The EPR spectra of the CcoP variants show the rhombic trio of the high potential his/his ligated heme, however the spectrum of each variant show differences and a signal for the mutated heme can not be conclusively accounted for. The EPR spectrum of H42C was surprising, as a signal correlating to a heme with His/Cys ligation was not observed. Recall however, that the His/His signal for the low midpoint redox potential heme was not observed in the EPR spectrum of CcoP (Chapter 3, Section 3.2.5). In a similar scenario to that hypothesized in CcoP, the high and low midpoint redox potential hemes of the CcoP variants may be spin-coupled, therefore explaining the population of low spin heme that is unaccounted for in the mutants. The coupling of two hemes creates an EPR silent species (Cheesman *et al.* 1998; Cheesman 2006). As previously discussed it was hypothesized that the low redox potential heme, in CcoP, would become five-coordinate upon mutation of His 42 to an alanine residue. The EPR spectrum of H42A shows no obvious high spin feature. The EPR result confirms the interpretation of the UV-visible spectrum, which suggests that H42A, unexpectedly contains two low spin heme species.

The EPR spectrum of H42M is dominated by the high spin signal ($g = 6$) which is large in comparison to the rhombic signals. The large $g = 6$ feature impedes the visualization of other signals in the spectrum. However, the height of the signal does not correspond to a large contribution from a high spin species and probably only accounts for approximately 10% of the total enzyme (Cheesman *et al.* 1998; Cheesman 2006). The UV-visible spectroscopy of H42M does not indicate that this CcoP variant contains a high spin species, therefore corresponding with the EPR spectrum.

On further study of the $g = 2.99$ feature in the EPR spectrum of H42M a broad underlying signal is visible to the left of the peak as indicated by the red arrow (Fig. 4.11). This signal at $g = 3.51$ can be assigned as the g_z feature of a low-spin heme with histidine-methionine ligands. A similar feature was observed in tr-CcoP, which has one heme with His/His ligation and one heme with His/Met ligation (Chapter 3, Sections 3.2.5 and 6). The high g -value of the signal together with the asymmetrical shape suggests that it is one component of a rhombic trio, in which two of the g_y and g_x features are below 2 and not easily detected (Cheesman *et al.* 1998). This leads overall to a broad “large g_{\max} ” type EPR spectrum. In the UV-Visible spectrum of H42M a CT band at 695nm was not observed. A 695 nm CT band is characteristic of a low intensity ligand to metal charge transfer transition that is present when a low spin ferric heme possesses at least one of the sulphur ligands methionine or cysteine (Moore and Pettigrew 1990). The absence of this CT band in the H42M UV-visible spectrum is not however conclusive proof that one of the hemes in this mutant is not His/Met ligated (Moore and Pettigrew 1990).

Despite this observed difference in the EPR spectrum of H42M, there were no distinguishable differences in the EPR spectrum of H42A and H42C compared to CcoP. The suggestion that His 42 is not the displaceable ligand to the low midpoint redox potential heme in CcoP, would account for no observed differences in the EPR spectra of the mutants and should therefore be considered further. The distal ligand to a *c*-type heme is commonly a histidine or a methionine residue; however the residues lysine and Arginine are regarded as potential alternatives (Moore and Pettigrew 1990; Cheesman 2006). Hemes with lysine or histidine ligation both present a band between 1480 - 1585 nm in LT MCD spectra. In CcoP, the 1585 nm band observed in the MCD spectra was assigned to a heme with His/His ligation (Chapter 3, Section 3.2.6). It is proposed that hemes with Arginine ligation also present a band at ~ 1585 nm however, there is little evidence to support this proposal (Cheesman 2006). In the sequence alignment of the CcoP subunit there is one

fully conserved lysine residue, K241 (*P. Stutzeri* numbering), however, the EPR of amine-bound hemes is unique in shape and position and the EPR spectrum of CcoP is not consistent with a heme lysine ligation (Chapter 3, Section 3.2.5) (Moore and Pettigrew 1990). A semi conserved Arginine, R56 (*P. Stutzeri* numbering) is also observed in the sequence alignment of the CcoP subunit. However, similarly to the EPR signal of amine bound hemes, the EPR spectrum of a His/Arg ligated heme is distinct and is not observed in the EPR spectrum of CcoP (Chapter 3, Section 3.2.5).

The EPR spectra of the CcoP mutants raise a number of hypotheses but do not suggest any conclusions to the identity of the displaceable distal ligand to the low potential heme in CcoP.

4.3 Conclusions

Previous investigations of the *cbb*₃ oxidase subunit, CcoP, indicated that the two *c* type hemes in CcoP were His/His ligated (Chapter 3). Biochemical characterization of the soluble form of CcoP, tr-CcoP, shows that upon deletion of the conserved histidine, His 42, the distal ligand to the low midpoint redox potential heme was replaced by a methionine and did not bind the exogenous ligand, CO (Chapter 3). Based on these results, the role of His 42 was investigated considering the hypothesis that His 42 is the distal ligand to the low midpoint redox potential heme in CcoP. Biochemical methods were used to investigate CcoP variants in which the residue His 42 was substituted for an alanine, cysteine or a methionine.

UV-Visible spectroscopy indicated that all the *c*-type hemes of the CcoP variants, H42A, H42C and H42M, were six-coordinate and low spin, as observed in the UV-Visible spectrum of CcoP. The mediated midpoint potential of the low redox potential heme in each of the mutant strains however differed to CcoP and to each other. These results

suggested that the point mutations in the Ccop variants disrupted either the coordinating ligands to the heme centre or the amino acids in the heme environment. Based on the mediated redox titrations it was concluded that mutation and subsequent replacement of His 42 affects the low redox potential heme in CcoP. Experimental results indicated that the low potential heme of all the CcoP variants bound the exogenous ligand CO, suggesting, despite the differing redox potentials of the low potential heme, that SDM had not affected the distal ligand to the low redox potential heme. Moreover, EPR spectroscopy of the CcoP variants H42A and H42C does not indicate any significant differences compared to the EPR spectrum of CcoP.

The experimental results presented here suggest that the amino acid residue His 42 is not the distal ligand to the low potential heme in CcoP. The identity of the displaceable distal ligand to the low midpoint redox potential heme in CcoP has not therefore been resolved; however, this should be the goal of a future study.

5 Cytochrome *Cbb*₃ oxidases from *P. Aeruginosa*

5.1 Introduction.....	182
5.2 Results and Discussion	187
5.2.1 Growth in batch culture under different oxygen regimes.....	187
5.2.2 Expression of the two predicted <i>P. aeruginosa cbb</i> ₃ Oxidases.....	190
5.2.3 Steady State Assay of Wild-type <i>P. aeruginosa</i> and mutants...	194
5.3 Conclusions.....	208

5.1 Introduction

The γ -Proteobacteria, *P. aeruginosa*, *P. putida*, *P. fluorescens* and *P. stutzeri* have tandem *ccoNOQP* operons (Stover *et al.* 2000; Nelson *et al.* 2002; Morales *et al.* 2006; Paulsen *et al.* 2005; Yan *et al.* 2008). In the bacterial pathogen, *P. aeruginosa* the operons, *ccoNOQP-1* and *ccoNOQP-2* encode the *cbb₃* oxidase and are thus designated *cbb₃-1* and *cbb₃-2* (Fig. 5.1) (Stover *et al.* 2000; Comolli and Donohue 2004). The functions of the two *cbb₃* oxidases have not been clearly defined, however independent roles have been suggested (Comolli and Donohue 2004).

In bacterial *cbb₃* oxidases, expression is maximal under oxygen limiting conditions (Batut *et al.*, 1989; Fischer, 1994; Swem *et al.*, 2001). Under aerobic conditions increased expression of the *P. aeruginosa* cytochrome *cbb₃-1* oxidase has been observed (Comolli and Donohue 2004; Alvarez-Ortega and Harwood 2007). Expression of the *cbb₃-1* oxidase does not increase or decrease significantly during growth under micro-aerophilic conditions (Comolli and Donohue 2004; Alvarez-Ortega and Harwood 2007). Expression of the *cbb₃-1* oxidase gene does, however, decrease under strict anaerobic growth conditions (Alvarez-Ortega and Harwood 2007). The observation that the *P. aeruginosa* *cbb₃-1* oxidase is expressed primarily under aerobic conditions, but also under semi-aerobic conditions suggests that this organism is prepared to cope with, and take advantage of sudden drops in oxygen without first having to mount a transcriptionally directed low oxygen response (Alvarez-Ortega and Harwood 2007).

In contrast, the *cbb₃-2* oxidase more closely resembles the canonical *cbb₃*-type oxidase. Expression of the *cbb₃-2* oxidase is increased in cells grown under semi-aerobic/anaerobic conditions (Comolli and Donohue 2004; Alvarez-Ortega and Harwood 2007). It is therefore hypothesized, that the two *P. aeruginosa* *cbb₃* oxidases differ in their respiratory

and regulatory functions. The *cbb₃-1* oxidase plays a role under aerobic conditions and the *cbb₃-2* oxidase plays a role under semi-aerobic conditions.

Evidence indicates that the two *cbb₃* operons are independently regulated from distinct promoters (Comolli and Donohue 2004). This is not surprising, considering that the two *ccoNOQP* operons of *P. aeruginosa* are differentially expressed in response to oxygen limitation. In the bacterial species *E. coli* the transcriptional regulator FNR responds to variations in cellular oxygen status by activating or repressing expression of respiratory enzymes (Crack *et al.* 2007). An FNR homologue, ANR, is present in *P. aeruginosa* (Vollack *et al.* 1998). As discussed previously, the global transcription factor, ANR, regulates the transcription of genes that encode for enzymes required for energy conservation under anaerobic and low oxygen conditions (Section 1.8) (Ray and Williams 1997; Vollack *et al.* 1998). A consensus binding site for ANR (TTGAT-N4-ATCAA) has been recognized in the region surrounding the transcription initiation point for *ccoNOQP-2* (Comolli and Donohue 2004). It is therefore not surprising that *P. aeruginosa* cells defective in, or lacking *anr*, demonstrated reduced expression of *ccoNOQP-2* under aerobic and anaerobic conditions (Comolli and Donohue 2004). In contrast, expression of *ccoNOQP-1* in the same *anr* mutant remained unchanged in both aerobic and semi aerobic conditions relative to the level of *ccoNOQP-1* in wild-type cells (Comolli and Donohue 2004; Alvarez-Ortega and Harwood 2007). The results therefore suggest that *ccoNOQP-2* is regulated using the FNR family member, ANR, to control its induction under oxygen limitation and the mechanisms influencing the *ccoNOQP-1* promoter appears to be distinct from *ccoNOQP-2*. (Comolli and Donohue 2004). The regulator of the *cbb₃-1* oxidase remains unclear, however other regulators responding to oxygen or other signals in *P. aeruginosa* have been recognized, for example the RoxRS system as discussed previously (Chapter 1, Section 1.8) (Comolli and Donohue 2004; Alvarez-Ortega and

Harwood 2007; Ugidos *et al.* 2008). These regulators respond to the signal and build the appropriate electron transport chain for the prevailing conditions.

Despite the specific roles proposed for the *cbb₃* isozymes the predicted subunits of *cbb₃-1* and *cbb₃-2* in *P. aeruginosa* share 82% amino acid identity (Table 5.1). There are limited differences in the CcoN, CcoO and CcoQ subunits of *cbb₃-1* and *cbb₃-2* scattered throughout the protein, but localized regions of high divergence are apparent in the CcoP subunits. The similarities between the *cbb₃* isozymes from *P. stutzeri* and *P. aeruginosa* suggest that the use of the non pathogenic *P. stutzeri* (Chapter 3 and 4) as a model organism substitute for the pathogenic *P. aeruginosa* is reasonable.

Organism	Organism	Similarity (%)
<i>P. aeruginosa cbb₃-1</i>	<i>P. aeruginosa cbb₃-2</i>	82
<i>P. aeruginosa cbb₃-1</i>	<i>P. stutzeri cbb₃-1</i>	83
<i>P. aeruginosa cbb₃-2</i>	<i>P. stutzeri cbb₃-2</i>	79
<i>P. aeruginosa cbb₃-2</i>	<i>P. stutzeri cbb₃-1</i>	79
<i>P. stutzeri cbb₃-1</i>	<i>P. stutzeri cbb₃-2</i>	82
<i>P. aeruginosa cbb₃-1</i>	<i>P. stutzeri cbb₃-2</i>	83

Table 5.1 Amino Acid similarity of *P. stutzeri cbb₃-1* and *cbb₃-2* and *P. aeruginosa cbb₃-1* and *cbb₃-2*. The amino acid sequence data of *P. aeruginosa* and *P. stutzeri* were obtained from the KEGG (Kyoto Encyclopedia of Genes and Genomes) database for comparison.

The biochemistry of *cbb₃-1* and *cbb₃-2* is poorly understood however it would appear that the two isoforms of the *cbb₃* oxidase have specialised roles under different prevailing oxygen levels (Comolli and Donohue 2004; Williams *et al.* 2007). To investigate the roles of the two *P. aeruginosa* enzymes *cbb₃-1* and *cbb₃-2*, *P. aeruginosa* strains with

disruptions in the locus encoding *cbb*₃-1 (Cco1.1), *cbb*₃-2 (Cco2.2), both *cbb*₃ oxidases (CcoΔ1) or the *aa*₃ oxidase (Cox Δ1) were created (Comolli and Donohue 2004) (Fig. 5.2). Wild-type and mutated *P. aeruginosa* strains were phenotypically characterized and the oxidase activity of each strain grown under aerobic and semi-aerobic conditions was investigated.

A

Strain	Genotype
WT	Wild type <i>P. aeruginosa</i> PAK
Cco1.1	PAK derivative, in-frame deletion in <i>cbb</i> ₃ -1
Cco2.2	PAK derivative, in-frame deletion in <i>cbb</i> ₃ -2
CcoΔ1	PAK derivative, in-frame deletion <i>cbb</i> ₃ -1 and <i>cbb</i> ₃ -2
CoxΔ1	PAK derivative, in-frame deletion <i>aa</i> ₃

B

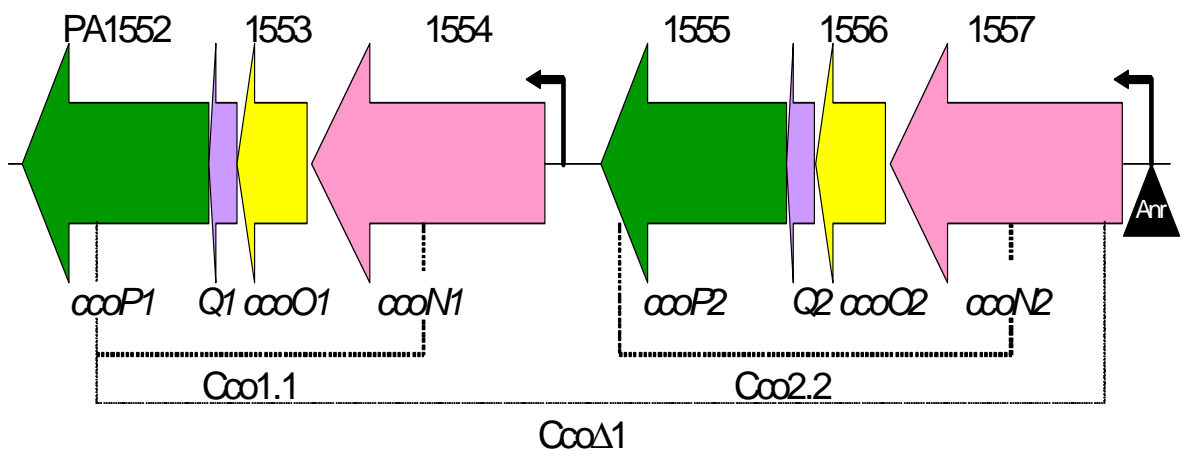


FIG. 5.1 (A) Nomenclature used for the description of strains used in this study.

(B) Map of the *P. aeruginosa* locus that contains two adjacent *ccoNOQP* operons *ccoNOQP-1* and *ccoNOQP-2*. The regions deleted in creation of mutant strains lacking *cbb*₃-1 (Cco1.1), *cbb*₃-2 (Cco2.2) or both *cbb*₃ oxidases (CcoΔ1) are indicated. The deletion construct CoxΔ1 lacks the cytochrome *c* oxidase *aa*₃ only and both *ccoNOQP* operons are present in the construct (Adapted from (Comolli and Donohue, 2004)).

5.2 Results and Discussion

5.2.1 Growth in batch culture under different oxygen regimes

All the *P. aeruginosa* strains were grown in asparagine medium, in which the carbon and nitrogen source, asparagine, is utilised for growth of the organism (Urbani *et al.* 2001). Expression and growth of each of the strains, outlined in Fig. 5.1A, were investigated under aerobic and anaerobic conditions. Aerobic conditions were obtained by growing the cells in 500 ml asparagine media in baffled flasks (2L) with agitation at 250 rpm. Semi-aerobic conditions were obtained by growing the cells in 1L asparagine media in un-baffled flasks (2L) with agitation at 135 rpm. Under both conditions, the cells were grown to late exponential phase. To clarify the role each *cbb*₃ oxidase plays in *P. aeruginosa* the growth rates of the WT strain and the strains with disruptions in the locus encoding *cbb*₃-1 (Cco1.1), *cbb*₃-2 (Cco2.2), both *cbb*₃ enzymes (CcoΔ1) and the *aa*₃ enzyme (CoxΔ1) were compared under aerobic and semi aerobic conditions (Fig. 5.3).

In highly aerated cultures, the growth of each *cbb*₃ oxidase strain was accelerated in comparison to growth under semi aerobic conditions, as observed by an increased cell density at the equivalent time points (Fig. 5.2). Previous evidence suggests that the isozyme, *cbb*₃-1 is primarily expressed under aerobic conditions and the isozyme *cbb*₃-2 is primarily expressed under semi aerobic conditions (Comolli and Donohue 2004). However, the growth curves of the deletion mutants Cco1.1 and Cco2.2 shown in Fig. 5.2 demonstrate that under aerobic and semi aerobic conditions the growth of each strain was indistinguishable from each other. As expected, however, the growth of these two mutants was slightly slower than observed for WT under similar conditions. An observed difference in both strains under different conditions was expected. The growth rate of the *cbb*₃ oxidase single mutants *cbb*₃-1 and *cbb*₃-2 was slightly reduced but comparable to that of WT suggesting that more than one oxidase is capable of sustaining microaerobic growth. This observation is supported by a similar finding by Alvarez-Ortega *et al.* when

the growth of *P. aeruginosa* deletion strains was monitored under specific controlled oxygen conditions (Alvarez-Ortega and Harwood 2007). They demonstrated that any one of the three terminal oxidases, *cbb₃-1*, *cbb₃-2* or CIO, that *P. aeruginosa* encodes, support microaerobic growth (Alvarez-Ortega and Harwood 2007). In comparison to the single *cbb₃* mutants, the double *cbb₃-1 cbb₃-2* mutant (CcoΔ1) grew slower than the WT strain under both aerobic and semi aerobic conditions.

The mutant strain lacking *aa₃*, CoxΔ1, was the slowest growing strain under both aerobic and semi aerobic conditions. In organisms other than *P. aeruginosa*, for example, *B. japonicum*, the *aa₃* oxidase is primarily expressed under aerobic conditions (Gabel and Maier 1993). The *aa₃* oxidase is conceivably the primary cytochrome *c* oxidase expressed by *P. aeruginosa* under aerobic conditions. The *cbb₃* oxidases influence bacterial gene expression in response to oxygen availability, as discussed previously (Chapter 1, Section 1.8) (Eraso and Kaplan 2000; Oh *et al.* 2000). Studies have shown that cytochrome *cbb₃* is less efficient at transducing energy than cytochrome *aa₃* (Chapter 1, Section 1.7). By controlling the expression of particular electron-transfer components, especially terminal oxidases, a bacterium constructs the most appropriate electron transport chain for the prevailing environmental conditions (Poole and Cook 2000). It is therefore possible that cytochrome *cbb₃* oxidase can not meet the cells energy requirements for rapid growth the way *aa₃* oxidase can.

In batch culture models manipulation of a changeable variables, for example oxygen or nutrient concentration, cannot be divorced from subsequent changes in growth rate of the bacterium. From the growth curves of the *P. aeruginosa* strains (Fig 5.2) the variable oxygen conditions do appear to alter the growth rate of the organism but this cannot be described with certainty.

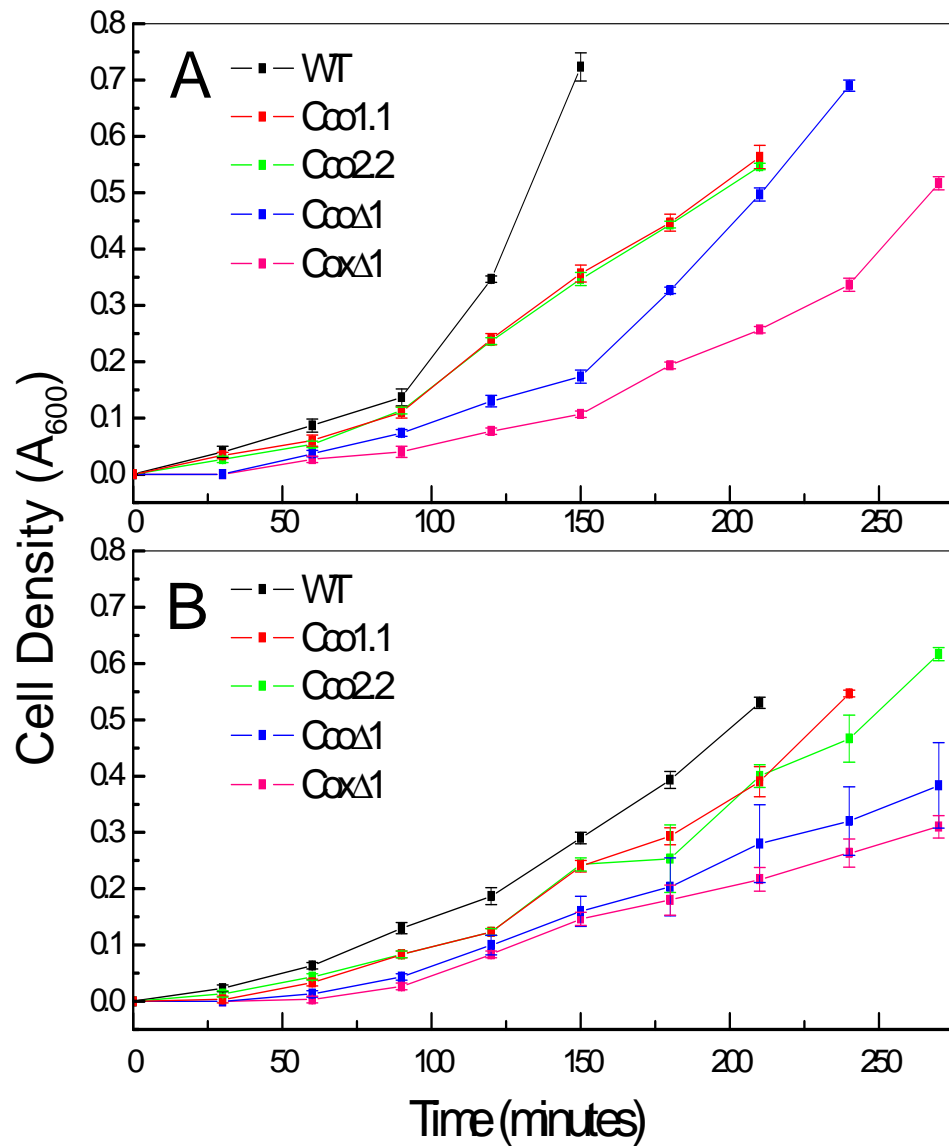


FIG. 5.2 Growth curves of *P. aeruginosa* strain PAK (WT) and mutated PAK, grown (A) aerobically and (B) semi aerobically. The coloured lines indicate the different strains as referred to in the figure legend. The growth of cells was monitored to an OD_{600} of approx 0.5. Each point represents $n = 3 \pm SE$.

5.2.2 Expression of the two predicted *P. aeruginosa* *cbb*₃ oxidases

Each of the two adjacent *P. aeruginosa* *ccoNOQP* operons, designated *ccoNOQP*-1 and *ccoNOQP*-2, encode the four canonical *cbb*₃ oxidase subunits, *cbb*₃-1 and *cbb*₃-2 respectively, according to their order on the chromosome of the *P. aeruginosa* strain PA01 (Stover *et al.* 2000). To assess the pattern of expression of the individual subunits in the *P. aeruginosa* *cbb*₃ oxidases, cells from aerobically and semi aerobically grown cultures were separated by SDS-PAGE and stained for covalently bound heme proteins (Fig. 5.3). The CcoO and CcoP subunits of the two *cbb*₃ oxidases differ slightly in amino acid compositions and therefore a variation in size of the subunits can be observed using SDS-PAGE (Fig. 5.4).

Membranes of the *P. aeruginosa* strain with a disruption in the locus encoding the *cbb*₃-1 oxidase (Cco1.1) show the band of CcoP2 (33.8 kDa) in cells grown under both aerobic and semi aerobic conditions; however this is more easily visualized in semi-aerobic membranes. Membranes of the *P. aeruginosa* strain with a disruption in the locus encoding the *cbb*₃-2 oxidase (Cco2.2) show the larger band of CcoP1 (34.6 kDa) in cells grown under both aerobic and semi aerobic conditions; however this is more easily visualized in aerobic membranes. Previously it was proposed that expression of *cbb*₃-1 is greatest under aerobic conditions (Comolli and Donohue 2004; Alvarez-Ortega and Harwood 2007). It was therefore, anticipated that expression of the subunit, CcoP1 would be greater when the cells were grown in oxygenated conditions. In cells grown under both aerobic and semi aerobic conditions the band of CcoP2 is also easily visible by heme peroxidase analysis, therefore suggesting that the abundance of CcoP2 did not vary under different growth conditions, despite the observation by Comolli *et al.* that expression of CcoP-2 was greater under semi-aerobic conditions than aerobic conditions (Comolli and Donohue 2004). The observation by Comolli *et al.* corresponds with the prediction that expression of the *cbb*₃-1 oxidase is greatest under aerobic conditions and expression of the *cbb*₃-2 oxidase greatest

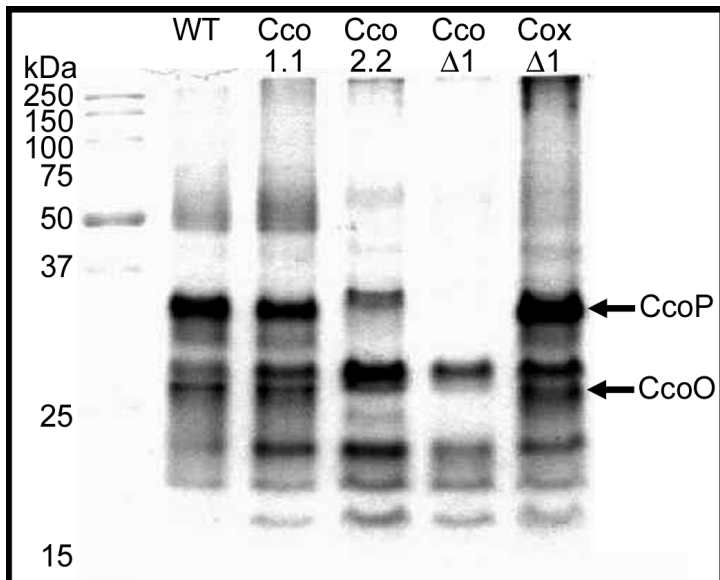
under micro-aerobic conditions (Comolli and Donohue 2004). Quantification through heme peroxidase staining is not however a precise technique and SDS PAGE is recognized as a qualitative method to separate proteins according to their electrophoretic mobility (Scopes 1994). Limitations in SDS PAGE therefore explain any minor discrepancies observed between the results presented previously by Comolli *et al.* and results presented in this study (Comolli and Donohue 2004).

The *c*-type heme of the subunit CcoO can also be detected by heme peroxidase staining; however, it co-migrates with the protein cytochrome *c*₁, which is also 28 kDa in size. (Fischer *et al.* 2001). As the CcoO subunit co-migrates with another protein and the predicted sizes of CcoO-1 and CcoO-2 are very close it is not possible to resolve CcoO-1 and CcoO-2 by mobility on SDS-PAGE. It was not clear from SDS PAGE if the Cco1.1 and Cco2.2 strains showed a reduction in the level of CcoO compared to wild-type as was previously observed (Comolli and Donohue 2004). Zufferey *et al.* previously found that the quantity of CcoO in the Proteobacteria *B. japonicum* is notable as a reporter of *cbb*₃ oxidase abundance as this subunit is required for stability of the enzyme (Zufferey *et al.*, 1996).

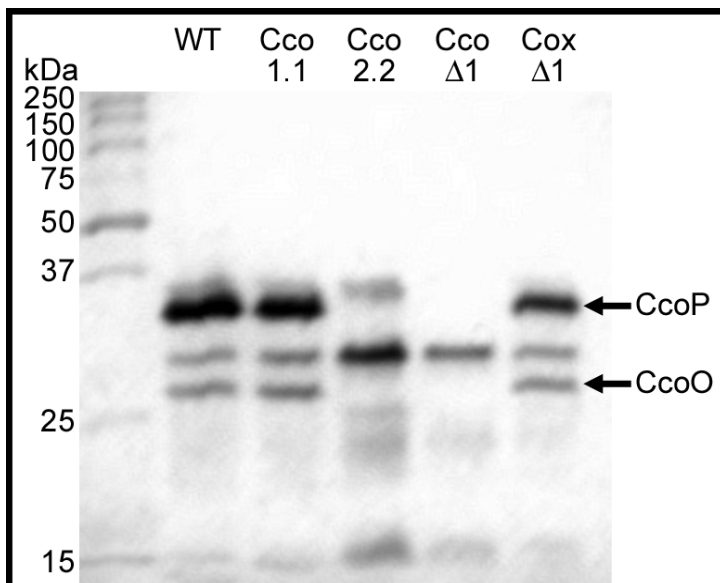
In addition to the bands of the two *c*-type cytochrome subunits of the *cbb*₃ oxidase from *P. aeruginosa*, two bands of molecular mass 28 and 20 kDa were also observed by SDS PAGE stained specifically for covalently attached hemes. These bands have previously been observed in *cbb*₃ rich membrane fractions from *B. japonicum* (Preisig *et al.* 1993). Heme staining of membranes from a *bc*₁ mutant lacked the 28 kDa band, therefore, this band was concluded to be cytochrome *c*₁ from the *bc*₁ complex (Preisig *et al.* 1993; Comolli and Donohue 2004). Interestingly the cytochrome *c*₁ band is more prominent under semi-aerobic conditions than aerobic conditions. The 20 kDa band is the cytochrome *c*₅₅₂, a product of the *cycM* gene (Bott *et al.* 1991; Fischer *et al.* 2001; Otten *et*

al. 2001). Cytochrome *c*₅₅₂ is a soluble cytochrome *c* protein which catalyses electron transfer from the cytochrome *bc*₁ complex to the terminal oxidase, cytochrome *aa*₃ (Bott *et al.* 1991; Otten *et al.* 2001). It would therefore be expected that this protein would be present in all strains of *P. aeruginosa* used in this study. The protein CycM is not easily visualized using SDS PAGE, however, it is more prominent in cells grown under aerobic conditions than those grown under semi-aerobic conditions. This observation is consistent with its role in electron transfer to the cytochrome *aa*₃ oxidase, an oxidase primarily expressed under aerobic conditions.

As expected, in the deletion strain CcoΔ1 the two subunits of the *cbb*₃-1 and *cbb*₃-2 were absent as adjudged by SDS-PAGE. The 28 kDa band of cytochrome *c*₁ and the 20 kDa band of the protein CycM were visible. Membranes of the *P. aeruginosa* strain with a disruption in the locus encoding the *aa*₃ oxidase (CoxΔ1) show similarities to WT in cells grown both aerobically and semi aerobically. The CcoP and CcoO subunits of *cbb*₃-1 and *cbb*₃-2 are prominent, the cytochrome *c* containing subunit of the *bc*₁ complex and the 20kDa band of CycM were visible on SDS PAGE.



A



B

FIG. 5.3 Heme peroxidase analysis of the *c*-type cytochromes present in the membranes of *P. aeruginosa* PAK WT and mutant strains. Strains were harvested after growth under aerobic (A) or semi-aerobic (B) conditions. 17.5 μ g of cell membranes was separated by SDS PAGE on 15% resolving gel before staining for heme-dependant peroxidase activity. Proteins with molecular weights corresponding to the *cbb*₃ oxidase subunits, CcoP and CcoO are indicated.

5.2.3 Steady State Assay of Wild-type *P. aeruginosa* and mutants

Based on the growth rates and SDS-PAGE analysis of wild-type and mutant strains different roles for the two *cbb₃* oxidases in *P. aeruginosa* has been considered (Section 5.2.1 and 5.2.2). It is proposed that the oxidase *cbb₃-1* is expressed under aerobic conditions and the oxidase *cbb₃-2* is primarily expressed under semi-aerobic conditions. To analyse the functional consequences of the different mutations the respiratory activity of these strains was examined.

P. aeruginosa wild-type strain and the mutants were grown under aerobic and semi-aerobic conditions with asparagine as the sole carbon and nitrogen source as described previously (Section 2.6.2). Cells were grown to their mid-exponential phase of growth, harvested, washed and resuspended in buffer. The oxygen consumption rates of these suspensions were determined using a Clark type oxygen electrode. Throughout these respiratory activity studies, the wild-type membranes were utilized as a positive control as there were no disruptions to the respiratory oxidases in this strain. The mutant strain with both *cbb₃* oxidases deleted was used as a negative control.

A cytochrome *c* oxidase, first identified as a cytochrome *co*-type oxidase, was previously purified and biochemically characterized from *P. aeruginosa* (Matsushita *et al.* 1980). This oxidase had a high TMPD-oxidizing activity and reacted preferentially with the membrane bound electron donor cytochrome *c*₅₅₁. This oxidase has since been recognised as the *cbb*₃ oxidase of *P. aeruginosa*, suggesting that cytochrome *c*₅₅₁ is the physiological electron donor to the *cbb*₃ oxidase *in vivo*. In *P. aeruginosa* cytochrome *cd*₁ the electron donors cytochrome *c*₅₅₁ and azurin are interchangeable and exist in equilibrium with each other, although cytochrome *c*₅₅₁ is the most efficient electron donor *in vitro* (Zumft 1997; Williams *et al.* 2007). To investigate the respiratory activity of wild-type and mutant *P. aeruginosa* strains a range of electron donors were used (Williams *et al.* 2007). The electron donors included NADH, azurin and *c*₅₅₁ and the artificial electron donor TMPD (Horio *et al.* 1961; Williams *et al.* 2007) (Fig. 5.4).

NADH Dependant Oxidase Activity

The pathway of electrons into the *cbb*₃ oxidase is thus far unclear; therefore the respiratory activity of all the strains was initially investigated using the electron donor NADH. NADH dependant oxidase activity was measured in WT and mutated *P. aeruginosa* membranes from both aerobically and semi aerobically grown cells (Fig. 5.5). This assay, which measures the total rate of oxygen consumption by all the quinol and cytochrome oxidases in the respiratory chain of *P. aeruginosa* is not specific to one oxidase. Overall, the results were as expected and are consistent with the hypothesis that the *cbb*₃-1 oxidase is primarily expressed under aerobic conditions and the *cbb*₃-2 oxidase is primarily expressed under semi aerobic conditions (Comolli and Donohue 2004).

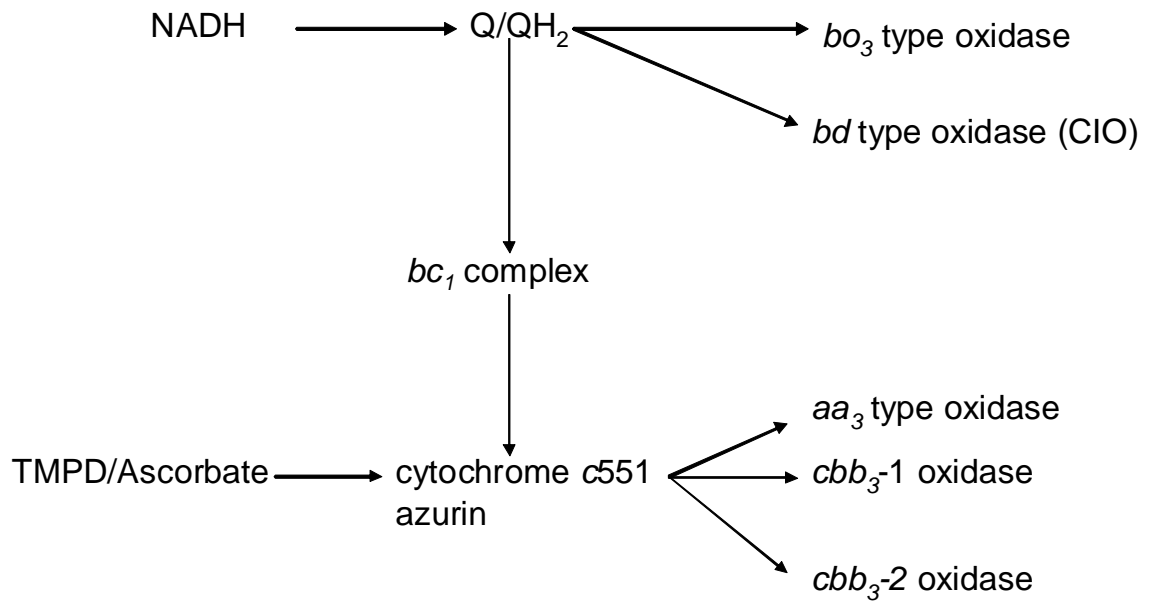


FIG. 5.4 Schematic representation of some of the predicted components of the *P. aeruginosa* respiratory pathway. This facultative organism can respire anaerobically by denitrification or aerobically using two quinol oxidases or three cytochrome *c* oxidases. NADH dehydrogenases reduce quinone and donate electrons to the terminal oxidases, as indicated. The figure shows the artificial electron donor TMPD/Ascorbate, and *P. aeruginosa* physiological donors, cytochrome c_{551} and azurin (Adapted from Comolli and Donohue 2004).

In membranes from aerobically and semi aerobically grown wild-type cells the NADH dependant activity differed by 20% (Fig. 5.5). The aerobically grown cells had the greatest activity and this result is consistent with three of the terminal oxidases in *P. aeruginosa* being primarily expressed under aerobic conditions. This compares to the expression of only two of the *P. aeruginosa* terminal oxidases under semi aerobic conditions. The NADH dependant oxidase activity observed in wild-type membranes was used as a benchmark for comparison of the other mutant strains.

When grown under aerobic conditions, the mutant strain Cco1.1 (*cbb₃-2* only) showed decreased NADH dependant oxidase activity compared to wild-type. In contrast, when the cells were grown under semi aerobic conditions the respiratory activity of this strain decreased only slightly compared to wild-type. These results therefore support the proposal that the *cbb₃-2* oxidase is primarily expressed under semi-aerobic growth conditions. In contrast to the respiratory activity observed in Cco1.1, respiratory activity in the aerobically grown mutant strain Cco2.2 (*cbb₃-1* only) decreased only slightly compared to wild-type. When the same strain was grown under semi aerobic conditions the membranes showed decreased NADH dependant activity. These results therefore support the suggestion that the *cbb₃-1* oxidase is primarily expressed under aerobic growth conditions (Section 5.2.2).

In comparison to wild-type, CcoΔ1 membranes grown under aerobic conditions showed a considerable decrease in activity. The same strain grown under semi aerobic conditions however, showed no change in respiratory activity compared to wild-type cells grown under the same conditions. The respiratory activity in the strain CcoΔ1 resembled activity observed in the strain Cco1.1 when the cells were grown under the same conditions. This result, surprisingly, suggests that the respiratory oxidases expressed under semi-aerobic conditions compensate for the loss of the *cbb₃* oxidases. In contrast, the respiratory

oxidases expressed under aerobic conditions do not compensate for the loss of the *cbb₃* oxidases. The results of the NADH dependant oxidase activity of Cco1.1 should however be questioned in light of the CcoΔ1 results. It was previously concluded that as the respiratory activity of Cco1.1 did not decrease in the semi-aerobically grown cells the result indicated that the *cbb₃-2* oxidase is primarily expressed under semi-aerobic conditions. However considering the CcoΔ1 results, it is possible that the other oxidases were compensating in this strain when grown under semi-aerobic conditions and the respiratory activity observed in the strain Cco1.1 is not reflective of the *cbb₃-2* expression.

Membranes from cells lacking the *aa₃* type oxidase (CoxΔ1) showed very little NADH dependant oxidase activity when grown under both aerobic and semi aerobic conditions. However, surprisingly the aerobically grown cells were more active than the semi-aerobically grown cells. This result possibly reflects the importance of the *aa₃* oxidase in the respiratory pathway of *P. aeruginosa* and deletion of this oxidase results in significant compensation, observed by the expression of the other oxidases.

NADH dependant oxidase activity is not specific to the *cbb₃* oxidases. It was therefore not clear if the respiratory activity observed in Cco1.1 and Cco2.2 was a result of increased *cbb₃* expression or increased expression of the other oxidases. To gather further information regarding the activity of the *cbb₃* oxidases, an assay, which is specific to *cbb₃* oxidases, was utilized.

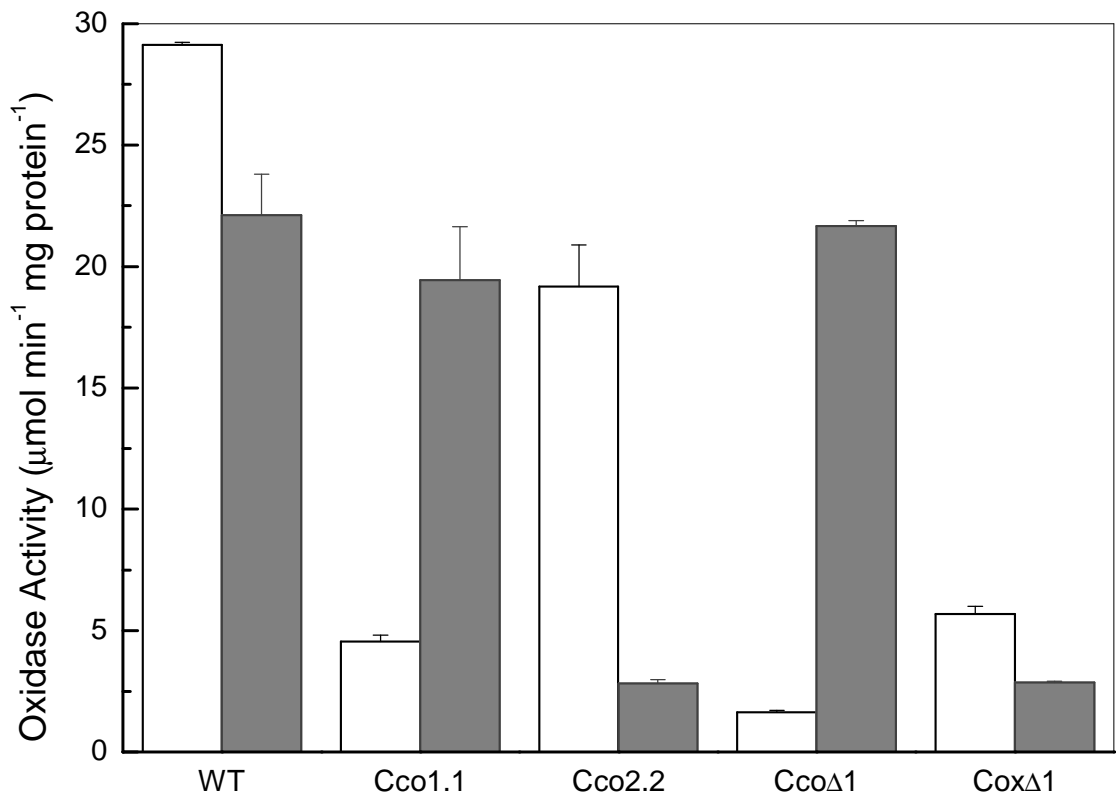


FIG. 5.5 NADH dependant oxidase activity with membranes of Wild-type *P. aeruginosa* and mutants lacking either one (Cco1.1 or Cco2.2) or both of the *cbb*₃ oxidases (CcoΔ1) or the *aa*₃ oxidases (CoxΔ1). Strains were grown under aerobic conditions (white) or semi-aerobic conditions (light grey). Values represent the average of three separate measurements, with error bars representing the standard deviation from the mean.

TMPD dependant Oxidase Assay

Oxidase activity in the wild-type and mutated strains grown under both aerobic and semi aerobic conditions was measured using the electron donor TMPD/ascorbate, which is specific for cytochrome *c* dependant oxidases (Fig. 5.6). In all the strains, a decrease in oxidase activity in comparison to NADH dependant oxidase activity was observed. This result was expected as the NADH dependant oxidase assay measures the total respiratory activity from all the quinol and cytochrome *c* oxidases compared to the TMPD/ascorbate assay, which only measures cytochrome *c* dependant oxidase activity. The decrease in TMPD/ascorbate oxidase activity was substantial however compared to NADH oxidase activity and suggesting that the majority of the observed NADH dependant activity in *P. aeruginosa* respiratory oxidases does not reflect the contribution of the cytochrome *c* dependant oxidases.

Membranes from aerobically grown cells lacking *cbb*₃-1 (Cco1.1) had 27% less TMPD dependant activity compared to wild-type membranes. In comparison, Cco1.1 membranes grown under semi aerobic conditions showed similar activity to wild-type membranes grown under the same conditions. These results are consistent with all previous observations that the *cbb*₃-2 oxidase is primarily expressed under semi aerobic conditions. In comparison, semi-aerobically grown cells lacking *cbb*₃-2 (Cco2.2) lost 59 % of their oxidase activity compared to wild-type membranes. Similarly to the results from the NADH dependant assay the oxidase activity of aerobically grown cells lacking *cbb*₃-2 was comparable to wild-type. Again these results are consistent with the previous observation that the *cbb*₃-1 oxidase is primarily expressed under aerobic conditions.

Membranes from cells lacking both *cbb*₃ oxidases (CcoΔ1) were considered a negative control since this strain lacks two of the three cytochrome *c* type oxidases in *P. aeruginosa*. Aerobically grown and semi aerobically grown CcoΔ1 membranes lost

more than 99 % oxidase activity compared to WT membranes suggesting that most of the cytochrome *c* dependant electron flow is blocked by inactivation of both of the *cbb₃* oxidases. It was anticipated that increased oxidase activity would be observed in the aerobically grown cells compared to the semi-aerobically grown cells due to increased expression of the *aa₃* oxidase under high oxygen concentration conditions(Kim *et al.* 2007). However, a slightly increased oxidase activity was observed in cells grown under semi aerobic conditions compared to aerobic conditions. The reason for this discrepancy is not clear.

The mutant lacking the *aa₃* oxidase shows a similar TMPD dependant oxidase activity pattern to both wild-type and the strain Cco1.1. As previously discussed, the *aa₃* oxidase is primarily expressed under aerobic conditions. It was therefore anticipated that a decrease in oxidase activity would be observed in the aerobically grown CoxΔ1 cells in comparison to wild-type cells. The oxidase activity of the strain CoxΔ1 was increased when the cells were grown under semi aerobic conditions compared to those grown under aerobic conditions. Moreover, in comparison to semi aerobically grown wild-type cells, the membranes of the semi aerobically grown cells lacking the *aa₃* oxidase (CoxΔ1) showed 36 % increased oxidase activity. The result therefore suggests that under semi aerobic conditions increased expression of the *cbb₃-2* oxidase compensates for the lack of *aa₃* oxidase despite the *aa₃* oxidase being primarily expressed aerobically.

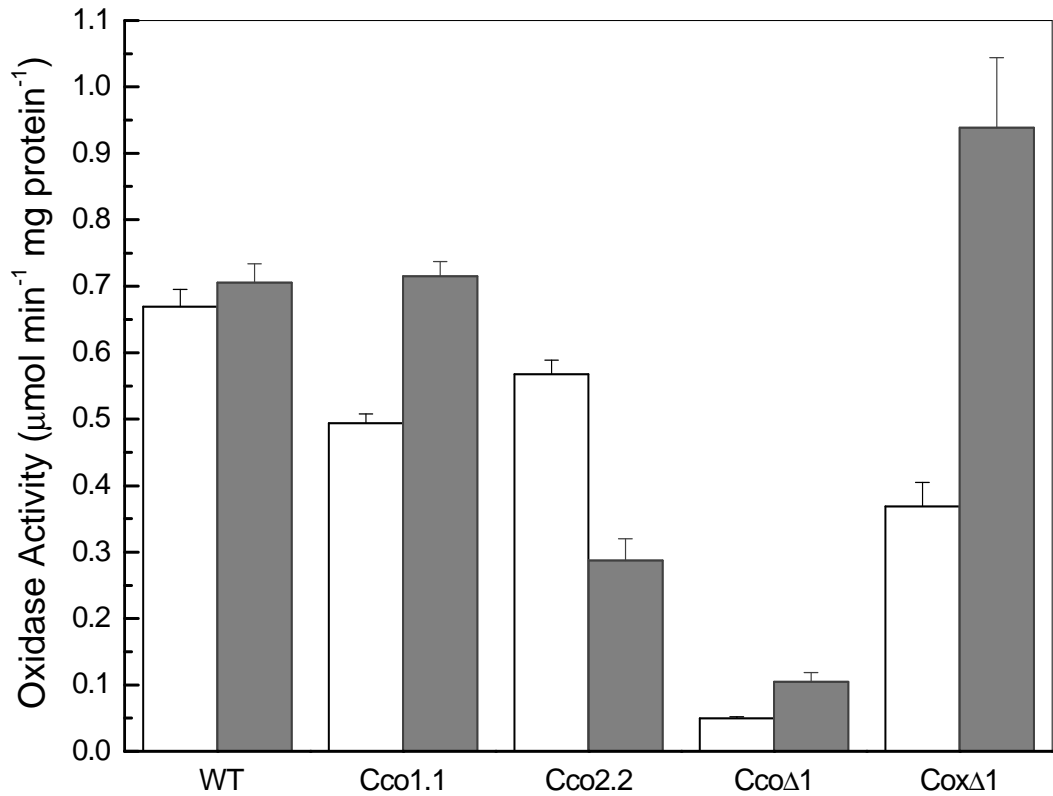


FIG. 5.6 TMPD dependant oxidase activity with membranes of Wild-type *P. aeruginosa* and mutants lacking either one (Cco1.1 or Cco2.2) or both of the *cbb*₃ oxidases (Cco Δ 1) or the *aa*₃ oxidases (Cox Δ 1). Strains were grown under aerobic conditions (white) or semi-aerobic conditions (light grey). Values represent the average of three separate measurements, with error bars representing the standard deviation from the mean.

Azurin dependant Oxidase Activity

A method for assaying *cbb*₃ oxidases using a physiologically relevant electron donor has not been reported (Comolli and Donohue 2004). Research has suggested that the two periplasmic proteins, cytochrome *c*₅₅₁ and azurin, can act as electron donors to the respiratory enzymes in *P. aeruginosa* (Barber *et al.* 1976). For example, the cytochrome *cd1* nitrite reductase isolated from *P. aeruginosa* is able to oxidise both reduced cytochrome *c*₅₅₁ and reduced azurin. Oxidase activity assays were used to investigate the role that the blue copper protein, azurin, and cytochrome *c*₅₅₁ play in mediating electron transfer to the *cbb*₃ oxidases. The methods used were as for the NADH dependant and TMPD dependant oxidase assays. These earlier results were used as a direct comparison to aid interpretation of the assay data. Overall the results for azurin dependant oxidase activity were similar to those observed for TMPD dependant oxidase activity in wild-type and mutant *P. aeruginosa* strains grown under both aerobic and semi aerobic conditions. At first sight, the results therefore suggest that azurin is a candidate as a physiological electron donor to the *cbb*₃ oxidases.

In aerated cultures the azurin dependant oxidase activity of membranes from wild-type, Cco1.1 and Cco2.2 cells was similar (Fig. 5.7). In contrast, when grown under semi aerobic conditions cells lacking *cbb*₃-1 (Cco1.1) showed increased azurin dependant oxidase activity compared to wild-type. Under the same conditions, the cells lacking *cbb*₃-2 (Cco2.2) had an azurin dependant oxidase activity similar to wild-type. These results are congruent with conclusions previously made regarding the expression of *cbb*₃-1 and *cbb*₃-2. The results suggest that the *cbb*₃-2 oxidase is primarily expressed under semi-aerobic conditions and the *cbb*₃-1 oxidase is primarily expressed under aerobic conditions. Expression of the electron donor, azurin, is under the control of the oxygen sensing transcriptional regulator ANR (Ray and Williams 1997; Vollack *et al.* 1998; Comolli and Donohue 2004). The isozyme *cbb*₃-2 is also under the control of the ANR box (Comolli

and Donohue 2004). *In vivo*, it would therefore be expected that activation of the *cbb₃-2* oxidase by ANR, in response to oxygen limitation, would correspond with an increase in azurin expression.

The cells with both *cbb₃* operons deleted (CcoΔ1) showed only 25% residual oxidase activity in comparison to wild-type, when grown under both aerobic and semi aerobic conditions. Semi aerobically grown membranes lacking the aerobically expressed *aa₃* complex (CoxΔ1) showed increased azurin dependant oxidase activity compared to wild-type. As observed in section 5.2.1, the growth rate of the *aa₃* mutant was slower compared to other *P. aeruginosa* strains under both aerobic and semi-aerobic conditions. This increased oxidase activity observed in the semi aerobically grown CoxΔ1 strain was only observed in the cells grown under semi aerobic conditions and membranes from cells grown under aerobic conditions showed similar activity to the mutant strain CcoΔ1. This observation therefore suggests that increased expression of semi-aerobically expressed oxidases *i.e.* *cbb₃-2* contributed to the elevated oxidase activity.

c₅₅₁ dependant oxidase activity

Overall the results for *c₅₅₁* dependant oxidase activity were similar to those observed for TMPD dependant oxidase activity when wild-type and mutant strains were grown under both aerobic and semi aerobic conditions. The results therefore suggest that, similarly to azurin, cytochrome *c₅₅₁* is a candidate as a physiological electron donor to the *cbb₃* oxidases.

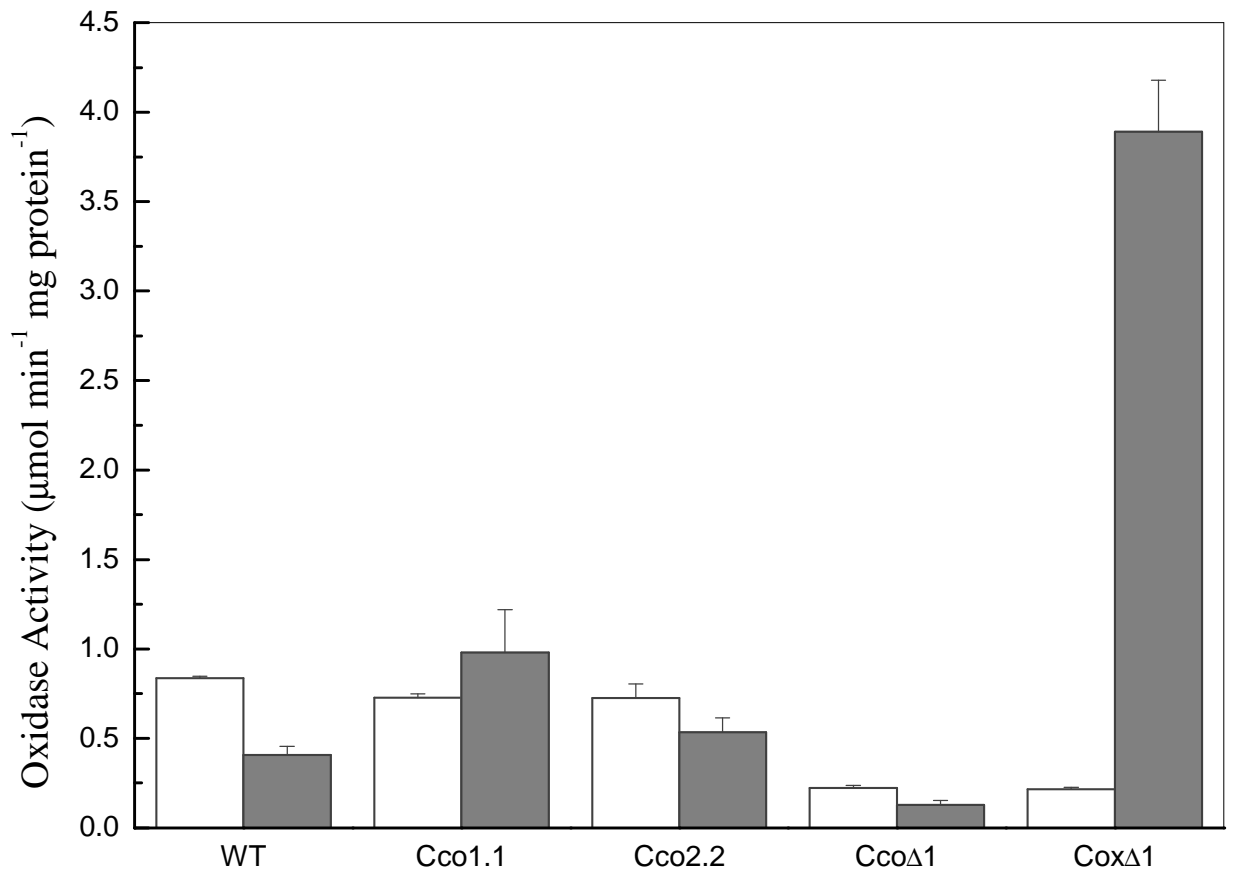


FIG. 5.7 Azurin dependant oxidase activity with membranes of wild-type *P. aeruginosa* and mutants lacking either one (Cco1.1 or Cco2.2) or both of the *cbb*₃ oxidases (Cco Δ 1) or the *aa*₃ oxidases (Cox Δ 1). Strains were grown under aerobic conditions (white) or semi-aerobic conditions (grey). Values represent the average of three separate measurements, with error bars representing the standard deviation from the mean.

In aerated cultures the c_{551} dependant oxidase activity of membranes from wild-type and Cco2.2 cells was similar (Fig. 5.8). However, the aerobically grown strain Cco1.1 showed increased oxidase activity in contrast to wild-type membranes. In comparison, a slight decrease in the oxidase activity of semi aerobically grown Cco1.1 membranes was observed. This result was unexpected as the assay results reported in the study suggest that the cbb_3-1 oxidase is primarily expressed under aerobic conditions and the cbb_3-2 oxidase is primarily expressed under semi aerobic. In contrast, when grown under semi aerobic conditions cells lacking cbb_3-2 (Cco2.2) showed decreased c_{551} dependant oxidase activity compared to wild-type and aerobically grown Cco2.2 showed increased oxidase activity in comparison to semi aerobically grown cells. The results observed for Cco2.2 are consistent with the current proposal. Examination of the *P. aeruginosa* strain with the cbb_3 operons deleted (Cco Δ 1) showed only a residual oxidase activity in comparison to wild-type, when grown under semi aerobic conditions. Interestingly, when grown under aerobic conditions the Cco Δ 1 strain showed only a 60 % decrease in oxidase activity compared to wild-type membranes grown under the same condition. A 75% decrease was observed in TMPD dependant and azurin dependant oxidase activity in aerobically grown Cco Δ 1 membranes. The smaller decrease in c_{551} dependant oxidase activity compared to TMPD dependant and azurin dependant oxidase activity suggests that the electron donor cytochrome c_{551} is more specific to the aa_3 oxidase, the only c -type cytochrome expressed in the Cco Δ 1 membranes. However, cells lacking the aerobically expressed aa_3 complex (Cox Δ 1) showed increased c_{551} dependant oxidase activity compared to the strain Cco Δ 1 when grown under both aerobic and semi aerobic conditions. The observed c_{551} dependant oxidase activity in the strain Cox Δ 1 is comparable to the azurin and TMPD dependant oxidase activity. In these three separate assays, the oxidase activity of Cox Δ 1 membranes from cells grown under semi-aerobic conditions was increased compared to the oxidase activity of aerobically grown cells. The explanation for this observation is unclear.

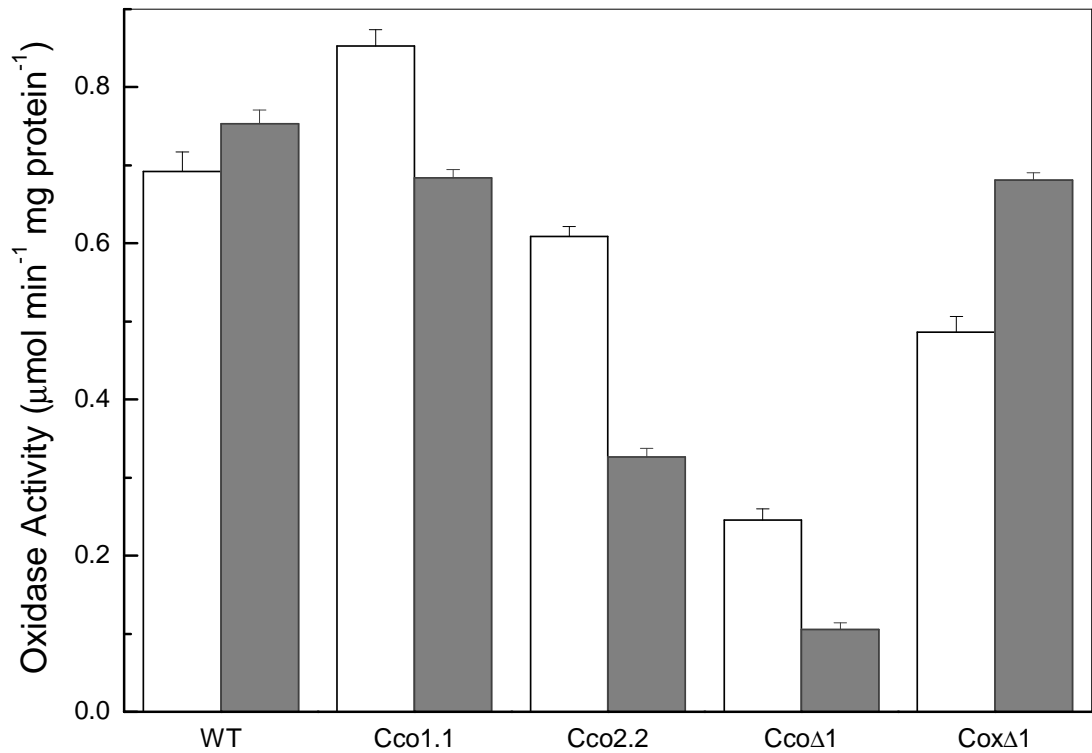


FIG. 5.8 c_{551} dependant oxidase activity with membranes of wild-type *P. aeruginosa* and mutants lacking either one (Cco1.1 or Cco2.2) or both of the cbb_3 oxidases (CcoΔ1) or the aa_3 oxidases (CoxΔ1). Strains were grown under aerobic conditions (white) or semi-aerobic conditions (grey). Values represent the average of three separate measurements, with error bars representing the standard deviation from the mean.

5.3 Conclusions

The results from this study support the previous suggestions by Comolli *et al.* that the *cbb₃-1* oxidase is primarily expressed under aerobic conditions and the *cbb₃-2* oxidase is primarily expressed under semi-aerobic conditions (Section 5.2.3). The results therefore reinforce the proposal that the *cbb₃-1* oxidase plays a physiological role at high oxygen tensions and suggests that this oxidase has an affinity for oxygen, which is lower than most *cbb₃* oxidases that are important under oxygen limiting conditions (Preisig *et al.* 1993; Zufferey *et al.* 1996; Jackson *et al.* 2006). The *cbb₃-2* oxidase appears to be more similar to canonical *cbb₃* type enzymes because in highly aerated cultures inactivation of this oxidase had a lesser impact on the oxidase activity of *P. aeruginosa* observed using a range of electron donors.

It remains unclear why the *P. aeruginosa cbb₃* oxidases play varying roles under differing oxygen conditions, however, it is predicted that variation in the expression of these two oxidases is one of the ways in which *P. aeruginosa* compensates for respiratory limitations and therefore continues to effectively generate energy in a number of different environments. The physiological electron donor specific to the *cbb₃* oxidases in *P. aeruginosa* also remains unclear. The azurin and *c₅₅₁* dependant oxidase activity assays do not make it clear whether the blue protein, azurin or the soluble protein cytochrome *c₅₅₁* is more specific to either *cbb₃-1*, *cbb₃-2* or both *cbb₃* oxidases. To resolve this outstanding question and to ascertain the affinity the *cbb₃-1* oxidase has for oxygen requires its purification from other *P. aeruginosa* oxidases.

6. Biochemical Characterization of *cbb*₃ oxidase isolated from *P. aeruginosa*.

6.1 Introduction.....	209
6.2 Results and Discussion.....	209
6.2.1 Purification of cytochrome <i>cbb</i> ₃ oxidase from <i>P. aeruginosa</i> ..	209
6.2.2 UV-Visible spectroscopy.....	213
6.2.3 TMPD mediated oxygen uptake activity.....	219
6.2.4 Mediated Redox potentiometry of <i>Cbb</i> ₃ -1 and <i>Cbb</i> ₃ -2.....	222
6.3 Conclusions.....	228

6.1 Introduction

Using *P. aeruginosa* strains with a disruption in the locus encoding *cbb₃-1* or *cbb₃-2* it has been demonstrated that expression of the two *cbb₃* oxidases differ depending upon the growth conditions (Chapter 5). The results intimate that the *cbb₃-1* oxidase plays a physiological role at high oxygen tensions in comparison to previously studied *cbb₃* oxidases, which are typically important under oxygen limiting conditions (Preisig *et al.* 1993; Zufferey *et al.* 1996; Jackson *et al.* 2006). This suggested that the *cbb₃-1* oxidase has an affinity for oxygen that is lower than that of *cbb₃* oxidases from other bacteria, which would require its purification from the other *P. aeruginosa* oxidases to ascertain. In contrast, the results suggest that the *cbb₃-2* oxidase plays a physiological role at low oxygen tension, a role more similar to the canonical *cbb₃* oxidases. The *cbb₃* oxidase from *P. stutzeri* has previously been studied in detail however, it is not clear which of the two *P. stutzeri* isozymes was analysed (Pitcher 2002; Pitcher *et al.* 2003). However, utilizing previous knowledge gained regarding the *cbb₃* oxidase from *P. stutzeri*, biochemical characterization has been used to investigate the two *cbb₃* oxidases in *P. aeruginosa* further. This study, using purified *cbb₃-1* and *cbb₃-2* enzymes represents the first detailed spectroscopic characterization of the *cbb₃* oxidases in *P. aeruginosa*.

6.2 Results

6.2.1 Purification of cytochrome *cbb₃* oxidase from *P. aeruginosa*

Previously, information was gathered on the basic phenotypes of the *P. aeruginosa* *cbb₃* oxidase using wild-type membranes and mutated *cbb₃* strains (Chapter 5). The purification of the two *cbb₃* oxidases of *P. aeruginosa*, *cbb₃-1* and *cbb₃-2* was simplified by using the strains Cco1.1 and Cco2.2, which lack either *cbb₃-1* or *cbb₃-2* respectively. The strain Cco1.1 was grown under semi-aerobic conditions and the strain Cco2.2 was grown under aerobic conditions. The steps employed in the purification of the *cbb₃* oxidase were the

same regardless of growth conditions *i.e.* aerobic or semi aerobic (Chapter 2, Section 2.6.3).

The method used for preparation of the *P. aeruginosa* membranes (Chapter 2, Section 2.6.2) was adapted from that described previously by Pitcher *et.al.* (Pitcher *et al.* 2002). The *P. aeruginosa* membranes were solubilised in detergent, (DM) and the cytochrome *cbb*₃ oxidases purified using anion exchange and metal-ion affinity chromatography (Chapter 2, Section 2.7.3).

The use of a step gradient during the first anion exchange column gave excellent separation of the *cbb*₃ oxidases from the superfluous oxidases, as shown in Fig. 6.1. The protein which eluted at each chromatographic peak was identified further using a combination of gel electrophoresis and UV-Visible spectroscopy. Spectroscopic analysis of the peaks obtained during the purification process revealed that the *aa*₃ oxidase eluted at a different salt concentration (200 mM) to either *cbb*₃-1 or *cbb*₃-2, which eluted at 300 mM and 250 mM NaCl respectively. The variation in salt concentration at which the oxidases eluted from the anion exchange column was conducive to easier protein separation but surprising as the *cbb*₃-2 oxidase from *P. aeruginosa* is slightly more negatively charged compared to *cbb*₃-1 oxidase. It was therefore anticipated that the binding of *cbb*₃-2 to the anion resin would be stronger and would elute from the anion exchange column after *cbb*₃-1.

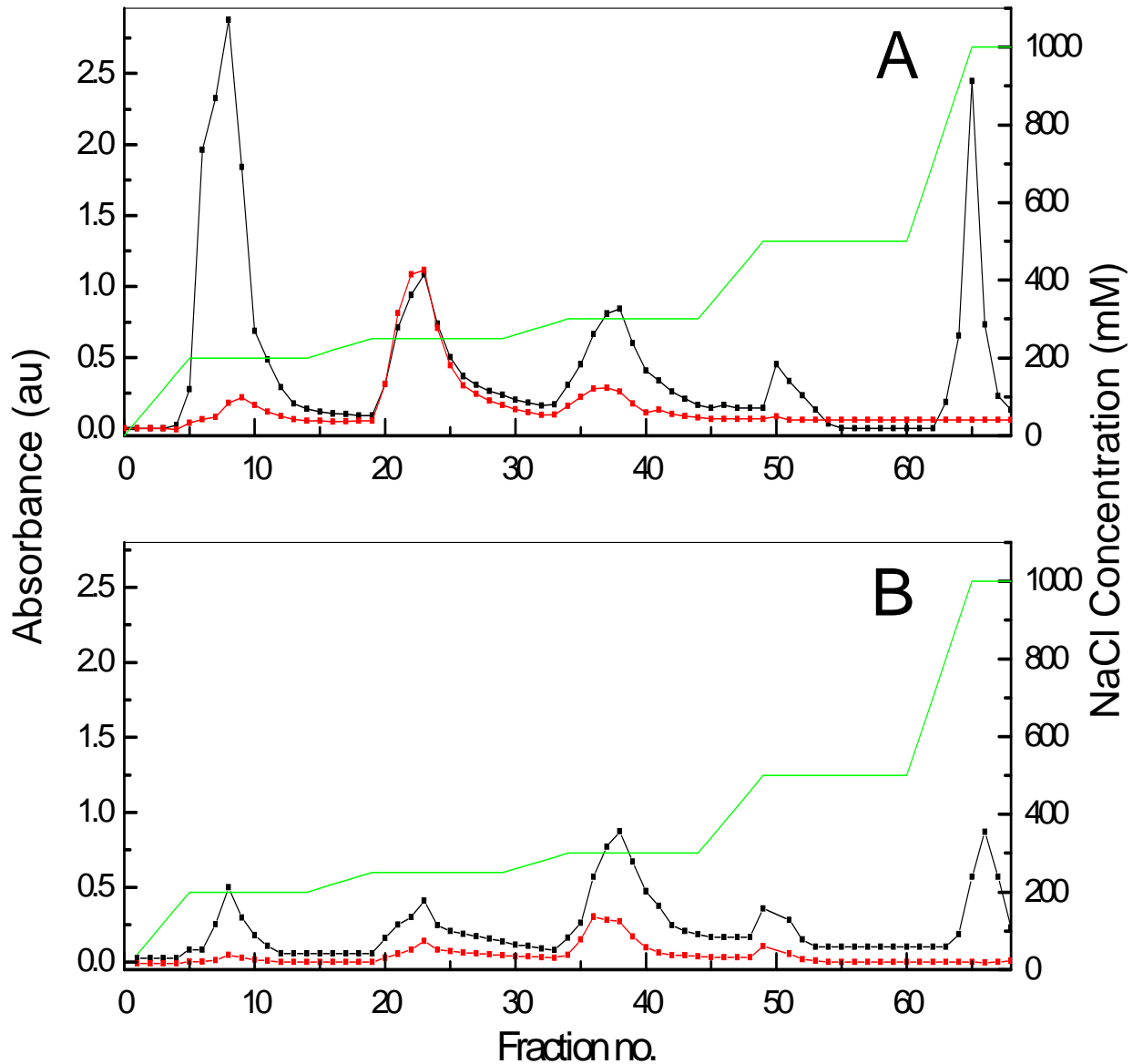


Fig. 6.1 Q sepharose chromatographic profile of the *P. aeruginosa* strains Cco1.1 (A) and Cco2.2 (B). The elution buffer was 20 mM Tris HCl, 50 μ M EDTA, 0.02% DM, 0-1000 mM NaCl, pH 8.5. The black trace indicates absorbance of the eluted protein at 280 nm. The red trace indicates absorbance of the eluted protein at 410 nm. The green line indicates the changes in NaCl concentration throughout the chromatographic process and the relation to the elution of different proteins.

Analysis of the purified *cbb₃-2* oxidase using Coomassie blue stained SDS PAGE gel indicates bands with apparent molecular masses of 42 kDa, 34 kDa, and 23 kDa (Fig. 6.2). These bands correspond to CcoN-2, CcoP-2 and CcoO-2 respectively. There was no evidence of CcoQ being part of the enzyme complex after purification. This is not however surprising as to date observation of the CcoQ subunit in a *cbb₃* preparation has not been reported (Zufferey *et al.* 1996; Kim *et al.* 2007; Verissimo *et al.* 2007). Analysis of the *cbb₃-1* oxidase by Coomassie staining SDS PAGE gel indicated that the CcoP subunit was not present in the final purified product, however the CcoO subunit was observed. The presence of major protein bands in the *cbb₃-1* sample similar to those observed in the *cbb₃-2* sample suggests that the protein concentration of the load sample was not underestimated. However, the CcoP-1 band does not appear to stain well and is light in comparison to other protein bands as demonstrated by the SDS PAGE gel of *P. aeruginosa* membranes stained for TMPZ mediated heme peroxidase activity (Chapter 5, Section 5.2.2). Upon purification of *cbb₃* oxidase from *R. sphaeroides* the subunits CcoN and CcoO were visualised using SDS-PAGE but the CcoP subunit stained poorly with Coomassie stain and was only detected by Western blot using an antibody against CcoP (Oh and Kaplan 2002). The CcoP-1 subunit was observed in the membranes of aerobically grown strain Cco2.2 (*cbb₃-1* only), suggesting that the CcoP subunit was lost during purification of the *cbb₃-1* oxidase (Fig. 5.4 Chapter 5, Section 5.2.2). During purification of the *cbb₃* oxidase isolated from *P. denitrificans* loss of the CcoP subunit was also observed. (de Gier *et al.* 1996). It has been established that the CcoNO subcomplexes isolated from both *P. denitrificans* and *B. japonicum* are catalytically competent (de Gier *et al.* 1996; Zufferey *et al.* 1996). The oxidase activity of the *P. aeruginosa* *cbb₃* oxidases will be discussed in Section 6.2.3.

Unfortunately, we were not able to attain a well-defined TMPZ mediated heme peroxidase heme stained gel. The lanes of the gel were smeared suggesting overloading of the protein;

however, at lower protein concentrations neither the CcoP nor CcoO bands were visible. The Coomassie stained SDS-PAGE gel shows that unfortunately the *cbb*₃ oxidases co-purified with other proteins. Co-purification of proteins, including cytochrome *c*_y was previously observed with purification of the *cbb*₃ oxidase from *R. sphaeroides* (Oh and Kaplan 2002). The lower purification yield of the *P. aeruginosa cbb*₃ oxidases possibly contributed to the poor gels.

6.2.2 UV-Visible Spectroscopy

Following purification of the *P. aeruginosa cbb*₃ oxidases, *cbb*₃-1 and *cbb*₃-2 were characterised spectroscopically.

*Cbb*₃-1

The electronic absorption spectrum of fully oxidized cytochrome *cbb*₃-1 isolated from aerobically grown *P. aeruginosa* shows a Soret maximum of 413 nm and two broad but well defined features in the visible region between 525 nm and 550 nm (Fig. 6.3A). Upon complete reduction with excess dithionite, the Soret band intensified and shifted to 420 nm with a visible shoulder at 422 nm. These two features are characteristic of ferrous *c*-type hemes and ferrous *b*-type heme respectively. The α and β bands in the visible region at 551 nm and 521 nm, with distinct shoulders at 559 nm and 528 nm respectively, intensify upon reduction. The 551 nm and 521 nm features are characteristic of ferrous *c*-type heme whilst the observed shoulders are characteristic of ferrous *b*-type heme. There was no evidence of a band near 600nm that would correspond to contamination with heme *a*.

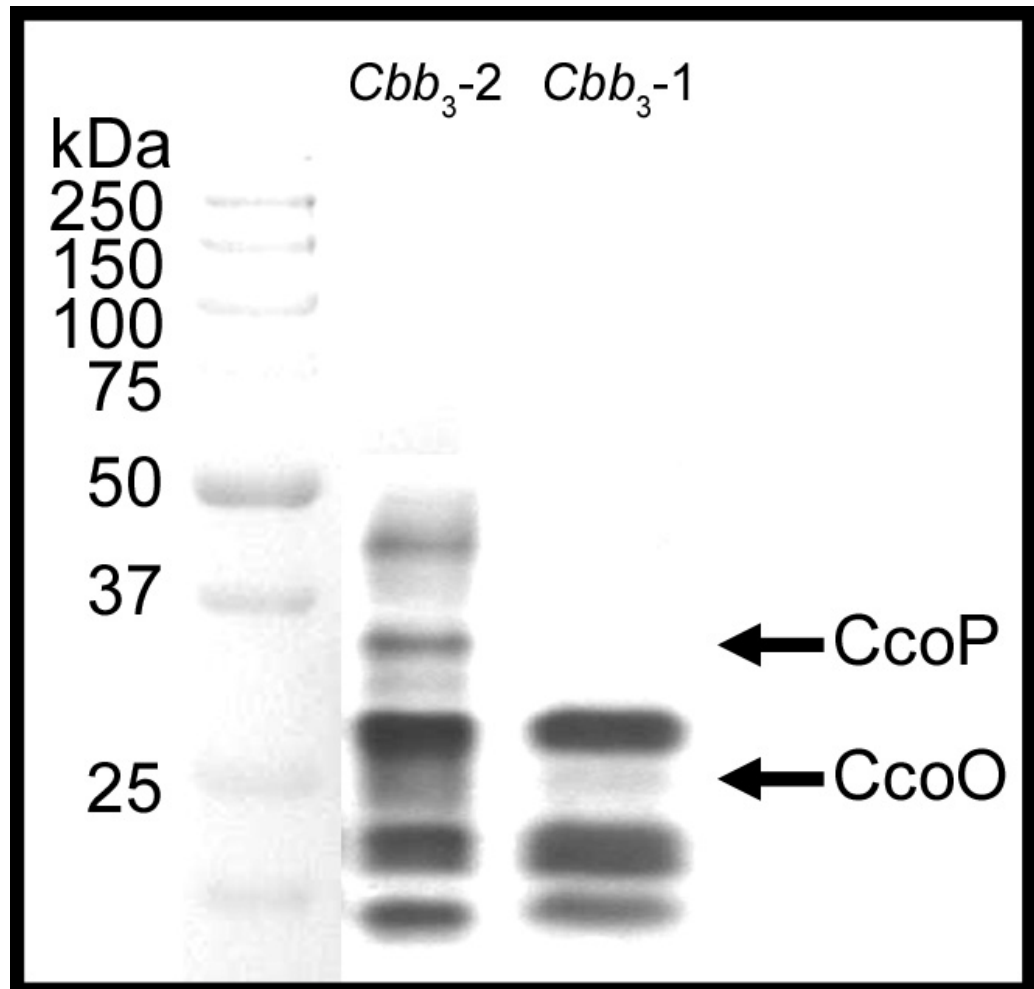


Fig. 6.2 SDS-PAGE gels of purified *cbb₃-1* and *cbb₃-2* oxidase from *P. aeruginosa*. Semi aerobically grown *cbb₃-2* and aerobically grown *cbb₃-1* were purified and the final concentrated product was subject to SDS PAGE. The gel was stained with Coomassie. The CcoQ subunit was not observed.

Cbb₃-2

The electronic absorption spectrum of fully oxidized cytochrome *cbb₃-2* isolated from semi-aerobically grown *P. aeruginosa* shows a Soret maximum of 412 nm and two broad but well defined features in the visible region between 525 nm and 550 nm (Fig. 6.3B). Upon complete reduction of *cbb₃-2* with excess dithionite, the Soret band intensified and shifted to 420 nm, with a distinct shoulder at 422 nm. These two features are characteristic of ferrous *c*-type hemes, and ferrous *b*-type heme respectively. The α and β bands in the visible region at 551 nm and 521 nm, with distinct shoulders at 559 nm and 528 nm respectively, intensify upon reduction. The 551 nm and 521 nm features are characteristic of ferrous *c*-type heme whilst the observed shoulders are characteristic of ferrous *b*-type heme. There was no evidence of a band near 600nm that would correspond to contamination with heme *a*. The UV-Visible spectroscopy of *cbb₃-1* and *cbb₃-2* are consistent with that reported for *P. stutzeri* (Pitcher *et al.* 2002).

Analysis of purified *cbb₃-1* by Coomassie stained SDS-PAGE, suggested that the CcoP subunit was lost during purification of this strain. However, analysis of the α and β bands in the UV-Visible spectrum *cbb₃-1* suggests that the ratio of *b*-type heme to *c*-type heme is 2:3 as would be expected to be observed in the *ccoNOP* complex relative to previous preparations (Pitcher *et al.* 2002; Verissimo *et al.* 2007). The same 2:3 ratio of *b*:*c* type hemes was observed in *cbb₃-2*. As discussed previously, the CcoP subunit was also lost during purification of the *cbb₃* oxidase from *P. denitrificans* (de Gier *et al.* 1996). The absence of the CcoP subunit was only recognised by close inspection of the reduced minus oxidized difference spectra compared to a previous preparation (de Gier *et al.* 1996). Loss of the CcoP subunit has not been reported during the purification of *cbb₃* oxidases isolated from other bacterial species (Pitcher *et al.* 2002; Kim *et al.* 2007; Verissimo *et al.* 2007). As shown by Coomassie stained SDS PAGE of the purified *P. aeruginosa* the CcoO-1 band was weak and it is plausible that the CcoP-1 band did not stain well. Moreover, in

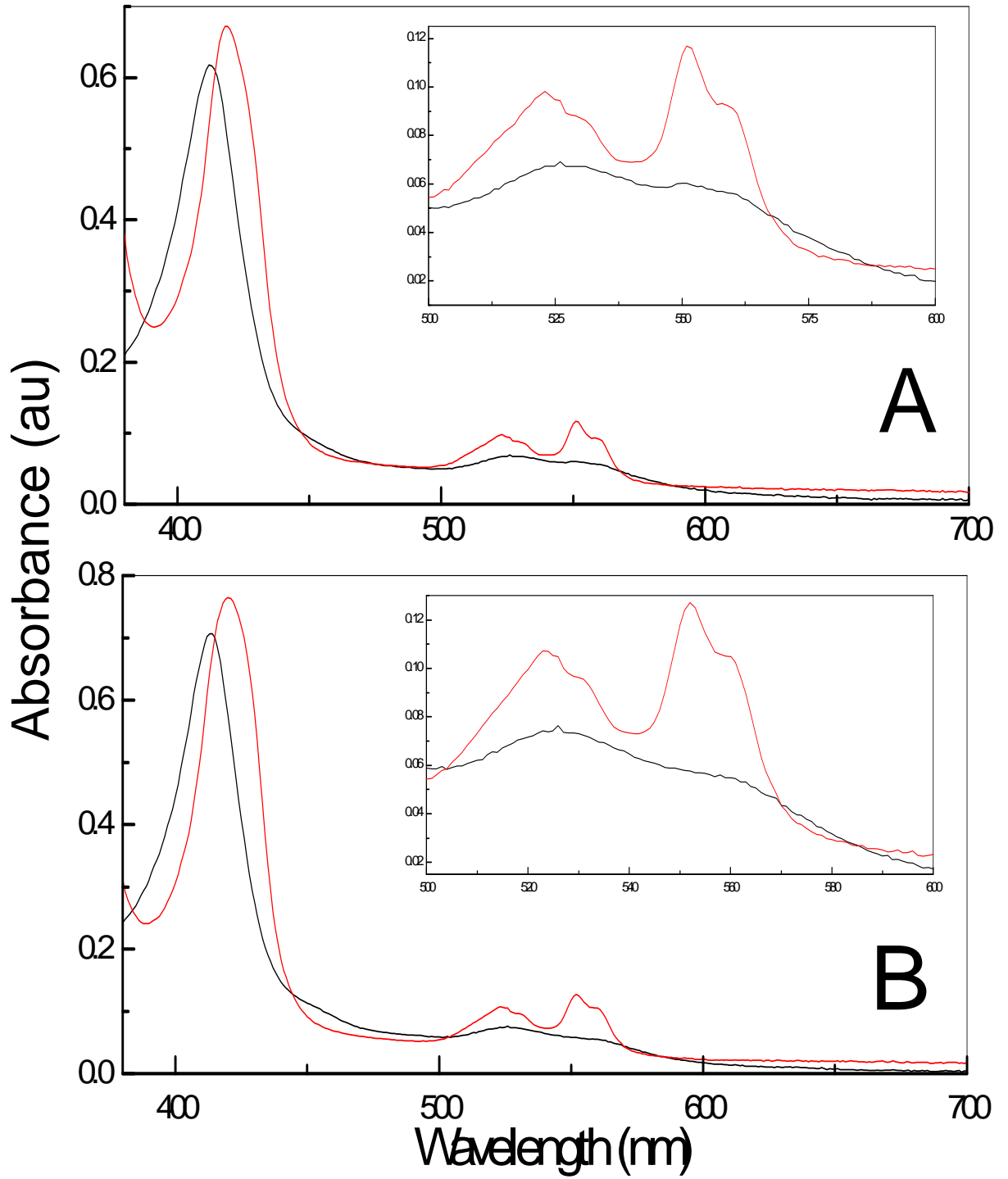
purified *R. sphaeroides* CcoP specific antibodies were used to visualise CcoP. Based on the comparable UV-visible spectra of *cbb₃-1* and *cbb₃-2* it can be surmised that the CcoP-1 subunit is present in the purified preparation of *cbb₃-1*.

The previously reported weak spectral feature at 642 nm in the preparation of *cbb₃* from *P. stutzeri* was not observed in either the preparation of *cbb₃-1* or *cbb₃-2* (Pitcher 2002). This feature was previously assigned to one of a pair of ligand to metal charge transfer bands of the high spin ferric heme *b₃*. It was not surprising however, that the feature was not observed as it was not consistently detected in *P. stutzeri* preparations (Pitcher 2002).

FIG. 6.3 UV-Visible absorption spectra of purified *P. aeruginosa cbb₃-1* (A) and *cbb₃-2* (B) isolated from aerobically grown cells and semi-aerobically grown *P. aeruginosa* cells respectively.

(A) The black trace depicts *cbb₃-1* oxidized with potassium ferricyanide (black) and fully reduced with sodium dithionite (red). A slight shift of the Soret band from 413 nm to 420 nm can be observed upon reduction of the enzyme with sodium dithionite. The inset shows a close up of the α and β regions of reduced *cbb₃-1* with peaks at 551 nm and 521 nm respectively. The spectrum was recorded at room temperature. The enzyme was in 20 mM Tris HCl, 50 μ M EDTA and 0.02% DM, pH 8.5.

(B) The black trace depicts *cbb₃-2* oxidized with potassium ferricyanide (black) and fully reduced with sodium dithionite (red). A slight shift of the Soret band from 412 nm to 420 nm can be observed upon reduction of the enzyme with sodium dithionite. The inset shows a close up of the α and β regions of reduced *cbb₃-2* with peaks at 551 nm and 521 nm respectively. The spectrum was recorded at room temperature. The enzyme was in 20 mM Tris HCl, 50 μ M EDTA and 0.02% DM, pH 8.5.



6.2.3 TMPD mediated oxygen uptake activity

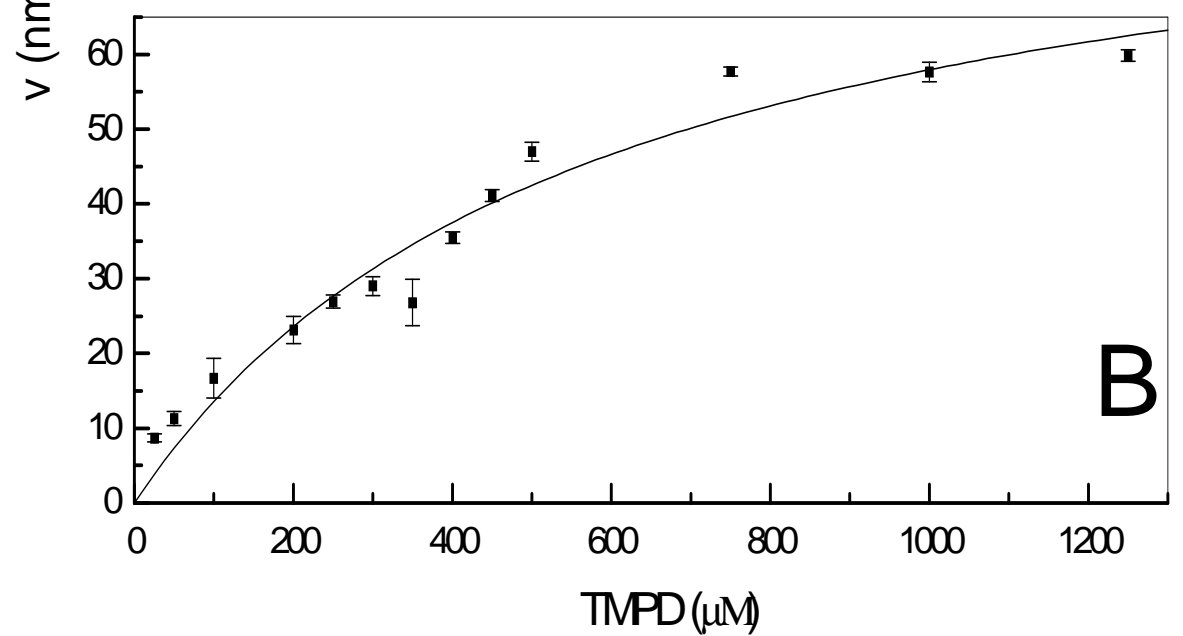
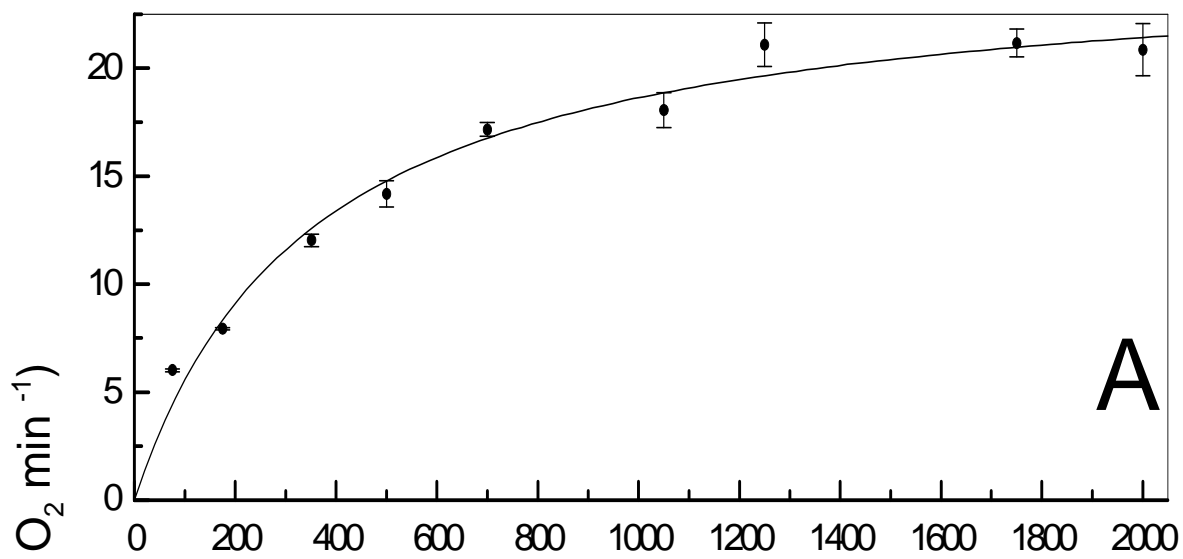
Previously oxidase activity assays were carried out using *P. aeruginosa* membranes (Chapter 5, Section 5.2.4). There were no observable differences of the oxidase activity in the *P. aeruginosa* membranes when the artificial electron donor TMPD or the physiological donors azurin and *c*₅₅₁ were used as electron mediators. The results therefore suggested that either azurin or cytochrome *c*₅₅₁ can donate electrons to the *cbb*₃ oxidases in the *P. aeruginosa* membranes.

To specifically investigate and compare the catalytic activity of the *cbb*₃-1 and *cbb*₃-2 the effect of varying substrate concentration on the oxygen consumption rate of the purified *cbb*₃-1 and *cbb*₃-2 from *P. aeruginosa* was investigated. The cytochrome *c* specific artificial electron donor, TMPD, was used to calculate the K_m and establish the methodology (Fig. 6.4). Using a Clark-type electrode, polarographic assays were carried out at a range of different concentrations of TMPD using purified *cbb*₃-1 and *cbb*₃-2. Prior to determining the K_m/V_{max} of the purified enzyme the optimal concentration of enzyme to be used was established. Optimization of this method was performed to ensure that the limiting factor in the experiment was the activity of the enzyme and not the amount of substrate available.

At each concentration of TMPD, the assay was repeated three times. The average rate and standard error of the mean are shown as squares and arrow bars respectfully (Fig. 6.4). The apparent K_m of purified *P. aeruginosa* strain *cbb*₃-1 for TMPD was estimated to be 200 μ M and the V_{max} was 18 nmol O₂ min⁻¹. The apparent K_m of *cbb*₃-2 for TMPD was estimated to be 167 μ M and the V_{max} was 40 nmol O₂ min⁻¹.

Fig. 6.4 TMPD dependent oxidase activity in purified *cbb₃-1* (A) and *cbb₃-2* (B). The graph shows the effect of varying the concentration of TMPD on the initial rate of oxygen consumption. Oxygen consumption was measured using a Clark-type platinum electrode polarized at - 0.7V with respect to a silver reference electrode. The reaction mixture (2.0 ml) comprised 20 mM Tris HCl buffer pH 7.6, 50 μ M EDTA, 100 mM NaCl, 0.02% DM, Ascorbate (4 mM), and purified protein (43 nM) were added and the reaction initiated by addition of TMPD (0-1500 μ M).

- (A) The effect of varying the concentration of TMPD on the initial rate of oxygen consumption by the purified *cbb₃-1*. The line of best fit to the Michaelis Menton equation yielded an apparent K_m value of 200 μ M and a V_{max} of 18 nmol O₂ min⁻¹.
- (B) The effect of varying the concentration of TMPD on the initial rate of oxygen consumption by the purified *P. aeruginosa cbb₃-2*. The line of best fit to the Michaelis Menton equation yielded an apparent K_m value of 167 μ M and a V_{max} of 40 nmol O₂ min⁻¹.



6.2.4 Mediated Redox Potentiometry of *Cbb*₃-1 and *Cbb*₃-2

The results presented in the chapter thus far suggest that the *P. aeruginosa cbb*₃-1 and *cbb*₃-2 purify as CcoNOP complexes that demonstrates TMPD mediated oxygen activity (Section 6.2.1 and 6.2.3). Mediated spectrophotometric redox potentiometry can be used to determine the reduction potentials of individual hemes. Studies of the thermodynamic redox behavior of oxidases can be an initial step towards understanding the mechanism of electron transfer within an oxygen reductase complex. Previously, redox titrations have been published for cytochrome *cbb*₃ oxidases isolated from *R. sphaeroides*, *R. capsulatus*, *P. stutzeri* and *B. japonicum* (García-Horsman *et al.* 1994; Gray *et al.* 1994; Pitcher 2002; Verissimo *et al.* 2007).

*Cbb*₃-1

Using the methods outlined in Section 2.8.1, spectra were collected between 500 – 700 nm at a number of redox potentials between 0 and 450 mV during reductive titrations of the *cbb*₃-1 oxidase from *P. aeruginosa*.

To determine the reduction potential of the *c*-type hemes values obtained for A₅₅₀-A₇₀₀ (*i.e.* the maximum absorbance in the visible region for reduced heme *c*, *minus* the reference absorbance) were plotted as a function of *E* (Fig. 6.5A). The best fit to the points was achieved with three *n* = 1 Nernstian components, centered at + 384 mV, + 243 mV, and + 113 mV assuming each heme contributes equally (*i.e.* 33%) to the absorbance change in the α -band maximum in the spectrum. Considering the previously speculated loss of the subunit CcoP during purification of the *cbb*₃-1 oxidase it was questionable if the best fit to the points would be effected with one *n* = 1 Nernstian component. The data points that contribute to the high redox potential species (+ 384 mV) do not show good resolution and the small absorbance change increments observed at the beginning of the mediated redox

titrations could be due to noise. The proposed loss of the CcoP subunit during purification could affect the redox properties and stability of the *cbb*₃ oxidase. However, the absorbance change of the *c*-type hemes during the mediated redox titration is consistent with the presence of three *c*-type hemes.

To determine the mediated reduction potential of the low spin *b*-type heme, values obtained for $A_{560}-A_{700}$ (*i.e.* the maximum absorbance in the visible region for reduced heme *b*, *minus* the reference absorbance) were plotted as a function of *E* (Fig. 6.5B). The best fit to the points was achieved with one $n = 1$ Nernstian component, centered at + 240 mV.

*Cbb*₃-2

Using the methods outlined in Section 2.8.1, spectra were collected between 500 – 700 nm at a number of redox potentials between 0 and 450 mV during reductive titrations of the *cbb*₃-2 oxidase from *P. aeruginosa*. To determine the reduction potential of the *c*-type hemes values obtained for $A_{550}-A_{565}$ (*i.e.* the maximum absorbance in the visible region for reduced heme *c* *minus* the absorbance at an isosbestic point) were plotted as a function of *E* (Fig. 6.6A). The best fit to the points was achieved with three independent $n = 1$ Nernstian components, centered at + 317 mV, + 245 mV, and + 186 mV assuming each heme contributes equally (*i.e.* 33%) to the absorbance change in the α -band maximum in the spectrum.

To determine the mediated reduction potential of the low spin *b*-type heme, values obtained for $A_{560}-A_{700}$ (*i.e.* the maximum absorbance in the visible region for reduced heme *b*, *minus* the reference absorbance) were plotted as a function of *E* (Fig. 6.6B). The best fit to the points was achieved with one $n = 1$ Nernstian component, centered at + 220 mV.

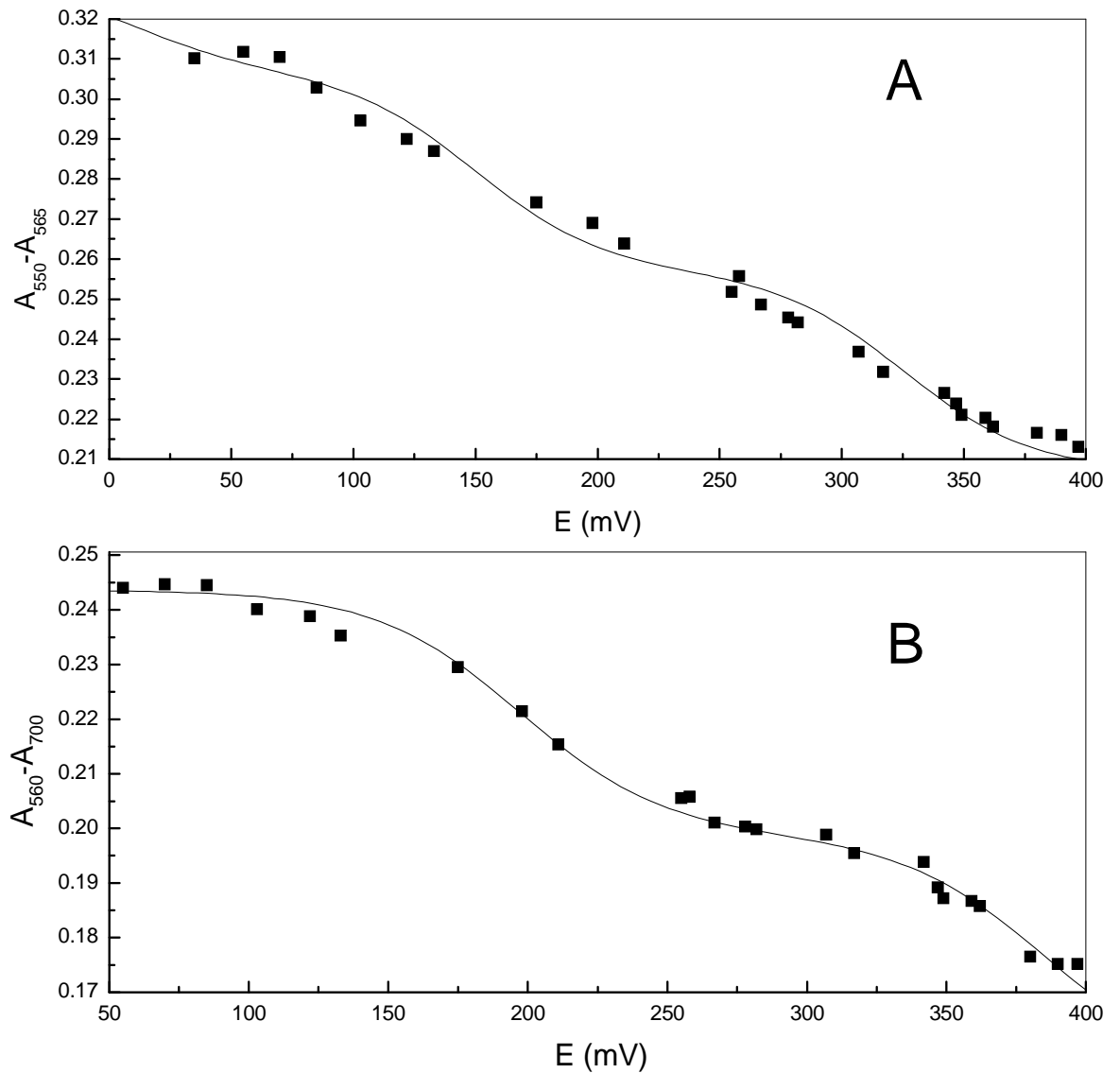


FIG. 6.5 Spectrophotometric reduction titration of *c*-type and *b*-type hemes present in *cbb₃-1*

(A) Normalised data fitted with three $n = 1$ Nernstian Curves centred at + 384 mV, + 243 mV and + 113 mV, assuming each heme contributes equally (i.e. 33%) to the absorbance change in the α -band maximum in the spectrum. r^2 value =0.9823

(B) Spectrophotometric reductive titration of low-spin *b*-type heme present in *cbb₃-1*. Normalised data fitted with a single $n = 1$ Nernstian curve centred at + 240 mV.

r^2 value =0.9891

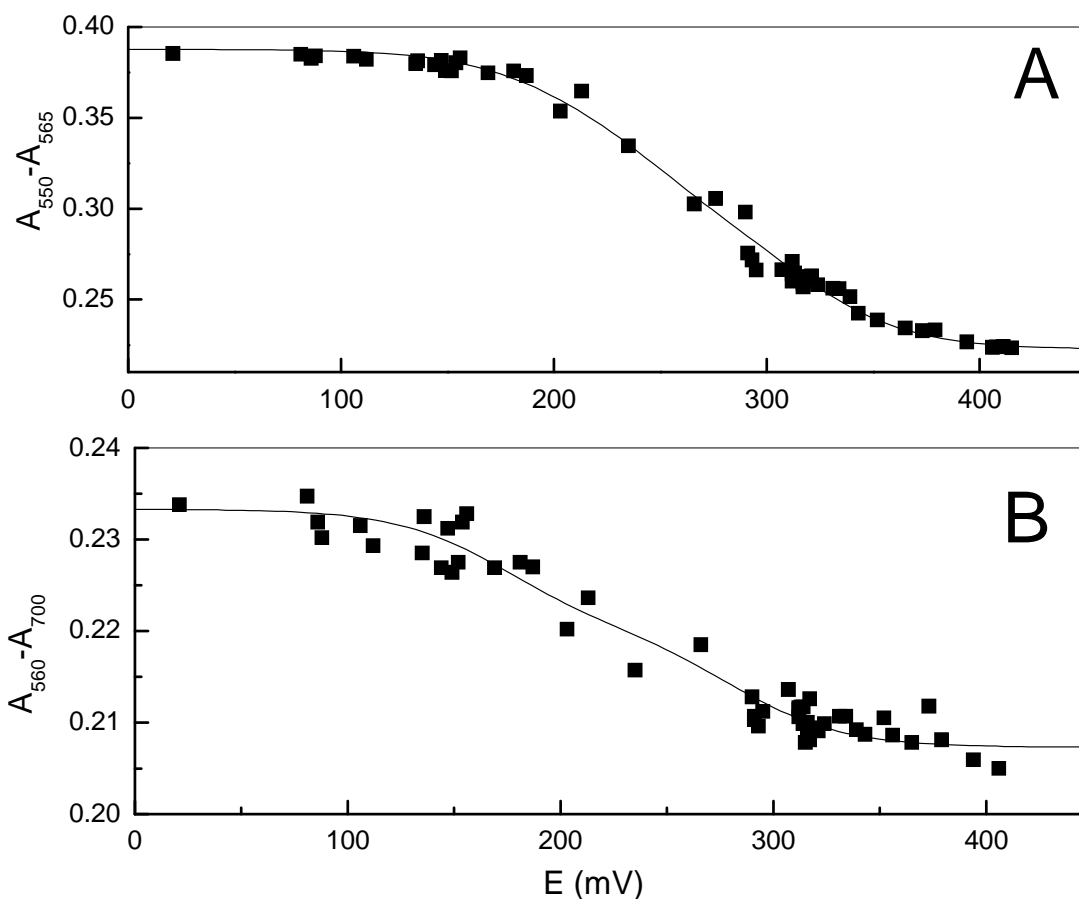


Fig. 6.6 Spectrophotometric reduction titration of *c*-type and *b*-type hemes present in *cbb*₃-2

(A) Normalised data fitted with three $n = 1$ Nernstian Curves centred at + 317 mV, + 245 mV and + 186 mV, assuming each heme contributes equally (i.e. 33%) to the absorbance change in the α -band maximum in the spectrum. r^2 value =0.9936

(B) Spectrophotometric reductive titration of the low-spin *b*-type heme present in *cbb*₃-2. Normalised data fitted with a single $n = 1$ Nernstian curve centred at + 220 mV. r^2 value =0.9561

The mediated redox potentiometry of CcoP isolated from *P. stutzeri* identified two *c*-type hemes with reduction potentials of + 185 mV and - 15 mV (Chapter 3, Section 3.2.3). These values correspond with the respective reduction potentials, + 245 mV and + 186 mV, observed in the *cbb*₃-2 oxidase isolated from *P. aeruginosa*. It is reasonable to suggest that as part of the *cbb*₃ oxidase complex, the electronic properties of the CcoP subunit are modulated by the other subunits in the complex. Assignment of the reduction potentials, + 245 mV and + 186 mV, to the two *c*-type heme in CcoP-2 assumes that the *c*-type heme in *cbb*₃-2 with a mediated reduction potential of + 317 mV in *cbb*₃-2 correspond to the *cbb*₃ subunit CcoO. The reduction potentials of the *cbb*₃-2 from *P. aeruginosa* are within the range of those reported for *P. stutzeri*, *B. japonicum* and *R. capsulatus* (Gray *et al.* 1994; Pitcher 2002; Verissimo *et al.* 2007).

The CT band centered at 642 nm has previously been attributed to the *b*₃ heme, with water as a sixth ligand (Pitcher 2002). The relatively weak contribution of a single high-spin ferric heme arising from the active site heme *b*₃ of CcoN, to the UV-visible spectrum of *cbb*₃-1 and *cbb*₃-2 is not easily deconvoluted against the background of four low spin hemes. In an attempt to determine the reduction potential of the *b*₃ heme, values obtained for $A_{642} - A_{565}$ (i.e. the disappearance of the feature at 642 nm *minus* the absorbance at an isosbestic point) were plotted as a function of *E*. The best fit to the points was obtained with a single Nernstian component centered at + 190 mV for *cbb*₃-1 and + 160 mV for *cbb*₃-2 (Figure 6.7). The redox potentials of the *b*₃ heme is somewhat lower than those calculated for *P. stutzeri* (+ 226 mV) and *B. japonicum* (+ 290 mV) (Pitcher 2002; Verissimo *et al.* 2007). However, the spacing of the potentials between heme *b* and heme *b*₃ in both *cbb*₃-2 and *cbb*₃-1 is little more than reported for the equivalent heme *a* and heme *a*₃ of bacterial *aa*₃ oxidases (Verissimo *et al.* 2008).

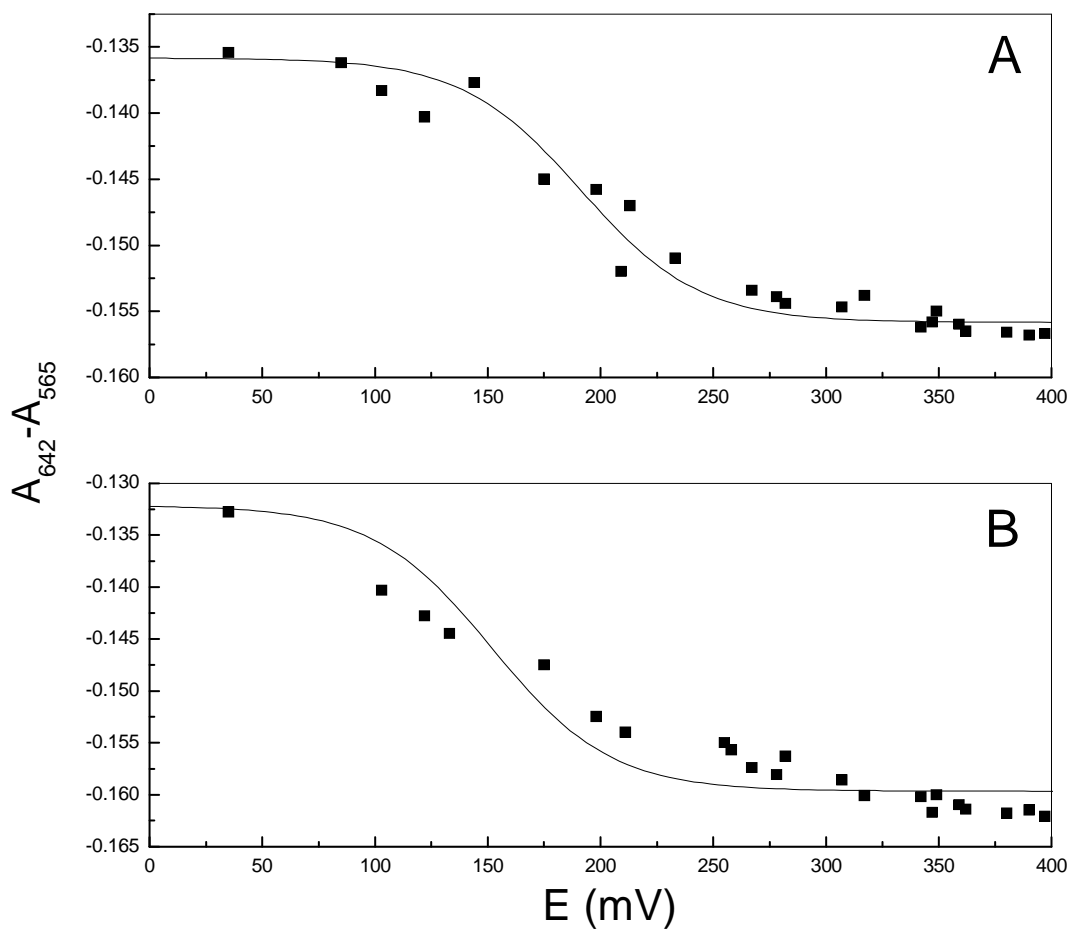


Fig. 6.7 Spectrophotometric reduction titration of transition centered at 642 nm in Cbb_3-1 (A) and Cbb_3-2 (B)

(A) Normalised data fitted with a single $n = 1$ Nernstian curve centred at + 190 mV.

r^2 value = 0.9811

(B) Normalised data fitted with a single $n = 1$ Nernstian curve centred at + 160 mV.

r^2 value = 0.9789

6.3 Conclusions

The present study, using the purified *cbb*₃ oxidases from *P. aeruginosa* represents the first spectroscopic study of the *cbb*₃ oxidases from this pathogenic bacterium. The biochemical properties of cytochrome *cbb*₃ oxidases purified from *P. aeruginosa* seem to be, unsurprisingly, similar to those reported for the *cbb*₃ oxidase isolated from *P. stutzeri*. This chapter does not however answer the question concerning how the two *cbb*₃ oxidases in *P. aeruginosa* oxidases differ with respect to their proposed distinct roles. The UV-Visible spectroscopies of *cbb*₃-1 and *cbb*₃-2 suggest the presence of five hemes in the enzymes, as previously observed in *P. stutzeri* (Pitcher *et al.* 2002). The *cbb*₃-1 and *cbb*₃-2 subunits isolated from *P. aeruginosa* have a high degree of similarity. There are limited differences in the CcoN, CcoO and CcoQ subunits of *cbb*₃-1 and *cbb*₃-2 scattered throughout the proteins but localized regions of high divergence in the CcoP subunits could define domains that are required for the differing roles of the two enzymes. Molecular dissection and further characterization of the CcoP subunit from the *cbb*₃-1 and *cbb*₃-2 could be used to investigate any differences between CcoP1 and CcoP2 and the function each one plays in the different roles of the two *cbb*₃ subunits.

7. General Discussion

The work presented in this thesis reports a molecular, biochemical and spectroscopic analysis of the cytochrome *cbb*₃ oxidase subunit, CcoP from *P. stutzeri*. The data is consistent with the CcoP subunit containing two His/His ligated *c*-type hemes, (but the residue His 42 could not be shown to be a heme ligand) one with a high reduction potential of + 188 mV and one with a low reduction potential of – 15 mV. The low potential heme binds the exogenous ligand, CO. Based on previous work it is hypothesized that the binding of an exogenous ligand is preceded by displacement of the distal histidine ligand (Pitcher *et al.* 2003). Displacement of a distal heme ligand by an exogenous ligand is an action commonly observed in heme based sensor proteins, *EcDos* and *CooA*, for example (Gilles-Gonzalez and Gonzalez 2005). As discussed previously, (Section 1.11) heme based sensors are the key regulators of adaptive responses to fluctuating levels of an exogenous ligand, oxygen, for example. These signal transducers achieve their response by coupling a regulatory heme-binding domain to a neighboring transmitter region of the same protein (Gilles-Gonzalez *et al.* 1994). As a group, heme based sensors commonly exploit histidine as a ligand. In CcoP, displacement of the distal histidine to the low potential heme and consequential binding of an exogenous ligand does not specifically define CcoP as a heme based sensor. However, if displacement of the distal histidine does not play a regulatory sensing role in the CcoP subunit, what is its function? Experimental results reported in this study have not lead to a definitive conclusion regarding the role of CcoP in *cbb*₃ oxidase but we will revisit observations previously discussed in section 1 considering the additional data gathered during this study.

The *cbb*₃ oxidases lack a redox active Cu_A electron-receiving domain in the (Section 1.4) and it is unclear how this *CcO* receives electrons from the electron donor. The high redox potential of one of the *c*-type hemes in CcoP suggests that this subunit could potentially fulfill the role as electron receiving domain in the *cbb*₃ complex. The subunit CcoO has,

however, been shown to be homologous to the electron-receiving domain in the enzyme NOR (Preisig *et al.* 1993; Cheesman *et al.* 1998; Sharma *et al.* 2006). It is therefore more favorable to suggest that electrons are passed from the electron donor to the heme *b* in the catalytic subunit, CcoN via CcoO. Moreover, the low potential of one of the *c*-type heme in CcoP is not consistent with electron transfer to CcoN. The CcoNO sub-complex isolated from *B. japonicum* is catalytically active, therefore supporting the role of CcoO as the electron-receiving domain (Zufferey *et al.* 1996). The proposed role of CcoO negates an electron receiving function for CcoP within the *cbb*₃ oxidase complex. It is therefore reasonable to suggest that CcoP plays an auxiliary role in the *cbb*₃ complex, possibly as a sensor of oxygen levels in the cell environment.

Recent completion of the *P. stutzeri* genome reveals that this γ -Proteobacterium contains a pair of *ccoNOQP* operons. The presence of an anaerobox upstream of CcoN-2 is indicative that the *P. stutzeri cbb*₃-2 is regulated by FNR under oxygen limiting conditions. The absence of an anaerobox upstream of CcoN-1 suggests that *cbb*₃-1 is regulated independently of FNR. This hypothesis is not, however, experimentally proven. The organism *E. coli* employs FNR to regulate gene expression required for anaerobic respiration but also utilizes the direct oxygen heme based sensor *EcDos* for activating signal transduction in response to environmental change. One of the distinguishing features of the *E. coli* heme sensor *EcDos* is its ability to regulate pre-existing proteins rather than trigger new gene expression (Gilles-Gonzalez and Gonzalez 2005; El-Mashtoly *et al.* 2008). In situations where oxygen scarcity is transient, it is more efficient to temporarily inhibit proteins rather than degrade proteins (El-Mashtoly *et al.* 2008). It is hypothesized that structural changes in the heme vicinity of the direct oxygen sensor *EcDos*, caused by an exogenous ligand binding to the heme, provide the initial event in the gas sensing; followed by intramolecular signal transduction from the heme to the function domain and thus having a regulatory effect (El-Mashtoly *et al.* 2008). It is proposed, that under

microaerophilic conditions CcoP functions in a similar way to a heme based oxygen sensor.

A speculative sequence of events for the passage of electrons and binding of oxygen in cytochrome *cbb*₃ oxidase has been derived based on results presented in this thesis and the current literature (Fig. 7.1). When the cell is subject to aerobic conditions, it is proposed that the *c*-type heme in CcoO, which has a high midpoint potential, accepts electrons from the electron donor (Fig. 7.1A). Internal electron transfer to heme *b*₃ and Cu_B in CcoN subsequently follows. Considering the redox potentials of the two *c*-type hemes in CcoP and the observation that the CcoNO sub complex is catalytically active, the subunit CcoP could potentially remain oxidized.

When the cell is subject to hypoxic conditions, electron turnover would decrease as reduced oxygen levels becomes a limiting factor. Decreased electron turnover in the CcoNO complex would precipitate redox cooperativity between CcoNO and CcoP and the intermolecular transfer of electrons to maintain electron flow (Fig. 7.1B). Intramolecular transfer of electrons resulting in reduction of the hemes in CcoP is possible if the hemes in the CcoN, CcoO and CcoP subunits are close. A crystal structure of the *cbb*₃ oxidase is not available; therefore, the distance between the hemes in the subunits is unknown. The rate of electron equilibration between the CcoNO complex and the CcoP subunit would be a function of the overall redox state of the enzyme.

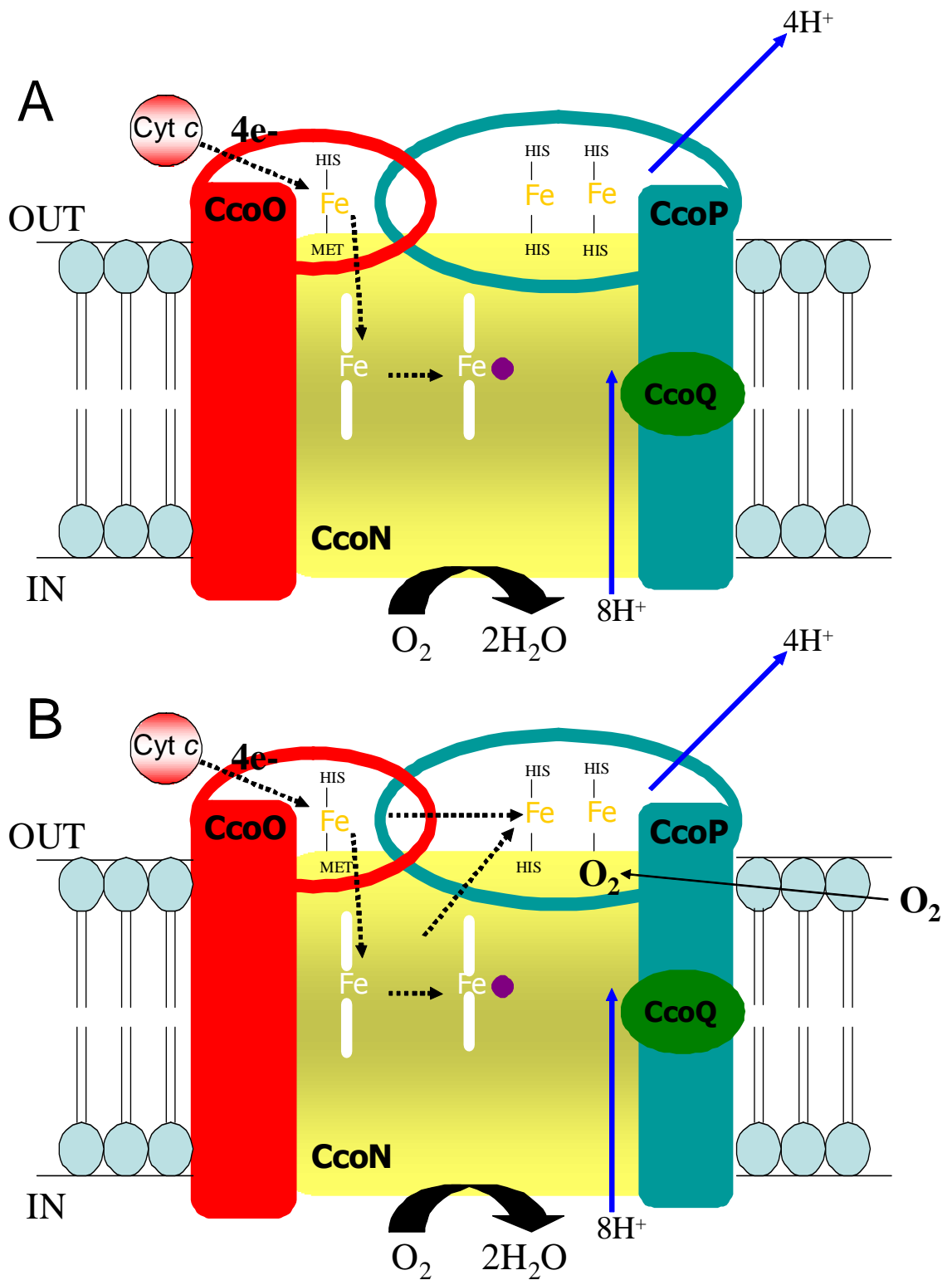


FIG. 7.1 Schematic illustrating the proposed passage of electrons in the *cbb*₃ oxidase. This cartoon illustrates the hypothetical passage of electrons (dotted lines) when the cell is under aerobic conditions (A) and hypoxic conditions (B). Under hypoxic conditions, it is proposed the CcoP subunit becomes fully reduced and that the distal histidine to the low potential heme in CcoP is displaced to bind any available O₂.

It is proposed that following full reduction of the low potential heme in CcoP the distal histidine displaces to bind available oxygen. This displacement of the distal ligand and binding of oxygen triggers a conformational change in the CcoP subunit, which concurrently triggers a response appropriate for adaptation of the cell to the prevailing environmental conditions. As previously discussed (Section 1.9), two component systems serve as a basic stimulus-response coupling mechanisms to allow organisms to sense and respond to changes in many different environmental conditions. It is proposed that the *cbb₃* oxidase is the redox sensor that controls the PrrB kinase/phosphate activities in response to changes in O₂ availability (Section 1.10) (Kim *et al.* 2007; Gomelsky *et al.* 2008). The interaction between the *cbb₃* oxidase and PrrB is unclear but it is possible that a redox linked conformational change in CcoP signals to modulate the sensory kinase/response regulator. A CcoP/sensory kinase-signaling pathway could act as a homeostatic regulator to aid fine-tuning of the respiratory system of Pseudomonads.

Reduction of the CcoP subunit by redox cooperative transfer of electrons between the *cbb₃* subunits would not be an energetically favorable reaction, and therefore would only occur if the bacterial cell were in distress, for example under hypoxic conditions to maintain function of the cell. This hypothetical sequence of events would ensure survival of the organism under hypoxic conditions. The proposed schemes are speculative based on the biochemical properties of CcoP observed during this study. Redox induced conformational changes in proteins are often small and fast making it difficult to measure and monitor. Moreover, the relative locations of the *c*-type hemes are unknown therefore, it is not clear if the hemes in CcoP and CcoO are sufficiently close to experience homotropic conditions. Crystal structures could potentially provide information regarding the reduced and oxidized forms of CcoP; however, no crystal structure of *cbb₃* oxidase is currently available. Efforts to obtain a crystal structure of the subunit CcoP are in progress (Geimeinhardt, 2006) with the hope of gaining further insight into this poorly understood

cbb₃ subunit. In CcoP, the amino acid residues around the proposed distal histidine to the low potential heme are highly conserved in all Proteobacteria. The high level of amino acid conservation is potentially important for modification of the protein following displacement of the distal ligand and subsequent binding of the exogenous ligand. Further information regarding the structure of CcoP would allude to the role of these conserved amino acids.

It remains unclear why some of Proteobacteria express two *cbb₃* oxidases, for example, *P. aeruginosa* and *P. stutzeri* but the plant pathogen *Pseudomonas syringe*, express only one *cbb₃* oxidase (Stover *et al.* 2000; Lindeberg *et al.* 2008; Yan *et al.* 2008). The expression of two oxidases may be consequential of a need for more efficient oxygen reduction complexes in the environmental conditions in which the organism thrives. This study has demonstrated that the two *cbb₃* oxidases in *P. aeruginosa* are always expressed under the tested conditions (aerobic and semi-aerobic), although the data indicates a higher level of expression of the *cbb₃-1* oxidase under aerobic conditions, and a higher level of expression of *cbb₃-2* under anaerobic conditions. Further work to characterize the CcoP subunit isolated from *cbb₃-1* and *cbb₃-2* considering the expression of the two isozymes under differing oxygen levels and the sensory roles suggested for CcoP, could be enlightening regarding the function of CcoP in the *cbb₃* oxidase. It would also be of interest to investigate any apparent differences in the ligand binding properties of CcoP from *cbb₃-1* and *cbb₃-2* reflecting on the proposal that the distal histidine to the low potential heme in CcoP is displaced to bind oxygen, as an indicator of the redox status of the cell.

In conclusion, the results presented in this thesis allude to the electron input and redox sensing strategies employed by the *cbb₃* oxidases.

8. References

- Aasa, R., T. Vänngård, (1975). "EPR signal intensity and powder shape: A reexamination." Journal of Magnetic Resonance **19**(3): 308-15.
- Abramson, J., S. Riistama, et al. (2000). "The structure of the ubiquinol oxidase from *Escherichia coli* and its ubiquinone binding site." Nat Struct Biol **7**(10): 910-7.
- Acha, S. J., I. Kuhn, et al. (2005). "Changes of viability and composition of the *Escherichia coli* flora in faecal samples during long time storage." J Microbiol Methods **63**(3): 229-38.
- Adachi, K., K. Oiwa, et al. (2007). "Coupling of rotation and catalysis in F(1)-ATPase revealed by single-molecule imaging and manipulation." Cell **130**(2): 309-21.
- Ådelroth, P., R. B. Gennis, et al. (1998). "Role of the pathway through K(I-362) in proton transfer in cytochrome c oxidase from *R. sphaeroides*." Biochemistry **37**(8): 2470-6.
- Almeida, M. G., S. Macieira, et al. (2003). "The isolation and characterization of cytochrome c nitrite reductase subunits (NrfA and NrfH) from *Desulfovibrio desulfuricans* ATCC 27774. Re-evaluation of the spectroscopic data and redox properties." Eur J Biochem **270**(19): 3904-15.
- Alvarez-Ortega, C. and C. S. Harwood (2007). "Responses of *Pseudomonas aeruginosa* to low oxygen indicate that growth in the cystic fibrosis lung is by aerobic respiration." Mol Microbiol **65**(1): 153-65.
- Antonini, E., Brunori, M., (1971). Hemoglobin and Myoglobin in their Reactions with Ligands, North Holland Publishing Company.
- Anzai, Y., H. Kim, et al. (2000). "Phylogenetic affiliation of the pseudomonads based on 16S rRNA sequence." Int J Syst Evol Microbiol **50 Pt 4**: 1563-89.
- Arai, H., T. Kodama, et al. (1997). "Cascade regulation of the two CRP/FNR-related transcriptional regulators (ANR and DNR) and the denitrification enzymes in *Pseudomonas aeruginosa*." Mol Microbiol **25**(6): 1141-8.
- Arredondo-Peter, R., M. S. Hargrove, et al. (1998). "Plant hemoglobins." Plant Physiol **118**(4): 1121-5.
- Arslan, E., A. Kannt, et al. (2000). "The symbiotically essential cbb(3)-type oxidase of *Bradyrhizobium japonicum* is a proton pump." FEBS Lett **470**(1): 7-10.
- Arslan, E., H. Schulz, et al. (1998). "Overproduction of the *Bradyrhizobium japonicum* c-type cytochrome subunits of the cbb3 oxidase in *Escherichia coli*." Biochem Biophys Res Commun **251**(3): 744-7.
- Babcock, G. T., L. E. Vickery, et al. (1976). "Electronic state of heme in cytochrome oxidase. I. Magnetic circular dichroism of the isolated enzyme and its derivatives." J Biol Chem **251**(24): 7907-19.
- Badrick, A. C., A. J. Hamilton, et al. (2007). "PrrC, a Sco homologue from *Rhodobacter sphaeroides*, possesses thiol-disulfide oxidoreductase activity." FEBS Lett **581**(24): 4663-7.
- Baker, S. C., S. J. Ferguson, et al. (1998). "Molecular genetics of the genus *Paracoccus*: metabolically versatile bacteria with bioenergetic flexibility." Microbiol Mol Biol Rev **62**(4): 1046-78.
- Bamford, V. A., H. C. Angove, et al. (2002). "Structure and spectroscopy of the periplasmic cytochrome c nitrite reductase from *Escherichia coli*." Biochemistry **41**(9): 2921-31.
- Barber, D., S. R. Parr, et al. (1976). "Some spectral and steady-state kinetic properties of *Pseudomonas* cytochrome oxidase." Biochem J **157**(2): 431-8.
- Betts, M., J., Russell R., B., (2003). Amino acid properties and consequences of substitutions. Bioinformatics for Geneticists. M. Barnes, R., Gray, I., C., Wiley.
- Bhairi, S. M. (2001). Detergents: A guide to the properties and uses of detergents in biological systems.

- Blumer, C. and D. Haas (2000). "Mechanism, regulation, and ecological role of bacterial cyanide biosynthesis." Arch Microbiol **173**(3): 170-7.
- Bordo, D. and P. Argos (1991). "Suggestions for "safe" residue substitutions in site-directed mutagenesis." J Mol Biol **217**(4): 721-9.
- Bott, M., D. Ritz, et al. (1991). "The Bradyrhizobium japonicum cycM gene encodes a membrane-anchored homolog of mitochondrial cytochrome c." J Bacteriol **173**(21): 6766-72.
- Boyer, P. D. (2002). "A research journey with ATP synthase." J Biol Chem **277**(42): 39045-61.
- Brown, S., A. J. Moody, et al. (1993). "Binuclear centre structure of terminal protonmotive oxidases." FEBS Lett **316**(3): 216-23.
- Brzezinski, P. and P. Adelroth (2006). "Design principles of proton-pumping haem-copper oxidases." Curr Opin Struct Biol **16**(4): 465-72.
- Buse, G., T. Soulimane, et al. (1999). "Evidence for a copper-coordinated histidine-tyrosine cross-link in the active site of cytochrome oxidase." Protein Sci **8**(5): 985-90.
- Butland, G., S. Spiro, et al. (2001). "Two conserved glutamates in the bacterial nitric oxide reductase are essential for activity but not assembly of the enzyme." J Bacteriol **183**(1): 189-99.
- Carterson, A. J., L. A. Morici, et al. (2004). "The transcriptional regulator AlgR controls cyanide production in Pseudomonas aeruginosa." J Bacteriol **186**(20): 6837-44.
- Castresana, J., M. Lubben, et al. (1994). "Evolution of cytochrome oxidase, an enzyme older than atmospheric oxygen." Embo J **13**(11): 2516-25.
- Cheesman, M., R., (2006) Personal Communication
- Cheesman, M., R., (2008) Personal Communication.
- Cheesman, M. R., P. J. Little, et al. (2001). "Novel heme ligation in a c-type cytochrome involved in thiosulfate oxidation: EPR and MCD of SoxAX from Rhodovulum sulfidophilum." Biochemistry **40**(35): 10562-9.
- Cheesman, M. R., W. G. Zumft, et al. (1998). "The MCD and EPR of the heme centers of nitric oxide reductase from Pseudomonas stutzeri: evidence that the enzyme is structurally related to the heme-copper oxidases." Biochemistry **37**(11): 3994-4000.
- Chepuri, V., L. Lemieux, et al. (1990). "The sequence of the cyo operon indicates substantial structural similarities between the cytochrome o ubiquinol oxidase of Escherichia coli and the aa3-type family of cytochrome c oxidases." J Biol Chem **265**(19): 11185-92.
- Clarke, P., H., Ornston, L., N., (1975). Metabolic Pathways and Regulation, Part I. Genetics and Biochemistry of Pseudomonas. P. Clarke, H., Richmond, M., H., John Wiley and Sons.
- Columbus, L., J. Lipfert, et al. (2006). "Expression, purification, and characterization of Thermotoga maritima membrane proteins for structure determination." Protein Sci **15**(5): 961-75.
- Comolli, J. C. and T. J. Donohue (2002). "Pseudomonas aeruginosa RoxR, a response regulator related to Rhodobacter sphaeroides PrrA, activates expression of the cyanide-insensitive terminal oxidase." Mol Microbiol **45**(3): 755-68.
- Comolli, J. C. and T. J. Donohue (2004). "Differences in two Pseudomonas aeruginosa cbb3 cytochrome oxidases." Mol Microbiol **51**(4): 1193-203.
- Cooper, M., G. R. Tavankar, et al. (2003). "Regulation of expression of the cyanide-insensitive terminal oxidase in Pseudomonas aeruginosa." Microbiology **149**(Pt 5): 1275-84.
- Cosseau, C. and J. Batut (2004). "Genomics of the ccoNOQP-encoded cbb3 oxidase complex in bacteria." Arch Microbiol **181**(2): 89-96.

- Cottet, S., I. Corthesy-Theulaz, et al. (2002). "Microaerophilic conditions permit to mimic in vitro events occurring during in vivo *Helicobacter pylori* infection and to identify Rho/Ras-associated proteins in cellular signaling." *J Biol Chem* **277**(37): 33978-86.
- Crack, J. C., J. Green, et al. (2007). "Superoxide-mediated amplification of the oxygen-induced switch from [4Fe-4S] to [2Fe-2S] clusters in the transcriptional regulator FNR." *Proc Natl Acad Sci U S A* **104**(7): 2092-7.
- Crack, J. C., J. Green, et al. (2006). "Detection of sulfide release from the oxygen-sensing [4Fe-4S] cluster of FNR." *J Biol Chem* **281**(28): 18909-13.
- Crofts, A. R., S. Lhee, et al. (2006). "Proton pumping in the bc1 complex: a new gating mechanism that prevents short circuits." *Biochim Biophys Acta* **1757**(8): 1019-34.
- Cunningham, L., M. Pitt, et al. (1997). "The *cioAB* genes from *Pseudomonas aeruginosa* code for a novel cyanide-insensitive terminal oxidase related to the cytochrome bd quinol oxidases." *Mol Microbiol* **24**(3): 579-91.
- Cunningham, L. and H. D. Williams (1995). "Isolation and characterization of mutants defective in the cyanide-insensitive respiratory pathway of *Pseudomonas aeruginosa*." *J Bacteriol* **177**(2): 432-8.
- de Gier, J. W., M. Lubben, et al. (1994). "The terminal oxidases of *Paracoccus denitrificans*." *Mol Microbiol* **13**(2): 183-96.
- de Gier, J. W., M. Schepper, et al. (1996). "Structural and functional analysis of *aa3*-type and *cbb3*-type cytochrome c oxidases of *Paracoccus denitrificans* reveals significant differences in proton-pump design." *Mol Microbiol* **20**(6): 1247-60.
- de Reuse, H. and S. Bereswill (2007). "Ten years after the first *Helicobacter pylori* genome: comparative and functional genomics provide new insights in the variability and adaptability of a persistent pathogen." *FEMS Immunol Med Microbiol* **50**(2): 165-76.
- Delgado-Nixon, V. M., G. Gonzalez, et al. (2000). "Dos, a heme-binding PAS protein from *Escherichia coli*, is a direct oxygen sensor." *Biochemistry* **39**(10): 2685-91.
- Dinwiddie, R. (2000). "Pathogenesis of lung disease in cystic fibrosis." *Respiration* **67**(1): 3-8.
- D'Mello, R., S. Hill, et al. (1995). "The oxygen affinity of cytochrome bo' in *Escherichia coli* determined by the deoxygenation of oxyleghemoglobin and oxymyoglobin: Km values for oxygen are in the submicromolar range." *J Bacteriol* **177**(3): 867-70.
- Dos Santos, V. A., S. Heim, et al. (2004). "Insights into the genomic basis of niche specificity of *Pseudomonas putida* KT2440." *Environ Microbiol* **6**(12): 1264-86.
- Driscoll, J. A., S. L. Brody, et al. (2007). "The epidemiology, pathogenesis and treatment of *Pseudomonas aeruginosa* infections." *Drugs* **67**(3): 351-68.
- Duncan, T. M., V. V. Bulygin, et al. (1995). "Rotation of subunits during catalysis by *Escherichia coli* F1-ATPase." *Proc Natl Acad Sci U S A* **92**(24): 10964-8.
- Dutta, R., L. Qin, et al. (1999). "Histidine kinases: diversity of domain organization." *Mol Microbiol* **34**(4): 633-40.
- Dutton, P. L. (1978). "Redox potentiometry: determination of midpoint potentials of oxidation-reduction components of biological electron-transfer systems." *Methods Enzymol* **54**: 411-35.
- Echalier, A., T. Brittain, et al. (2008). "Redox-linked structural changes associated with the formation of a catalytically competent form of the diheme cytochrome c peroxidase from *Pseudomonas aeruginosa*." *Biochemistry* **47**(7): 1947-56.
- El-Mashtoly, S. F., S. Nakashima, et al. (2008). "Roles of Arg-97 and Phe-113 in regulation of distal ligand binding to heme in the sensor domain of Ec DOS protein. Resonance Raman and mutation study." *J Biol Chem* **283**(27): 19000-10.
- Eraso, J. M. and S. Kaplan (1994). "prrA, a putative response regulator involved in oxygen regulation of photosynthesis gene expression in *Rhodobacter sphaeroides*." *J Bacteriol* **176**(1): 32-43.

- Eraso, J. M. and S. Kaplan (2000). "From redox flow to gene regulation: role of the PrrC protein of *Rhodobacter sphaeroides* 2.4.1." Biochemistry **39**(8): 2052-62.
- Farver, O., H. J. Hwang, et al. (2007). "Reorganization energy of the CuA center in purple azurin: impact of the mixed valence-to-trapped valence state transition." J Phys Chem B **111**(24): 6690-4.
- Fischer, H. M., L. Velasco, et al. (2001). "One of two hemN genes in *Bradyrhizobium japonicum* is functional during anaerobic growth and in symbiosis." J Bacteriol **183**(4): 1300-11.
- Foster, D. L. and R. H. Fillingame (1982). "Stoichiometry of subunits in the H⁺-ATPase complex of *Escherichia coli*." J Biol Chem **257**(4): 2009-15.
- Fu, H. A., S. Iuchi, et al. (1991). "The requirement of ArcA and Fnr for peak expression of the *cyd* operon in *Escherichia coli* under microaerobic conditions." Mol Gen Genet **226**(1-2): 209-13.
- Gabel, C. and R. J. Maier (1993). "Oxygen-dependent transcriptional regulation of cytochrome aa3 in *Bradyrhizobium japonicum*." J Bacteriol **175**(1): 128-32.
- Gall, B. and H. Scheer (1998). "Stabilization of photosystem II reaction centers: influence of bile salt detergents and low pH." FEBS Lett **431**(2): 161-6.
- Garbers, D. L. and D. G. Lowe (1994). "Guanylyl cyclase receptors." J Biol Chem **269**(49): 30741-4.
- García-Horsman, J. A., B. Barquera, et al. (1994). "The superfamily of heme-copper respiratory oxidases." J Bacteriol **176**(18): 5587-600.
- García-Horsman, J. A., E. Berry, et al. (1994). "A novel cytochrome c oxidase from *Rhodobacter sphaeroides* that lacks CuA." Biochemistry **33**(10): 3113-9.
- Geimeinhardt, S. (2006). Personal Communication.
- Gilles-Gonzalez, M. A., G. S. Ditta, et al. (1991). "A haemoprotein with kinase activity encoded by the oxygen sensor of *Rhizobium meliloti*." Nature **350**(6314): 170-2.
- Gilles-Gonzalez, M. A. and G. Gonzalez (2005). "Heme-based sensors: defining characteristics, recent developments, and regulatory hypotheses." J Inorg Biochem **99**(1): 1-22.
- Gilles-Gonzalez, M. A., G. Gonzalez, et al. (1994). "Heme-based sensors, exemplified by the kinase FixL, are a new class of heme protein with distinctive ligand binding and autoxidation." Biochemistry **33**(26): 8067-73.
- Gohlke, U., A. Warne, et al. (1997). "Projection structure of the cytochrome bo ubiquinol oxidase from *Escherichia coli* at 6 Å resolution." Embo J **16**(6): 1181-8.
- Gomelsky, L., O. V. Moskvina, et al. (2008). "Hierarchical regulation of photosynthesis gene expression by the oxygen-responsive PrrBA and AppA-PpsR systems of *Rhodobacter sphaeroides*." J Bacteriol **190**(24): 8106-14.
- Gomes, C. M., C. Backgren, et al. (2001). "Heme-copper oxidases with modified D- and K-pathways are yet efficient proton pumps." FEBS Lett **497**(2-3): 159-64.
- Gonzalez, G., E. M. Dioum, et al. (2002). "Nature of the displaceable heme-axial residue in the EcDos protein, a heme-based sensor from *Escherichia coli*." Biochemistry **41**(26): 8414-21.
- Good, N. E., G. D. Winget, et al. (1966). "Hydrogen ion buffers for biological research." Biochemistry **5**(2): 467-77.
- Goodhew, C. F., Brown, K.R., Pettigrew, G.W., (1986). "Heme staining in gels. a useful tool in the study of bacterial c-type cytochromes." Biochim Biophys Acta **852**: 288-94.
- Govan, J. R. W. (1997). Pseudomonads and non-fermenters. Medical Microbiology. R. S. D. Greenwood, J. Peutherer, Churchill Livingstone.
- Gray, K. A., M. Grooms, et al. (1994). "*Rhodobacter capsulatus* contains a novel cb-type cytochrome c oxidase without a CuA center." Biochemistry **33**(10): 3120-7.
- Hargrove, M. S. (2000). "A flash photolysis method to characterize hexacoordinate hemoglobin kinetics." Biophys J **79**(5): 2733-8.

- Hebelstrup, K. H., A. U. Igamberdiev, et al. (2007). "Metabolic effects of hemoglobin gene expression in plants." *Gene* **398**(1-2): 86-93.
- Hemp, J., C. Christian, et al. (2005). "Helix switching of a key active-site residue in the cytochrome cbb3 oxidases." *Biochemistry* **44**(32): 10766-75.
- Hemp, J., H. Han, et al. (2007). "Comparative Genomics and Site-Directed Mutagenesis Support the Existence of Only One Input Channel for Protons in the C-Family (cbb(3) Oxidase) of Heme-Copper Oxygen Reductases." *Biochemistry*.
- Hendler, R. W. and G. S. Sidhu (1988). "A new high potential redox transition for cytochrome aa3." *Biophys J* **54**(1): 121-33.
- Hendler, R. W. and H. V. Westerhoff (1992). "Redox interactions in cytochrome c oxidase: from the "neoclassical" toward "modern" models." *Biophys J* **63**(6): 1586-604.
- Holm, L., M. Saraste, et al. (1987). "Structural models of the redox centres in cytochrome oxidase." *Embo J* **6**(9): 2819-23.
- Horio, T., T. Higashi, et al. (1961). "Purification and properties of cytochrome oxidase from *Pseudomonas aeruginosa*." *J Biol Chem* **236**: 944-51.
- Hwang, H. J. and Y. Lu (2004). "pH-dependent transition between delocalized and trapped valence states of a CuA center and its possible role in proton-coupled electron transfer." *Proc Natl Acad Sci U S A* **101**(35): 12842-7.
- Ibrahim, M., R. L. Kerby, et al. (2006). "Heme displacement mechanism of CooA activation: mutational and Raman spectroscopic evidence." *J Biol Chem* **281**(39): 29165-73.
- Iwata, S., C. Ostermeier, et al. (1995). "Structure at 2.8 Å resolution of cytochrome c oxidase from *Paracoccus denitrificans*." *Nature* **376**(6542): 660-9.
- Jackson, R. J., K. T. Elvers, et al. (2006). "Oxygen reactivity of both respiratory oxidases in *Campylobacter jejuni*: the "cydAB" genes encode a cyanide-resistant, low-affinity oxidase that is not of the cytochrome bd-type." *J Bacteriol.* **189**; 1604-15
- Junemann, S. (1997). "Cytochrome bd terminal oxidase." *Biochim Biophys Acta* **1321**(2): 107-27.
- Junemann, S. and J. M. Wrigglesworth (1995). "Cytochrome bd oxidase from *Azotobacter vinelandii*. Purification and quantitation of ligand binding to the oxygen reduction site." *J Biol Chem* **270**(27): 16213-20.
- Kahn, D., M. David, et al. (1989). "Rhizobium meliloti fixGHI sequence predicts involvement of a specific cation pump in symbiotic nitrogen fixation." *J Bacteriol* **171**(2): 929-39.
- Kamen, M. D., T. Kakuno, et al. (1973). "Spin-state correlations in near infrared spectroscopy of cytochrome c'." *Proc Natl Acad Sci U S A* **70**(6): 1851-4.
- Kayalar, C., J. Rosing, et al. (1977). "An alternating site sequence for oxidative phosphorylation suggested by measurement of substrate binding patterns and exchange reaction inhibitions." *J Biol Chem* **252**(8): 2486-91.
- Khoroshilova, N., H. Beinert, et al. (1995). "Association of a polynuclear iron-sulfur center with a mutant FNR protein enhances DNA binding." *Proc Natl Acad Sci U S A* **92**(7): 2499-503.
- Khoroshilova, N., C. Popescu, et al. (1997). "Iron-sulfur cluster disassembly in the FNR protein of *Escherichia coli* by O₂: [4Fe-4S] to [2Fe-2S] conversion with loss of biological activity." *Proc Natl Acad Sci U S A* **94**(12): 6087-92.
- Kim, Y. J., I. J. Ko, et al. (2007). "Dominant role of the cbb3 oxidase in regulation of photosynthesis gene expression through the PrrBA system in *Rhodobacter sphaeroides* 2.4.1." *J Bacteriol* **189**(15): 5617-25.
- Kirisits, M. J. and M. R. Parsek (2006). "Does *Pseudomonas aeruginosa* use intercellular signalling to build biofilm communities?" *Cell Microbiol* **8**(12): 1841-9.
- Kirk, M. L. and K. Peariso (2003). "Recent applications of MCD spectroscopy to metalloenzymes." *Curr Opin Chem Biol* **7**(2): 220-7.

- Kita, K., K. Konishi, et al. (1984). "Terminal oxidases of *Escherichia coli* aerobic respiratory chain. II. Purification and properties of cytochrome b558-d complex from cells grown with limited oxygen and evidence of branched electron-carrying systems." J Biol Chem **259**(5): 3375-81.
- Kita, K., K. Konishi, et al. (1986). "Purification and properties of two terminal oxidase complexes of *Escherichia coli* aerobic respiratory chain." Methods Enzymol **126**: 94-113.
- Koch, H. G., C. Winterstein, et al. (2000). "Roles of the ccoGHIS gene products in the biogenesis of the cbb(3)-type cytochrome c oxidase." J Mol Biol **297**(1): 49-65.
- Krogh, A., B. Larsson, et al. (2001). "Predicting transmembrane protein topology with a hidden Markov model: application to complete genomes." J Mol Biol **305**(3): 567-80.
- Kulajta, C., J. O. Thumfart, et al. (2006). "Multi-step assembly pathway of the cbb3-type cytochrome c oxidase complex." J Mol Biol **355**(5): 989-1004.
- Lalucat, J., A. Bennasar, et al. (2006). "Biology of *Pseudomonas stutzeri*." Microbiol Mol Biol Rev **70**(2): 510-47.
- Li, X. Z., D. Ma, et al. (1994). "Role of efflux pump(s) in intrinsic resistance of *Pseudomonas aeruginosa*: active efflux as a contributing factor to beta-lactam resistance." Antimicrob Agents Chemother **38**(8): 1742-52.
- Lindeberg, M., C. R. Myers, et al. (2008). "Roadmap to new virulence determinants in *Pseudomonas syringae*: insights from comparative genomics and genome organization." Mol Plant Microbe Interact **21**(6): 685-700.
- Liu, M. C., W. J. Payne, et al. (1983). "Comparison of cytochromes from anaerobically and aerobically grown cells of *Pseudomonas perfectomarinus*." J Bacteriol **154**(1): 278-86.
- Ludwig, B. and G. Schatz (1980). "A two-subunit cytochrome c oxidase (cytochrome aa3) from *Paracoccus denitrificans*." Proc Natl Acad Sci U S A **77**(1): 196-200.
- Lund, S., S. Orłowski, et al. (1989). "Detergent structure and associated lipid as determinants in the stabilization of solubilized Ca²⁺-ATPase from sarcoplasmic reticulum." J Biol Chem **264**(9): 4907-15.
- Malatesta, F., F. Nicoletti, et al. (1998). "Electron entry in a CuA mutant of cytochrome c oxidase from *Paracoccus denitrificans*. Conclusive evidence on the initial electron entry metal center." FEBS Lett **434**(3): 322-4.
- Mandon, K., P. A. Kaminski, et al. (1993). "Role of the fixGHI region of *Azorhizobium caulinodans* in free-living and symbiotic nitrogen fixation." FEMS Microbiol Lett **114**(2): 185-9.
- Marchal, K., J. Sun, et al. (1998). "A cytochrome cbb3 (cytochrome c) terminal oxidase in *Azospirillum brasilense* Sp7 supports microaerobic growth." J Bacteriol **180**(21): 5689-96.
- Marina, A., C. D. Waldburger, et al. (2005). "Structure of the entire cytoplasmic portion of a sensor histidine-kinase protein." Embo J **24**(24): 4247-59.
- Mascher, T., J. D. Helmann, et al. (2006). "Stimulus perception in bacterial signal-transducing histidine kinases." Microbiol Mol Biol Rev **70**(4): 910-38.
- Matsui, H., V. E. Wagner, et al. (2006). "A physical linkage between cystic fibrosis airway surface dehydration and *Pseudomonas aeruginosa* biofilms." Proc Natl Acad Sci U S A **103**(48): 18131-6.
- Matsushita, K., M. Yamada, et al. (1980). "Membrane-bound respiratory chain of *Pseudomonas aeruginosa* grown aerobically." J Bacteriol **141**(1): 389-92.
- Mauk, A., G., Moore, G., R., (1997). "Control of metalloprotein redox potentials: what does site-directed mutagenesis of heme proteins tell us?" Journal of Biological and Inorganic Chemistry **2**: 119-125.

- McPherson, A., S. Koszelak, et al. (1986). "An experiment regarding crystallization of soluble proteins in the presence of beta-octyl glucoside." J Biol Chem **261**(4): 1969-75.
- Meadow, P. (1975). Wall and Membrane Structures in the Genus Pseudomonas. Genetics and Biochemistry of Pseudomonas. P. Clarke, H., Richmond, M., H., John Wiley and Sons.
- Mitchell, P. (1975). "Protonmotive redox mechanism of the cytochrome b-c1 complex in the respiratory chain: protonmotive ubiquinone cycle." FEBS Lett **56**(1): 1-6.
- Moore, G. R., G. W. Pettigrew, et al. (1986). "Factors influencing redox potentials of electron transfer proteins." Proc Natl Acad Sci U S A **83**(14): 4998-9.
- Moore, G. R., Pettigrew, G.W., (1990). Cytochromes c: Evolutionary, Structural and Physiochemical Aspects, Springer-Verlag.
- Moore, L. J., E. L. Mettert, et al. (2006). "Regulation of FNR dimerization by subunit charge repulsion." J Biol Chem **281**(44): 33268-75.
- Morales, G., A. Ugidos, et al. (2006). "Inactivation of the *Pseudomonas putida* cytochrome o ubiquinol oxidase leads to a significant change in the transcriptome and to increased expression of the CIO and *cbb3-1* terminal oxidases." Environ Microbiol **8**(10): 1764-74.
- More, C., V. Belle, et al. (1999). "EPR spectroscopy: a powerful technique for the structural and functional investigation of metalloproteins." Biospectroscopy **5**(5 Suppl): S3-18.
- Musser, S. M., M. H. Stowell, et al. (1993). "Comparison of ubiquinol and cytochrome c terminal oxidases. An alternative view." FEBS Lett **327**(2): 131-6.
- Nelson, K. E., C. Weinel, et al. (2002). "Complete genome sequence and comparative analysis of the metabolically versatile *Pseudomonas putida* KT2440." Environ Microbiol **4**(12): 799-808.
- Neidle, E. L. and S. Kaplan (1992). "Rhodobacter sphaeroides *rdxA*, a homolog of *Rhizobium meliloti* *fixG*, encodes a membrane protein which may bind cytoplasmic [4Fe-4S] clusters." J Bacteriol **174**(20): 6444-54.
- Nicholls, D., G., Ferguson, S., J., (2002). Bioenergetics **3**, Academic Press.
- Nyquist, R. M., D. Heitbrink, et al. (2003). "Direct observation of protonation reactions during the catalytic cycle of cytochrome c oxidase." Proc Natl Acad Sci U S A **100**(15): 8715-20.
- O'Gara, J. P., J. M. Eraso, et al. (1998). "A redox-responsive pathway for aerobic regulation of photosynthesis gene expression in *Rhodobacter sphaeroides* 2.4.1." J Bacteriol **180**(16): 4044-50.
- Oh, J. I. (2006). "Effect of mutations of five conserved histidine residues in the catalytic subunit of the *cbb3* cytochrome c oxidase on its function." J Microbiol **44**(3): 284-92.
- Oh, J. I., J. M. Eraso, et al. (2000). "Interacting regulatory circuits involved in orderly control of photosynthesis gene expression in *Rhodobacter sphaeroides* 2.4.1." J Bacteriol **182**(11): 3081-7.
- Oh, J. I. and S. Kaplan (1999). "The *cbb3* terminal oxidase of *Rhodobacter sphaeroides* 2.4.1: structural and functional implications for the regulation of spectral complex formation." Biochemistry **38**(9): 2688-96.
- Oh, J. I. and S. Kaplan (2000). "Redox signaling: globalization of gene expression." Embo J **19**(16): 4237-47.
- Oh, J. I. and S. Kaplan (2002). "Oxygen adaptation. The role of the CcoQ subunit of the *cbb3* cytochrome c oxidase of *Rhodobacter sphaeroides* 2.4.1." J Biol Chem **277**(18): 16220-8.
- Oh, J. I., I. J. Ko, et al. (2001). "The default state of the membrane-localized histidine kinase PrrB of *Rhodobacter sphaeroides* 2.4.1 is in the kinase-positive mode." J Bacteriol **183**(23): 6807-14.

- Oh, J. I., I. J. Ko, et al. (2004). "Reconstitution of the *Rhodobacter sphaeroides* cbb3-PrrBA signal transduction pathway in vitro." Biochemistry **43**(24): 7915-23.
- Ostermeier, C., A. Harrenga, et al. (1997). "Structure at 2.7 Å resolution of the *Paracoccus denitrificans* two-subunit cytochrome c oxidase complexed with an antibody FV fragment." Proc Natl Acad Sci U S A **94**(20): 10547-53.
- Otten, M. F., J. van der Oost, et al. (2001). "Cytochromes c₅₅₀, c₅₅₂, and c₁ in the electron transport network of *Paracoccus denitrificans*: redundant or subtly different in function?" J Bacteriol **183**(24): 7017-26.
- Ouchane, S. and S. Kaplan (1999). "Topological analysis of the membrane-localized redox-responsive sensor kinase PrrB from *Rhodobacter sphaeroides* 2.4.1." J Biol Chem **274**(24): 17290-6.
- Ozturk, M., E. Gurel, et al. (2007). "Site-directed mutagenesis of five conserved residues of subunit i of the cytochrome cbb3 oxidase in *Rhodobacter capsulatus*." J Biochem Mol Biol **40**(5): 697-707.
- Palleroni, N. J. (1975). General Properties and Taxonomy of the Genus *Pseudomonas*. Genetics and Biochemistry of Pseudomonas. P. Clarke, H., Richmond, M., H., John Wiley and Sons.
- Palleroni, N. J. (2003). "Prokaryote taxonomy of the 20th century and the impact of studies on the genus *Pseudomonas*: a personal view." Microbiology **149**(Pt 1): 1-7.
- Parkhill, J., B. W. Wren, et al. (2000). "The genome sequence of the food-borne pathogen *Campylobacter jejuni* reveals hypervariable sequences." Nature **403**(6770): 665-8.
- Parkinson, J. S. (1995). Genetic Approachs for signalling pathways and proteins. Two-Component Signal Transduction. J. Hoch and T. Silhavy. Washington DC, ASM Press.
- Parkinson, J. S. and E. C. Kofoid (1992). "Communication modules in bacterial signaling proteins." Annu Rev Genet **26**: 71-112.
- Paulsen, I. T., C. M. Press, et al. (2005). "Complete genome sequence of the plant commensal *Pseudomonas fluorescens* Pf-5." Nat Biotechnol **23**(7): 873-8.
- Pedersen, P. L. and L. M. Amzel (1993). "ATP synthases. Structure, reaction center, mechanism, and regulation of one of nature's most unique machines." J Biol Chem **268**(14): 9937-40.
- Penin, F., V. Brass, et al. (2004). "Structure and function of the membrane anchor domain of hepatitis C virus nonstructural protein 5A." J Biol Chem **279**(39): 40835-43.
- Pereira, M. M., M. Santana, et al. (2001). "A novel scenario for the evolution of haem-copper oxygen reductases." Biochim Biophys Acta **1505**(2-3): 185-208.
- Pieracci, F. M. and P. S. Barie (2007). "Strategies in the prevention and management of ventilator-associated pneumonia." Am Surg **73**(5): 419-32.
- Pitcher, R. S. (2002). Biochemical and Spectroscopic studies of cytochrome cbb₃ oxidases. School of Biological Sciences. Norwich, University of East Anglia.
- Pitcher, R. S., T. Brittain, et al. (2002). "Cytochrome cbb(3) oxidase and bacterial microaerobic metabolism." Biochem Soc Trans **30**(4): 653-8.
- Pitcher, R. S., T. Brittain, et al. (2003). "Complex interactions of carbon monoxide with reduced cytochrome cbb3 oxidase from *Pseudomonas stutzeri*." Biochemistry **42**(38): 11263-71.
- Pitcher, R. S., M. R. Cheesman, et al. (2002). "Molecular and spectroscopic analysis of the cytochrome cbb(3) oxidase from *Pseudomonas stutzeri*." J Biol Chem **277**(35): 31474-83.
- Pitcher, R. S. and N. J. Watmough (2004). "The bacterial cytochrome cbb3 oxidases." Biochim Biophys Acta **1655**(1-3): 388-99.
- Poole, R. K. and G. M. Cook (2000). "Redundancy of aerobic respiratory chains in bacteria? Routes, reasons and regulation." Adv Microb Physiol **43**: 165-224.

- Preisig, O., D. Anthamatten, et al. (1993). "Genes for a microaerobically induced oxidase complex in *Bradyrhizobium japonicum* are essential for a nitrogen-fixing endosymbiosis." Proc Natl Acad Sci U S A **90**(8): 3309-13.
- Preisig, O., R. Zufferey, et al. (1996). "The *Bradyrhizobium japonicum* fixGHIS genes are required for the formation of the high-affinity cbb3-type cytochrome oxidase." Arch Microbiol **165**(5): 297-305.
- Preisig, O., R. Zufferey, et al. (1996). "A high-affinity cbb3-type cytochrome oxidase terminates the symbiosis-specific respiratory chain of *Bradyrhizobium japonicum*." J Bacteriol **178**(6): 1532-8.
- Prive, G. G. (2007). "Detergents for the stabilization and crystallization of membrane proteins." Methods **41**(4): 388-97.
- Puustinen, A., M. Finel, et al. (1991). "Properties of the two terminal oxidases of *Escherichia coli*." Biochemistry **30**(16): 3936-42.
- Puustinen, A., M. I. Verkhovsky, et al. (1996). "Reaction of the *Escherichia coli* quinol oxidase cytochrome bo₃ with dioxygen: the role of a bound ubiquinone molecule." Proc Natl Acad Sci U S A **93**(4): 1545-8.
- Rauhamaeki, V., M. Baumann, et al. (2006). "Identification of a histidine-tyrosine cross-link in the active site of the cbb3-type cytochrome c oxidase from *Rhodobacter sphaeroides*." Proc Natl Acad Sci U S A **103**(44): 16135-40.
- Ray, A. and H. D. Williams (1997). "The effects of mutation of the *anr* gene on the aerobic respiratory chain of *Pseudomonas aeruginosa*." FEMS Microbiol Lett **156**(2): 227-32.
- Rensing, C., B. Fan, et al. (2000). "CopA: An *Escherichia coli* Cu(I)-translocating P-type ATPase." Proc Natl Acad Sci U S A **97**(2): 652-6.
- Richardson, D. J. (2000). "Bacterial respiration: a flexible process for a changing environment." Microbiology **146** (Pt 3): 551-71.
- Rothery, E. L., C. G. Mowat, et al. (2003). "Histidine 61: an important heme ligand in the soluble fumarate reductase from *Shewanella frigidimarina*." Biochemistry **42**(45): 13160-9.
- Russo, F. D. and T. J. Silhavy (1993). "The essential tension: opposed reactions in bacterial two-component regulatory systems." Trends Microbiol **1**(8): 306-10.
- Saifutdinov, R., G., Larina, L., I., Vakulskaia, T., I., Voronkov, M., G., (2000). Electron Paramagnetic Resonance in Biochemistry and Medicine, Kluwer Academic.
- Sambrook, J., Fritsch, E., F., Maniatis, T., (1989). Molecular Cloning: A laboratory Manual, Cold Spring Harbour Press.
- Sapay, N., R. Montserret, et al. (2006). "NMR structure and molecular dynamics of the in-plane membrane anchor of nonstructural protein 5A from bovine viral diarrhea virus." Biochemistry **45**(7): 2221-33.
- Saraste, M. and J. Castresana (1994). "Cytochrome oxidase evolved by tinkering with denitrification enzymes." FEBS Lett **341**(1): 1-4.
- Schwem, B. E. and R. H. Fillingame (2006). "Cross-linking between helices within subunit a of *Escherichia coli* ATP synthase defines the transmembrane packing of a four-helix bundle." J Biol Chem **281**(49): 37861-7.
- Scopes, R. K. (1994). Protein Purification: Principles and Practice, Springer-Verlag.
- Shapleigh, J. P., J. P. Hosler, et al. (1992). "Definition of the catalytic site of cytochrome c oxidase: specific ligands of heme a and the heme a₃-CuB center." Proc Natl Acad Sci U S A **89**(11): 4786-90.
- Sharma, V., A. Puustinen, et al. (2006). "Sequence analysis of the cbb3 oxidases and an atomic model for the *Rhodobacter sphaeroides* enzyme." Biochemistry **45**(18): 5754-65.
- Shelver, D., R. L. Kerby, et al. (1997). "CooA, a CO-sensing transcription factor from *Rhodospirillum rubrum*, is a CO-binding heme protein." Proc Natl Acad Sci U S A **94**(21): 11216-20.

- Shifman, J. M., B. R. Gibney, et al. (2000). "Heme redox potential control in de novo designed four-alpha-helix bundle proteins." Biochemistry **39**(48): 14813-21.
- Smith, P. K., R. I. Krohn, et al. (1985). "Measurement of protein using bicinchoninic acid." Anal Biochem **150**(1): 76-85.
- Sowa, A. W., S. M. Duff, et al. (1998). "Altering hemoglobin levels changes energy status in maize cells under hypoxia." Proc Natl Acad Sci U S A **95**(17): 10317-21.
- Spiers, A. J., A. Buckling, et al. (2000). "The causes of *Pseudomonas* diversity." Microbiology **146** (Pt 10): 2345-50.
- Spiro, S. and J. R. Guest (1991). "Adaptive responses to oxygen limitation in *Escherichia coli*." Trends Biochem Sci **16**(8): 310-4.
- Stevens, T. H. and S. I. Chan (1981). "Histidine is the axial ligand to cytochrome alpha 3 in cytochrome c oxidase." J Biol Chem **256**(3): 1069-71.
- Stover, C. K., X. Q. Pham, et al. (2000). "Complete genome sequence of *Pseudomonas aeruginosa* PA01, an opportunistic pathogen." Nature **406**(6799): 959-64.
- Sun, Y., K. Jin, et al. (2001). "Neuroglobin is up-regulated by and protects neurons from hypoxic-ischemic injury." Proc Natl Acad Sci U S A **98**(26): 15306-11.
- Svensson-Ek, M., J. Abramson, et al. (2002). "The X-ray crystal structures of wild-type and EQ(I-286) mutant cytochrome c oxidases from *Rhodobacter sphaeroides*." J Mol Biol **321**(2): 329-39.
- Taccetti, G., S. Campana, et al. (1995). "Cystic fibrosis and episodic arthritis." J Pediatr **126**(5 Pt 1): 848-9.
- Takeda, S., T. Nakai, et al. (2007). "In vitro and in vivo activities of a new cephalosporin, FR264205, against *Pseudomonas aeruginosa*." Antimicrob Agents Chemother **51**(3): 826-30.
- Tavares, P., A. S. Pereira, et al. (2006). "Metalloenzymes of the denitrification pathway." J Inorg Biochem **100**(12): 2087-100.
- Thöny-Meyer, L., C. Beck, et al. (1994). "The *ccoNOQP* gene cluster codes for a cb-type cytochrome oxidase that functions in aerobic respiration of *Rhodobacter capsulatus*." Mol Microbiol **14**(4): 705-16.
- Thöny-Meyer, L., P. Kunzler, et al. (1996). "Requirements for maturation of *Bradyrhizobium japonicum* cytochrome c550 in *Escherichia coli*." Eur J Biochem **235**(3): 754-61.
- Thorndycroft, F. H., G. Butland, et al. (2007). "A new assay for nitric oxide reductase reveals two conserved glutamate residues form the entrance to a proton-conducting channel in the bacterial enzyme." Biochem J **401**(1): 111-9.
- Toledo-Cuevas, M., B. Barquera, et al. (1998). "The *cbb3*-type cytochrome c oxidase from *Rhodobacter sphaeroides*, a proton-pumping heme-copper oxidase." Biochim Biophys Acta **1365**(3): 421-34.
- Tomb, J. F., O. White, et al. (1997). "The complete genome sequence of the gastric pathogen *Helicobacter pylori*." Nature **388**(6642): 539-47.
- Towner, K. (1997). *Bacterial Genetics. Medical Microbiology*. C. Livingstone.
- Traylor, T., G., Mitchell, M., J., Tsuchiya, S., Campbell, D., H., Stynes, D., V., Koga, N., (1981). "Cyclophane Hemes: Steric Effects on Dioxygen and Carbon Monoxide Binding to Hemes and Heme Proteins." Journal of the American Chemistry Society **103**: 5234-5236.
- Tsukihara, T., H. Aoyama, et al. (1995). "Structures of metal sites of oxidized bovine heart cytochrome c oxidase at 2.8 Å." Science **269**(5227): 1069-74.
- Tuckerman, J. R., G. Gonzalez, et al. (2002). "Ligand and oxidation-state specific regulation of the heme-based oxygen sensor FixL from *Sinorhizobium meliloti*." Biochemistry **41**(19): 6170-7.
- Ugidos, A., G. Morales, et al. (2008). "The coordinate regulation of multiple terminal oxidases by the *Pseudomonas putida* ANR global regulator." Environ Microbiol.

- Uden, G. and J. R. Guest (1985). "Isolation and characterization of the Fnr protein, the transcriptional regulator of anaerobic electron transport in *Escherichia coli*." Eur J Biochem **146**(1): 193-9.
- Uno, T., D. Ryu, et al. (2004). "Residues in the distal heme pocket of neuroglobin. Implications for the multiple ligand binding steps." J Biol Chem **279**(7): 5886-93.
- Urbani, A., S. Gemeinhardt, et al. (2001). "Properties of the detergent solubilised cytochrome c oxidase (cytochrome cbb(3)) purified from *Pseudomonas stutzeri*." FEBS Lett **508**(1): 29-35.
- Van Alst, N. E., K. F. Picardo, et al. (2007). "Nitrate sensing and metabolism modulate motility, biofilm formation, and virulence in *Pseudomonas aeruginosa*." Infect Immun **75**(8): 3780-90.
- van der Oost, J., P. Lappalainen, et al. (1992). "Restoration of a lost metal-binding site: construction of two different copper sites into a subunit of the *E. coli* cytochrome c quinol oxidase complex." Embo J **11**(9): 3209-17.
- Van Niel, C. B. and M. B. Allen (1952). "A note on *Pseudomonas stutzeri*." J Bacteriol **64**(3): 413-22.
- Van Spanning, R. J., A. P. De Boer, et al. (1997). "FnrP and NNR of *Paracoccus denitrificans* are both members of the FNR family of transcriptional activators but have distinct roles in respiratory adaptation in response to oxygen limitation." Mol Microbiol **23**(5): 893-907.
- Verissimo, A. F., F. L. Sousa, et al. (2007). "Thermodynamic redox behavior of the heme centers of cbb3 heme-copper oxygen reductase from *Bradyrhizobium japonicum*." Biochemistry **46**(46): 13245-53.
- Verissimo, A. F., F. L. Sousa, et al. (2008). "Thermodynamic redox behavior of the heme centers in A-type heme-copper oxygen reductases: comparison between the two subfamilies." Biophys J **95**(9): 4448-55.
- Vollack, K. U., E. Hartig, et al. (1999). "Multiple transcription factors of the FNR family in denitrifying *Pseudomonas stutzeri*: characterization of four fnr-like genes, regulatory responses and cognate metabolic processes." Mol Microbiol **31**(6): 1681-94.
- Vollack, K. U., J. Xie, et al. (1998). "Localization of denitrification genes on the chromosomal map of *Pseudomonas aeruginosa*." Microbiology **144** (Pt 2): 441-8.
- Wallace, C. J. and I. Clark-Lewis (1992). "Functional role of heme ligation in cytochrome c. Effects of replacement of methionine 80 with natural and non-natural residues by semisynthesis." J Biol Chem **267**(6): 3852-61.
- Welter, R., L. Q. Gu, et al. (1994). "Identification of the ubiquinol-binding site in the cytochrome bo₃-ubiquinol oxidase of *Escherichia coli*." J Biol Chem **269**(46): 28834-8.
- Wenger, R. H. (2002). "Cellular adaptation to hypoxia: O₂-sensing protein hydroxylases, hypoxia-inducible transcription factors, and O₂-regulated gene expression." Faseb J **16**(10): 1151-62.
- Wikstrom, M. (2004). "Cytochrome c oxidase: 25 years of the elusive proton pump." Biochim Biophys Acta **1655**(1-3): 241-7.
- Wikstrom, M. and M. I. Verkhovskiy (2007). "Mechanism and energetics of proton translocation by the respiratory heme-copper oxidases." Biochim Biophys Acta **1767**(10): 1200-14.
- Wikstrom, M. K. (1977). "Proton pump coupled to cytochrome c oxidase in mitochondria." Nature **266**(5599): 271-3.
- Williams, H. D., J. E. Zlosnik, et al. (2007). "Oxygen, cyanide and energy generation in the cystic fibrosis pathogen *Pseudomonas aeruginosa*." Adv Microb Physiol **52**: 1-71.
- Wood, P. M. (1984). "Bacterial proteins with CO-binding b- or c-type haem. Functions and absorption spectroscopy." Biochim Biophys Acta **768**(3-4): 293-317.

- Worlitzsch, D., R. Tarran, et al. (2002). "Effects of reduced mucus oxygen concentration in airway *Pseudomonas* infections of cystic fibrosis patients." J Clin Invest **109**(3): 317-25.
- Wraight, C. A. (2006). "Chance and design--proton transfer in water, channels and bioenergetic proteins." Biochim Biophys Acta **1757**(8): 886-912.
- Xia, D., C. A. Yu, et al. (1997). "Crystal structure of the cytochrome bc1 complex from bovine heart mitochondria." Science **277**(5322): 60-6.
- Yan, Y., J. Yang, et al. (2008). "Nitrogen fixation island and rhizosphere competence traits in the genome of root-associated *Pseudomonas stutzeri* A1501." Proc Natl Acad Sci U S A **105**(21): 7564-9.
- Yang, K., J. Zhang, et al. (2007). "Glutamate 107 in subunit I of the cytochrome bd quinol oxidase from *Escherichia coli* is protonated and near the heme d/heme b595 binuclear center." Biochemistry **46**(11): 3270-8.
- Youn, H., R. L. Kerby, et al. (2003). "The role of the hydrophobic distal heme pocket of CooA in ligand sensing and response." J Biol Chem **278**(4): 2333-40.
- Zhou, Y., T. M. Duncan, et al. (1997). "Subunit rotation in *Escherichia coli* FoF1-ATP synthase during oxidative phosphorylation." Proc Natl Acad Sci U S A **94**(20): 10583-7.
- Zlosnik, J. E., G. R. Tavankar, et al. (2006). "Investigation of the physiological relationship between the cyanide-insensitive oxidase and cyanide production in *Pseudomonas aeruginosa*." Microbiology **152**(Pt 5): 1407-15.
- Zufferey, R., E. Arslan, et al. (1998). "How replacements of the 12 conserved histidines of subunit I affect assembly, cofactor binding, and enzymatic activity of the *Bradyrhizobium japonicum* cbb3-type oxidase." J Biol Chem **273**(11): 6452-9.
- Zufferey, R., O. Preisig, et al. (1996). "Assembly and function of the cytochrome cbb3 oxidase subunits in *Bradyrhizobium japonicum*." J Biol Chem **271**(15): 9114-9.
- Zumft, W. G. (1997). "Cell biology and molecular basis of denitrification." Microbiol Mol Biol Rev **61**(4): 533-616.